The structure and function of hyaluronan-binding proteins in extracellular matrix assembly

Nicholas T. Seyfried

Green College

University of Oxford

A thesis submitted in partial fulfilment of the requirements for the Degree of Doctor of Philosophy in Biochemistry

Michaelmas Term, 2004

The structure and function of hyaluronan-binding proteins in extracellular matrix assembly

Thesis submitted for the degree of D.Phil. in Biochemistry, Michaelmas Term 2004
Nicholas T. Seyfried, Green College

The chondroitin sulfate proteoglycan (CSPG) aggrecan forms link protein-stabilised complexes with hyaluronan (HA), via its N-terminal G1-domain, that provide cartilage with its load bearing properties. Similar aggregates (potentially containing new members of the link protein family), in which other CSPGs (i.e., versican, brevican and neurocan) substitute for aggrecan, may contribute to the structural integrity of many other tissues including skin and brain. In this thesis, cartilage link protein (cLP) and the G1-domains of aggrecan (AG1) and versican (VG1) were expressed in *Drosophila* S2 cells, purified to homogeneity and functionally characterised. The recombinant human proteins were found to have properties similar to those described for the native molecules. For example cLP formed dimers, and HA decasaccharides (HA 10-mers) were the minimum size that could compete effectively for their binding to polymeric HA. In addition, gel filtration and protein cross-linking/MALDI-TOF peptide fingerprinting showed that cLP and AG1 interact in the absence or presence of HA. Conversely, cLP and VG1 did not bind directly to each other in solution yet formed ternary complexes with HA24. *N*-linked glycosylation of VG1 and AG1 was demonstrated to be unnecessary for either HA binding or the formation of ternary complexes. Additionally, the length of HA required to accommodate two G1-domains was found to be significantly larger for aggrecan than versican, which may reflect differences in the conformation of HA stabilised on binding these proteins. To further investigate protein-HA interactions, fluorescent HA oligosaccharides were prepared and characterised. HA oligosaccharides labelled with the fluorophore 2-aminobenzoic acid (2AA) from four to 40 residues in length were purified to homogeneity by ion exchange chromatography using a logarithmic gradient. Molecular weight and purity characterisation of HA oligosaccharides was facilitated by 2AA derivitisation since it enhanced signals in MALDI-TOF mass spectrometry and improves fluorophore-assisted carbohydrate electrophoresis (FACE) analysis by avoiding the inverted parabolic migration characteristic of 2-aminoacridone (AMAC) labelled sugars. The small size and shape of the fluorophore maintains the biological activity of the derivatised oligosaccharides, as demonstrated by their ability to compete for polymeric hyaluronan binding to VG1, AG1 and cLP. An electrophoretic mobility shift assay was used to study VG1 binding to 2AA-labelled HA 8-, 10-, 20-, 30- and 40-mers and although no stable VG1 binding was observed to labelled 8-mers, the equilibrium dissociation constant (100 nM) for VG1 with HA 10-mers was estimated from densitometry analysis of the free oligosaccharide. Interactions involving 2AA labelled HA 20-, 30-, and 40-mers with VG1 also displayed positive cooperativity. Therefore, oligosaccharides labelled with 2-aminobenzoic acid are biologically active and show excellent potential as probes in fluorescence-based assays that investigate protein-carbohydrate interactions.

Declaration

I declare that the work present in this thesis is my own. Other work performed in collaboration with other scientists is clearly indicated in the relevant sections of this thesis and below.

Collaborations

Some of the work presented in this thesis was performed in collaboration. The expression of link protein and the G1-domains of aggrecan and versican in *Drosophila* S2 cells was performed by Dr. Gillian F. McVey as reported in her D.Phil thesis (McVey GF, 2002), for which 1 am greatly indebted. The biotinylated rooster comb hyaluronan used in microtitre plate assays and the defined hyaluronan oligosaccharides used in Chapters 3 and 4 were provided by Dr. David Mahoney (MRC Immunochemistry Unit, University of Oxford). Immunostaining using biotinylated VG1 and AG1 was performed by Dr. Carol de la Motte (Cleveland Clinic, OH, USA). Work involving the production of fluorescently labelled HA oligosaccharides and was done in collaboration with Dr. Andrew Almond (University of Oxford), where his advice and direction were invaluable. Experiments using multi-angle laser light scattering (MALLS) were also done in collaboration with Dr. Andrew Almond in the laboratory of Professor Timothy Hardingham (University of Manchester). I would also like to thank Dr. Thomas Jowett (University of Manchester) for his helpful technical advice regarding MALLS and Dr. David Neville and Dr. David Priestman (University of Oxford) for their help with oligosaccharide labelling and fluorimetry, respectively. The NMR of hyaluronan oligosaccharides and molecular modelling was performed by Dr. Charles Blundell (University of Oxford). Amino acid analysis and protein sequencing was carried out by Mr. Tony C. Wills (MRC Immunochemistry Unit, University of Oxford).

Acknowledgments

First and foremost I need to thank my supervisor Tony Day for providing me the opportunity to work in his laboratory and the freedom to pursue my own research endeavours. I have learned so much in the past three years. Your guidance and vision have made me a better scientist.

I would like to thank the Arthritis Research Campaign, which partially funded this project. This funding greatly relieved financial burden and allowed me to focus more on my science rather than expenses.

In regard to other important co-workers, I would like to especially thank Julia Presanis and Stefanos Tsiftsoglou for their friendship and helpful scientific advice. Special thanks also to Dr. Andrew Almond, whose direction and inspiration provided a very enriching and rewarding research collaboration.

I must thank all members of F1 and the MRC Immunochemsitry Unit, especially Marilyn Rugg and Tony Willis for keeping such organisation in a chaotic laboratory environment. As always, I could not have done any of these things without Shannon Hook, and my parents who have supported and cared for me over the last three years.

Publications

1. Seyfried, N.T., McVey G.F., Almond A., Mahoney D.J., Dudhia J., and Day A.J. (2005) Expression and purification of functionally active hyaluronan-binding domains from human cartilage link protein, aggrecan and versican; formation of ternary complexes with defined hyaluronan oligosaccharides. *J. Biol. Chem.*, **280**, 5435-5448.

2. Seyfried, N.T., Blundell C.D., Day A.J., and Almond A. (2005) The preparation and application of biologically active fluorescent hyaluronan oligosaccharides. *Glycobiology*, **15**, 303-312.

3. Blundell, C.D., Seyfried N.T., and Day A.J. 2004. Structural and functional diversity of hyaluronan-binding proteins. In: *Chemistry and Biology of Hyaluronan* (H.G. Garg, and C.A. Hales eds.), pp. 189-204. Elsevier Press, Amsterdam.

Selected poster abstracts

Seyfried, N.T., McVey, G.F., Dudhia, J, Day, A.J. The expression, purification and characterisation of functional human recombinant link protein and the G1-domains of aggrecan and versican. Presented at the *British Society for Matrix Biology (BSMB),* 2004, Manchester, UK.

Seyfried, N.T., McVey, G.F., Dudhia, J, Day, A.J. Interactions between hyaluronan, human recombinant cartilage link protein and the G1-domains of aggrecan and versican. Presented at *Hyaluronan,* 2003, Cleveland, OH, USA.

Seyfried, N.T., McVey, G.F., Dudhia, J, Day, A.J. The *in vitro* assembly of ternary complexes with human recombinant link protein and the G1-binding domains of aggrecan and versican. Presented at the *British Society for Matrix Biology (BSMB)*, 2003, Oxford, UK.

McVey G.F., Seyfried N.T., Willis A.C., Dudhia J and Day A.J. Expression of functional hyaluronan-binding proteins in Drosophila Schneider 2 cells. Presented at the *Federation of the European Connective Tissue Societies (FECTS),* 2002, Brighton, UK.

Abbreviations

2AA	2-aminobenzoic acid = anthranilic acid
AG1	G1-domain of human recombinant aggrecan
CCP	complement control protein
CD44	cluster of differentiation 44
cLP	cartilage link protein
CUB	complement subcomponents
CS	chondroitin sulphate
EGF	epidermal growth factor
AMAC	2-aminoacridone
ANTS	8-amino-1,3,6-naphthalene trisulfonic acid
ECM	extracellular matrix
EMSA	electrophoretic mobility shift assay
FPLC	fast performance liquid chromatography
FACE	fluorophore-assisted carbohydrate electrophoresis
GAG	glycosaminoglycan
GlcNAc	*N*-acetyl glucosamine
GlcUA	glucuronic acid
HA	hyaluronic acid = hyaluronan
HAX	hyaluronan fragment with a GluUA moiety at the non-reducing terminus and X sugar rings in total
HAPLN	HA and proteoglycan link protein
HAS	hyaluronan synthase
HPLC	high performance liquid chromatography
IαI	inter-α-inhibitor
Ig	immunoglobulin
K_d	dissociation constant
Link_TSG6	the Link module from human TSG-6, expressed in *E. coli*,
MALDI-TOF MS	matrix-assisted laser desorption/ionization mass spectrometry with time-of-flight analysis
MALLS	multi-angle laser light scattering
MES	2-(N-morpholine)ethane sulphonic acid
M_r	molecular mass
N-glycosidase F	PNGase F
NMR	nuclear magnetic resonance
PSB	protein sample buffer
TSG-6	TNF-stimulated gene 6
S.D	standard deviation
S.E	standard error of the mean
SDS-PAGE	sodium dodecyl sulphate-polyacrylamide gel electrophoresis
SPR	surface plasmon resonance
U	unit of enzyme
VG1	G1-domain of human recombinant versican

Contents

1 Introduction

1.1 Glycosaminoglycans

Glycosaminoglycans (Figure 1.1), important constituents in the extracellular matrix (ECM), are composed of linear repeating disaccharide backbones containing either the amino sugar derivative glucosamine or galactosamine (Jackson *et al.* 1991). Therefore, glycosaminoglycans (GAGs) can be separated into two groups, the galactosaminoglycans, which include chondroitin sulphate, and its epimerised homologue dermatan sulphate (Trowbridge and Gallo 2002; Kusche-Gullberg and Kjellen 2003) or the glucosaminoglycans, which include keratan sulphate, heparan sulphate, heparin and hyaluronan (Laurent and Fraser 1992; Funderburgh 2000; Esko and Lindahl 2001).

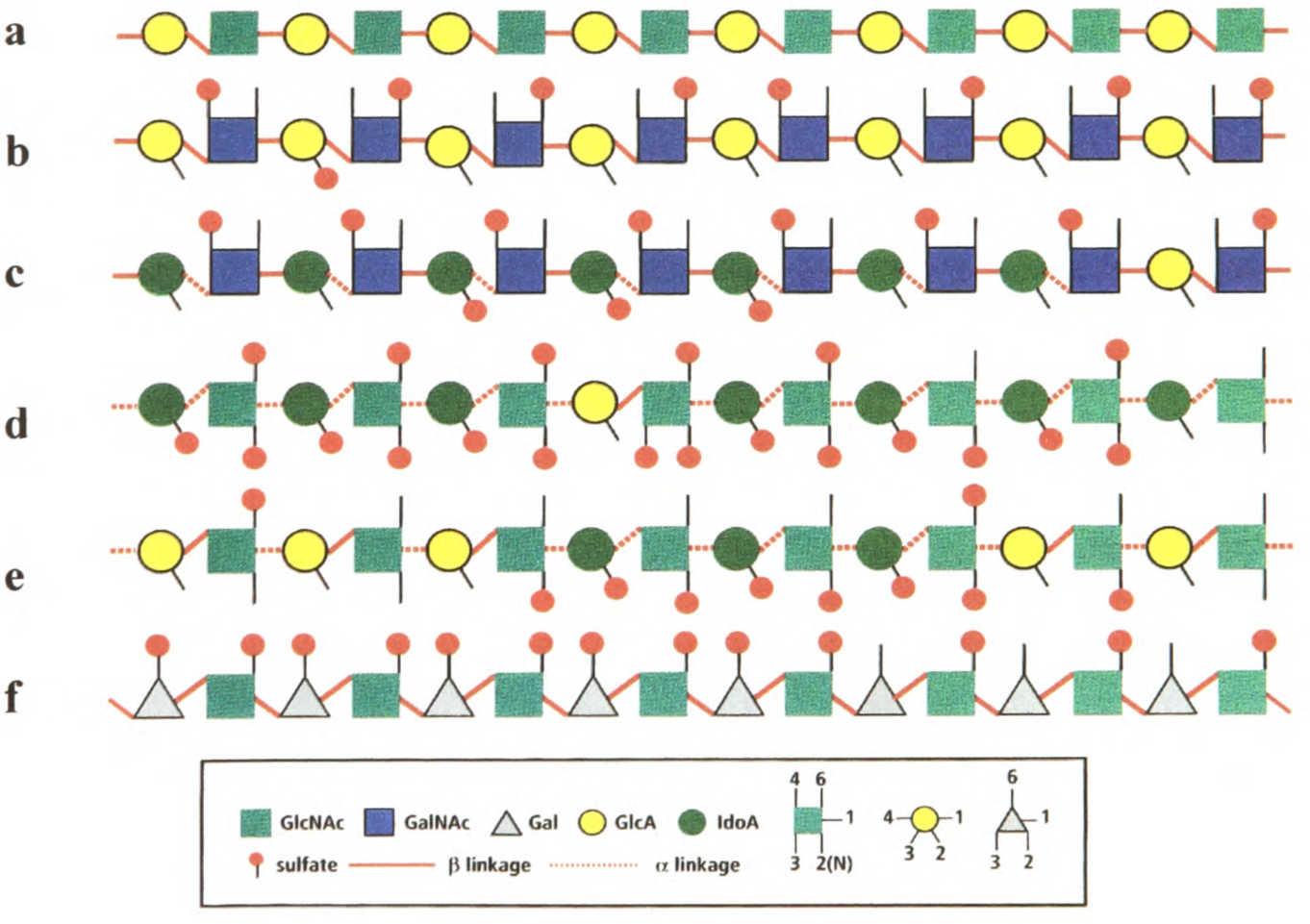

Figure 1.1 The polysaccharide backbones of a) hyaluronan, b) chondroitin sulphate, c) dermatan sulphate, d) heparin, e) heparan sulphate and f) keratan sulphate. Heparan sulphate is distinguished from heparin by the level and pattern of sulphation where heparin (primarily produced in mast cells) is more highly sulphated (Wedemeyer *et al.* 2000). This figure was provided by Dr. Anthony J. Day.

Glycosaminoglycan structure can also differ on the type of linkages (i.e., α or β), and the degree of sulphation or epimerisation; glucuronic acid can be epimerised to iduronic acid in heparin/heparan sulphate and dermatan sulphate, respectively (Figure 1.1). Additionally, almost all GAGs are found covalently linked to a core protein creating proteoglycans (Iozzo 1998) that have various functions in the extracellular matrix ranging from mechanical support to cellular adhesion, proliferation and differentiation (Hardingham and Fosang 1992; Iozzo 1998; Perrimon and Bernfield 2000).

1.2 Hyaluronan

1.2.1 Structure and properties

Hyaluronan (HA) was first described in the vitreous of the eye (Meyer and Palmer 1934) before its precise structure consisting of repeating D-glucuronic acid and *N*-acetyl-D-glucosamine linked by alternative β1-3 and β1-4 linkages (Figure 1.2) was reported 20 years later (Weissmann and Meyer 1954). Hyaluronan is distinct from other glycosaminoglycans in that it is not found covalently attached to a core protein, sulphated or epimerised rendering its structure the simplest of all the glycosaminoglycans. Depending on the tissue source, the polymer usually consists of 2500-25000 disaccharides, giving rise to molecular weights ranging from 10^6 to 10^7 Daltons and extended lengths of 2-25 μm (Laurent and Fraser 1992). HA as a polymer in physiological solution is best described as a stiffened and expanded random coil due to hydrogen bonding of adjacent sugar units and mutual repulsion between carboxyl groups (Laurent *et al.* 1960; Laurent and Fraser 1992; Hardingham 2004). However, HA never forms stable gels even with increasing concentration

indicating the absence of stable chain-chain self association (Almond *et al.* 1998a). Therefore, hyaluronan is highly dynamic in solution which may influence its interactions with proteins (Day and Sheehan 2001; Blundell *et al.* 2004b).

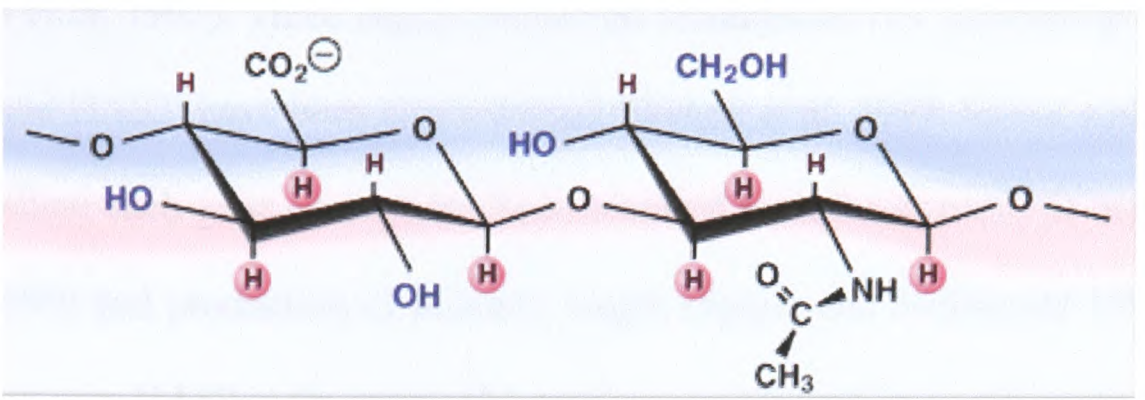

Figure 1.2 The disaccharide structure of hyaluronic acid showing the β (1→3) linkage between D-glucuronic acid (GlcUA) and *N*-acetyl-D-glucosamine (GlcNAc) residues.

1.2.2 Distribution, synthesis and degradation

Hyaluronan (HA) is found in all vertebrates and is a major constituent in the vitreous of the human eye, the synovial joint fluid, and the extracellular matrices of cartilage and brain (Fraser *et al.* 1997). It is also expressed in the matrix produced by the cumulus located around the oocyte, prior to ovulation (Fraser *et al.* 1997; Tammi *et al.* 2002). However, the largest amount of HA resides in the skin, where it is present in both the dermis and epidermis (Fraser *et al.* 1997). Hyaluronan is also a found in the glycocalyx of some strains of bacteria such as *Streptococci*, where it can act as a host defence mechanism (DeAngelis 1999, 2002). In addition to being found in the extracellular space of tissue, HA is also found intracellular where it is involved in growth regulation (Evanko and Wight 1999; Hascall *et al.* 2004). HA is unique from other glycosaminoglycans because it is synthesised by an HA synthase (HAS) at the inner face of the plasma membrane by addition of new sugar units to the reducing end of the polymer (Philipson and Schwartz 1984; Prehm 1984; Weigel 2004). The advantage of hyaluronan synthesis at the cell membrane is that HA can be

simultaneously assembled and extruded through the membrane into the extracellular space, which allows huge molecular weight polymers to be produced that would otherwise be limited in size by the constraints of Golgi or post-Golgi compartments (Weigel *et al.* 1997). Three highly conserved mammalian HA synthase genes (HAS1, HAS2 and HAS3) have been characterised (Weigel *et al.* 1997; Spicer and McDonald 1998) where each gene product has been reported to differ in catalytic activity (Itano *et al.* 1999) and production of polymer length (Spicer and McDonald 1998). Of the three enzymes HAS2 is the major HA synthase implicated in development since mice lacking HAS2 are embryonic lethal while HAS3 and HAS1 knockouts survive (Camenisch and McDonald 2000). Hyaluronan turnover in the body is remarkably high (~ 5 g/day (Fraser *et al.* 1997)). HA is endocytosed in the liver by endothelial cells and then catabolised in the lysosome by three enzymes, a hyaluronidase and two exoglycosidases (ß-glucuronidase and ß-*N*-acetyl glucosamindase) that remove sugars sequentially from the non-reducing termini (Laurent and Fraser 1992; Stern 2003; Stern 2004). The human genome contains six hyaluronidase-like genes, HYAL1, HYAL2, HYAL3, HYAL4 and PH-20/SPAM1 with one pseudogene HYALP1 (Csoka *et al.* 2001). The two major mammalian hyaluronidases (Hyal-1 and Hyal-2) act in concert to degrade high molecular weight hyaluronan to the tetrasaccharide level and can regulate HA size in tissue (Csoka *et al.* 2001). This is important because HA can have different biological activities, depending on polymer size where it has been reported that high and low molecular weight HA have opposite effects. For example, high molecular weight (10^6- 10^7 Da) hyaluronan chains are space filling molecules which hydrate tissues, and inhibit proliferation, inflammation and angiogenesis (Camenisch and McDonald 2000; Termeer *et al.* 2003). In contrast low molecular weight HA oligosaccharides (~ 1-10 kDa) can trigger signalling cascades

and cause changes in cell behaviour including stimulation of angiogenesis, and inflammation (Noble *et al.* 1996; Slevin *et al.* 1998; Horton *et al.* 1999; Termeer *et al.* 2003). Low molecular weight HA oligosaccharides (HA 4-10-mers) have also been shown to suppress tumour growth (Toole 2004). Therefore, it has been proposed that larger HA polymers protect the cell from access to the small HA oligosaccharides thereby suppressing stress responses and signalling cascades. (Camenisch and McDonald 2000; Termeer *et al.* 2003).

1.2.3 Hyaluronan in disease states

Given the high rate of HA turnover in tissue and the differential effects that high and low molecular weight HA has on cellular behaviour it is apparent that the mechanisms which control HA synthesis and degradation are of critical importance in physiological homeostasis. For example, an increase in hyaluronan expression is observed during ovulation where HA is responsible for forming a pericellular matrix around the oocyte, a process known as cell-oocyte complex (COC) expansion, which facilitates ovulation and fertilisation (Salustri *et al.* 1999). Changes in hyaluronan expression are also involved in the progression of disease states where the abnormal metabolism and catabolism of hyaluronan are associated with arthritis (Engstrom-Laurent 1989; Scher *et al.* 1996), vascular disease (Wight and Merrilees 2004) and cancer (Toole 2002; Toole 2004); almost all types of tumours are associated with an increased level of hyaluronan expression (Toole and Hascall 2002; Toole 2004). Furthermore, inhibiting HAS gene products significantly reduced prostate tumour size in mice (Simpson *et al.* 2002) and loss of HYAL-1 activity has been shown to promote tumour metastasis (Csoka *et al.* 2001). Therefore, it seems that the ability of HA to influence cellular proliferation, migration and adhesion via its interactions with

HA-binding proteins might contribute to the malignancy and survival of several cancers (Toole 2002).

1.3 The hyaluronan-binding proteins: structure and function

1.3.1 Link module superfamily

Although HA is a simple polysaccharide it has diverse functions in vertebrates mainly due to its ability to interact with different HA-binding proteins (termed hyaladherins (Toole 1990)). Over the last few years much progress has been made in our understanding of the structural basis of HA-protein interactions (Day and Sheehan 2001; Day and Prestwich 2002; Blundell *et al.* 2004b). For example, the majority of HA-binding proteins contain a common structural domain of approximately 100 amino acids, termed the Link module (also referred to as a proteoglycan tandem repeat, (Kohda *et al.*, 1996, Blundell *et al.* 2003)). Figure 1.3 shows the domain structures for the members of the Link module superfamily, which currently has 14 members and the majority of these contain a variety of other domain types. It has been suggested that the Link module superfamily can be divided into three subgroups (Figure 1.4) according to the known or expected size of their HA-binding domains (Day 1999; Day and Prestwich 2002; Blundell *et al.* 2004b). For instance Type A domains comprise a single independently folded Link module which can support high affinity HA binding as found in the protein product of tumour necrosis factor stimulated gene-6 (TSG-6); see Blundell *et al.* 2003. Type B domains, however, require N-and C-terminal extensions flanking the Link module for the correct folding and functional activity, which is exemplified by the ~150 amino acid HA-binding domain of CD44 (Teriete *et al.* 2004).

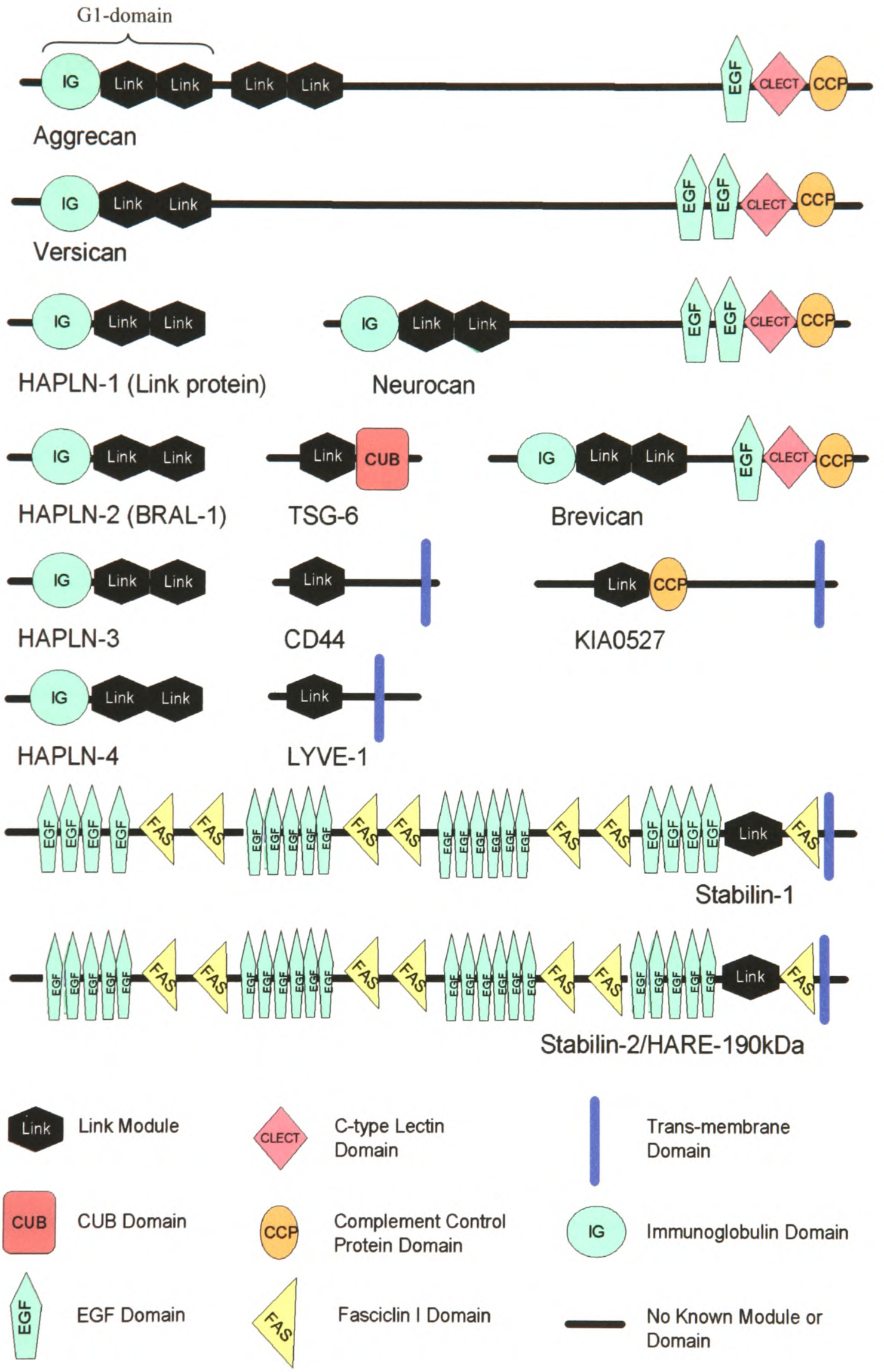

Figure 1.3 The domain organisation of the Link module superfamily. The symbols depicting the various modules are derived from the SMART datatbase (http://smart.embl-heidelberg.de/). This figure was reproduced from Blundell CD, Seyfried NT and Day AJ (2004).

Type	Protein	Binding Domain	Structure
A	TSG-6	Link ~100aa	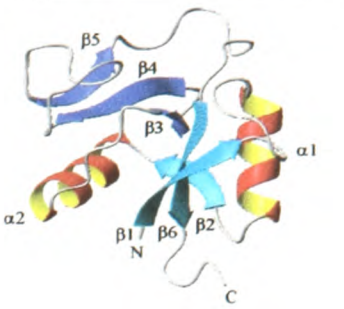
B	CD44	N Link C ~150aa	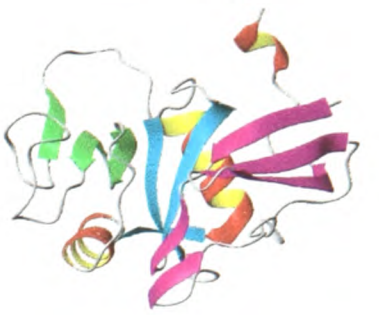
C	Link protein Aggrecan Versican	Ig Link Link ~330aa	No 3D structure

Figure 1.4 Members of Link module superfamily can be divided into three subgroups according to the known or expected size of their HA-binding domains (Day 1999; Day and Prestwich 2002). Tertiary structures have been determined for the Type A (Blundell *et al.* 2003) and Type B (Teriete *et al.* 2004) domains. However, there is currently no structural data for the Type C domains. Figure adapted from Blundell CD, Seyfried NT and Day AJ (2004).

The third class, Type C domains, contain an N-terminal immunoglobulin fold (Ig) followed by two contiguous Link modules as found in cartilage link protein and members of the chondroitin sulphate proteoglycan (CSPG) family, (i.e., aggrecan, versican, neurocan and brevican). The structure and biological function of superfamily members for each domain class are covered in detail below.

1.3.1.1 Type A domains

The HA-binding properties TSG-6 are probably the best characterised of any member of the Link module superfamily. TSG-6, a ~35 kDa secreted protein is comprised almost entirely of a Link module and CUB module (Wisniewski and Vilcek 1997; Milner and Day 2003). Its expression is not constitutive in adult tissues but induced in response to inflammatory mediators and growth factors (Wisniewski and Vilcek 1997;

Milner and Day 2003; Wisniewski and Vilcek 2004). The tertiary structure of the Link module from human TSG-6 (Link_TSG6) was determined by NMR spectroscopy in solution and has defined the consensus fold for the entire superfamily (Kohda *et al.* 1996; Blundell *et al.* 2003). The Link module, comprised of two α-helices and two triple stranded anti-parallel β-sheets arranged around a large hydrophobic core, was found to have a very similar fold to that of the C-type lectin module from which it may have evolved (Drickamer 1999; Blundell *et al.* 2003). The critical residues involved in HA binding have been mapped in Link_TSG6, which include Lys^{11}, Tyr^{12}, Tyr^{59}, Phe^{70} and Tyr^{78} (Mahoney *et al.* 2001b). Other members of the Type A subgroup potentially include the HA receptors stabilin-1 and stabilin-2 (Zhou *et al.* 2000; Politz *et al.* 2002); recent molecular modelling indicates that they may have Type B domains (discussed below) with N- and C- terminal sequences composed of two halves of an EGF domain (Blundell CD and Day AJ, unpublished). Both genes code for homologous transmembrane proteins (~40 percent amino acid identity) that contain one Link module, seven fasciclin-like adhesion domains and multiple EGF/EGF-like domains (Figure 1.3). Since both are expressed in the liver and lymph nodes it has been suggested that they function as receptors for HA clearance (Zhou *et al.* 2000; Politz *et al.* 2002). Stabilin-2 is also related to the 190 kDa subunit of human HARE, the Hyaluronan Receptor for Endocytosis (Zhou *et al.* 2003). HARE is specific for both HA and chondroitin sulphate clearance in the liver and lymph nodes (Weigel and Weigel 2003). It must be noted that Stabilin-1 does not bind HA (Prevo *et al.* 2004). In addition, the binding properties of KIA0527 (Figure 1.3), cloned from brain tissue (Nagase *et al.* 1998), is still uncertain (Mahoney *et al.* 2001b).

1.3.1.2 Type B domains

Recently the solution structure and crystal structure for the Type B HA binding domain of CD44 has been determined (Teriete *et al.* 2004). This structure revealed that the N- and C-terminal extensions that flank the Link module come together in space to form an additional lobe, comprised of β-strands that extend the Link module β-sheet structure (Figure 1.4). A second protein also reported to have N- and C-terminal extensions is the Lymphatic Vessel Endothelial HA receptor or LYVE-1 (Jackson *et al.* 2001; Jackson 2003), which is primarily expressed on lymphatic endothelial cells (Banerji *et al.* 1999). LYVE-1, which shares 43 % homology with CD44, is capable of internalising HA after binding. Therefore, it has been suggested to be involved in the transport of HA from tissue to lymph (Prevo *et al.* 2001). The LYVE-1 HA binding domain is likely to be significantly smaller than that of CD44 due to a shorter C-terminal extension (Teriete *et al.* 2004). As described above Stabilin-1 and -2 may also contain an extended Link module.

1.3.1.3 Type C domains

The largest HA binding domain (~330 amino acids) is the Type C domain, which is found in cartilage link protein, where the Link module was first identified from rat chondrosarcoma (Neame *et al.* 1986). Previous studies have shown that with link protein both Link modules are involved in the interactions with HA (Goetinck *et al.* 1987; Grover and Roughley 1994). The full length link protein has the same domain organisation as the G1-domain domain of the CSPGs aggrecan, versican, neurocan and brevican (Figure 1.3 and 1.4), which suggests that they share a common ancestral gene (Spicer *et al.* 2003). Similar to cartilage link protein, studies on aggrecan have

also shown that both Link modules in the G1-domain are required for HA binding (Watanabe *et al.*, 1997a). In addition, the immunoglobulin domain has been reported to enhance the binding of aggrecan to HA compared to just the double link modules alone (Watanabe *et al.* 1997a). To date there is no high resolution structure for the Type C HA-binding domain.

1.3.2 Non-Link module HA-binding proteins

A number of HA-binding proteins have been identified that lack a Link module domain and are unrelated to each other at the primary sequence level. For example, inter-α-inhibitor (IαI) a serine protease inhibitor found in serum, was found to be covalently associated with HA in rheumatoid arthritis fluid (Sandson *et al.* 1965). More recently it has been shown to stabilise the cumulus via covalent interactions with HA during ovulation (Bost *et al.* 1998; Day AJ *et al.* 2004). Other proteins that have been reported to bind HA but do not contain a Link module are the HA-binding protein known as HABP-1 or P-32 (Deb and Datta 1996), the receptor for HA-mediated cell motility (RHAMM) (Yang *et al.* 1994; Cheung *et al.* 1999) and the human interphotoreceptor matrix receptor SPACRCAN (Acharya *et al.* 2000; Chen *et al.* 2004). It has been proposed that linear sequences termed BX_7B motifs (where B is either a lysine or arginine and X can be any amino acid other than acidic residues) might represent the minimum requirement for HA binding in RHAMM and other HA-binding proteins (Yang *et al.* 1994). However, there are few convincing data to indicate that they mediate hyaluronan binding in these proteins (Chen *et al.* 2004). Additionally, the spacing of basic amino acids is extremely common in protein sequences (Day and Prestwich 2002). Therefore, the presence of a BX_7B motif should not be interpreted as an indicator that a protein will bind hyaluronan nor should it be

assumed that this is necessarily the site of hyaluronan binding activity in a known hyaladherin (Day and Prestwich 2002).

1.4 The Link protein family

The first complete amino acid sequence of cartilage link protein (cLP) was that determined from protein isolated the rat chondrosarcoma (Neame *et al.* 1986) followed by the human sequence (Dudhia and Hardingham 1990). Human cartilage link protein is ~96 % homologous to that of the rat and porcine protein (Neame and Barry 1993). Link protein is an extracellular glycoprotein, initially characterised in cartilage, with a molecular mass of 40-48 kDa (Oegema *et al.* 1975). Three forms of the protein from cartilage have been identified and shown to arise through differences in *N*-linked glycosylation and proteolysis (Neame and Barry 1993). The largest, termed LP1, has two *N*-linked oligosaccharides, whereas LP2 and LP3 have a single glycan and, additionally, LP3 lacks the first 16 amino acids (Mort *et al.* 1983). Link protein in cartilage, stabilises the interaction of aggrecan with hyaluronan, forming large multimolecular aggregates that are highly hydrated and give the tissue its load bearing properties (Hardingham and Fosang 1992) discussed in more detail in section 1.6. Immunochemistry with anti-cLP antibodies indicated that cLP is widely expressed (Gardell *et al.* 1980; Ripellino *et al.* 1989). Recently, two distinct brain link proteins termed BRAL1 and BRAL2 (sharing ~ 45 % homology with cLP) have also been identified (Hirakawa *et al.* 2000; Bekku *et al.* 2003). This lead to the identification of a human link protein gene family consisting of four members denoted 'HAPLN' or HA and Proteoglycan LiNk protein family (Spicer *et al.* 2003) where in this new nomenclature cLP is renamed HAPLN-1 and the two brain specific link

proteins (BRAL1 and BRAL2) correspond to HAPLN-2 and HAPLN-4, respectively (Figure 1.3). HAPLN-3 was also reported to be the most widely expressed link protein by Northern and tissue array analyses (Spicer *et al.* 2003). Each link protein gene was found to be located immediately adjacent to one of the four CSPG genes forming HAPLN-1/versican, HAPLN-2/brevican, HAPLN-3/aggrecan and HAPLN-4/neurocan gene pairs (Nomoto *et al.* 2002; Czipri *et al.* 2003; Spicer *et al.* 2003). The four encoded HAPLN proteins share 45-52 % overall amino acid identity where the least amount of similarity is seen in the immunoglobulin domain (Spicer *et al.* 2003). The critical importance of link protein in development is exemplified by knockout studies. Most cartilage link protein deficient mice die shortly after birth due to respiratory failure, which is believed to be a consequence of insufficient cartilage function in the upper respiratory tract (Watanabe and Yamada 1999). Those that survived developed progressive dwarfism and lordosis of the cervical spine.

1.5 The CSPGs: aggrecan, versican, neurocan and brevican

1.5.1 Aggrecan

Aggrecan is a large macromolecule with a protein core size of 225-250 kDa that is crucial in the extracellular matrix of cartilage where its function is distributing load in weight bearing joints (Bayliss 1990; Hardingham *et al.* 1994; Muir 1995). Aggrecan can also be found expressed in the developing brain and heart (Schwartz *et al.* 1996; Zanin *et al.* 1999). The primary structure of human cartilage aggrecan has been cloned and sequenced (Doege *et al.* 1991).

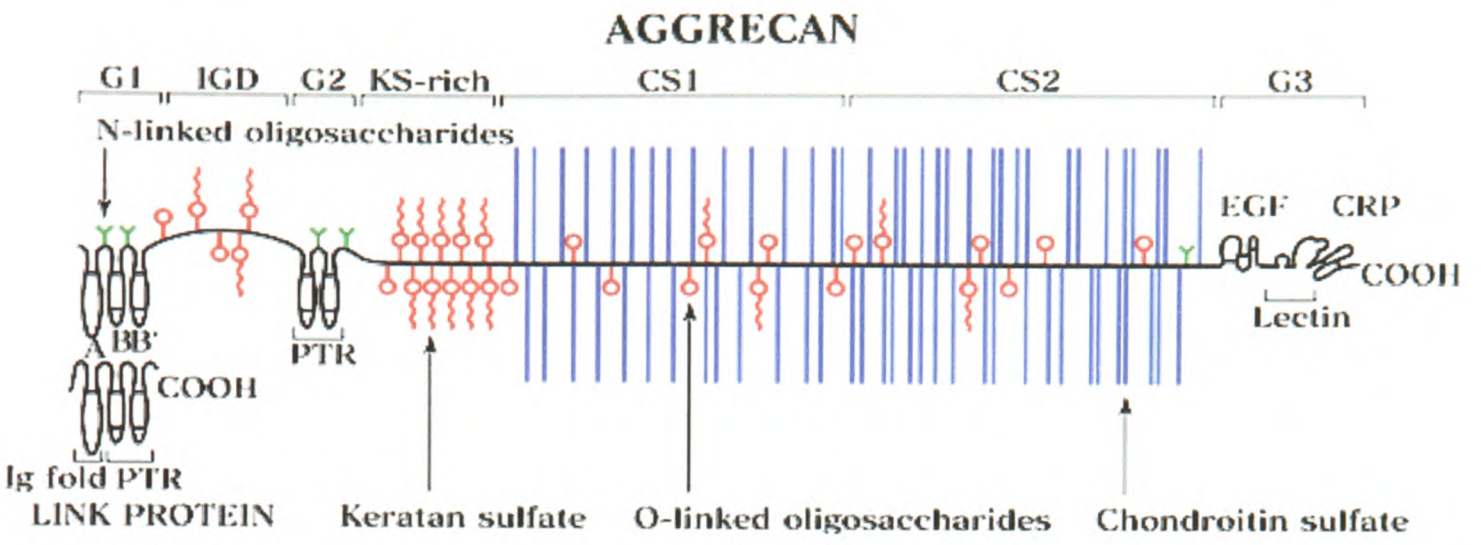

Figure 1.5 Aggrecan contains three globular domains (G1, G2, G3) and a two extended regions: The interglobular domain (IGD) and glycosaminoglycan attachment domain, which is composed of a variable keratan sulphate rich region and two chondroitin sulphate regions (CS-1 and CS-2). The domain structure of link protein is also shown, which is similar to the aggrecan G1 domain. This figure was taken from a glycoforum web article by Hardingham (1998).
See http://www.glycoforum.gr.jp/science/hyaluronan/HA05/HA05E.html.

Approximately 90 % of the mass of aggrecan is composed of glycosaminoglycans, predominantly chondroitin sulphate with some keratan sulphate in addition to *N*- and *O*-linked oligosaccharides bound covalently to the core protein (Figure 1.5). A fully glycosylated aggrecan molecule may contain up to 100 chondroitin sulphate and 30 keratan sulphate side chains giving the proteoglycan a mass of >2 MDa. (Hardingham and Fosang 1992). Aggrecan has three globular domains the G1, G2 and G3 domains (Figure 1.5). The G1 and G2 each contain two contiguous Link modules, where those in the G2 do not show any HA-binding activity (Fosang and Hardingham 1989). The G3 domain contains an EGF domain followed by a carbohydrate recognition domain (C-type lectin domain) and a complement control protein (CCP) domain at the C-terminus (Figure 1.5). In aggrecan mRNA, alternative splicing may result in the deletion of the EGF domain and the CCP domain (Baldwin *et al.* 1989; Doege *et al.* 1991). However, most transcripts in human cartilage lack the EGF domain, but contain the CCP domain (Grover and Roughley 1993). It has been shown that the G3 domain and more specifically the C-type lectin domain in aggrecan can interact with tenascin-C and -R, extracellular matrix proteins expressed in the central nervous

system (Aspberg *et al.* 1997; Day *et al.* 2004). The G3 domain can also bind to Fibulin-1, -2 and -3 (Aspberg *et al.* 1997; Olin *et al.* 2001; Isogai *et al.* 2002), proteins with elongated structures and many EGF-like domains, which are found associated with microfibrils in elastic fibers (Timpl *et al.* 2003). Therefore, hyaluronan and proteoglycan complexes can be found cross-linked through fibulins or tenascins in the extracellular matrix of various tissues (Lundell *et al.* 2004 and section 1.6). The crucial role of aggrecan in extracellular matrix assembly is exemplified in cartilage matrix deficiency (*cmd*), an autosomal recessive disorder caused by a genetic defect of aggrecan, resulting in the absence of the proteoglycan in cartilage (Watanabe *et al.* 1997b). Homozygotes (−/−) are characterised by cleft palate and short limbs, tail, and snout. They also die just after birth because of respiratory failure (Watanabe *et al.* 1997b) similar to cLP deficient mice (section 1.4).

1.5.2 Versican

Versican was originally characterised as a large chondroitin sulphate proteoglycan expressed in the prechondrogenic mesenchymal of developing chick limb buds (Kimata *et al.* 1986). Versican displays a ubiquitous distribution in connective tissues. In most tissues the staining pattern of versican is similar to that of the elastic fiber network (Zimmermann *et al.* 1994; Bode-Lesniewska *et al.* 1996). The C-terminal portion of human versican was initially identified in fibroblasts (Krusius *et al.* 1987) and two years later the complete amino acid sequence was reported (Zimmermann and Ruoslahti 1989). Alternative RNA splicing occurs in the two large exons encoding the GAG attachment sites (αGAG or βGAG) resulting in four versican mRNA transcripts producing the V0, V1, V2 and V3 variants (Dours-Zimmermann and Zimmermann 1994; Wight 2002). The variants differ in size and potential GAG

attachment sites, where V3 has no GAGs attachment sites (Figure 1.6). Versican also shares similar properties to aggrecan in that it interacts with other extracellular matrix proteins such as tenascin R via the lectin-binding domain (Aspberg *et al.* 1997). This lectin binding domain participates in other interactions such as those with fibulin-1 and fibulin-2 (Aspberg *et al.* 1999; Olin *et al.* 2001), and fibrillin-1 (Isogai *et al.* 2002). It has therefore been proposed that fibulin might serve as a bridge between versican and fibrillin, forming highly ordered multimolecular structures important to the assembly of elastic fibers (Wight 2002).

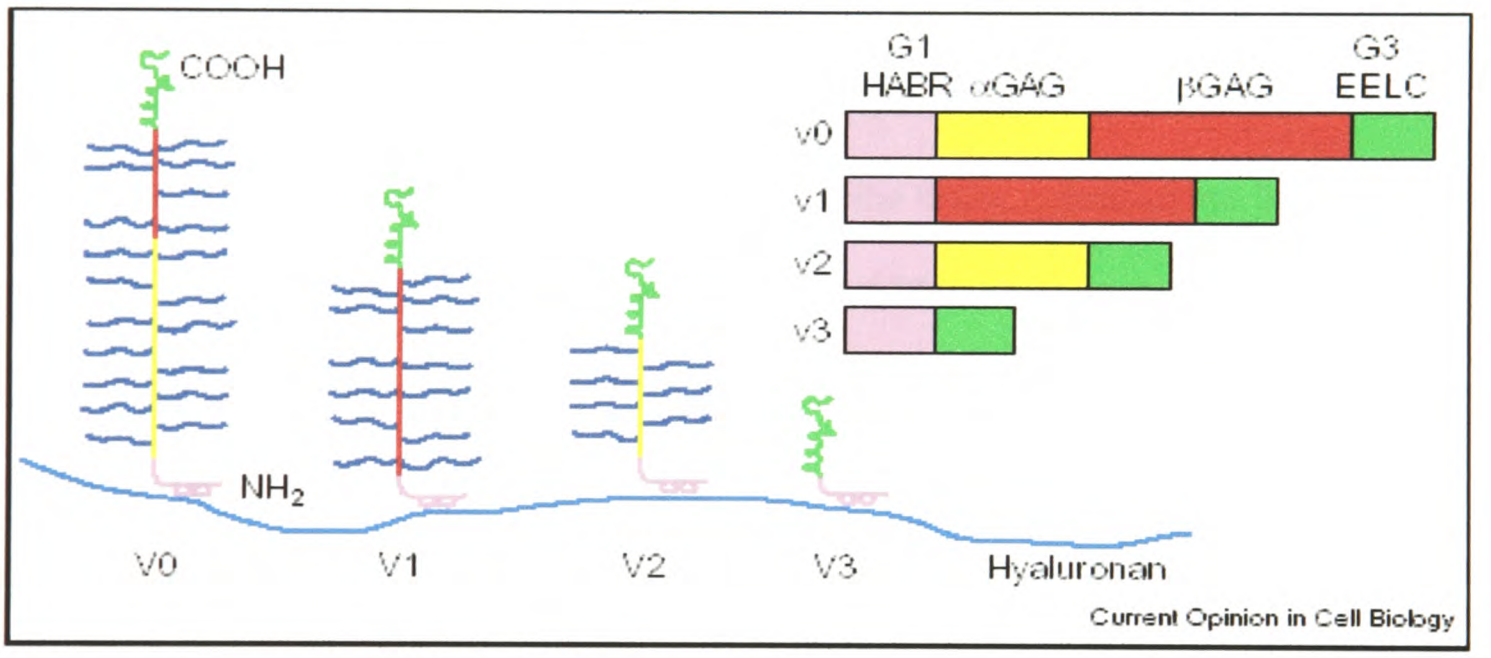

Figure 1.6 A model of the different isoforms generated by alternative splicing of the mRNA transcript for versican. Different colours denote specific domains in the gene and in the protein product. Purple = hyaluronan binding region (G1-domain); yellow = the α GAG exon and the protein product; red = β GAG exon and the protein product; green = two epidermal growth factor repeats (EE), a lectin binding domain (L) and a complement regulatory region (C), which make up the G3 domain. The GAG chains are shown in blue. This figure was reproduced from Wight 2002.

Like aggrecan, versican also has a crucial role in development. For example, the heart defect mouse (*dhf*) is a recessive lethal because the *Cspg2* (versican) gene is disrupted resulting in death at embryonic day 10.5 indicating the importance of versican in endocardial cushion swellings and heart segmentation that gives rise to the right ventricle (Mjaatvedt *et al.* 1998).

1.5.3 Neurocan and brevican

The chondroitin sulphate proteoglycans neurocan and brevican are specifically expressed in the central nervous system (Yamaguchi 2000; Rauch 2004). Neurocan was originally cloned from rat brain (Rauch *et al.* 1991) and is developmentally regulated with regards to mass, concentration, carbohydrate composition, sulphation and localisation (Rauch *et al.* 1992); it accounts for almost 20 % of total brain proteoglycan during early development. Neurocan has a core protein with a molecular mass of ~300 kDa and 3-4 potential chondroitin sulphate attachment sites (Margolis and Margolis 1994). Similar to the G3 domain of versican, neurocan has two epidermal growth factor domains, a C-type lectin domain, and a CCP-domain (Rauch *et al.* 1992). In the extracellular matrix of the brain, neurocan has been shown to interact with tenascin R and C (Grumet *et al.* 1994; Aspberg *et al.* 1997; Rauch 2004), the neural cell adhesion molecule (N-CAM) and neuron glial cell adhesion molecule (Rauch 2004). Soluble neurocan was also found to inhibit neural adhesion and neuron outgrowth *in vitro* and therefore, was suggested to play an important role in axon guidance and neurite growth (Grumet *et al.* 1993; Friedlander *et al.* 1994). However, these interactions are clearly not crucial to successful development as knockout mice lacking neurocan show no defects and develop normally (Zhou *et al.* 2001). The CSPG brevican was initially cloned by Yamada *et al.* 1994. Like other members of the CSPG family, brevican contains a G1 domain and a G3 domain with an epidermal growth factor domain, a C-type lectin domain and a CCP-domain at the C-terminus (Figure 1.3). However, the central GAG-attachment region of brevican is much shorter than that of aggrecan, versican, or neurocan, and shows little homology with these proteoglycans (Yamada *et al.* 1994). The brevican core protein exists as a 145 kDa full-length protein and an 80 kDa N-terminally truncated form. In addition, a

significant amount of brevican lacks glycosaminoglycan chains indicating that brevican is a "part-time" proteoglycan (Yamada *et al.* 1994). Unlike other members of the CSPG family, brevican occurs in tissue as both secreted and glycosylphosphatidylinositol-anchored isoforms (Seidenbecher *et al.* 1995). The role of brevican in the extracellular matrix assembly of the brain is still unclear since brevican deficient mice show no defects and develop normally (Brakebusch *et al.* 2002). However, these mice do have significant deficits in the maintenance of hippocampal long-term potentiation (LTP). Additionally, human gliomas (an aggressive form of brain cancer) show an increase in brevican expression, which may be a requisite for tumour invasion into the surrounding extracellular environment (Gary *et al.* 1998; Gary and Hockfield 2000).

1.6 The role of CSPGs and link protein in the extracellular matrix

Chondroitin sulphate proteoglycans are essential components of articular cartilage, the thin tissue that covers and protects bone surfaces from wear (Bayliss 1990; Hardingham and Fosang 1992; Muir 1995; Knudson and Knudson 2001). Articular cartilage has few cells (<5% of its volume) being composed mainly of extracellular matrix (Hardingham and Fosang 1992; Muir 1995; Knudson and Knudson 2001). The important biophysical properties of cartilage are the result of the composition of the extracellular matrix. Cartilage contains a dense network of fine collagen fibrils (mainly types II, VI, IX and XI), which are responsible for the form and tensile properties of the tissue (Muir 1995; Knudson and Knudson 2001). Hyaluronan can anchor itself to the chondrocytes cell surface through its interaction with CD44 (Figure 1.7) and possibly other cell surface HA receptors that might be able to compensate for CD44 (Nedvetzki *et al.* 2004). However, it is the CSPGs, mainly

aggrecan, together with cartilage link protein (HAPLN-1) and hyaluronan that form large multimolecular aggregates, which draw water into the tissue by osmosis and exert a swelling pressure on the collagen network that provides cartilage with its load-bearing properties (Figure 1.7). The first evidence for the involvement of hyaluronan in aggregate formation was discovered by Hardingham and Muir 1972. They found that the viscosity of a proteoglycan (aggrecan and link protein) solution dramatically increased with the addition of a small amount of hyaluronan (~1 %). The proteoglycan aggregate, referred to as a ternary complex, was also extensively characterised by Hascall and Heinegaard 1974a, where they estimated that the ratio of aggrecan to link protein was approximately 1:1.

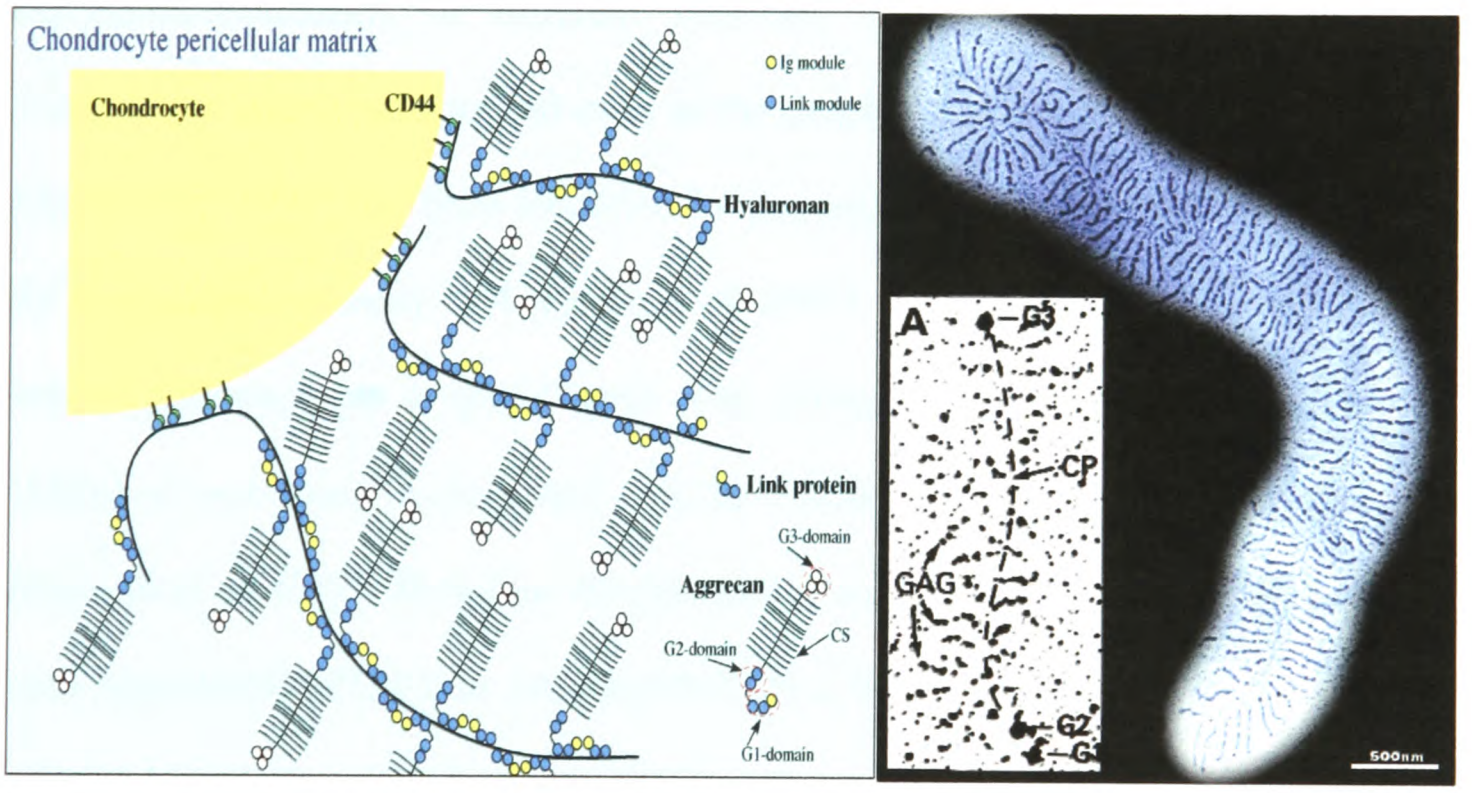

Figure 1.7 A schematic representation of the chondrocyte extracellular matrix (left) in cartilage where alternating arrays of aggrecan and link protein molecules are found bound to a core hyaluronan filament, which can be anchored to the cell surface by CD44. This figure was taken from a glycoforum web article by Day (2001). See http:www.glycoforum.gr.jp/science/hyaluronan/HA16/HA16E.html. Electron micrographs (right) depicting a hyaluronan filament densely packed with up to 200 aggrecan and link protein molecules (Buckwalter and Rosenberg 1982). This figure was taken from a glycoforum web article Hardingham (1998). See http://www.glycoforum.gr.jp/science/hyaluronan/HA05/HA05E.html.

This was later substantiated by the work of Faltz *et al.* 1979. It was also proposed that the role of link protein in these complexes was to stabilise the interaction of aggrecan to HA possibly by bridging the proteoglycan and the hyaluronan chain (Hascall and

Heinegaard 1974a). Link protein effectively locks each proteoglycan to HA to form essentially an un-dissociable complex under physiological conditions (Hardingham 1979; Tang *et al.* 1979) due to the cooperative interactions of cLP with aggrecan and HA. This interaction between cLP and aggrecan is thought to be mediated via the Ig domains, whilst their Link modules bind to hyaluronan (Perin *et al.* 1987; Grover and Roughley 1994; Matsumoto *et al.* 2003). Similar aggregates containing one of four link proteins (HAPLN-1, 2, 3 and 4) and other members of the CSPG family (versican, neurocan or brevican) are likely to contribute to the structural integrity of many other tissues including brain (Yamaguchi 2000) and aorta (Wight and Merrilees 2004). This is interesting in light of the recent work showing the co-expression/localisation of different HAPLNs with CSPGs. For example cLP (HAPLN-1), which is expressed early in the developing brain (Ripellino *et al.* 1989; Rauch *et al.* 1991) has been identified in neurocan preparations from rat brain with the monoclonal antibody 8A4 (Rauch *et al.* 1991); HAPLN-1 has also been shown to interact with neurocan *in vitro* (Rauch *et al.* 2004). In addition, the brain link protein HAPLN-2 was found co-localised with the versican V2 splice variant in the brain (Oohashi *et al.* 2002). Therefore, the presence of ternary aggregates consisting of HA, with neurocan/HAPLN-1 or versican/HAPLN-2 has been proposed by Rauch 2004 (Figure 1.8). Interactions between CSPGs with tenascin-C and –R, which contribute to the structural organisation of brain tissue, are also schematically portrayed (Figure 1.8 and section 1.5). The diversity in the interactions between CSPGs and members of the link protein family is not restricted to brain. For example, in smooth muscle HAPLN-3 and versican have also been observed co-localised (Ogawa *et al.* 2004), suggesting that together with hyaluronan, they may contribute to the structural assembly of this tissue.

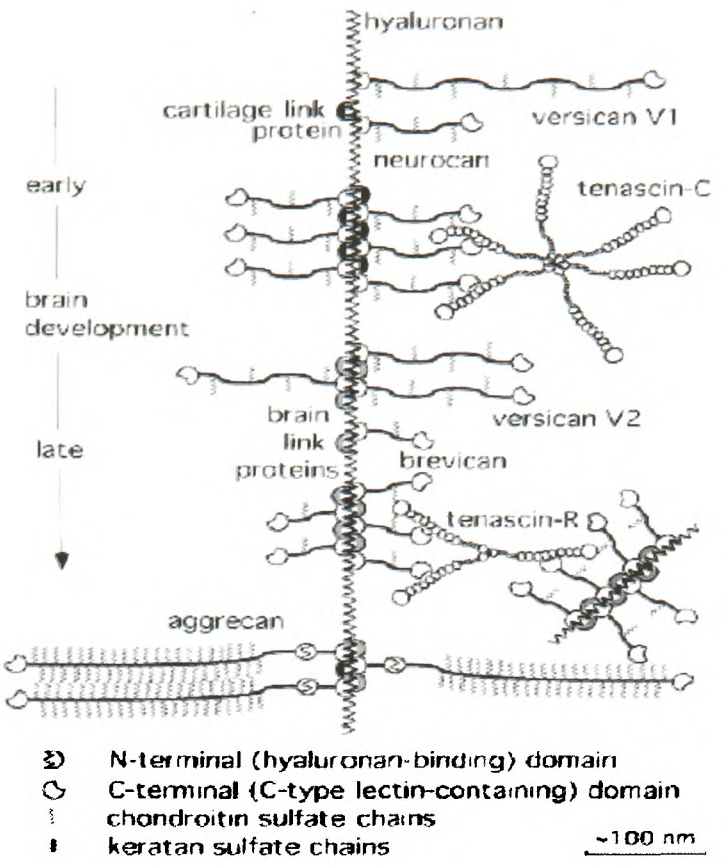

Figure 1.8 Developmental changes in the expression of chondroitin sulphate proteoglycans, tenascins and link proteins (HAPLNs) in brain (Rauch 2004). Characteristic molecules of the early developing brain are versican (V1), neurocan, tenascin-C and cartilage link protein. Characteristic molecules of the mature brain are versican (V2), brevican, aggrecan, tenascin-R and brain link proteins. Due to their polyvalency, tenascins are able to interconnect and cross-link CSPG-hyaluronan aggregates. This figure was modified from Rauch (2004),

Therefore, it appears that a wide range of aggregates containing one of four HAPLNs and CSPGs can be formed and contribute to the structural integrity of many different tissues as exemplified in brain (Figure 1.8). Clearly, a better understanding of the temporal expression between members of the link protein family, CSPGs and HA will be important in understanding differences in tissue specific extracellular matrix assembly.

1.7 Aim and rationale for this project

Interactions between chondroitin sulphate proteoglycans with members of the link protein family and hyaluronan play a crucial role in the formation and stability of the extracellular matrix in various tissues. Therefore, information on the exact molecular basis of these interactions is essential if we are to understand the organisation of healthy tissue and how this changes in disease states. The aim of this project was to purify and functionally characterise human recombinant cartilage link protein (cLP) and the G1-domains of aggrecan (AG1) and versican (VG1) (previously expressed by McVey 2002)). The ultimate goal of this research is to use these recombinant proteins and defined hyaluronan oligosaccharides to reconstruct ternary aggregates for structural determination. This will provide novel information on the structural organisation of cartilage and may facilitate attempts to repair cartilage by tissue engineering.

2 Materials and methods

2.1 Chemicals and materials

HEPES, MES, guanidine-HCl, tricine buffers, rooster comb hyaluronan, and Tween-20 and general lab chemicals were all purchased from Sigma Aldrich. Tris buffer was purchased from Calbiochem. Sodium acetate and acetonitrile were from Riedel-de-Haën and trifluoroacetic acid (TFA) from Pierce. The EDTA, sodium carbonate, glycerol, SDS, Urea, and NaCl were all purchased from VWR International. ProtoFlowGel (30 % (w/v) acrylamide, 0.8 % (w/v) bisacrylamide) was purchased from National Diagnostics, UK. The biotinylated rooster comb hyaluronan used in microtitre plate assays and the defined HA oligosaccharides used in Chapters 3 and 4 were prepared as described in Mahoney *et al.* 2001b and Mahoney *et al.* 2001a, respectively and provided by Dr. David Mahoney (MRC Immunochemistry Unit, University of Oxford). Medical grade hyaluronan was purchased from Genzyme Corporation, MA. Ovine testicular hyaluronidase was purchased from Calbiochem, where one unit (U) is defined as the amount of enzyme that will cause the same turbidity reduction as 1.0 unit of International Standard Preparation. The 2-aminobenzoic acid and sodium cyanoborohydride were purchased from Sigma Aldrich, and ammonium acetate from Fluka Chemicals.

2.2 General Methods

2.2.1 SDS-PAGE

Protein samples were analysed by Tris/Tricine SDS-PAGE essentially as described by Schagger and von Jagow 1987. Using a Bio-Rad Miniprotean II electrophoresis system, 10 % (w/v) acrylamide resolving gels (7 cm x 8 cm) and 4% (w/v) acrylamide

stacking gels (1 cm x 8 cm) were prepared as described in Table 2.1. Samples were typically resuspended into protein sample buffer (PSB) containing β-mercaptoethanol (125 mM Tris-HCl, 6 % v/v SDS, 20 % v/v glycerol, 10 % v/v β-mercaptoethanol, 0.02 % bromophenol blue pH 6.8) boiled for 5 min and run at 80 mA for 1.5 h using anode (0.2 M Tris-HCl, pH 8.9) and cathode (0.1 M Tris, 0.1 M Tricine, 1 % (w/v) SDS, pH 8.25) buffers. Pre-stained SeeBlue® Plus2 protein standards (Invitrogen) or low range SDS-PAGE standards (BioRad) were used as molecular weight markers (Table 2.2). To visualise protein, gels were stained with 1 % (w/v) coomassie brilliant blue R (Sigma Aldrich) in 40 % (v/v) ethanol and 10 % (v/v) acetic acid for 1 h and then de-stained in 7 % (v/v) acetic acid and 10 % (v/v) ethanol overnight.

Table 2.1: Compositions of resolving gel and stacking gel in SDS-PAGE

Gel solutions	10 % Resolving Gel	4 % Stacking Gel
30 % (w/v) Acrylamide Solution	3.33 ml	0.40 ml
Water	1.21 ml	1.95 ml
50 % glycerol	2.12 ml	-
3x Gel buffer[a]	3.33 ml	0.78 ml
10 % ammonium persulphate	100 µl	50 µl
TEMED	10 µl	6 µl

[a] 3 M Tris-HCl, 0.3 % (w/v) SDS pH 8.45

Table 2.2: Molecular weight markers

SeeBlue® Plus2	Apparent MW (kDa)
Phosphorylase B	105
Bovine Serum Albumin	78
Glutamic Dehydrogenase	55
Alcohol Dehydrogenase	45
Carbonic Anhydrase	34
Myoglobin Red	17
Lysozyme	16

Bio-Rad Low Range Standards	Apparent MW (kDa)
Phosphorylase B	97
Bovine Serum Albumin	66
Ovalbumin	45
Carbonic Anhydrase	31
Trypsin Inhibitor	22
Myoglobin Red	14

2.2.2 Preparation of non-reduced/alkylated and reduced/alkylated SDS-PAGE samples

For reduced samples, 1 volume of protein sample and 1 volume of 200 mM Tris, 8 M Urea, 2 % (w/v) SDS, pH 8.8 (Tris-SDS-Urea) containing 6.2 mg/ml dithiothreitol (20 mM final concentration) were incubated for 30 min at 37 °C. Then 0.2 volumes of Tris-SDS-Urea, containing 83 mg/ml iodoacetamide (41 mM final concentration), were added and incubated for 5 min at 37 °C. For non-reduced samples, 1 volume of sample and 1.2 volumes Tris-SDS-Urea, containing 13.8 mg/ml iodoacetamide (41 mM final concentration), were incubated for 30 min at 37 °C. Bromophenol blue (0.1 volumes) was added to the samples as a marking dye. The samples were boiled for 5 minutes and loaded onto a 10 % (w/v) acrylamide gel and run as described in section 2.2.1.

2.2.3 Amino acid analysis and N-terminal sequencing

All amino acid analysis and N-terminal protein sequencing was performed by Mr. Antony C. Willis (MRC Immunochemistry Unit, Department of Biochemistry, University of Oxford). Amino acid analysis (Heinrikson and Meredith 1984), was performed using an Applied Biosystems 420A derivatiser/analyser with an on-line narrow bore high performance liquid chromatography system (Applied Biosystems) to determine protein concentrations. Each protein sample was run in triplicate and the average value for amino acids Ala, Phe and Val, which represent mole percents of 7.1, 5.3 and 7.4 in cLP, 9.0, 2.7, and 8.1 in AG1 and 8.5, 4.5 and 9.4 in VG1, respectively were used to determined the number of moles per sample. From this, the protein concentrations were determined using the theoretical molecular mass of 37162 Da for AG1, 38480 Da for cLP and 36546 Da for VG1. Automated edman degradation was

performed for N-terminal sequencing using an Applied Biosystems 470 gas-phase sequencer with on-line PTH analysis for 15 cycles. Liquid samples were applied to a glass-fiber disc pre-treated with polybrene and run using the standard program provided by the manufacturer.

2.2.4 Determination of hyaluronan concentration

When necessary HA concentrations were calculated by the method of Blumenkrantz and Asboe-Hansen 1973. Briefly, 8 μg of HA oligosaccharides (6-, 8-, 10-, 12-mers) and rooster comb HA were diluted into 200 μl Milli-Q water, in glass pyrex test tubes on ice. To this 1.2 ml of 12.5 mM sodium tetraborate (final concentration) in concentrated sulphuric acid was added and the samples vortexed. Tubes were then heated in a dry block in a fume hood at 100 ˚C for 5 min and then cooled in ice. Biphenyl reagent (20 μl of 0.15 % m-hydroxybiphenol (w/v) in 0.5 % (w/v) NaOH was added to all tubes, vortexed and incubated on ice. Rooster comb standards were diluted from a 10 mg/ml stock in water provided by Dr. Anthony Day prepared on the basis of dry weight. The amount of uronic acid was derived by linear regression analysis from the standard curve.

2.3 Vector construction and expression

The vector construction was carried out by Dr. Gillian McVey as described in McVey 2002. The cLP coding sequence was amplified by PCR from a full-length human cartilage link protein plasmid (nucleotides 1-1062 in (Dudhia and Hardingham 1990), encoding amino acids 1-354); the forward and reverse primers were:

Forward 5'-TATGGTACC**ATG**AGGAGTCTACTTCTTCTGG-3'

Reverse 5'-ATATCTAGATTATCAGTTGTATGCTCTGAAGCAG-3'

The engineered *Kpn*I and *Xba*I restriction sites are underlined and the ATG start codon is in bold typeface. DNAs for the G1 domains from both human aggrecan (nucleotides 61-1119 in (Doege *et al.* 1991), encoding amino acids 1 to 353 of the preprotein) and human versican (nucleotides 267-1316 in (Zimmermann and Ruoslahti 1989), encoding amino acids 1 to 350 of the preprotein) were obtained by carrying out RT-PCR on total RNA extracted from human chondrocytes. The forward and reverse primers used for AG1 were:

Forward 5'-TATGGTACC**ATG**ACCACTTTACTCTGGGTTTTC-3'

Reverse 5'-ATATCTAGATTATTAGTCTTCACCTGTGTAGCAGATG-3'

The forward and reverse primers used for VG1 were:

Forward 5'-TATGGTACC**ATG**TTCATAAATATAAAGAGCATC-3'

Reverse 5'-ATATCTAGATTATTACATTCGACGTTTAAAGCAGTAG-3'

The DNA was amplified for 30 cycles of 94°C, 57°C and 72°C (1 min each) with *Tli* polymerase (Promega). The PCR products were digested with *KpnI/Xba*I and cloned into the corresponding sites in the *Drosophila* Expression System (DES) vector pMT/V5-His B (Invitrogen) downstream of a metallothionein inducible promoter. In the case of the cLP and VG1 constructs, plasmids were identified that had insert sequences identical to those reported previously (Zimmermann and Ruoslahti 1989; Dudhia and Hardingham 1990). However, for AG1 all the clones analysed (8 in total) contained an identical sequence change, relative to the published sequence (Doege *et al.* 1991), corresponding to the inversion of nucleotides CG to GC at positions 865/866. This caused a two amino acid alteration of His^{285} to Gly and Val^{286} to Leu in the aggrecan sequence; it is possible this represents a novel allelic variant of the aggrecan gene. However, in order to generate a plasmid corresponding to the published AG1 sequence (Doege *et al.* 1991), mutagenesis was performed using the

Transformer site directed mutagenesis kit (CLONTECH) as described previously by Nentwich *et al.* 2002. The mutant primer (5'-CCACGGGCCA**C**G**T**CTACCTGGCC-3' with mutated bases in bold), and selection primer (5'-AGAGGGCCCTAGGTTCGAAGG-3'), which changes a unique *Sac*II site in the polylinker of the DES vector to *Avr*II (underlined), were both synthesised with 5'-phosphate groups. A construct with the corrected sequence was selected by DNA sequencing. Stable transfectants were generated for each of the DES expression plasmids encoding cLP, AG1 or VG1 by co-transfection of Schneider 2 (S2) cells with a vector carrying the hygromycin B resistance gene (pCoHygro) as described previously in (Nentwich *et al.* 2002). Stably transfected cell lines were maintained at 25 °C in Schneider's *Drosophila* Medium (Invitrogen) supplemented with 10% (v/v) fetal calf serum (Sigma) and penicillin/streptomycin (Invitrogen) at 50 U/ml and 50 mg/ml, respectively. Hygromycin (Invitrogen) was added at a concentration of 300 μg/ml to ensure selection of recombinant clones.

2.4 Protein purification using reverse phase HPLC

The recombinant proteins were purified from the culture supernatant using a combination of ion exchange chromatography and reverse-phase HPLC, essentially as described previously for full length TSG-6 (Nentwich *et al.* 2002). S2 cells were scaled into T500 cm^2 triple flasks (Nunc) containing 150 ml of serum free medium containing 18 mM L-Glutamine (Invitrogen) and 1 % (w/v) penicillin/streptomycin. Protein expression was induced by adding $CuSO_4$ to a final concentration of 500 μM approximately 3 h after cells had been transferred into serum-free medium. Culture supernatants for the three proteins (cLP, VG1 and AG1) were harvested after 72 h and clarified by centrifugation at 6500 x g for 10 min. To culture supernatants of cLP and

VG1 (900 ml), 20 ml of 50 % (v/v) of SP-Sepharose (Amersham Biosciences) in 300 mM sodium acetate pH 4.0, was added. In contrast the AG1 supernatants (900 ml) received 20 ml of 50 % (v/v) of Q-Sepharose (Amersham Biosciences) in 20 mM MES pH 6.5. The supernatant/sepharose slurry mixtures were incubated for 20 min, followed by washing of the resin with 300 ml of either the acetate (cLP and VG1) or MES (AG1) buffers. The sepharose resins with bound protein were transferred to sintered columns and washed again with ~50 ml of the appropriate buffer. VG1 and cLP were eluted from the SP-sepharose in 150 mM NaCl, 20 mM MES, pH 6.0 or 500 mM NaCl, 20 mM MES, 5 mM EDTA, pH 6.5, respectively. AG1 was recovered from the Q-Sepharose in 150-200 mM NaCl, 20 mM MES, pH 6.0. Fractions containing cLP (combined and diluted 1:20 (v/v) in 300 mM sodium acetate, pH 4.0) were subjected to a second round of ion-exchange batch purification as before. Fractions from the respective protein preparations were pooled and applied to a Phenomenex 250 x 10-mm Jupiter C5 column (300 Å, 5 μm) equilibrated in 17 % (v/v) solvent B (95 % (v/v) acetonitrile, 0.09 % (v/v) trifluoroacetic acid) in solvent A (0.1 % (v/v) trifluoroacetic acid (TFA)) at a flow rate of 3 ml/min. Initial conditions were maintained for 10 min followed by one of two linear acetonitrile gradients. VG1 and AG1 were eluted by gradients of 17-65 %, 65-95 % solvent B (in A) over 10, and 30 min respectively, while cLP was eluted by linear gradients of 17-55 % (10 min), 55-75 % (20 min), 75-95 % (5 min) solvent B (in A). The absorbance was continuously monitored at 220 nm and peaks were collected manually. Proteins were lyophilised and their concentrations were determined by amino acid analysis as described in section 2.2.3. The purified proteins were analysed on 10 % (w/v) Tris-Tricine SDS-PAGE following reduction and alkalyation with dithiothreitol and

iodoacetamide, respectively or alkylation with iodoacetamide alone and stained with coomassie brilliant blue R as described in section 2.2.2.

2.5 MALDI-TOF mass spectrometry of HPLC purified proteins

An Ettan MADLI-TOF/Pro instrument (Amersham Biosciences, UK) was used for all mass spectrometry experiments. Aliquots of VG1 (4 μg), cLP (13.7 μg), and AG1 (2.7 μg) untreated or treated with PNGase F (section 2.7) were dried under vacuum and resuspended in 5 μl 0.1 % (v/v) TFA. The PNGase F enzyme (~1μg) was also run alone as a control. Samples were then mixed 1:1 (v/v) with saturated matrix solution (α-cyano-4-hydroxycinnamic acid in 50 % (v/v) acetonitrile, 0.1 % (v/v) trifluoroacetic acid) and analysed in positive-ion linear mode with a 20 kV potential and the low mass rejection at 1000 m/Z. External calibration was performed using apomyoglobin $[M+H]^+ = 16952.27$ and bovine albumin $[M+H]^+ = 66430.09$.

2.6 Alternative protein purification using FPLC

2.6.1 Purification from conditioned supernatants

Conditioned supernatants (900 ml) for cLP and VG1 were clarified by centrifugation and pH adjusted from ~6.5 to 5.0 with 5 M HCl prior to purification. Using a Waters 650E Advanced Protein Purification System, a XK-26 column packed with 25 ml of SP-Sepharose fast flow resin (Amersham Biosciences) was first equilibrated with 300 mM sodium acetate, pH 4.0 for 5 column volumes (~125 ml) at 30 ml/min. After equilibration the conditioned protein (cLP or VG1) supernatant was pumped over the column followed by equilibration back into 300 mM sodium acetate, pH 4.0 to wash away any non-specific protein binding. The column was then removed from the Waters 650E pump and connected to an ÄKTA FPLC 950 purifier (Amersham

Biosciences). For VG1 the column was equilibrated with buffer C (20 mM MES, pH 6.0) for 1.5 column volumes (~40 ml) and protein eluted with a linear gradient of 0-50 % buffer D (20 mM MES, 1 M NaCl, pH 6.0) over 240 ml at 2 ml/min. The column was then washed with 30 ml of buffer D to remove any residual bound protein and equilibrated back into buffer C. For cLP purification, the column was equilibrated in buffer E (20 mM MES, pH 6.5) for 1.5 column volumes and protein eluted with a linear gradient of 0-50 % buffer F (20 mM MES, 1 M NaCl, pH 6.5) over 250 ml at 5 ml/min followed by washing (buffer F) and equilibration (buffer E) as described above for VG1. The pH for the AG1 culture supernatant was not adjusted prior to purification over a XK-26 column packed with ~25 ml Q-Sepahorse fast flow (Amersham Biosciences). The column was equilibrated with buffer E (20 mM MES, pH 6.5) and the supernatant pumped over the column at 30 ml/min using the Waters 650E Advanced Protein Purification System. The column was then equilibrated back into buffer E. Using an ÄKTA FPLC purifier, a linear gradient from 0-50 % buffer F (20 mM, 1 M NaCl, pH 6.5) was employed over 210 ml total at 5 ml/min to elute AG1 from the column. For all proteins, the absorbance was continuously monitored at 280 nm and 10 ml fractions were collected automatically using a Frac-900 fraction collector (Amersham Biosciences).

2.6.2 Mono-S purification of cLP and VG1

As an alternative to HPLC protein purification, VG1 and cLP were purified from ion-exchange batches using a Mono-S HR 5/5 (Amersham Biosciences) high resolution cation-exchange column (1 ml total volume) with an ÄKTA 950 FPLC purification system. Fractions containing VG1 after SP-Sepharose fast flow purification as described in section 2.6.1 were pooled and diluted 1:1 (v/v) into 300 mM sodium

acetate, pH 4.0 and loaded onto the column equilibrated in buffer E run at 1 ml/min. The protein was eluted using a linear gradient of 0-40 % F over 30 ml and fractions collected (1 ml). The column was then washed for 5 ml in buffer F and equilibrated back into 5 ml buffer E. Fractions were analysed on SDS-PAGE as described previously (section 2.2.1). cLP fractions after SP-sephaorse fast flow purification were pooled and diluted 1:5 (v/v) into 300 mM sodium acetate, pH 4.0 and loaded onto the column equilibrated in buffer E run at 1 ml/min. The protein was eluted from the column using a linear gradient of 0-50 % buffer F over 30 ml total at 1 ml/min. Fractions were collected manually using an ÄKTA 950 peak fraction collector. SDS-PAGE was used to analyse peak fractions (section 2.2.1).

2.6.3 Resource-Q purification of AG1

As an alternative to HPLC purification, AG1 was re-purified using a Resource-Q (Amersham Biosciences, UK) anion-exchange column (1 ml total volume) with an ÄKTA 950 FPLC purification system. Samples containing AG1 after Q-Sepharose fast flow purification as described above were pooled and diluted 1:1 (v/v) into buffer E and loaded onto the column equilibrated in buffer E at 1 ml/min. The protein was eluted using a linear gradient of 0-30 % buffer F over 24 ml and fractions collected manually. The column was then washed for 10 ml in buffer F and equilibrated in 10 ml buffer E. Fractions were analysed on SDS-PAGE as described previously (section 2.2.1).

2.7 Deglycosylation of cLP, AG1 and VG1

Samples of cLP, AG1 and VG1 (0.05 μg/μl in water) were incubated in the absence and presence of 0.1 U/ml N-glycosidase F (PNGase F; Roche Diagnostics) for 1 h at

37 °C. An equal volume of 2x PSB (containing 10 % (v/v) ß-mercaptoethanol) was then added and boiled for 5 min followed by SDS-PAGE.

2.8 Polyclonal antibody production

A polyclonal antibody against human cLP was raised against a 16 amino acid peptide (DEAVQACLNDGAQIAK; residues 273-288 in the pre-protein) located in the second Link module. Molecular modelling of this domain (C.D. Blundell, A. Almond and A.J. Day, in preparation) based on the knowledge of the Link module tertiary structure (Blundell *et al.* 2003) indicates that this region of cLP is likely to be surface

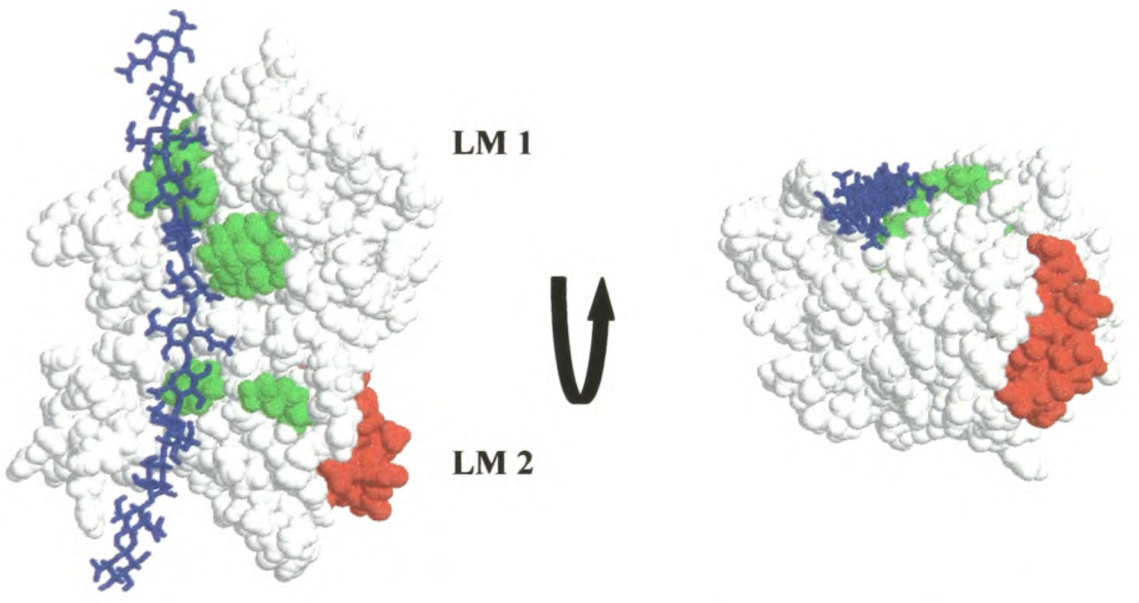

Figure 2.1 This shows a model of the two Link modules (LM1 and LM2) of human cartilage link protein. An antibody was raised against cartilage link protein amino acids 273-288 (shown in red), which resides in the second link module. Amino acids numbered from the full length protein thought to be involved in HA-binding are highlighted in green (R (168), Y (169), R (236), Y (238), Y (217), K (343), Y (316)). Additionally, a HA decasaccharide is shown in the binding site highlighted in blue. The model was provided by Dr. Charles Blundell (Oxford).

exposed (Figure 2.1). The peptide was synthesised and coupled to keyhole limpet hemocyanin via its authentic cysteine residue, which is disulphide bonded to cysteine 279 in the native protein. (Mimotopes, UK). Antibodies were raised against the conjugated peptide in rabbits by Chemicon (San Diego, CA) as described in (Carrette

et al. 2001) and all bleeds were shown to be reactive against the unconjugated peptide by dot blot analysis.

2.9 Western blotting

The western blotting protocol was followed essentially as described in Nentwich *et al.* 2002. Briefly, samples of link protein were run under reducing conditions on 10 % (w/v) Tris-Tricine SDS-PAGE as described in section 2.2.1 and electroblotted onto Hybond-P membranes (Amersham Biosciences). Washes were performed in phosphate buffered saline (PBS), containing 0.1 % (v/v) Tween-20, after each stage of the western blotting procedure, carried out at room temperature. The membrane was blocked overnight in PBS containing 10 % (w/v) milk powder, 0.1 % (v/v) Tween-20, 0.02 % (w/v) bovine serum albumin and washed thoroughly. The blot was then incubated with a 1:1000 dilution of the rabbit anti-human link protein antiserum and following washing, with a 1:5000 dilution of horseradish peroxidase-conjugated donkey anti-rabbit secondary antibody for 1 h each in 10 % (v/v) blocking solution diluted in PBS containing 0.1 % (v/v) Tween-20. After a final wash, antibody binding was visualised by enhanced chemiluminescence system, according to the instructions of the supplier (Amersham Biosciences).

2.10 Protein biotinylation

High molecular weight medical grade polymeric hyaluronan (~1000 kDa) at 5 mg/ml in 162 µl of water was combined with 2.5 ml of ion exchange purified VG1 or AG1 (~10-20 µg/ml) and incubated at room temperature for 1 h to fully saturate active HA-binding sites (i.e., to protect any functionally active important lysine residues in the

HA-binding site from modification). This was followed by 18 µl of ovine testicular hyaluronidase at 7000 U/ml (in 20 mM MES, 5 mM EDTA, pH 6.5) and incubation at 37 °C for 1 h to remove the high molecular weight HA prior to HPLC. To this 2.5 ml of NHS-LC biotin (Pierce) at 0.034 mg/ml in 100 mM $NaHCO_3$, pH 8.5 was added and rotated at room temperature for 1 h. For cLP, HA at 5 mg/ml in 810 µl water was combined with 10 ml of ion-exchanged purified cartilage link protein (~10 µg/ml) and incubated at room temperature for 1 h. This was followed by 90 µl of ovine testicular hyaluronidase at (7000 U/ml) and incubation at 37 °C for 1 h followed by addition of an equal volume of NHS-LC biotin (0.034 mg/ml) in 20 mM MES, 1 mM EDTA, pH 6.5 and rotation for 1 h at room temperature as described above. The biotinlyated-AG1, -VG1 and -cLP (annotated bAG1, bVG1 and bLP) proteins were then purified by HPLC as described in section 2.4 for the unmodified proteins, and quantified using amino acid analysis (section 2.2.3).

2.11 HA-binding assays

2.11.1 Binding of cLP, VG1 and AG1 coated plates to biotinylated-HA

The HA-binding activities of cLP, AG1 and VG1 were first examined using a microtitre plate-based assay essentially as described in Parkar *et al.* 1998; Mahoney *et al.* 2001b with slight modifications. All dilutions, incubations and washes were preformed in Standard Assay Buffer (SAB; 50 mM HEPES, 100 mM NaCl, 0.05 % (v/v) Tween-20 pH 7.4). Lyophilised aliquots of AG1 and VG1 were resuspended into Milli-Q water. In the case of cLP due to its poor solubility in water it was resuspended in 4 M guanidine-HCl, 5 mM sodium acetate, 1 mM EDTA pH 5.8 as described previously for the native pig protein (Bonnet *et al.* 1985; Parkar *et al.* 1998). Maxisorp F96 plates were coated overnight with varying dilutions of AG1 (0-600

ng/well), VG1 (0-71 ng/well) and cLP (0-300 ng/well), in 20 mM Na_2CO_3, pH 9.6 (200 µl/well). The coating solution was removed and the plates washed three times. Non-specific binding sites were blocked by incubation with 1 % (w/v) bovine serum albumin for 90 min at 37 °C followed by three more washes. Plates were then incubated at room temperature for 4 h with 12.5 ng/well biotinylated-HA (prepared from rooster comb; see section 2.1). Plates were washed three times, and 200 µl of a 1:10,000 dilution of ExtraAvidin alkaline phosphatase (Sigma) was added and incubated for 30 min. After three more washes, wells were incubated for 10 min with 200 µl of a 1 mg/ml solution of disodium p-nitrophenyl phosphate (Sigma) in 100 mM Tris-HCl, 100 mM NaCl, 5 mM $MgCl_2$, pH 9.3. The absorbance at 405 nm was determined and corrected by subtracting values from the uncoated control wells. In competition assays, plates were coated with 5 pmol cLP, 4.5 pmol AG1 or 1.2 pmol VG1 in 200 µl (final volume) of Na_2CO_3 pH 9.6 at concentrations shown to be near minimum that give maximal bHA binding (see Figure 3.6). Plates were washed and blocked as described above and then incubated with 12.5 ng/well bHA in the absence or presence of unlabelled polymeric HA or defined HA oligosaccharides (6-, 8-, 10- and 12-mers, produced as described in section 2.1). Plates were developed for 10 min as described above and all absorbance measurements at 405 nm were corrected by subtracting values from the uncoated wells; values are plotted as mean percentages (n=8) ±S.E. of binding in absence of competing HA.

2.11.2 Binding of to biotinylated cLP, VG1 and AG1 to HA coated wells

Maxisorp F96 microtitre plates were coated overnight with 5 µg/well umbilical cord HA (uHA) in 20 mM Na_2CO_3, pH 9.6. All dilutions, incubations and washes were preformed as described above (section 2.11.1) but with SAB containing 0.2 % (v/v)

Tween-20; these conditions have been used previously for plate assays with biotinylated-AG1 prepared from bovine laryngeal cartilage (Parkar *et al.* 1998). Plates were incubated with increasing amounts of bLP (0-7.4 pmol/well), bVG1 (0-10.6 pmol/well) or bAG1 (0-42 pmol/well) diluted in SAB for 4 h at room temperature. Competition experiments were performed at concentrations close to the minimum that give maximal uHA binding for bLP (2.7 pmol/well), bVG1 (2.9 pmol/well), or bAG1 (11.7 pmol/well) in the absence or presence of increasing amounts of rooster comb HA (0-2500 ng/well). Plates were developed for 10-20 min and all absorbance measurements at 405 nm were corrected by subtracting values from the uncoated wells.

2.11.3 Protein-protein interactions using a microtitre plate assay

To study bLP binding to AG1 and VG1, Maxisorp F96 microtitre plates were coated overnight (0-1000 ng/well) with AG1 or VG1 as described in section 2.11.1. All dilutions, incubations and washes were performed as in section 2.11.2. bLP was initially resuspended in 50 µl of 4 M guanidine-HCl, 50 mM sodium acetate, 1 mM EDTA, pH 5.8, then diluted 379-fold into SAB to a final concentration of 33 pmol/ml. Plates were incubated with 200 µl/well bLP (6.6 pmol/well) for 4 h at room temperature and bound protein detected as described in 2.11.1. To assay bLP binding in high salt or at lower pH the experimental protocol described above were replicated with the SAB changed to 50 mM HEPES, 500 mM NaCl, 0.2 % Tween-20, pH 7.4 or 50 mM sodium acetate, 100 mM NaCl, 0.2 % Tween-20, pH 5.8, respectively. To study bAG1 and bVG1 binding to cLP, plates were coated overnight (0-3650 ng/well) with cLP as described in 2.11.1, and washed/blocked as described above. Plates were then incubated with 200 µl/well bVG1 (3.3 pmol/well) or bAG1 (13.3 pmol/well) for

4 h at room temperature and protein detected as described in 2.11.1. In all instances plates were developed for 10-20 min and all absorbance measurements at 405 nm were corrected by subtracting values from the control wells that were not coated with protein overnight.

2.12 Complex formation using analytical gel filtration

Gel filtration experiments were conducted on a Phenomenex 300 x 7.8 mm Biosep-SEC-S2000 column run in 10 mM HEPES, 500 mM NaCl, pH 7.0 at 0.5 ml/min at a constant temperature of 25 °C and data analysed using Chromeleon software (Dionex). The column was calibrated with globular protein standards (Sigma Molecular Weight Marker Kit; i.e., Cytochrome C (12,400 Da), carbonic anhydrase (29,000 Da), bovine serum albumin (66,000 Da), alcohol dehydrogenase (150,000 Da), and ß-amylase (200,000 Da)), which were loaded individually (5 µg) onto the column and monitored at 280 nm. The log of the molecular weight for each calibrant was plotted against its distribution coefficient K_{av}, which were derived using the formula $K_{av}= (V_e-V_o)/ (V_T-V_o)$ where V_e is the elution volume (peak apex) of the sample; V_T is the total liquid volume of the column, calculated on the basis of its radius and length, while V_o is the void volume of the column, which was determined from the elution volume of blue dextran (5.65 ml). The formation of HA-protein complexes was based on the method described previously for the native proteins (Bonnet *et al.* 1985). To study the individual protein interactions with HA, lyophilised cLP, AG1 and VG1 were resuspended to a final concentration of 0.3 µg/µl, 0.15 µg/µl and 0.25 µg/µl respectively in 20 µl 4 M guanidine-HCl, 50 mM sodium acetate, 1 mM EDTA, pH 5.8. To these, 1-3 µl of HA oligosaccharides (i.e., 10-, 14-, 20-, 24-, 28-, 32- or 40-mers prepared from umbilical cord HA as described

in Mahoney *et al.* 2001a at 0.5-1 mg/ml in water were added to give ≥2-fold molar excess HA over total protein; equivalent volumes of water were added to samples without HA. Prior to gel filtration samples were diluted ~10-fold with 50 mM sodium acetate, pH 5.8 in order to convert from dissociative to associative conditions (see Bonnet *et al.* 1985); i.e., to give a final concentration of ~0.4 M guanidine-HCl. This dilution was done in 5 steps, the first being the addition of 20 µl buffer, followed by 4 identical additions of 40 µl, where there was a 10 min incubation at room temperature between each step. The samples were loaded onto the gel filtration column and the eluent monitored at 280 nm. To study protein-protein interactions and ternary complex formation, cLP was combined with AG1 or VG1 under dissociative conditions with the individual proteins at the same final concentrations as described above, prior to addition of HA/water and stepwise dilution into associative conditions.

2.13 Protein-protein cross-linking experiments

For protein cross-linking experiments, samples (100 µl) in associative buffer conditions (prepared as described in section 2.12) were treated with 1.25 µl of 10 mM BS^3; Bis(sulfosuccinimidyl)suberate (Pierce) cross-linking reagent for 30 min at room temperature. The reaction was quenched by adding 2 µl of 1 M Tris-HCl, pH 7.5. Protein was recovered using 10 µl strataclean resin (Stratagene) and then loaded directly onto SDS-PAGE gels after boiling the resin in 25 µl PSB. The gel bands of interest were excised with a scalpel, split into 3 ~1x1 mm squares and destained by washing three times with 50 % (v/v) acetonitrile in 50 mM ammonium bicarbonate, for 20 min. The gels were dehydrated by addition of 70 % (v/v) acetonitrile in water for 20 min and then dried under vacuum. Gel slices were rehydrated by adding 40 µl of 20 mM ammonium bicarbonate with 20 ng/µl of sequencing grade trypsin

(Promega), and incubated at 37 °C for 12-16 h. Peptides were extracted from the gel slices by adding 50 µl of solution containing 50 % (v/v) acetonitrile in 0.1 % (v/v) trifluoroacetic acid and incubating at room temperature for 20 min. This was repeated two further times and supernatants pooled and evaporated to dryness under vacuum. The peptides were resuspended in 0.1 % (v/v) trifluoroacetic acid and added 1:1 to saturated matrix solution (α-cyano-4-hydroxycinnamic acid in 50 % (v/v) acetonitrile, 0.1 % (v/v) trifluoroacetic acid) and analysed in positive-ion reflectron mode with a 20 kV potential. Internal calibration was carried out using the autolytic peaks of trypsin ($[M+H]^+ = 842.5$ and $[M+H]^+ = 2211.1$).

2.14 Multi-angle laser light scattering (MALLS)

MALLS experiments were done in collaboration with Dr. Andrew Almond, (University of Oxford) and conducted in the laboratory of Professor Timothy Hardingham (University of Manchester). A 300 x 10-mm Superdex-200 (23.6 ml) gel filtration column (Amersham Biosciences, UK) was equilibrated in 10 mM HEPES, 500 mM NaCl, pH 7.0 at 0.5 ml/min at a constant temperature of 25 °C and calibrated using the globular protein standards and blue dextran as described in section 2.12 for the Biosep-SEC-S2000 column; the void volume was determined to be 7.56 ml. The resulting calibration curve (Figure 4.2) shows that the two gel filtration columns (Biosep-SEC-S2000 and Superdex-200) used have similar separation properties over the molecular weight range used here. Samples of VG1 alone (20 µg) or a mixture of VG1 (50 µg) and cLP (40 µg) in the presence of a 2-fold molar excess of HA32 over protein were prepared in associative conditions (200 µl final volume) as described (section 2.12) and loaded onto the Superdex-200 column (Amersham Biosciences, UK); a sample of HA32 (90 µg) in 200 µl 50 mM sodium acetate, 1 mM EDTA, pH

5.8 was run individually as a control. During the elution period measurements of the UV absorbance at 280 nm, the refractive index and laser light scattering were made every 0.5 s. Laser light scattering (30 mW GaAs laser, 690 nm) was recorded at 18 fixed angles using a DAWN EOS system (Wyatt Technology Corp.). Refractive index measurements (at 690 nm) were made using an Optilab rEX refractometer (Wyatt Technology Corp.). The concentration (c) was calculated from refractive index (n) using a dn/dc value of 0.19 ml/g. In processing the data, the 9 angles with the greatest signal to noise ratio were used (69°–163°). Analysis of the data followed the standard Debye theory and extrapolation techniques, as described in (Chu 1991), and was performed using ASTRA version 4 software (Wyatt Technology Corp.).

Production of Fluorescent HA oligosaccharides

2.15 Oligosaccharide production

Hyaluronan was dissolved at a concentration of 1 mg/ml in digest buffer (100 mM sodium acetate, 150 mM NaCl, adjusted to pH 5.2 with glacial acetic acid) and pre-incubated for 10 min at 37 °C. To this, ovine testicular hyaluronidase (1 U/µl in reaction buffer) was added to give a final concentration of 1, 5 or 10 U enzyme per mg of HA and the mixture was incubated for 1 h at 37 °C. The reaction was terminated by boiling for 10 min and centrifuged to remove denatured enzyme.

2.16 Fluorescent labelling of HA oligosaccharides

2.16.1 Labelling of HA oligosaccharides with 2-aminacridone (AMAC)

Oligosaccharides individually (4-, 6-, 8- or 10-mers) or from a testicular hyaluronidase digest mixture (provided by Dr. Andrew Almond, Oxford Biochemistry Department) were prepared as described by Blundell *et al.* 2004a and derivatised with

2-aminoacridone (AMAC) on the reducing end sugar essentially as described by Calabro *et al.* 2000a. Briefly, 40 µl 12.5 mM AMAC dissolved in 15 % (v/v) acetic acid in DMSO was added to lyophilised oligosaccharide samples and incubated for 15 min at room temperature. To this 40 µl of 1.25 mM sodium cyanoborohydride in Milli-Q water was added and the resultant mixture incubated overnight at 37 °C to complete the reaction.

2.16.2 Labelling of HA oligosaccharides with 2-aminobenzoic acid (2AA)

Oligosaccharides in the resultant digest mixture (see section 2.15) were derivatised with 2AA by reductive amination at the reducing end sugar essentially as described by Neville *et al.* 2004. Briefly a 5 ml stock solution of 2-aminobenzoic acid (2AA) (150 mg) and sodium cyanoborohydride (225 mg) dissolved in 2 % (v/v) acetic acid in methanol was prepared and added to the HA oligosaccharides at a 3:1 (v/v) ratio in microcentifuge tubes. Samples were heated at 80 °C for 45 min to complete the reaction. Excess 2AA was removed by a Sephadex G-10 desalting column (Amersham Biosciences, UK) on an ÄKTA 900 FPLC system (Amersham Biosciences, UK) in 50 mM ammonium acetate, and then the oligosaccharides lyophilised repeatedly to remove residual acetate buffer. Purified HA 4-, 6-, 8- and 10-mers, prepared as described in Blundell, *et al.* 2004a were also labelled individually.

2.17 Anion-exchange oligosaccharide purification

Lyophilised unlabelled or 2AA-labelled HA digests were resuspended in water and purified on a Mono-Q 5/50 GL anion-exchange column (Amersham Biosciences, UK) using an ÄKTA 950 FPLC system (Amersham Biosciences, UK) with UNICORN

software. The column was equilibrated in Milli-Q water (buffer A) at a flow rate of 2 ml/min. Labelled HA oligosaccharides (2 ml at ~1 mg/ml in water) were loaded onto the column and the initial conditions (100 % buffer A) were maintained for 5 min. Oligosaccharides were then eluted with buffer B (500 mM NaCl) using a logarithmic gradient described by the equation % B = 8.4 x $\log_e(1.0 + 0.45t)$, where t represents time in minutes. The fractions were monitored at both 215 nm and 330 nm, respectively, the latter being a wavelength specific for 2AA (Ito, *et al.* 1998). A 2AA-labelled 10-mer (produced and characterised as described in Blundell, *et al.* 2004a) was used to calibrate peak elution positions. Fractions of each length oligosaccharide were pooled and desalted on a G-10 Sephadex column, equilibrated in 50 mM ammonium acetate lyophilised and resuspended in Milli-Q water and analysed by FACE analysis as described below in section 2.18.2. An additional anion exchange chromatography step was performed to ensure homogeneity prior to EMSA. Each peak fraction was then collected, lyophilised and desalted as described above. Oligosaccharide fractions were finally lyophilised repeatedly from Milli-Q water to remove any residual ammonium acetate.

2.18 Fluorophore-assisted carbohydrate electrophoresis (FACE)

2.18.1 Electrophoresis of AMAC-labelled HA oligosaccharides

Native polyacrylamide (27 % (w/v) resolving and 4 % (w/v) stacking gels) were made up in the Tris-Borate-EDTA (TBE) running buffer (90 mM Tris, 90 mM boric acid, 2.5 mM EDTA, pH 8.3); gels were polymerized with 1 % ammonium persulphate and 0.1 % TEMED. AMAC-labelled oligosaccharide samples were diluted 1:1 (v/v) with 20 % (v/v) glycerol and run 1.5 hr at 300 V at 4 °C. Gels were analysed with a UV light source using a green emission filter (~600 nm).

2.18.2 Electrophoresis of 2AA-labelled HA oligosaccharides

Purified 2AA-labelled oligosaccharides were diluted from water with 50 % (v/v) glycerol to give a final concentration of 16 % (v/v) glycerol. Native polyacrylamide, 27 % (w/v), gels (without stacking gel) were made up in the running buffer: 192 mM glycine, 25 mM Tris pH 8.4; polymerized as described above. Approximately equimolar amounts of each labelled oligosaccharide and the unfractionated digest were loaded and run at 300 V, 4 °C for 3 h using a Protean gel apparatus (BioRad, UK) employing a constant cooled water pump system.

2.19 MALDI-TOF MS of 2AA-labelled HA oligosaccharides

Tetra to decasaccharides of 2AA-labelled oligosaccharides (4-10-mers) were analysed in negative-ion reflectron mode with a 20 kV potential. Briefly, a mixture in water of 2AA-labelled HA4, HA6, and HA8 all at 0.625 mg/ml with 2AA-HA10 at 0.125 mg/ml were diluted 1:100 (v/v) with water and mixed 1:1 (v/v) with 2.5 mg/ml 2,5-dihydroxybenzoic acid (DHB) as described previously by Blundell *et al.* 2004a. Solutions for external calibration were composed of a mixture of adrenocorticotrophic hormone fragment 18-39 (ACTH; $[M-H]^-$ = 2463.20 Da) and angiotensin II ($[M-H]^-$ = 1044.54 Da) in 50 % (v/v) acetonitrile, 0.5 % (v/v) TFA. A ladder of longer oligosaccharides (12-36-mers) was analysed in negative-ion linear mode with a 20 kV potential and a low mass rejection of 2000 m/Z. Oligosaccharide samples in water were mixed 1:1 (v/v) with saturated 3,5-dimethoxy-4-hydroxycinnamic acid (Sinapinic acid) in 50 % (v/v) ACN, 0.5 % (v/v) TFA. Solutions for external calibration were composed of a mixture of ACTH (see above) and oxidized insulin ($[M-H]^-$ = 3492.65). Samples of labelled HA 38- and 40-mers were analysed individually (data not shown). To assess the sensitivity of MALDI-TOF mass

spectrometry for 2AA labelled oligosaccharides, a mixture of unlabelled HA10 and labelled HA10 at equivalent concentrations (0.125 μg/μl) were mixed 1:1 (v/v) with 2,5-DHB (2.5 mg/ml) matrix and analysed (62.5 ng/spot) in negative-ion reflectron mode.

2.20 NMR spectroscopy of 2AA-labelled HA oligosaccharides

All NMR was performed by Dr. Charles Blundell, Biochemistry Department, University of Oxford. Oligosaccharide samples for NMR (2AA-labelled 4-, 6-, 8- and 10-mers) were prepared from lyophilised material reconstituted in 10 % (v/v) D_2O and adjusted to pH 6.0 with 0.1 M HCl and NaOH. A 1 mM sample of 2AA was also prepared. Homonuclear 1D spectra were recorded on these samples at 750 MHz, 25 °C with an acquisition time of 113.66 ms over 1024 complex points. All spectra were referenced externally to the water resonance at 4.765 ppm downfield of 2,2-dimethyl-2-silapentane-5-sulphonate (DSS). Concentrations of oligosaccharides were measured by comparing the integrated peak intensities from the aromatic ring protons at 7.7 ppm and 7.3 ppm in the 1D spectra from each sample with that of a 1 mM 2AA control sample.

2.21 Electrophoretic gel mobility assay (EMSA)

2.21.1 Preliminary EMSA with cLP, AG1 and VG1

Samples were prepared by adding 18 μl of HA oligosaccharides (approximately equimolar amounts) in 50 mM sodium acetate, 1 mM EDTA, pH 5.8 to 2 μl of VG1, AG1 or cLP (2.5 μg/μl) in 4 M guanidine·HCl, 50 mM sodium acetate, 1 mM EDTA, pH 5.8, and incubated at room temperature for 1 h at this concentration of guanidine (400 mM) known to be associative (Bonnet *et al.* 1985). Prior to loading, 8 μl of 50 %

(v/v) was added and samples run on a native 10 % (w/v) polyacrylamide gels prepared in 640 mM glycine, 83 mM Tris pH 8.4 in 10 % glycerol with a stacking gel (4.5 % (w/v) acrylamide, 480 nM glycine, 62.5 nM Tris, pH 8.4) at 50 V and 4 °C for 60 min. Gels were visualised as described in section 2.22.

2.21.2 EMSA with VG1 and longer length 2AA-labelled HA oligosaccharides

Samples were prepared by adding 18 µl of HA oligosaccharides (3.4 µM) in 50 mM sodium acetate, 1 mM EDTA, pH 5.8 to 2 µl of VG1 (0-6 mg/ml) in 4 M guanidine·HCl, 50 mM sodium acetate, 1 mM EDTA, pH 5.8, and incubated at room temperature for 1 h. Prior to loading, 8 µl of 50 % (v/v) glycerol was added to give final concentration of 2.2 µM for all HA oligosaccharides. Native 4.5 % (w/v) polyacrylamide gels (7 cm x 8 cm) were prepared without a stacking gel, containing 10 % glycerol (v/v) and 1 M Tris (pH 8.45). Samples were loaded into separate lanes and electrophoresed (Miniprotean II, BioRad, UK) for 40 min at 40 V and 4 °C, using a 100 mM Tris, 100 mM Tricine pH 8.6 running buffer. Visualisation of the gel was performed as described below in section 2.22. Gels were stained with 1 % (w/v) coomassie brilliant blue R (Sigma Aldrich), 40 % (v/v) ethanol and 10 % (v/v) acetic acid to detect protein after UV visualisation.

2.22 Gel imaging and densitometry for 2AA-labelled oligosaccharides

Gels were visualised using a UV transilluminator (Uvi Tec, UK) using a digital camera fitted with a 430 nm band pass blue filter (Andover Corp., NH) over the camera. A UG1 glass plate (H.V. Skan Ltd, UK) was placed between the UV lamp source and the gel to block visible light, essentially as described before (Turnbull, *et al.* 1999; Drummond, *et al.* 2001). The aperture was adjusted to avoid saturating the

camera CCD and multiple images were recorded with different exposure times. Densitometry analysis was performed using the Scion Image software (Scion Corp., MD). The concentration of 2AA-labelled HA 20-, 30- and 40-mer stocks were determined by densitometry after FACE analysis (2.18.2). Briefly, equivalent volumes (1 µl) of HA10-2AA control (0.125 µg/µl) and labelled oligosaccharide stocks (20,- 30- and 40-mers) of unknown concentration were run on a 27 % (w/v) acrylamide gel (Miniprotean II, BioRad, UK) for 2 h at 200 V with the same gel and running buffer conditions as those described in 2.18.2. Total fluorescence (T_f) was calculated using the formula T_f = (band area)x(band intensity-background intensity). The T_f ratio of 2AA-labelled HA10 compared to labelled 20-, 30-, or 40-mers was then used to quantify and normalise stock solutions.

2.23 Fluorimetry

For fluorimetry experiments, samples of 2AA-labelled HA10 (HA10-2AA), alone or mixed with equimolar amounts of VG1 (VG1 + HA10-2AA) were diluted into associative buffer conditions as described for the EMSA (2.21.2). The samples were incubated at room temperature for 1 h and emission scans (200-550 nm) recorded using a Jasco FP-777 Spectrofluorometer (excitation 330 nm). Fluorescent intensity between 375-475 nm, spanning the maximum emission range for 2AA (Ito, *et al.* 1998), was calculated by subtracting recorded control values (buffer or VG1 alone) from HA10·2AA and VG1 + HA10·2AA values, respectively. Samples of 2AA (5 µM) were also run as controls.

2.24 X-Ray crystallography

Attempts were made to crystallise VG1 using the Tecan Genesis 150 crystallisation robot (Laboratory of Molecular Biophysics, Oxford Biochemistry Department). Briefly, VG1 (943 μg) purified by reverse-phase HPLC was resuspended (10 mg/ml) with water. Two commercially available crystal screens from Molecular Dynamics (wizard screen 1 and 2) and two from Hampton Research (PEG-ion screen and crystal screen lite) were used although no crystals growth was observed.

3 Protein purification and characterisation

3.1 Introduction

All of the proteins investigated here comprise an identical organisation of domains with an N-terminal Immunoglobulin (Ig) fold followed by two Link modules. Previously a Link module pair from human cartilage link protein was expressed in *E. coli* and following purification and refolding the protein was found to exhibit some HA binding using a microtitre plate assay (McVey 2002). However, equivalent aggrecan and versican constructs were inactive, which is consistent with the finding that the Ig domain, N-terminal to the Link module pair, stabilises the binding to hyaluronan in these proteins (Watanabe *et al.* 1997; Matsumoto *et al.* 2003). In addition, it was proposed that *N*-linked glycosylation may also be necessary for correct folding and functional activity of the Link module pairs (Watanabe *et al.* 1997). For the above reasons, the Ig-Link-Link construct for cartilage link protein (i.e. the full length protein) and the G1-domain of aggrecan and versican were expressed in *Drosophila* S2 cells (McVey 2002). This expression system was also selected since it had been utilised with success for the expression of full-length TSG-6 (Nentwich *et al.* 2002).

3.2 Preliminary protein expression and protein sequencing

Small scale protein expression studies indicated that the heterologous gene products for cartilage link protein (cLP), G1-aggrecan (AG1) and G1-versican (VG1) were being secreted into the culture medium and amino acid sequencing of blotted material indicated that the proteins had N-termini corresponding to those of the native proteins (McVey 2002). VG1 ran as a doublet after SDS-PAGE analysis where both species

were found by amino acid sequencing to have the expected N-terminal sequence beginning at amino acid 21 (LHKVKVGKSP) of the versican pre-protein (Zimmermann and Ruoslahti 1989). N-terminal sequencing of this preparation revealed that the AG1 preparation contained two species (SDHDNSLSV and AVTVETSDHD), in addition to the expected VETSDHDNSL sequence for native aggrecan (Doege *et al.* 1991); the relative initial yield of each sequence was 51, 33 and 16 percent, respectively. cLP had the expected N-terminal sequence (DHLSDXYTLD) where no amino acid was detected at position 6 (an asparagine), indicating that this *N*-linked glycosylation site is fully occupied (Dudhia and Hardingham 1990). Preliminary studies of the semi-pure material also showed that these proteins were functionally active with regard to HA binding (McVey 2002). This chapter describes the large scale isolation/purification and characterisation of these proteins using a range of analytical methods.

3.3 Isolation and HPLC purification of cLP, AG1 and VG1

Proteins were eluted from the ion-exchange resin with the elution buffers described in section 2.4 and 10 ml fractions were collected. Analysis of consecutive protein fractions by SDS-PAGE after ion-exchange chromatography (Figure 3.1) indicated that each of the three preparations contained protein products of the expected molecular weight (~40 kDa); cLP is also shown both before and after its second ion-exchange purification step (Figure 3.1c and 3.1d), where the latter step enhanced purity of the protein fractions. However, all preparations still contained significant amounts of protein contaminant and an additional purification step was deemed necessary. Due to the success of purifying recombinant full length TSG-6 using reverse-phase HPLC (Nentwich *et al.* 2002) the same approach was investigated for

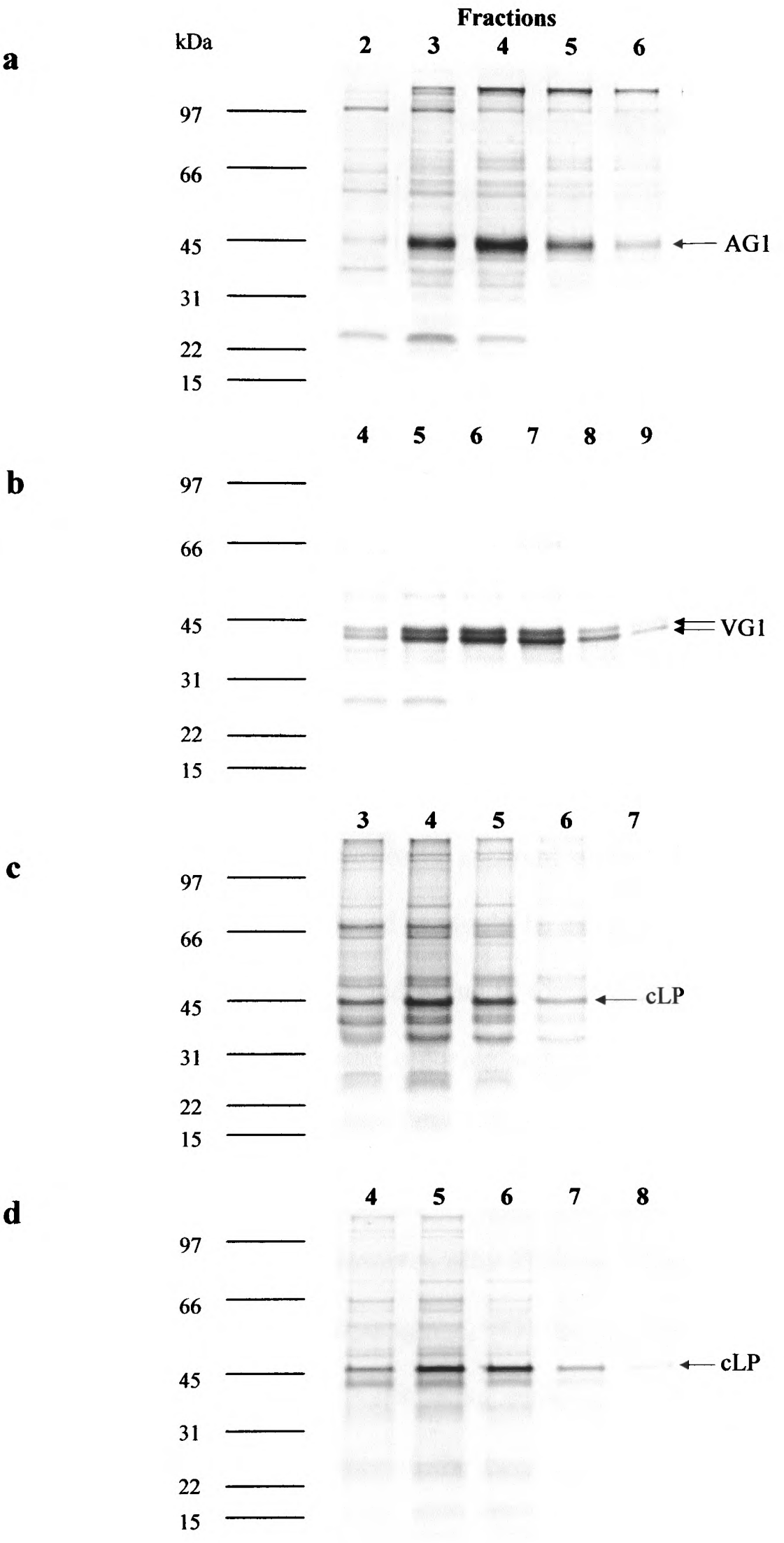

Figure 3.1 SDS-PAGE analysis of AG1, and VG1 and cLP purified by ion-exchange chromatography. Consecutive salt fractions from each recombinant human protein preparation were analysed. **a)** AG1 was eluted from Q-Sepharose in 150-200 mM NaCl, 20 mM MES, pH 6.0. **b)** VG1 was eluted as a doublet from the SP-Sepharose in 150 mM NaCl, 20 mM MES, pH 6.0 fractions. cLP was eluted from SP-sepharose in 500 mM NaCl, 20 mM MES, 5 mM EDTA, pH 6.5 in both a primary **(c)** and **(d)** secondary purification step.

cLP, AG1 and VG1. Figure 3.2 shows HPLC chromatograms for the recombinant proteins. Peak fractions from HPLC were analysed by SDS-PAGE, which indicated that the recombinant proteins elute from the column after approximately 25 min at 65 % buffer B (in buffer A) (see Figure 3.2, arrows). The recovery for each protein preparation on HPLC was approximately 50 %.

3.4 Characterisation of HPLC purified proteins

Fractions containing target protein after HPLC were combined, freeze dried and analysed by SDS-PAGE under reducing and non-reducing conditions (Figure 3.3a). The proteins (VG1, AG1 and cLP) were essentially purified to homogeneity when compared to the pre-purified ion-exchange fractions (Figure 3.1). In all cases the proteins (VG1, AG1 and cLP) have lower apparent molecular weights under non-reducing conditions than when reduced as would be expected for protein containing disulfide bonds. The VG1 doublet (Band A and B, Figure 3.3a) runs with an apparent molecular weight of 38-40 kDa under reducing and 36-38 kDa under non-reducing conditions which, is in good agreement the masses obtained in MALDI-TOF mass spectrometry (Figure 3.4a); two species (1 and 2) are observed with average masses at 37.7 and 38.5 kDa, respectively. However, after PNGase F treatment, which cleaves the amide bond linking glycans to asparagines, VG1 runs primarily as a single species on SDS-PAGE (band G; Figure 3.3b) under reducing conditions with a lower apparent molecular weight than either of the two species in the untreated sample. Thus the A/B doublet is likely to represent different glycoforms of the protein. MALDI-TOF mass spectrometry analysis of the PNGase F treated VG1 preparation also reveals a single species at 37.7 kDa (arrow 3, Figure 3.4a), where no major

a

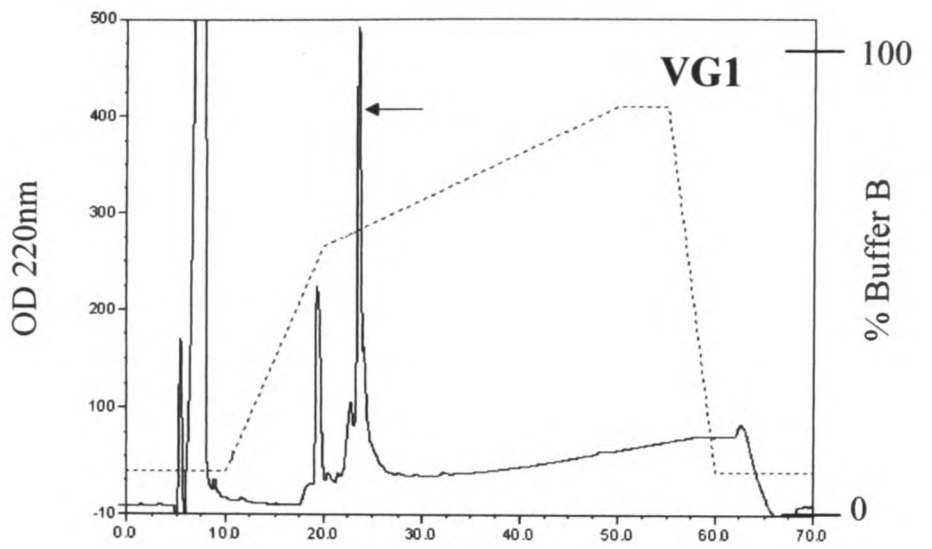

b

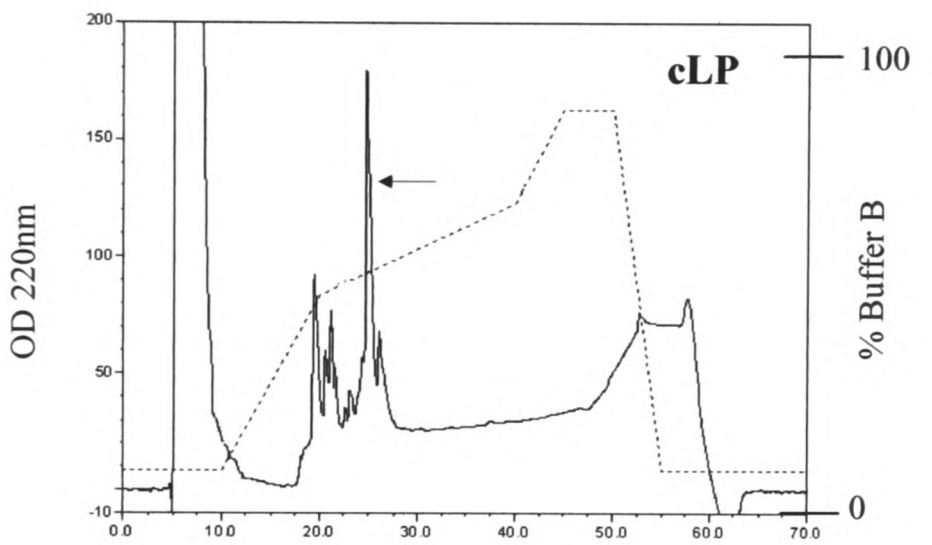

c

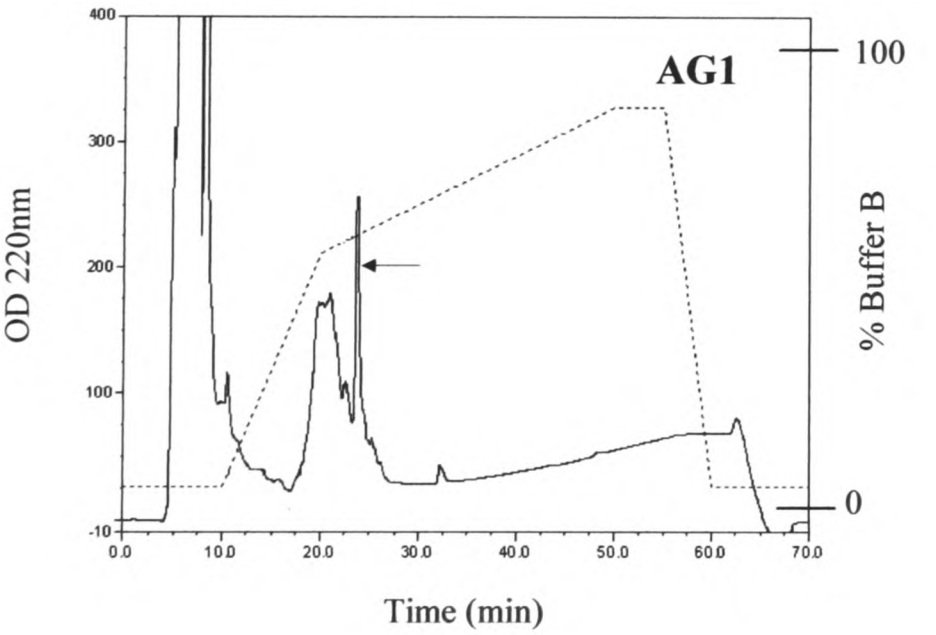

Figure 3.2 HPLC Chromatograms of **a)** VG1 **b)** cLP and **c)** AG1. Arrows denote peaks corresponding to the recombinant proteins determined by SDS-PAGE analysis. The dotted line represents the gradient of % buffer B.

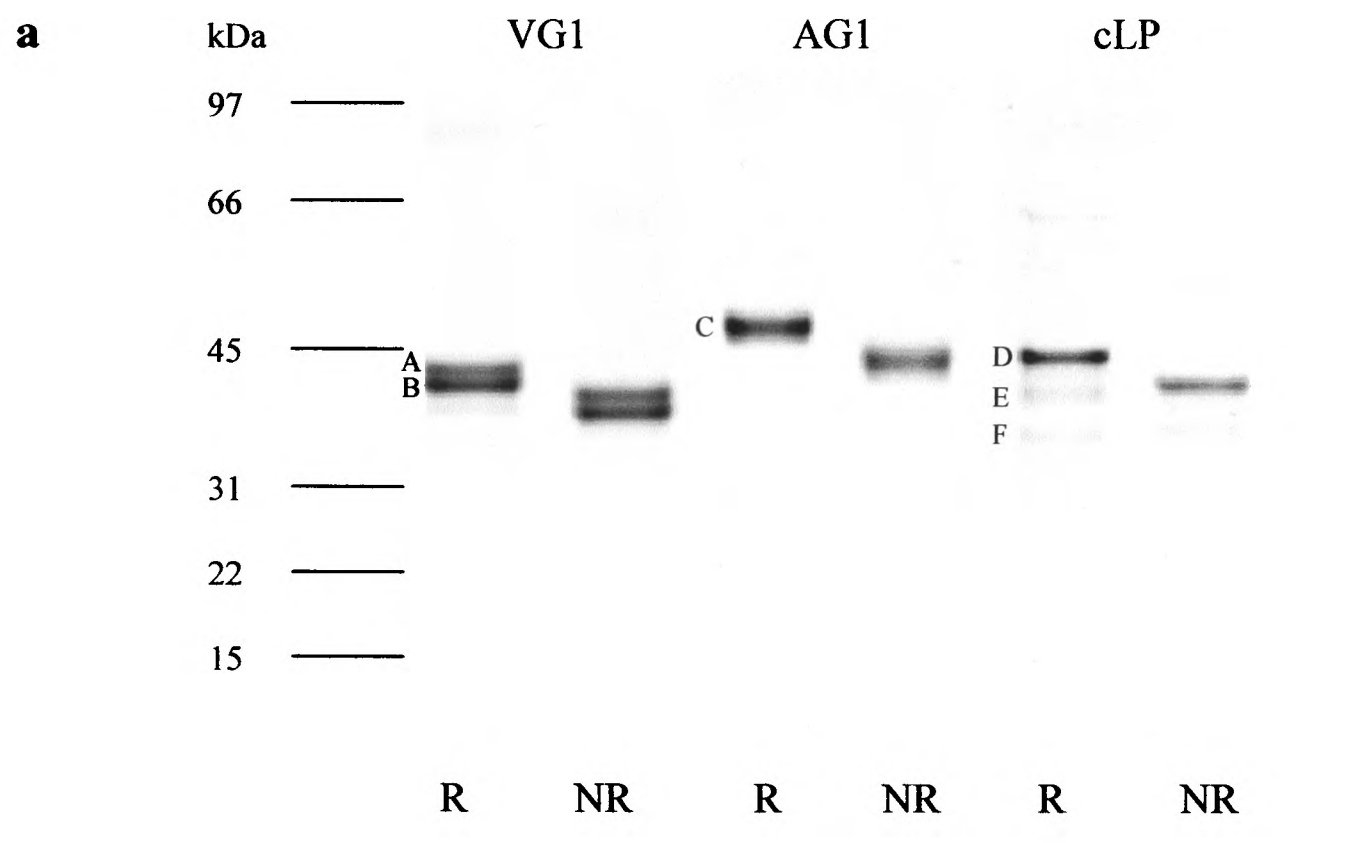

Figure 3.3 SDS-PAGE of purified recombinant and PNGase F-treated proteins. **a**) VG1, AG1 and cLP were analysed under reducing (R: reduction/alkylation) and non-reducing (NR: alkylation) conditions. VG1 runs as a doublet (A and B), AG1 as a diffuse band (C) and cLP as multiple species (D, E, and F). **b**) Analysis of VG1, AG1 and cLP with (+) and without (-) PNGase F (*N*-glycosidase F) treatment. After treatment the VG1 doublet (A and B) runs as a single band (G) and AG1 (C) runs as a tighter band (H). The expected (D) and truncated (E) link protein species are seen in the untreated sample. The black arrows (I and J) represent the two link protein species seen after treatment. The lower MW band (*) seen in all treated samples is the PNGase F enzyme.

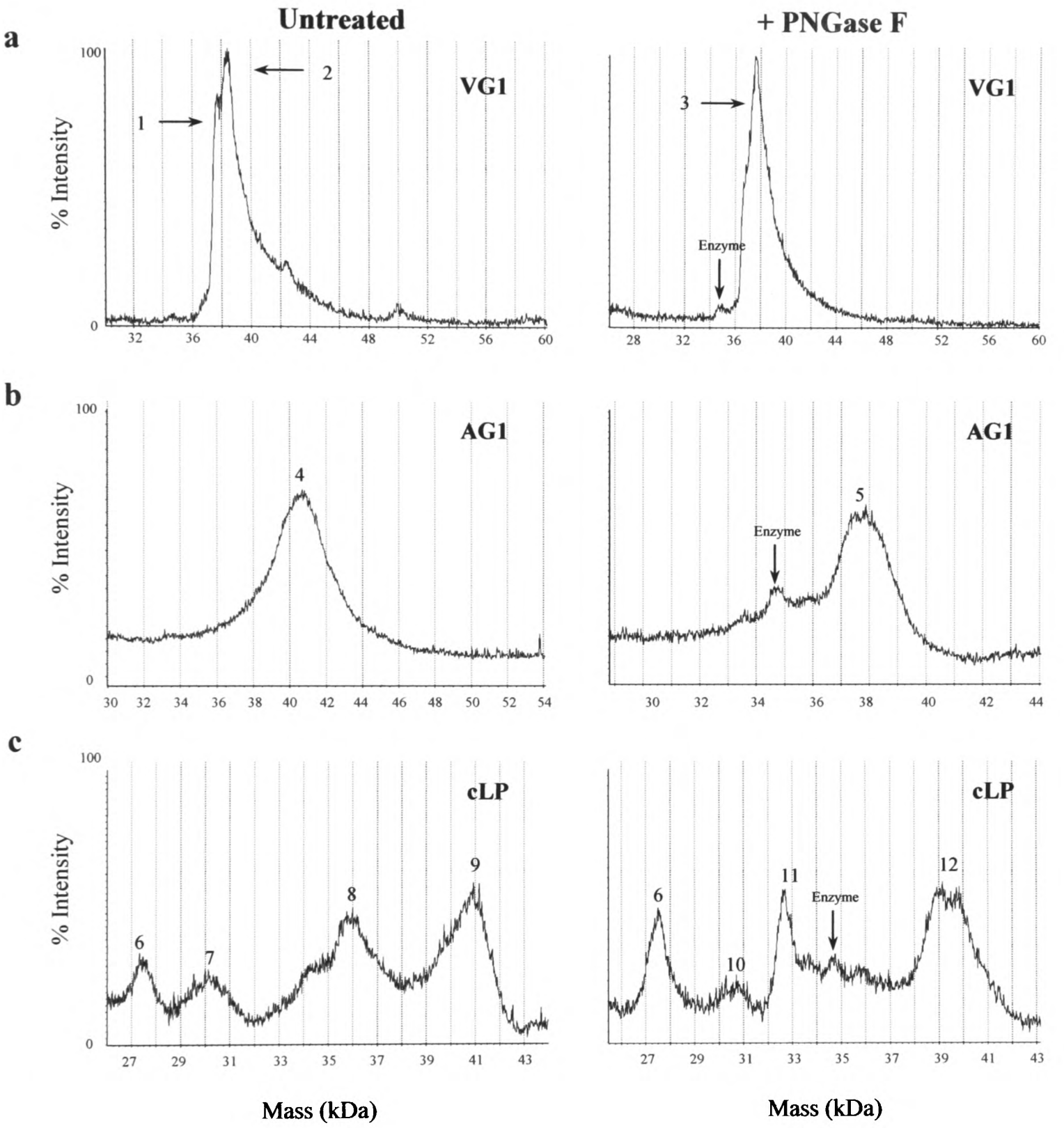

Figure 3.4 Samples of VG1, AG1 and cLP were analysed before and after PNGase F treatment by MALDI-TOF mass spectrometry in positive-ion linear mode. **a**) For VG1, two species (1 and 2) at of 37.7 and 38.5 kDa are observed in the untreated sample while a single species (3) is observed at 37.7 kDa after PNGase F treatment. **b)** AG1 has a mass of 40.4 kDa before (4) and 37.8 kDa after (5) PNGase F treatment. **c)** Three cLP species (7, 8, and 9) have masses of 30.3, 36.3, and 40.7 kDa, respectively before treatment while three cLP species (10, 11 and 12) have masses of 30.6, 32.7, and 39.4 kDa after PNGase F treatment, respectively. A lower species at 27.5 kDa (species 6) is observed for cLP both before and after PNGase F treatment. The PNGase F enzyme has a mass of 34.9 kDa (black arrow).

difference in mass is seen compared to species 1 in the untreated preparation (Figure 3.4a); this observed mass is approximately 1.2 kDa larger than the theoretical mass of the protein (36546.01 Da). Therefore, in MALDI-TOF MS, which is non-quantitative, species 1 may represent a small fraction of unglycosylated protein (that may ionize better than the glycosylated species) in the untreated VG1 preparation whereas species 2 represents a mixture of the A/B doublet seen in SDS-PAGE analysis (Figure 3.3a). This would also indicate that the sugar moieties on recombinant VG1 represent approximately 2 percent of the protein mass. The G1-domain of versican has two potential sites for *N*-linked glycosylation at Asn-57 and Asn-330 (numbered as in the pre-protein (Zimmermann and Ruoslahti 1989) and it seems likely that these sites are occupied in the *Drosophila* expressed protein and removed by PNGase F treatment.

The AG1 preparation runs as a single, rather broad, species of ~47–50 kDa under reducing and ~43-46 kDa under non-reducing conditions (band C on Figure 3.3a), which is slightly larger than the average molecular mass (40.4 kDa) determined for AG1 by MALDI-TOF mass spectrometry (species 4, Figure 3.4b). The broad band observed in SDS-PAGE may result in part from the AG1 length variation (see section 3.2) where the preparation contains two additional species that are 3 amino acids shorter or longer (corresponding to masses of 36833.2 and 37433.9 Da, respectively) in addition to the expected VETSDHDNSL sequence (37162.6 Da). After PNGase F treatment AG1 ran as a tighter band at a lower molecular weight (~45 kDa) by SDS-PAGE analysis (species H; Figure 3.3b), which is consistent with a reduced average mass (37.8 kDa) observed in MALDI-TOF mass spectrometry compared to the untreated AG1 (species 5, Figure 3.4b). The aggrecan G1-domain has three consensus

sites for *N*-linked glycosylation at Asn-126, Asn-239 and Asn-333 (pre-protein numbering; (Doege *et al.* 1991)) and one or more appear occupied and removed by PNGase F since band H and species 5 have significantly lower apparent molecular weights compared to the untreated material on both SDS-PAGE and MALDI-TOF mass spectrometry, respectively. Therefore, for AG1, it is likely that combined differences in glycosylation and length heterogeneity contribute to the broad band seen on SDS-PAGE (Figure 3.3a).

The cLP preparation runs mainly as a species of ~45 kDa (species D on Figure 3.3a) under reducing conditions and ~42 kDa under non-reducing conditions with faint lower molecular weight species visible at approximately 40 and 35 kDa (E and F), respectively under reducing conditions. Four species (6, 7, 8 and 9) are observed in MALDI-TOF mass spectrometry (Figure 3.4c) having average masses of 27.5, 30.3, 36.3, and 40.7 kDa, respectively. Species 7-9 are all approximately 5 kDa smaller than the apparent molecular weights observed for species F, E and D on SDS-PAGE under reducing conditions; these values are in better agreement with the apparent molecular weights observed for species F, E, and D on SDS-PAGE under non-reducing conditions (Figure 3.3a). N-terminal sequence analysis of purified cLP showed this preparation to contain two species in a 5:1 molar ratio (based on their initial yields). The major species (band D) corresponded to the expected N-terminal sequence (DHLSDXYTLD; having a theoretical mass of 38480 Da for the non-glycosylated protein) where no amino acid was detected at position 6 (an asparagine), indicating that this *N*-linked glycosylation site is fully utilised as noted before (McVey 2002). The minor sequence (AENGPHLLVE), having a theoretical mass of 36335 Da, corresponds to a truncated form that is 18 amino acids shorter (~2 kDa

smaller) than the full-length protein. This may result from N-terminal proteolysis as reported previously for the native protein (Neame and Barry 1993). Two species were also shown to be immunoreactive with a rabbit anti-human link protein antibody raised against a peptide sequence from the second Link module domain (Figure 3.5), indicating that species D and E most likely correspond to the intact and truncated cLP, respectively. Longer exposure also revealed the presence of a lower molecular weight species (~35 kDa), which were in the vicinity of band F (Figure 3.3a and 3.4c). As can be seen in Figure 3.3b, PNGase F treatment of cLP resulted in the appearance of bands I and J. The former has a ~2 kDa lower apparent molecular weight than the intact protein (band D), while J has similar mobility as species E. The two predominant cLP species (11 and 12) observed after PNGase F treatment in MALDI-TOF (Figure 3.4c) mass spectrometry have average masses of 32.7 and 39.4 kDa, respectively with another species 10 (30.7 kDa) that has approximately the same mass as species 7 (30.3 kDa). The peaks seen at ~35-36 kDa, represent the PNGase enzyme itself (34.9 kDa) and possibly some residual glycosylated species 8. Since the MALDI-TOF protein samples analysed are mixtures and are not individually separated, direct comparisons with SDS-PAGE analysis may be misleading. Thus, taking only the SDS-PAGE analysis of cLP into consideration and given that native human cartilage link protein has two *N*-linked oligosaccharides (at Asn-6 and Asn-41) where the latter site is always reported to be occupied (Neame and Barry 1993) it seems likely from PNGase F treated cLP, that only the carbohydrate from Asn-6 is removed (i.e. band 1 is a partially deglycosylated from of band D), while band E and J could represent the truncated form of cLP (lacking the N-terminal glycopeptide) with an N-glycan on Asn-41. However, further detailed analysis will be necessary to confirm this.

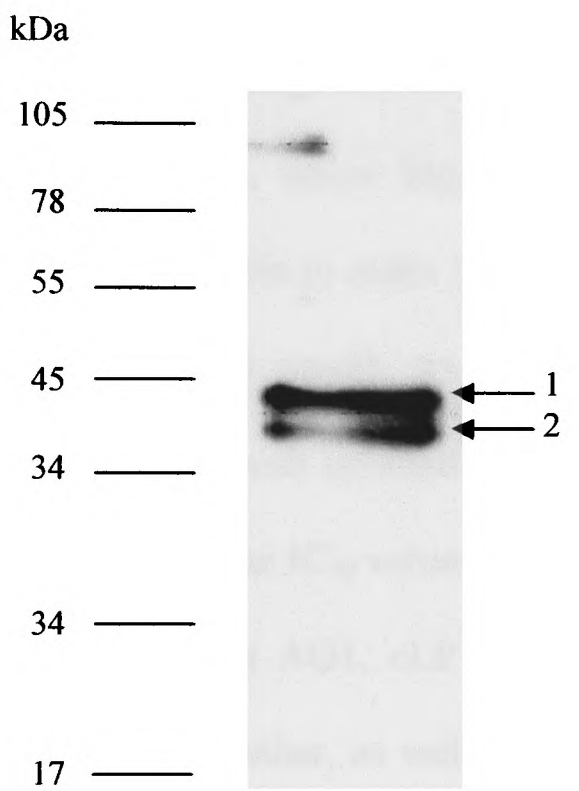

Figure 3.5 Western blotting revealed that the cLP preparation (0.5 μg) contains two major species, which are immunoreactive with an anti-cLP polyclonal antibody, that run at ~45 and 40 kDa (arrows 1 and 2) under reducing conditions. The larger species represents the full-length protein while the smaller species is likely a N-terminal truncated product.

3.5 Functional activity of HA-binding proteins

3.5.1 Binding of HA to protein-coated plates

A microtitre plate assay using biotinylated-HA (Mahoney *et al.* 2001b) was used to determine the functional activity of the recombinant proteins (see section 2.11.1). Increasing amounts of cLP, AG1 and VG1 were coated onto plates at a range of concentrations and their HA binding was determined colourimetrically. All proteins were found to interact with HA, where binding was saturable (Figure 3.6); VG1 required the least amount of protein to attain binding saturation (1.2 pmol) compared to AG1 (4.5 pmol) and cLP (5 pmol). As can be seen from Figure 3.7, these interactions could be competed with unlabelled rooster comb polymeric HA (pHA) indicating that they are specific; the IC_{50} values for pHA competition were determined to be 38, 25 and 20 ng/well for AG1, cLP and VG1, respectively, which are in reasonable agreement with each other, as well as to the expected IC_{50} value of 12.5 ng/well (i.e, the amount of bHA/well) given the inaccuracy of measuring HA by the carbazole assay (section 2.2.4). In the case of cLP and AG1, experiments with defined HA oligosaccharides (Mahoney *et al.* 2001a) indicated that HA10 is the minimum size that can compete maximally for bHA binding; HA6 and HA8 did not act as effective competitors (Figure 3.7). Previous gel filtration studies on the native link protein and aggrecan binding domain gave equivalent results (Hardingham and Muir 1973; Hascall and Heinegaard 1974b; Rosenberg *et al.* 1988). Similarly for VG1, HA10 and HA12 compete much more effectively than HA6 and HA8, as has been reported for human hyaluronectin, a proteolytic fragment of versican (Bertrand and Delpech 1985). However, from Figure 3.7 it can be seen that HA10 and HA12 are less efficient competitors than pHA; HA10 competes less well than HA12 (IC_{50} values of 562 and 222 ng/well, respectively). Equivalent assays using PNGase F

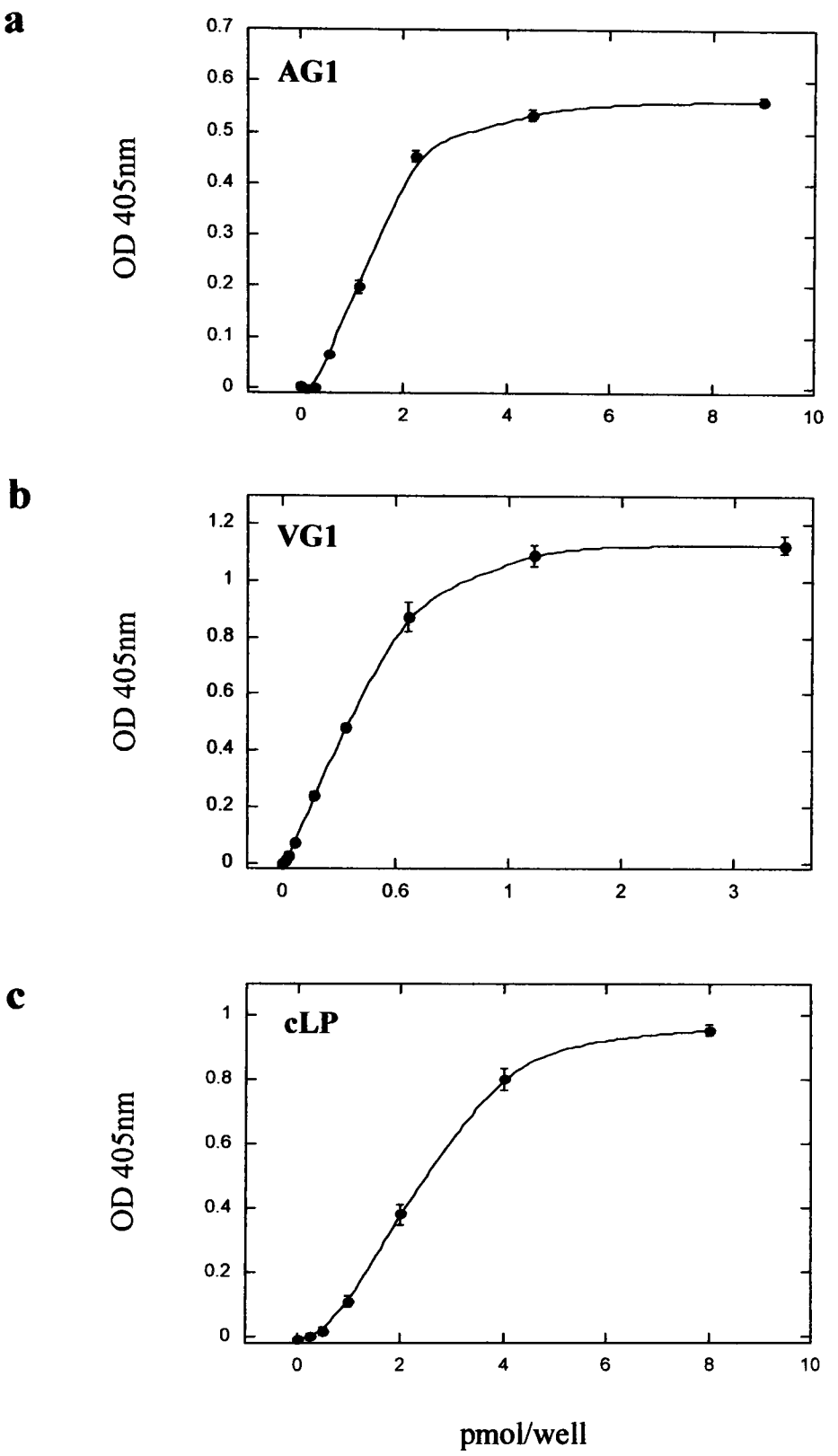

Figure 3.6 HA-binding assays for G1-aggrecan, G1-versican and cartilage link protein. The binding of biotinylated-HA (bHA; 12.5 ng/well) to protein-coated plates was determined colorimetrically at 405 nm after 10 mins for **(a)** AG1 n=8 ±S.E. **(b)** VG1 n=12 ±S.E. and **(c)** cLP n=8 ±S.E.

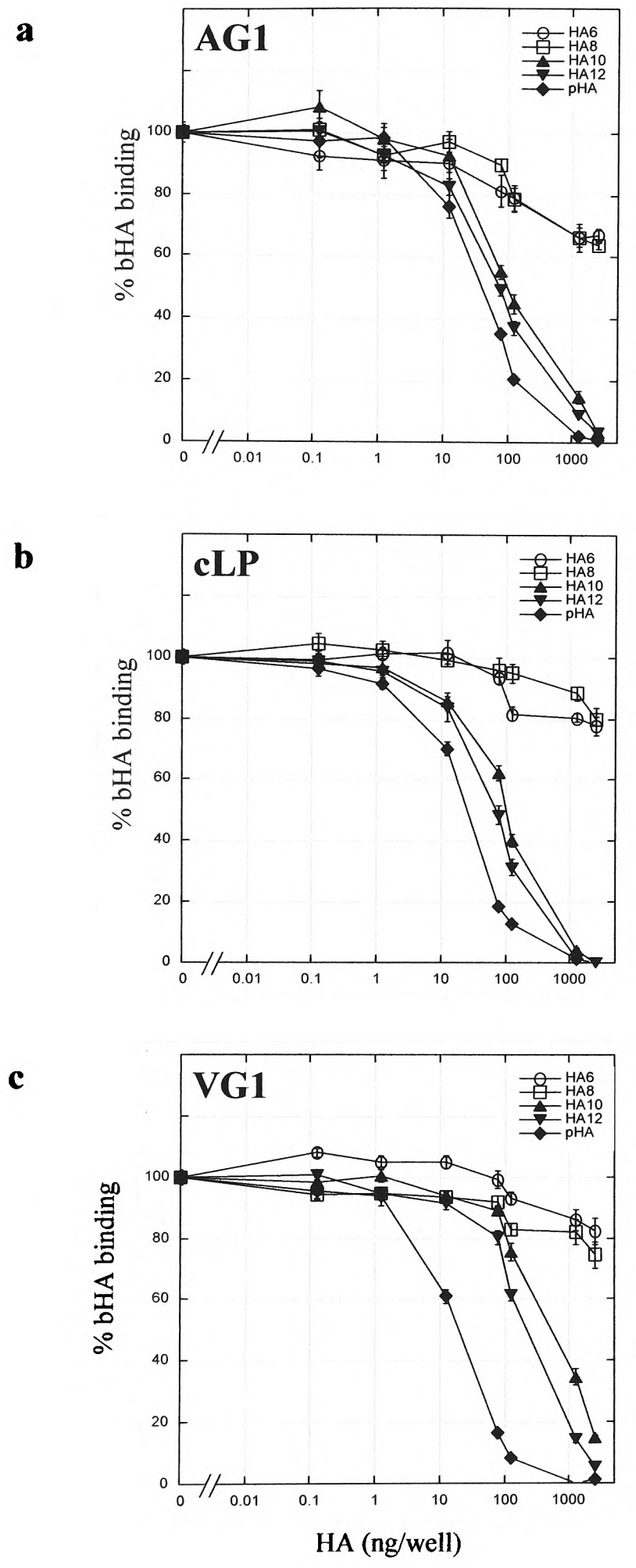

Figure 3.7 HA-binding assays for cartilage link protein, G1-aggrecan and G1-versican. The binding of biotinylated-HA (bHA; 12.5ng/well) to protein-coated plates in the presence or absence of competing unlabelled polymeric HA (pHA) or HA oliogosaccharides of defined size. Values are plotted as mean percentages (n=8) ±S.E. of binding in absence of competing HA for AG1 (**a**), cLP (**b**) and VG1 (**c**); OD_{405nm} values of 0.65, 0.85 and 1.00 were seen for AG1, cLP and VG1, respectively, after 10 min development time.

treated AG1 revealed that the deglycosylated AG1 was inactive (Figure 3.8) in this solid phase assay; a similar finding has been reported previously for this domain expressed in human embryonic kidney cells and analysed in ligand blotting assays (Watanabe *et al.* 1997). However, PNGase F treatment of VG1 or cLP did not affect their HA-binding properties (Figure 3.8).

3.5.2 Binding of protein to HA-coated plates and tissue staining

cLP, AG1 and VG1 were biotinylated in the presence of HA to avoid modification of lysine residues essential for ligand binding (see section 2.10). These biotinylated proteins (bLP, bAG1 and bVG1, respectively) were incubated (at a range of concentrations) with HA-coated plates and the binding was determined colorimetrically (see section 2.11.2). All three biotinylated-proteins were capable of interacting with umbilical cord HA (Figure 3.9) where bLP required the least amount of protein/well to attain near saturation (2.7 pmol) compared to bVG1 (2.9 pmol) and bAG1 (11.7 pmol). This binding was determined to be specific since it could be competed by unlabelled rooster comb HA (Figure 3.10). This also indicates that biotinylation does not interfere with the functional activity of the proteins. Both bVG1 and bAG1 were also used as probes to stain for HA in tissue (Figure 3.11, performed by Dr. Carol de la Motte, Cleveland Clinic, OH) essentially as described in de la Motte *et al.* 2003. The staining of bVG1 and bAG1 compared favorably to the commercially available S-HABP (Seikagaku Corporation, Japan), which is essentially a biotinylated HA-binding domain of bovine aggrecan with ~ 20 % biotinylated bovine cartilage link protein. Staining using bLP was not attempted due to its inherent insolubility in aqueous buffers (Parkar *et al.* 1998). Therefore biotinylated cLP, AG1 and VG1 were determined to be functionally active in regard to their HA

a

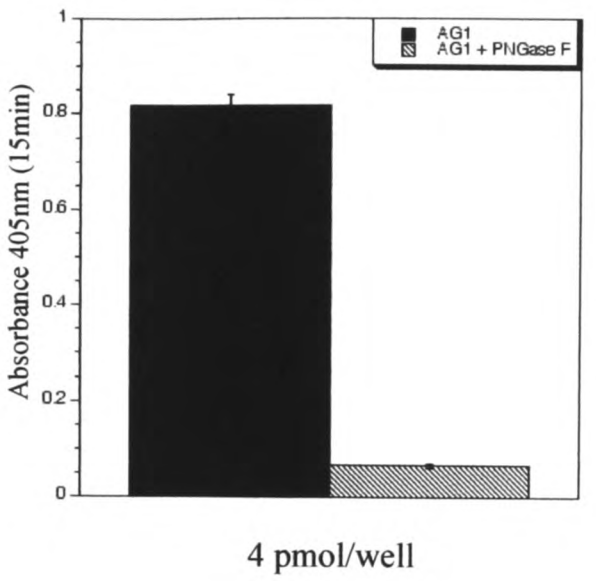

b

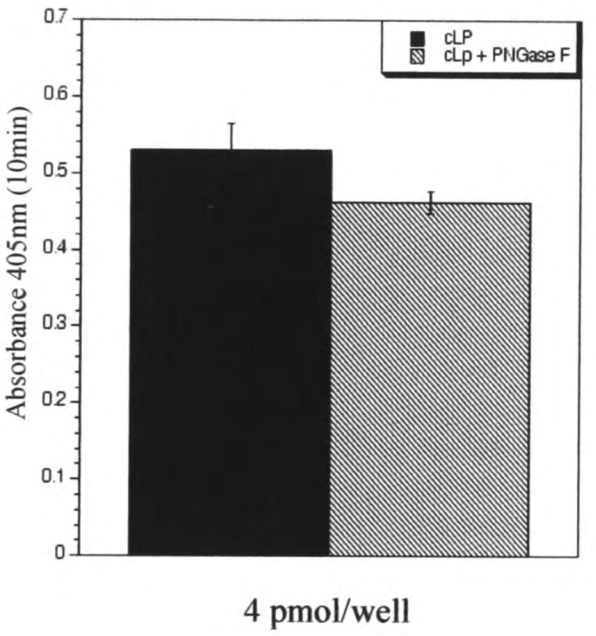

c

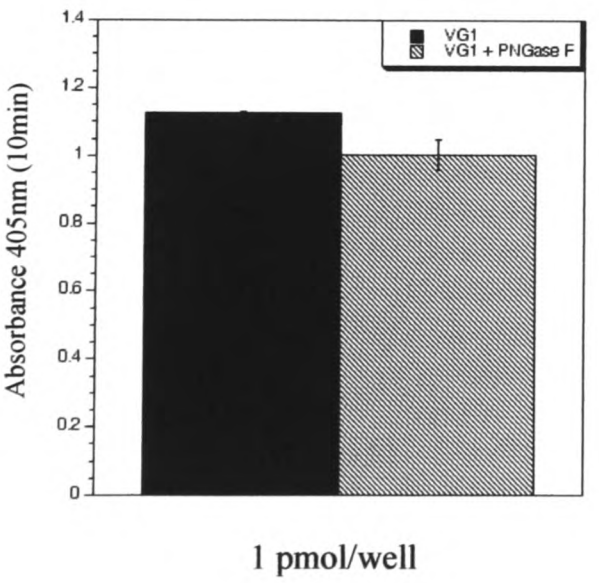

Figure 3.8 Binding of biotinylated-HA to PNGase F-treated and untreated AG1 (**a**) cLP (**b**) and VG1 (**c**) were analysed in a microtitre plate assay where the AG1 and cLP proteins were coated at 4 pmol/well and VG1 at 1 pmol/well, respectively; these concentrations of untreated protein give close to maximal HA binding (see Figure 3.6). Values are plotted as mean absorbance (n=4) ±S.E.

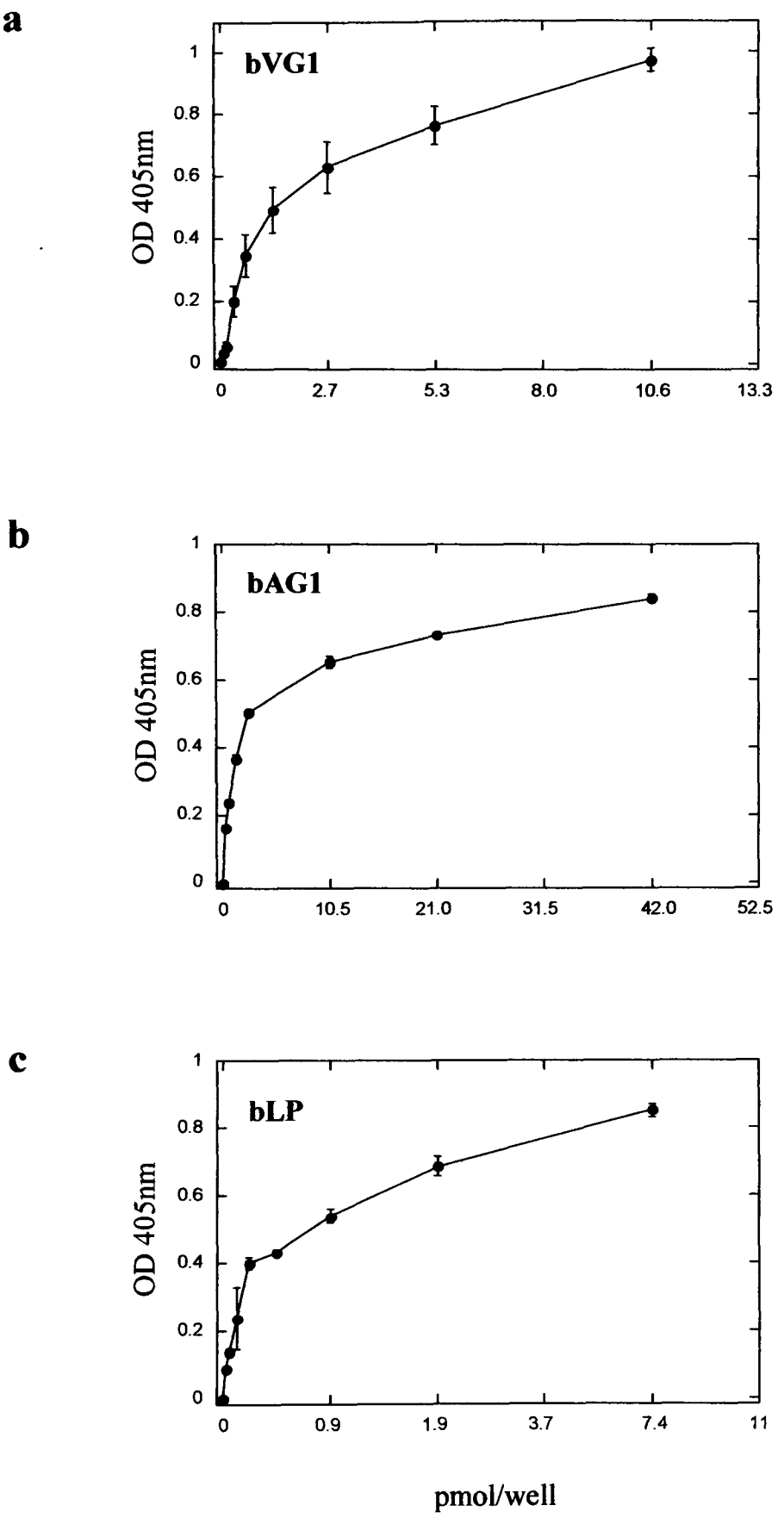

Figure 3.9 Binding of biotinylated VG1 (**a**) AG1 (**b**) and cLP (**c**) to umbilical cord HA coated plates were analysed colorimetrically. Values are mean absorbance (n=4) ±S.E.

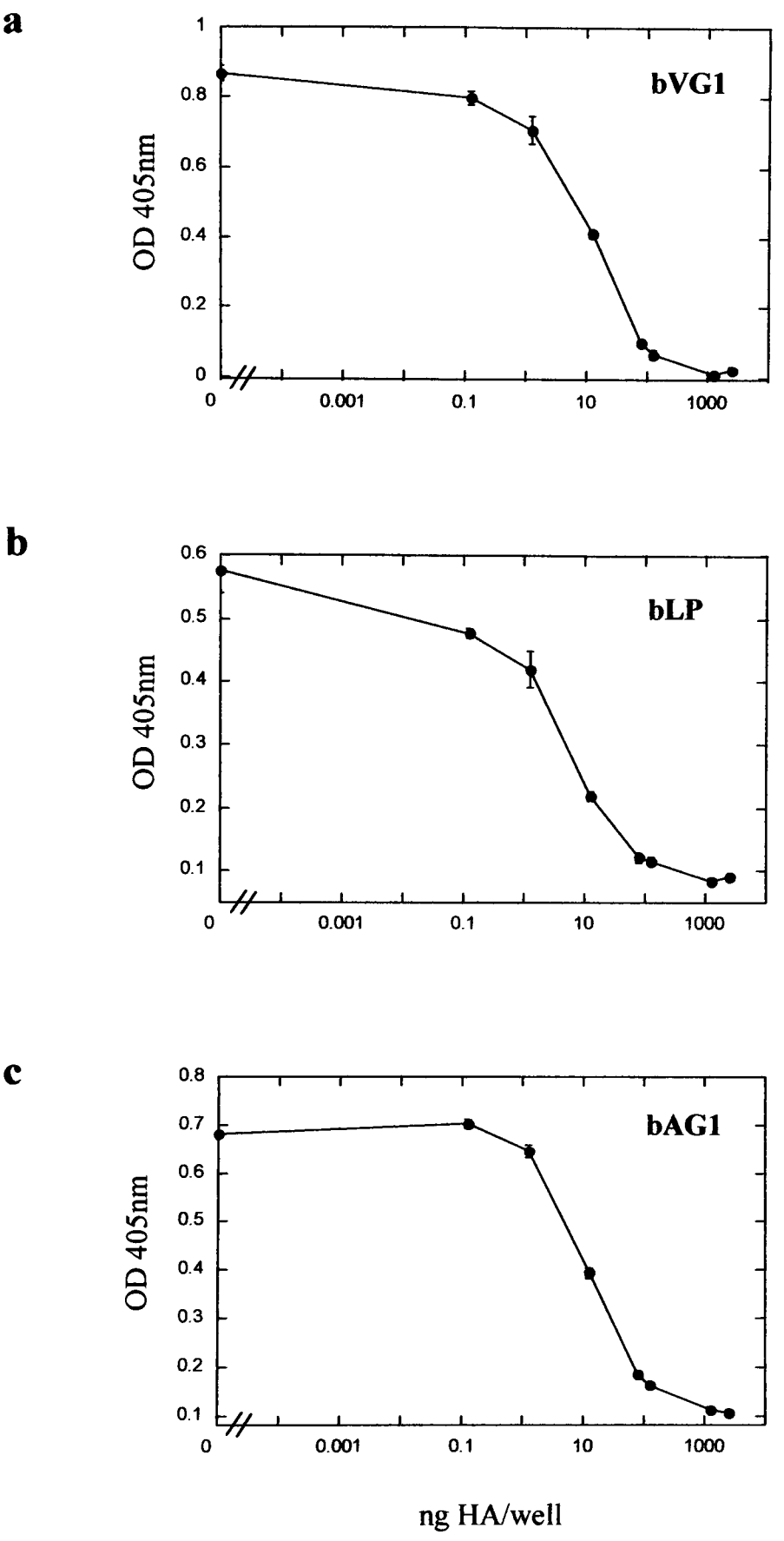

Figure 3.10 The binding of biotinylated 2.9 pmol/well VG1 (**a**), 2.7 pmol/well cLP (**b**) and 11.7 pmol/well AG1 (**c**) to umbilical cord HA coated plates in the absence or presence of competing unlabelled rooster comb polymeric HA. Values are mean absorbance (n=4) ±S.E.

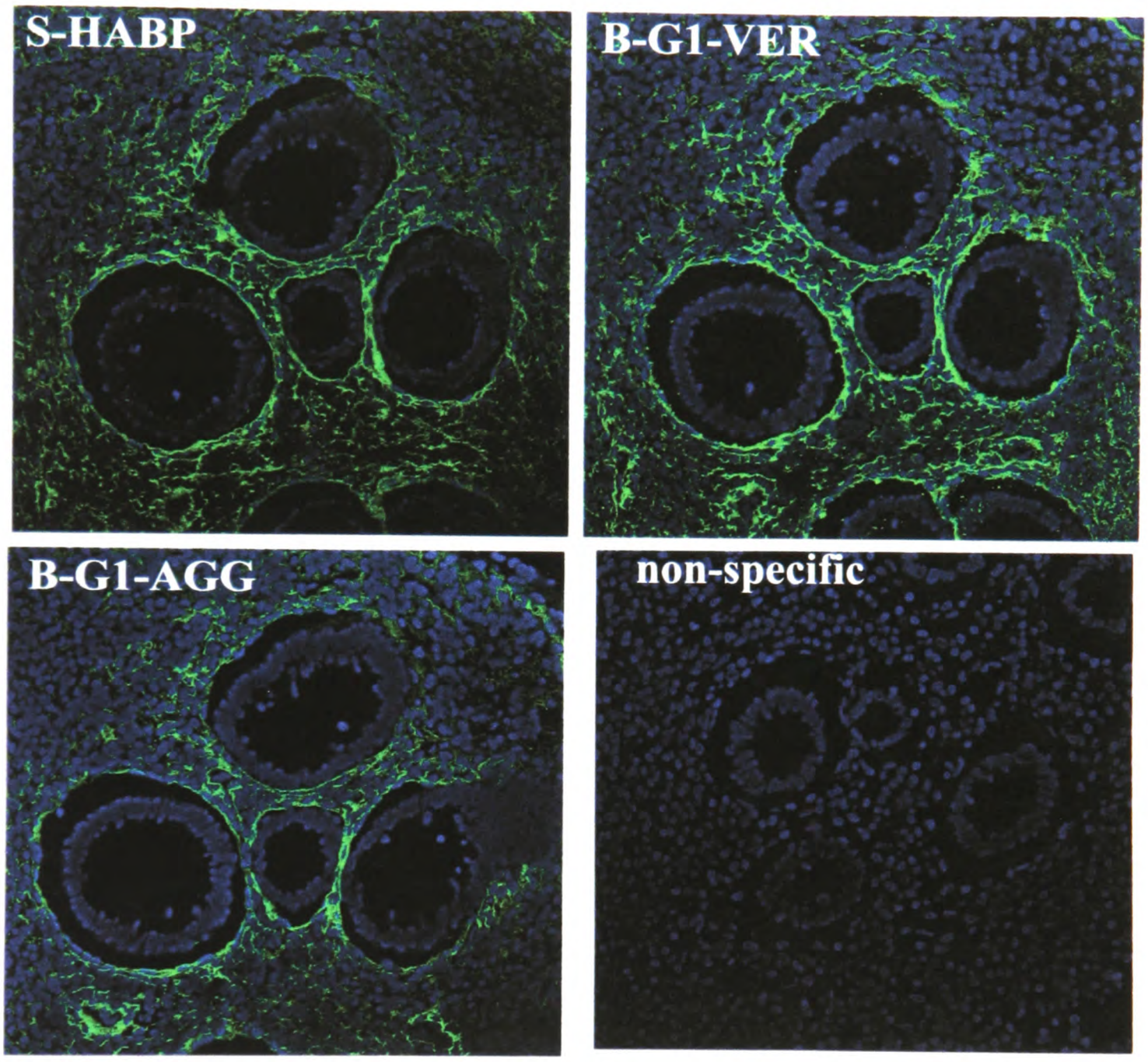

Figure 3.11 Staining for hyaluronan in human inflammatory bowel tissue with biotinylated AG1 (B-G1-AGG) or VG1 (B-G1-VER) compared to commercially available Seikagaku HABP (S-HABP) using a secondary FITC-conjugated reagent. A control lacking biotinylated protein (non-specific) is shown in the lower right panel. Staining was performed by Dr. Carol de la Motte, Cleveland Clinic, OH.

binding properties and therefore, useful reagents for studying protein-protein (chapter 4) or protein-HA interactions *in vitro*.

3.6 Alternative FPLC protein purification

Initial crystallisation trials with VG1 did not yield any crystals (see section 2.24). One possible reason for this is that VG1 was purified by reverse-phase HPLC (see section 2.4), which is thought to interfere with crystallisation due to the denaturing conditions causing aggregation, or residual TFA adhering to the protein. Therefore, an alternative method of purification was investigated to avoid the use of HPLC and organic buffers. It was also hoped that the method chosen would be more efficient in recovering protein from the S2 culture supernatants than the 'batch' ion-exchange used previously. Therefore, cLP, AG1 and VG1 were purified by ion-exchange column chromatography using an ÄKTA FPLC purification system (Amersham Biosciences) in aqueous (non-organic) buffers. Unlike the previous batch purification scheme where the conditioned supernatant is incubated with the sepharose and the protein eluted by washes of particular salt strength, the purification method used here flowed the *Drosophila* S2 supernatant through SP- or Q-Sepharose columns; this increases the accessible surface area of the sepharose encountered by the protein. For VG1, the pH of the media was reduced from ~6.5 to 5.0 with HCl (i.e., ~2 two pH units below the theoretical isoelectric point of VG1 (6.82)) to ensure that the protein has a net positive charge. As seen in Figure 3.12a and 3.12b, SDS-PAGE indicates that VG1 is eluted from the negatively charged SP-sepharose column between 100-250 mM NaCl. Comparison of the protein yields from the two procedures by SDS-PAGE indicates that an increased amount of VG1 is recovered from the supernantant using the column scheme compared to the batch scheme (Figure 3.1b). Integration of

a

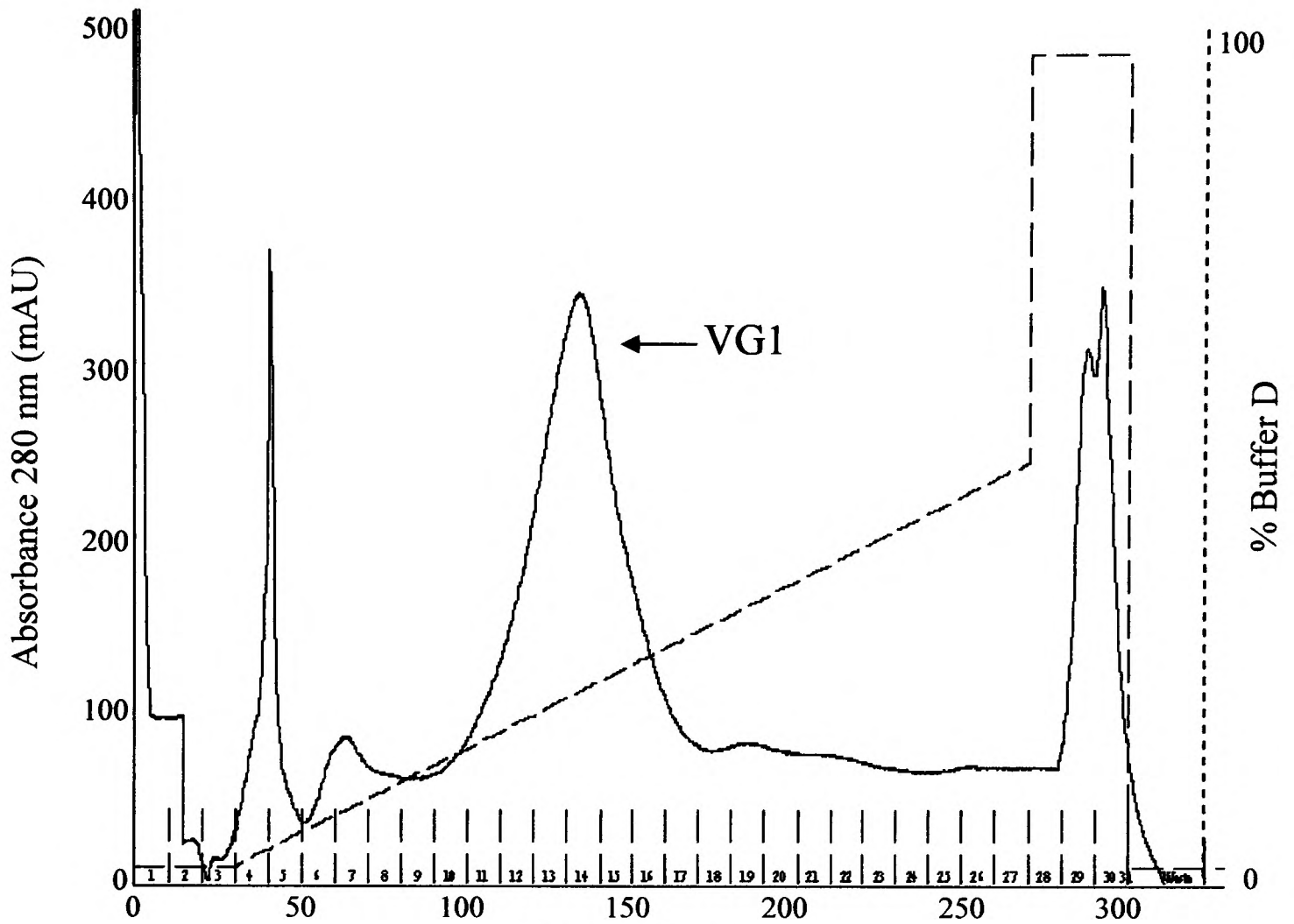

b

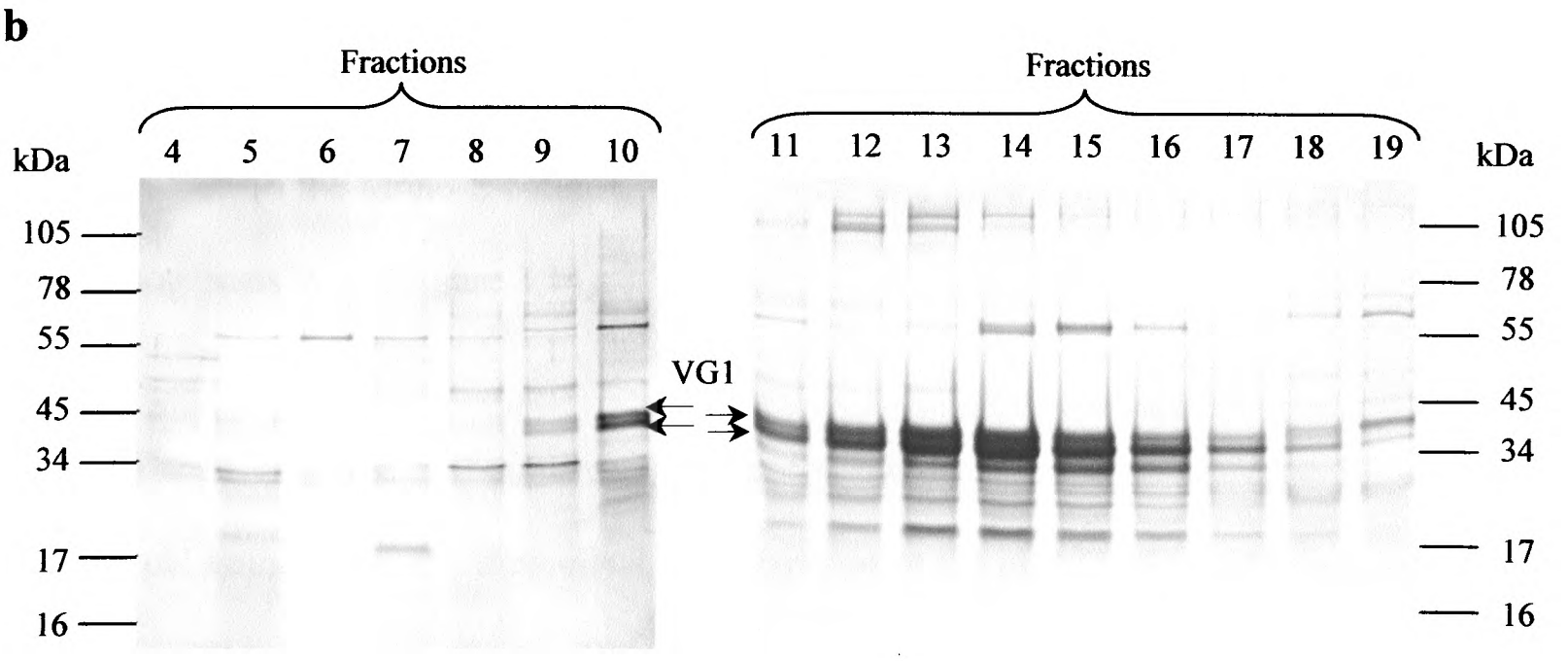

Figure 3.12 Cation-exchange purification of VG1 conditioned supernatant using an ÄKTA FPLC system. **a)** VG1 (black arrow) elutes as a symmetric peak from the SP-Sepharose column between 100-250 mM NaCl as determined by SDS-PAGE analysis (**b**) where the VG1 doublet is seen in (double arrows) fractions 9-17.

the area under the curve using the Unicorn 5.0 software (Amersham Biosciences) yielded the total protein absorbance at 280 nm. Dividing the total absorbance by the theoretical distinction coefficient for VG1 (OD_{280} = 1 mg/ml = 1.19) revealed that ~7 mg of protein was purified from 900 ml of conditioned media. This is ~8 times more protein than attained using the batch approach, estimated at 900 µg by SDS-PAGE analysis from equivalent starting volumes (900 ml) of conditioned supernatant. However, it must be noted that other *Drosophila* protein contaminants may also be contributing to the OD_{280} observed in Figure 3.12. Additionally the increased protein yield could be influenced by the expression ability of the *Drosophila* S2 cells themselves which appear to alter over time in culture. Therefore, using a SP-sepharose column and adjusting the pH of the conditioned medium prior to purification results in increased VG1 yields. Fractions containing VG1 were then pooled, diluted and re-purified using a high resolution Mono-S ion-exchange column (section 2.6.2). As can be seen on Figure, 3.13a and 3.13b, more than one peak was identified that contained VG1 by SDS-PAGE, most likely indicating differences in absorbance caused by protein contaminants. Fractions 5 and 6 were combined and repurified on the Mono-S column, which results in a more symmetric peak profile and homogenous VG1 (Figure 3.14).

Similar to VG1, the cLP culture supernatant was reduced in pH to 5.0, approximately two pH units below the theoretical isoelectric point for cLP (7.18), and then purified over a SP-Sepharose column (Figure 3.15a). Fractions were collected and analysed by SDS-PAGE (Figure 3.15b), which indicated that the cLP (black arrow) eluted from the column over a salt concentration of 80-200 mM NaCl (fractions 8-14). The broad elution profile is likely due to cLP heterogeneity or *Drosophila* host contaminants.

a

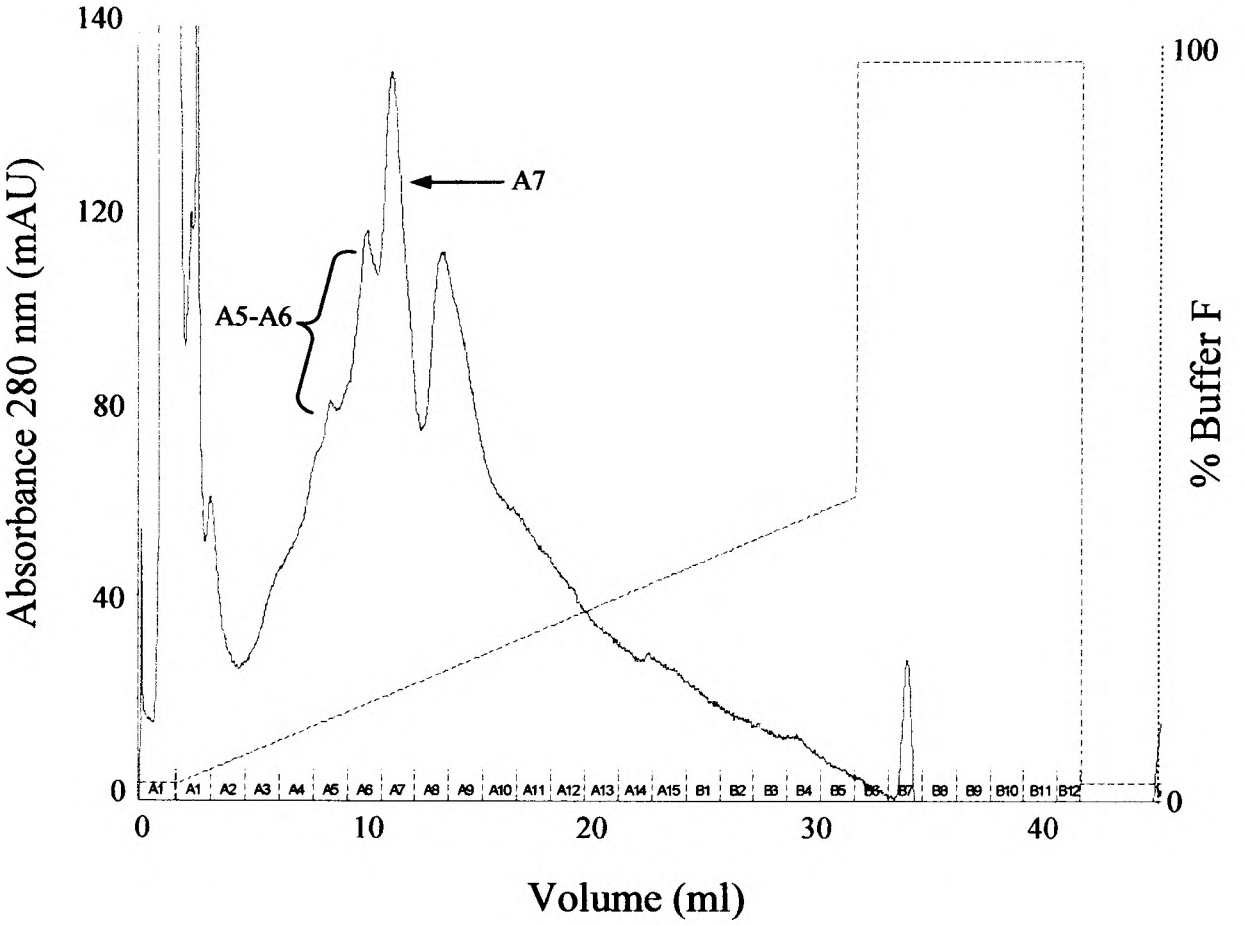

b

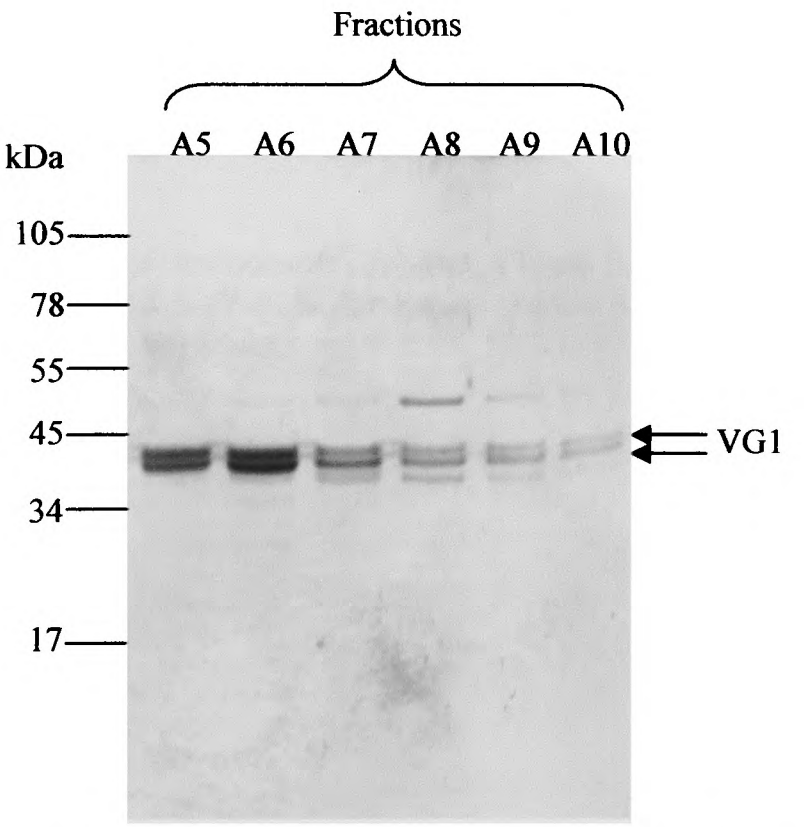

Figure 3.13 High resolution cation-exchange purification of VG1 was performed using a Mono-S column **a)** VG1 elutes in multiple peak fractions (A5-A10) as determined by SDS-PAGE analysis **(b)**.

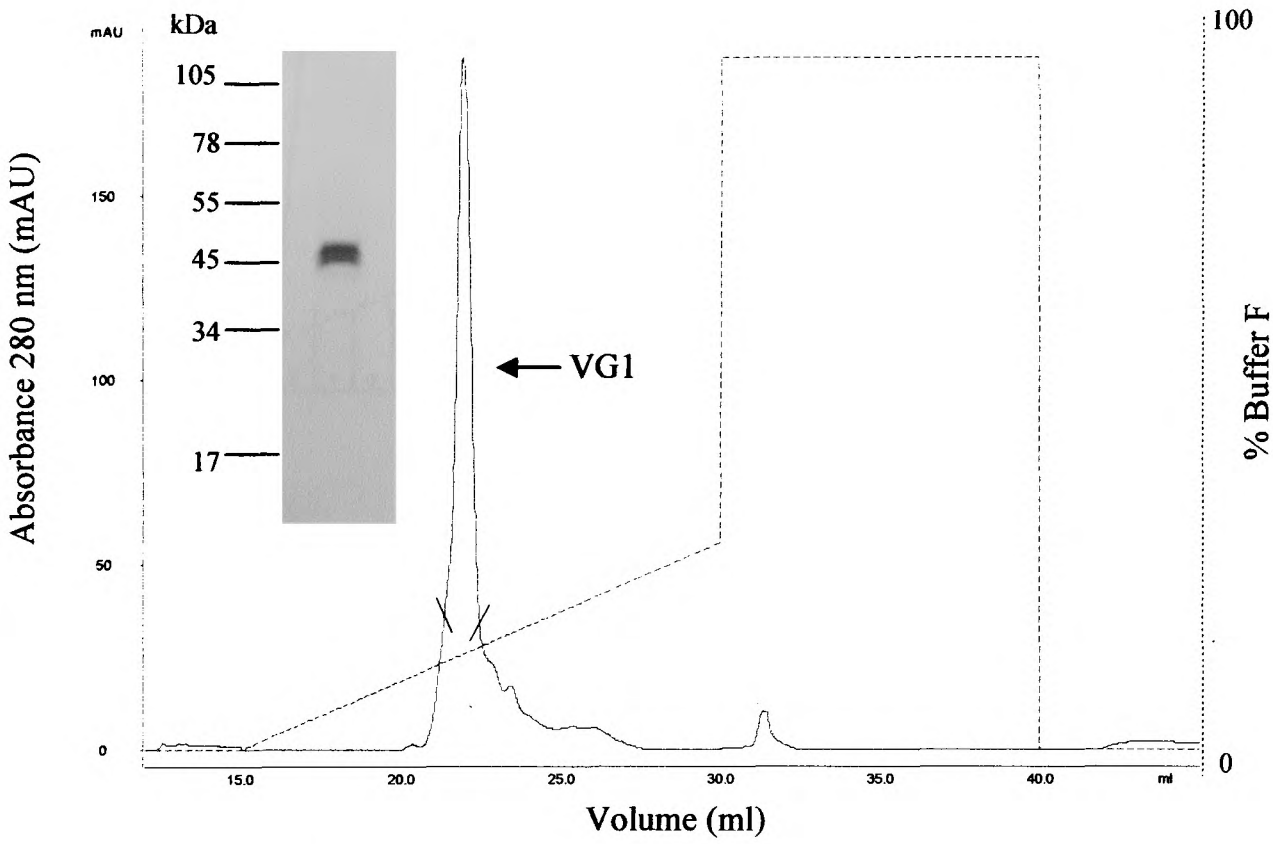

Figure 3.14 Re-purification of fractions A5-A6 (see Figure 3.13) on a Mono-S column with a linear gradient of 0-30 % buffer F (see section 2.6.2) over a 15 ml volume produces a symmetrical VG1 peak.

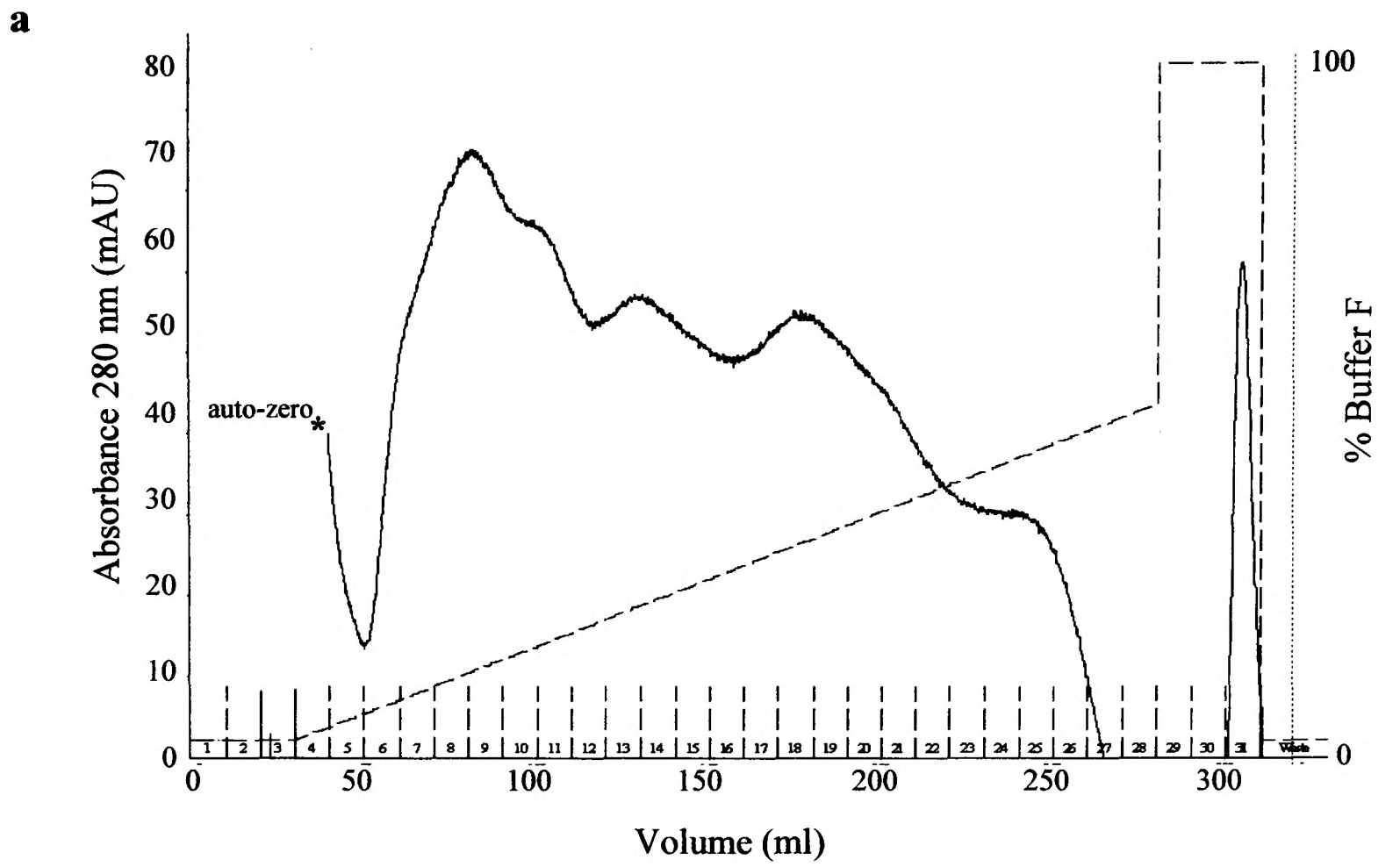

Figure 3.15 Cation-exchange purification of cLP conditioned supernatant using an ÄKTA FPLC system. **a)** cLP elutes in multiple fractions from the SP-Sepharose column between 80-200 mM NaCl as determined by SDS-PAGE analysis. The * indicates an auto-zero performed in the run prior to cLP elution. (**b**) where cLP is indicated (black arrow) in fractions 8-14.

Therefore, the peak integration from the elution profile was not attempted. Fractions containing link protein were pooled, diluted and repurified over a high resolution Mono-S ion-exchange column (Figure 3.16). The large peak (black arrow) was collected and analysed by SDS-PAGE (Figure 3.16, inset), which indicated it was indeed cLP (species 1). The lower molecular weight product species 2 likely represents bands E seen after HPLC purification (Figure 3.3a). The cLP purified solely by ion-exchange chromatography has a similar level of purity as cLP isolated by reverse-phase HPLC (Figure 3.3a) indicating that Mono-S purification of cLP is a viable purification alternative.

AG1 was purified from culture supernatant using a positively charged Q-sepharose column (Figure 3.17a). In this case, the pH of the conditioned media (~6.5) was not altered because it is already ~1.5 units above the theoretical isoelectric point of AG1 (5.07) providing the protein with a net negative charge. The eluent from the column gave a high UV absorbance at 280 nm, which saturated the detector, so that no clear peaks were visible (Figure 3.17a). Analysis of the eluent by SDS-PAGE (Figure 3.17b) indicates the presence of AG1 in three fractions (15-18) corresponding to 160-250 mM NaCl; the bands observed were weaker than seen in the batch method (Figure 3.1a), which may be due to a change in *Drosophila* S2 expression levels. AG1 fractions were pooled, and repurified down a Resource-Q anion-exchange column (Figure 3.18), where a shallow elution gradient (section 2.6.3) was employed to facilitate removal of high molecular contaminants in the AG1 preparation. As can be seen from Figure 3.18, AG1 elutes from the column between 180-190 mM NaCl as determined by SDS-PAGE analysis. Therefore the shallow gradient was effective at removing majority of the high molecular weight contaminants (see Figure 3.17b)

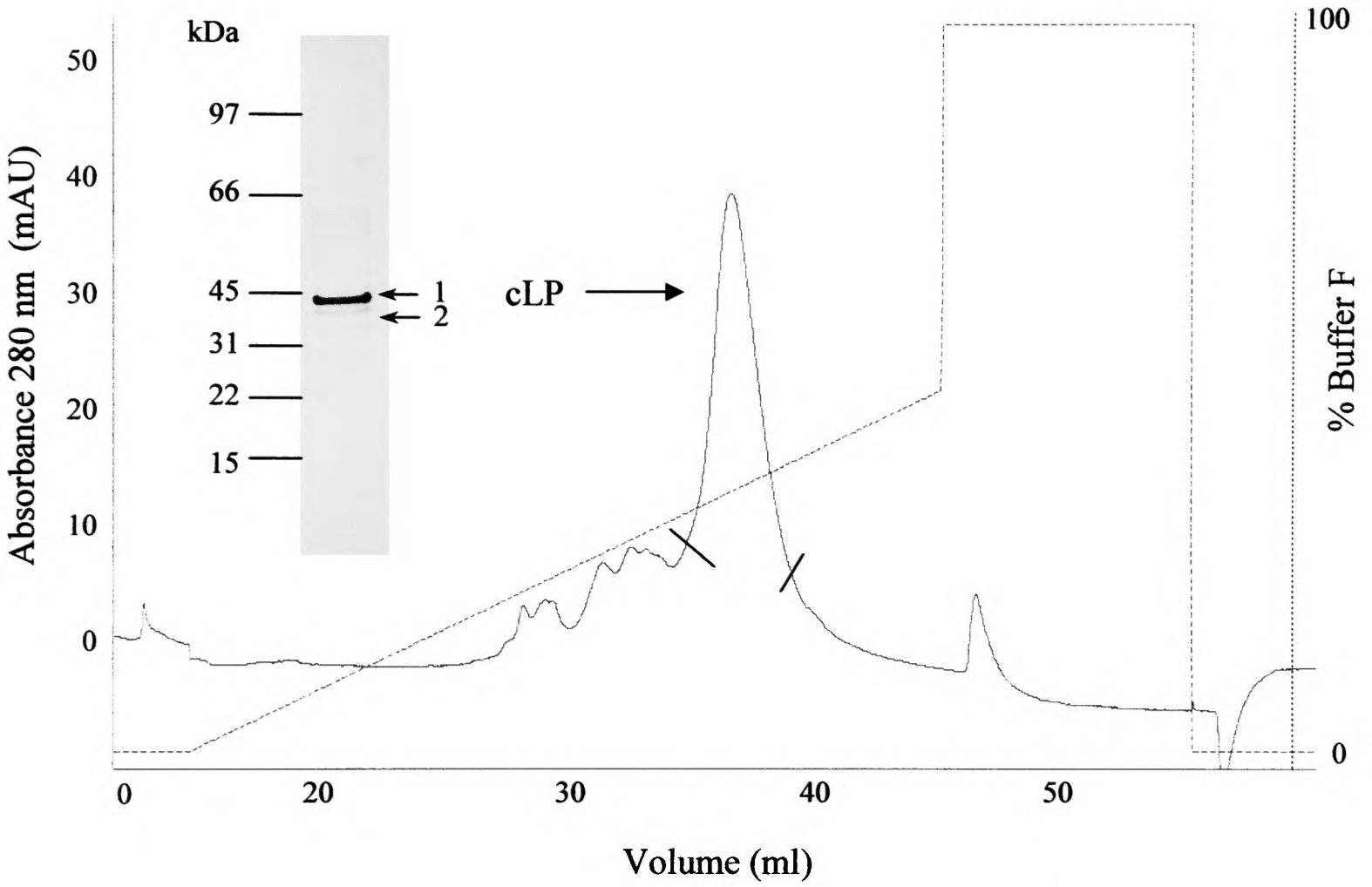

Figure 3.16 High resolution cation-exchange for cLP purification was performed using a Mono-S column. **a**) cLP (black arrow) elutes as a symmetric peak from column confirmed by SDS-PAGE analysis (inset) where the protein is present as a major species of ~42 kDa (band 1) and a minor species at ~40 kDa (band 2).

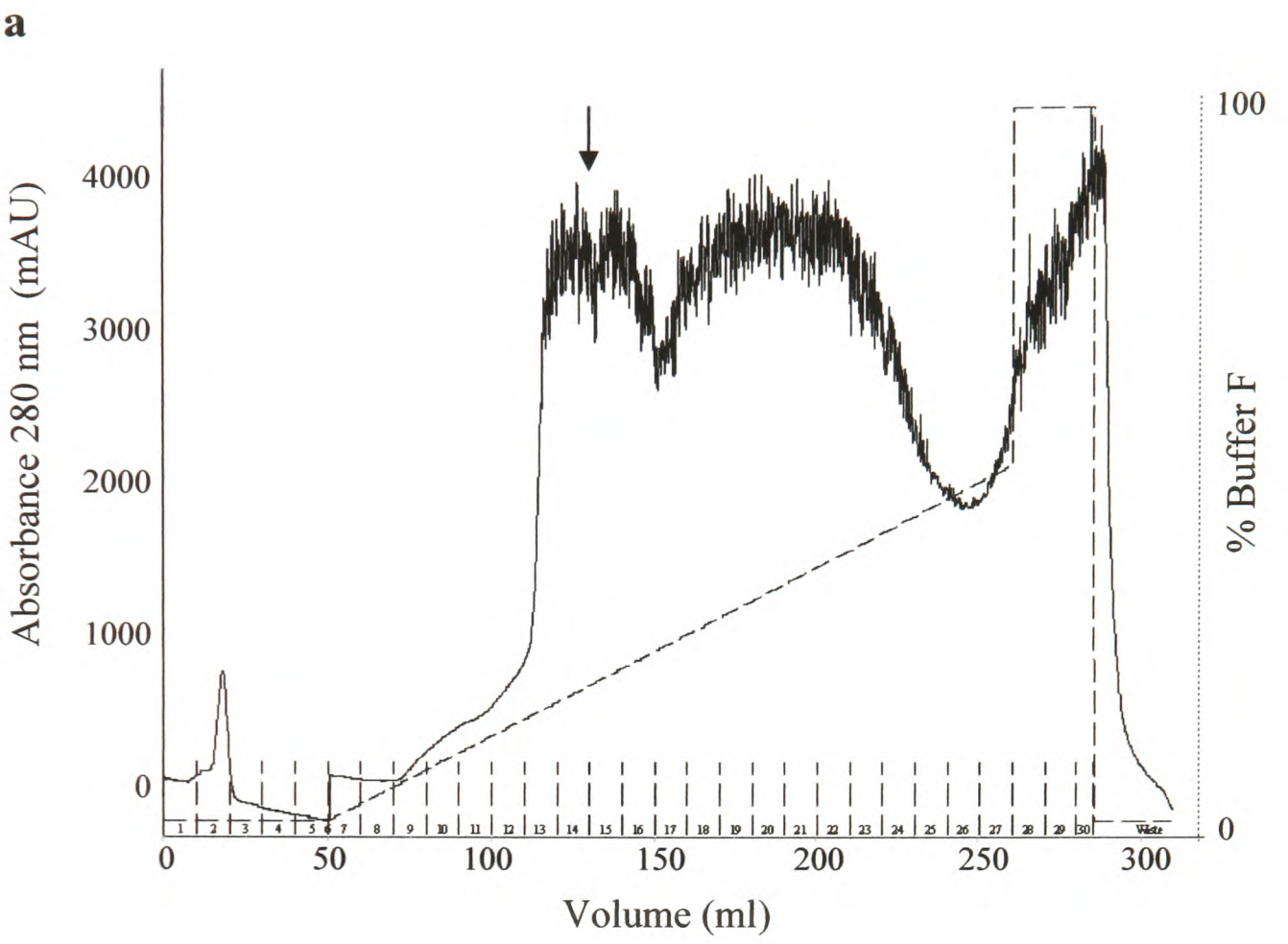

Figure 3.17 Anion-exchange purification of AG1 conditioned supernatant using an ÄKTA FPLC system. **a)** AG1 (black arrow) elutes from the Q-Sepharose column between 100-200 mM NaCl, confirmed by SDS-PAGE analysis (**b**) where AG1 is indicated (black arrow) fractions 15-17.

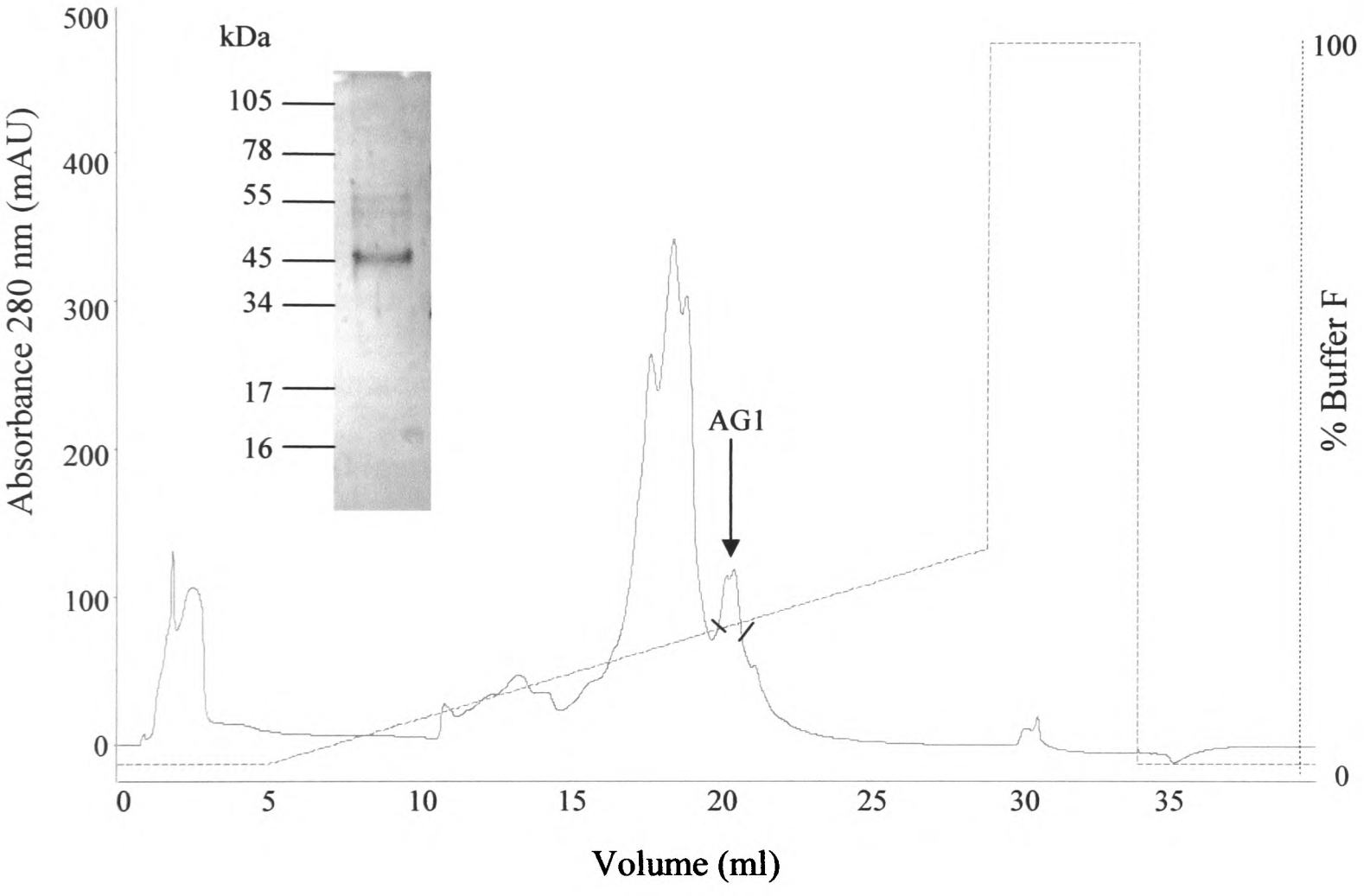

Figure 3.18 High resolution anion-exchange purification of AG1 was performed using a Resource-Q column. **a)** AG1 elutes as a double peak from column as determined by SDS-PAGE analysis (inset).

although some residual contaminants are still observed at ~69-55 kDa (Figure 3.18).

3.7 Discussion

Human recombinant cartilage link protein (cLP) and the G1-domains of aggrecan (AG1) and versican (VG1) expressed in *Drosophila* S2 cells were purified to homogeneity and characterised by N-terminal sequencing and MALDI-TOF mass spectrometry. All three recombinant proteins also contained *N*-linked glycans (Figure 3.3b) characteristic of proteins expressed in insect cell hosts (Altmann *et al.* 1999). Interestingly, after treatment with PNGase F, which removes *N*-linked glycans, both cLP and VG1 maintained their ability to bind HA whereas AG1 displayed no detectable binding (Figure 3.8). The lack of HA binding observed for treated AG1 is consistent with a previous study where PNGase treated human recombinant G1-aggrecan was unable to bind HA in transblot assays (Watanabe *et al.* 1997). Therefore, it appears that at least for cLP and VG1, *N*-linked glycosylation is not essential for functional activity. Further investigation into the functional activity of VG1 and AG1 after PNGase F treatment is provided in Chapter 4.

The recombinant proteins were demonstrated to be functionally active in regard to their HA-binding properties, as reported previously for the native proteins. For example, cLP, AG1 and VG1 were all found to interact with biotinylated-HA in microtitre plate assays, where HA10 was the minimum size oligosaccharide that can compete for polymeric HA binding to the proteins (Figure 3.7). For cLP and AG1 the IC_{50} values for HA10 and HA12 competition were reasonably similar to that determined with polymeric HA (see Figure 3.7), which is consistent with these individual interactions being non-cooperative as reported previously for the native

proteins (see Hardingham and Muir 1973; Morgelin *et al.* 1995). However, for VG1, HA10 and HA12 are less efficient competitors than polymeric HA, which may suggest that the affinity of VG1 for HA may increase with the molecular weight of the sugar (i.e. positive cooperativity) discussed in more detail in chapters 4 and 5. All three proteins maintained their functional activity after biotinylation, where the binding to HA coated plates was competed with polymeric rooster comb HA. In addition, both bAG1 and bVG1 were capable of staining for hyaluronan in human tissue sections as seen for a mixture of native cLP and the HA binding domain of aggrecan (de la Motte *et al.* 2003 and figure 3.11).

The FPLC purification scheme proved a viable alternative to reverse-phase HPLC purification, in particular for VG1, which showed a significant increase in protein yield when the conditioned supernatant was run through a packed AK-26 SP-Sepharose fast flow column. All proteins were also capable of being purified to near homogeneity by high resolution ion-exchange using a Mono-S (VG1 and cLP) or a Resource-Q (AG1) pre-packed column, respectively. One clear advantage with the non-organic purification procedure was that cLP did not show any observable insolubility after purification, however this could also be due to the lower concentration of cLP (162 nM) in the ion-exchange purified material (Rosenberg *et al.* 1991). Therefore, the residual amounts of TFA present in HPLC purified cLP after lyophilisation may have been responsible for its insolubility. In conclusion, these purification techniques may provide useful in the future for protein production and purification for crystallography studies.

4 Protein interactions with defined HA oligosaccharides

4.1 Introduction

In this chapter the interactions of the recombinant proteins with HA or with each other were investigated using gel filtration, multi-angle laser light scattering (MALLS), protein cross-linking and microtitre plates assays. All work was performed with HPLC purified proteins (see Chapter 3) unless otherwise stated.

4.2 Protein-protein and protein-HA interactions

In Figure 4.1a, gel filtration chromatograms are shown for cLP, AG1 and VG1 run individually in the absence of HA. The aggrecan and versican G1-domains gave peaks that eluted at 14.5 and 15.2 min, corresponding to apparent molecular weights of 67 and 45 kDa, respectively, as determined by linear regression analysis using the calibration curve in Figure 4.2a. A molecular weight of ~40 kDa was determined by MALLS analysis on VG1 (Figure 4.3a), which is in good agreement with value obtained from the calibration curve (i.e., 45 kDa). In the case of AG1 the apparent molecular weight (67 kDa) is significantly larger than the estimate from MALLS (33 ±18 kDa; data not shown). This and the absence of AG1 dimers in the protein cross-linking studies (Figure 4.4a) indicate that the aggrecan G1-domain is monomeric, with a non-globular shape. The presence of HA10 did not have a significant effect on the elution positions of either AG1 or VG1 (Figure 4.1a and 4.1b). cLP gave rise to a broad elution profile (~14 min) having an apparent molecular weight of ~80 kDa indicating the possibility of dimer formation (Figure 4.1a). Protein cross-linking experiments (see Figure 4.4a) supported this finding, where cLP forms a cross-linking

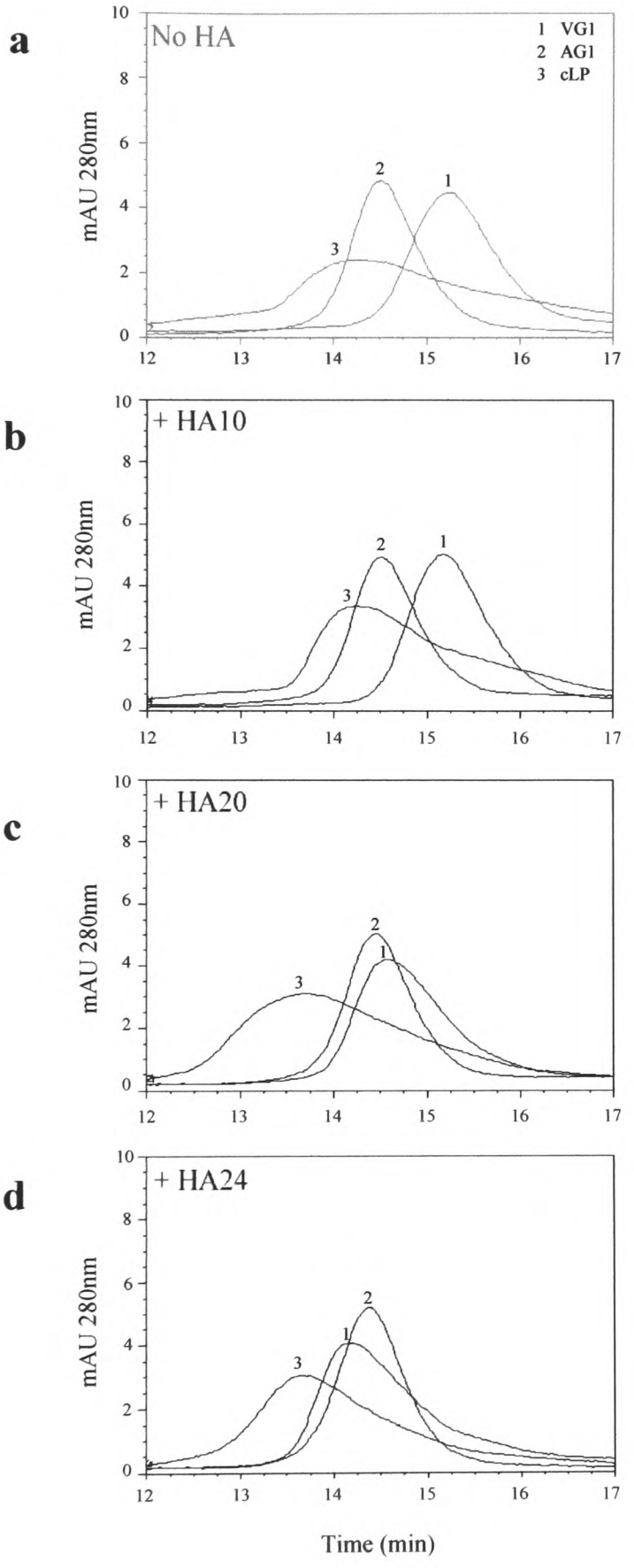

Figure 4.1 Protein-HA interactions in solution using a Biosep-SEC-S2000 gel filtration column. Chromatograms for VG1 (1), AG1 (2), or cLP (3) in the absence (**a**) or presence of HA10 (**b**), HA20 (**c**), or HA24 (**d**) oligosaccharides. cLP and VG1 both exhibit a higher apparent MW in the presence of HA20 or HA24, while the elution position of AG1 remained unchanged.

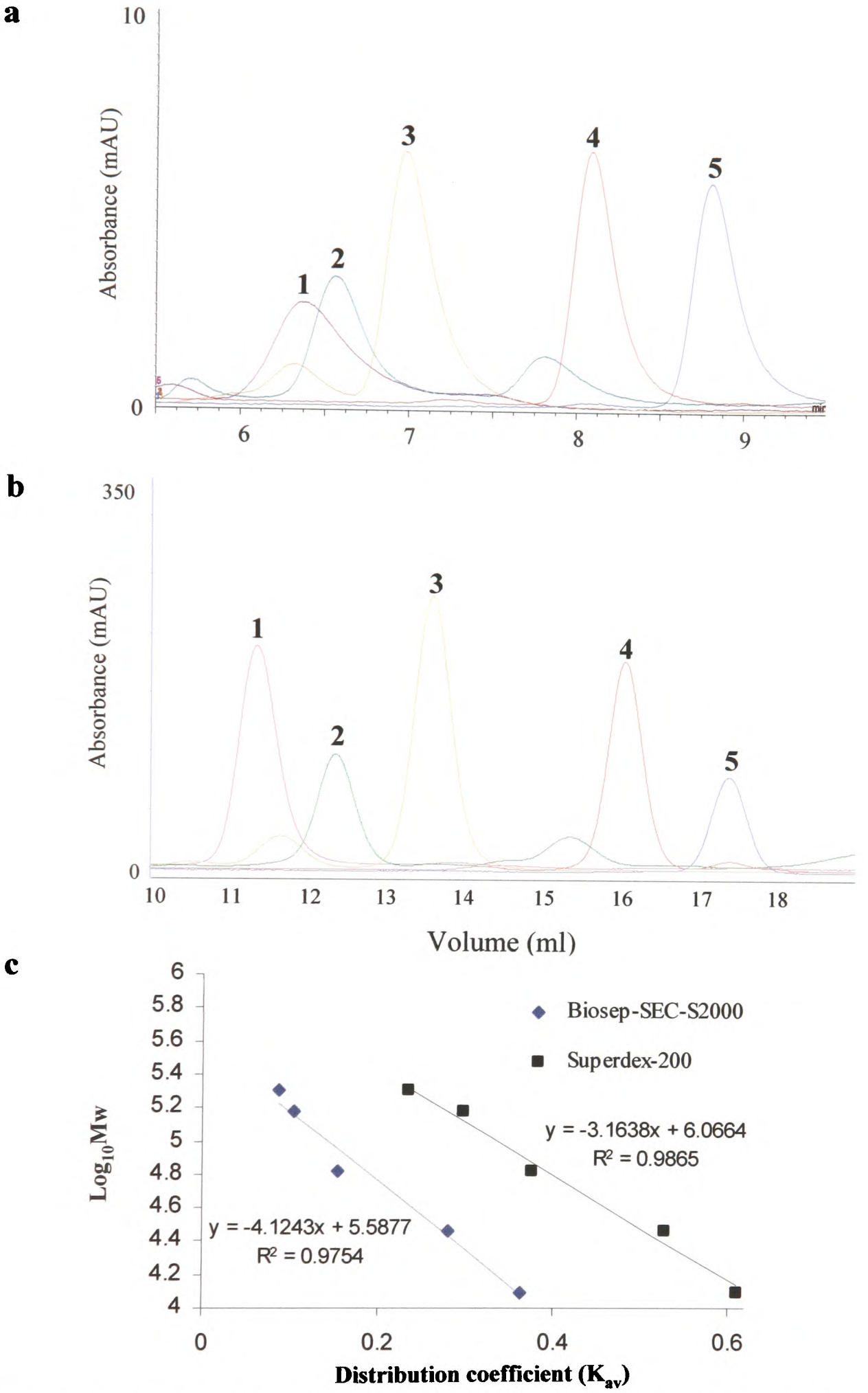

Figure 4.2 Calibration of the gel filtration columns. Globular protein standards of known molecular weight were used to calibrate the Biosep-SEC-S2000 (**a**) and Superdex-200 (**b**) gel filtration columns; the latter being used for MALLS analysis. The standards are ß-amylase (200,000 Da; peak 1), alcohol dehydrogenase (150,000 Da; peak 2), bovine serum albumin (66,000 Da peak 3), carbonic anhydrase (29,000 Da; peak 4) and cytochrome C (12,400 Da; peak 5). **c**) Linear regression analysis of the gel filtration standards. K_{av} values were calculated using the formula $K_{av}= (V_e-V_o)/(V_T-V_o)$ where V_e is the elution volume of the sample, V_T and V_o are the total liquid volume and the void volume of the column, respectively. The y intercept values for the Biosep-SEC-S2000 and Superdex-200 columns (1.2×10^6 Da and 3.9×10^5 Da, respectively) are in good agreement the exclusion values quoted by the manufacturers (i.e., 1.3×10^6 and 3×10^5 Da, respectively). Proteins eluted on the two columns have K_{av} values that differ by only 0.1–0.2 indicating that they have similar separation properties between 12.4 kDa and 200 kDa; this small discrepancy results from the different exclusion limits of the columns.

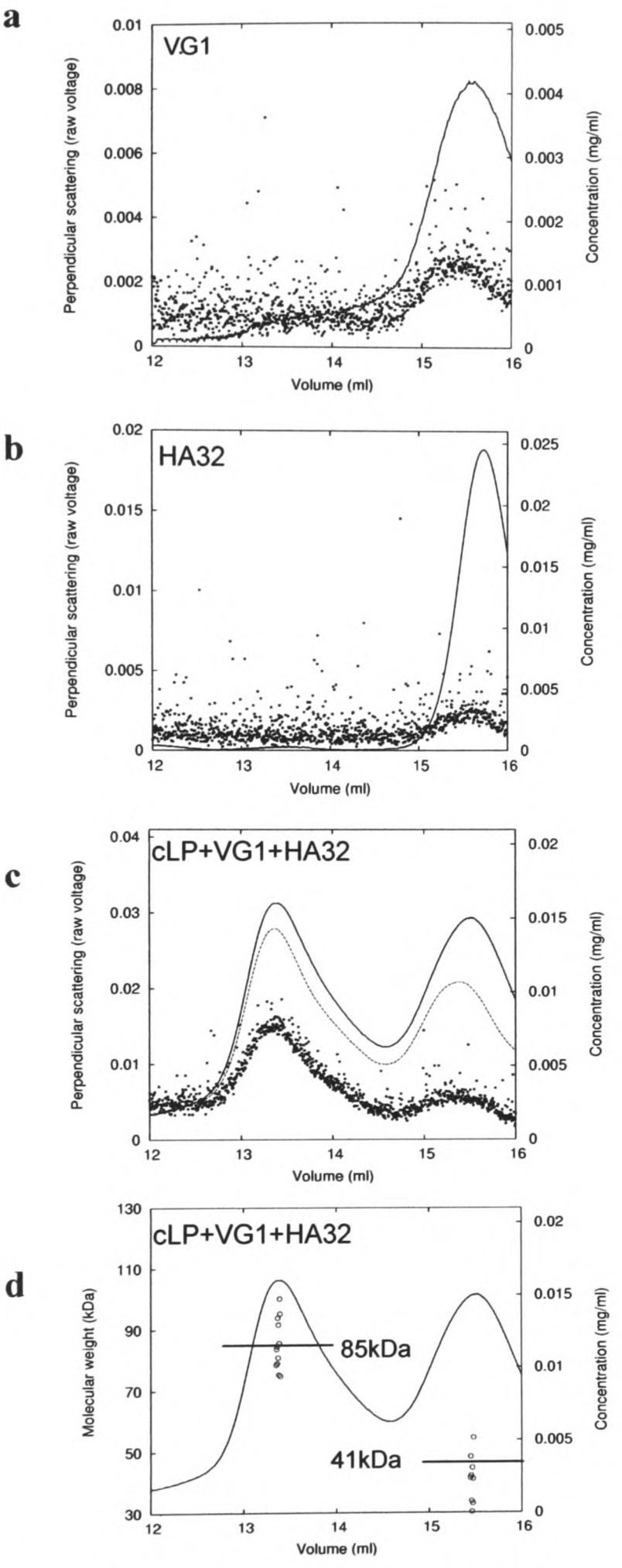

Figure 4.3 MALLS analysis of VG1 and the cLP/VG1/HA32 ternary complex. VG1 (**a**), H32 (**b**) and cLP + VG1 + HA32 (**c**) were run on a Superdex-200 gel filtration column and the eluate (from between 12–16 ml) analysed by MALLS; the perpendicular (90°) scattering (dots), concentration (solid line) and absorbance at 280 nm (dashed line) are shown. (**d**) The scattering data corresponding to the peak apexes of the two major species in (**c**) were used to calculate molecular weights (open circles) by the Debye method (Tanford 1961). The horizontal lines denote the average molecular weight; i.e., 41 kDa ± 5 kDa (S.D.) for VG1 (based on the measured concentration of 15 µg/ml) and 85 ± 5 kDa for cLP/VG1/HA32 (at 17 µg/ml). As can be seen from trace (**b**) HA32 elutes at a significantly higher apparent molecular weight (31 kDa) than would be expected for a molecule of 6 kDa, which is consistent with previous observations of HA's hydrodynamic properties (Almond *et al.*, 1998b).

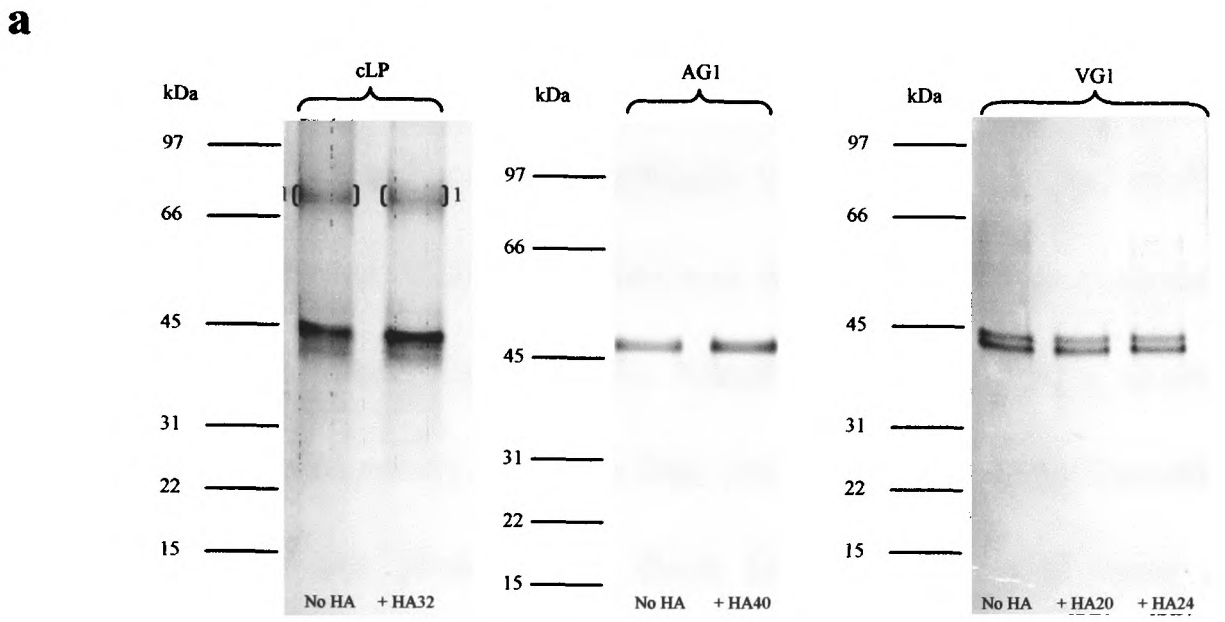

Figure 4.4 SDS-PAGE analysis of protein cross-linking experiments. **a)** The individual recombinant proteins were treated with the BS^3 cross-linker in the absence or presence of HA oligosaccharides (i.e., HA32 for cLP, HA20 or HA24 for VG1, and HA40 for AG1; see text); bands were excised from the gel and proteins identified by in-gel trypsin digestions and mass spectrometry (see Figure 4.9 and Tables 4.1 and 4.2). cLP runs as a dimer (band 1) with or without HA32; no cross-linking products were observed for VG1 or AG1 either in the absence or presence of HA. **b)** AG1/cLP or VG1/cLP mixtures were cross-linked in the absence or presence of HA32. A protein cross-linking product is seen between cLP and AG1 in the absence (band 2) and presence of HA (band 3); the cLP dimer is also seen (band 1) in both cases. Only the cLP dimer was observed (band 4) when VG1 and cLP were crosslinked in the absence of HA. However, a cross-linking product containing both proteins was seen in the presence of HA32 (band 5).

product at ~80 kDa on SDS-PAGE. Therefore, human recombinant cartilage link protein behaves as a homodimer as observed previously for the native protein (Tang *et al.* 1979; Bonnet *et al.* 1985; Thornton *et al.* 1987). The cLP elution profile in the presence of HA10 is less broad (in particular with regard to higher molecular weight species eluting between 12.0-13.5 min) and shows an increased absorbance at the dimer position (~14 min; Figure 4.1b), which supports previous studies where the binding of HA (10-16-mers) to native link protein inhibited the formation of higher oligomers but did not prevent cLP from forming dimers (Bonnet *et al.* 1985; Rosenberg *et al.* 1991). SDS-PAGE analysis of peak fractions collected at the dimeric position (13.5-16.0 min) followed by densitometry indicated that the cLP protein band was more intense in samples containing HA10 compared to cLP alone (Figure 4.5a and 4.5b). Therefore, the observed increased absorbance at 280 nm for cLP in the presence of HA10 is likely to result from an increase in cLP solubility caused by the reduction of the formation of higher oligomeric species and possibly due to an increased solubility.

In the presence of HA20 (3.8 kDa) or HA24 (4.6 kDa) the elution positions for cLP were 13.7 and 13.6 min corresponding to apparent molecular weights of 104 and 109 kDa, respectively (Figure 4.1c and 4.1d). Similarly, VG1 in the presence of these oligosaccharides, also eluted earlier than with HA10 (i.e., 14.6 and 14.2 min) corresponding to 63 and 79 kDa, respectively (Figure 4.1c and 4.1d). This suggests that two molecules of cLP and VG1 can interact with HA20 or HA24, respectively. Additionally, for both cLP and VG1, their apparent molecular masses appear to increase proportionally to oligosaccharide size (Figure 4.6). In contrast, the elution position of AG1 changes only slightly in the presence of 10-, 14-, 20-, or 24-, and 28-,

a

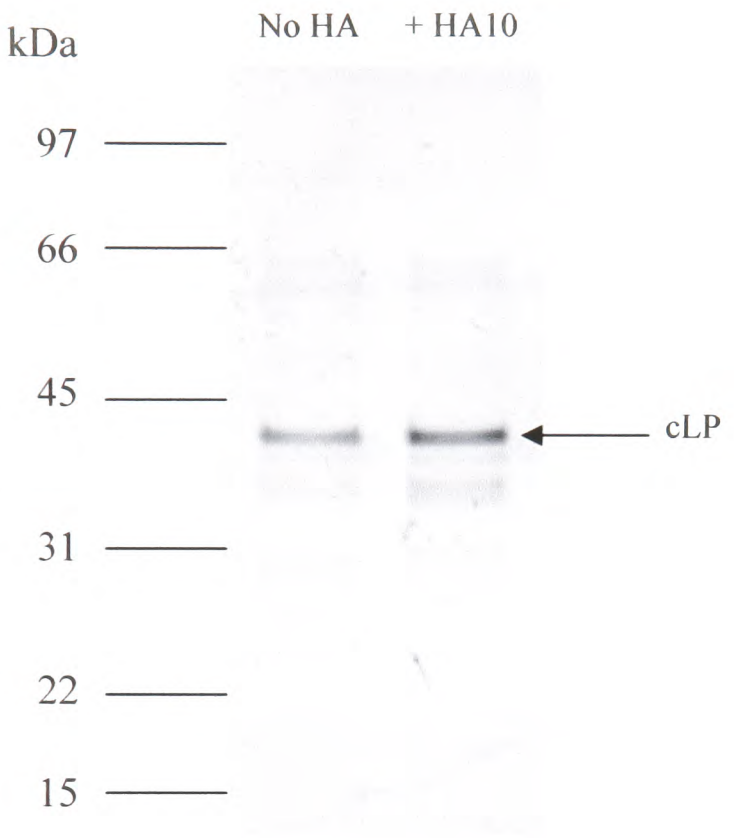

b

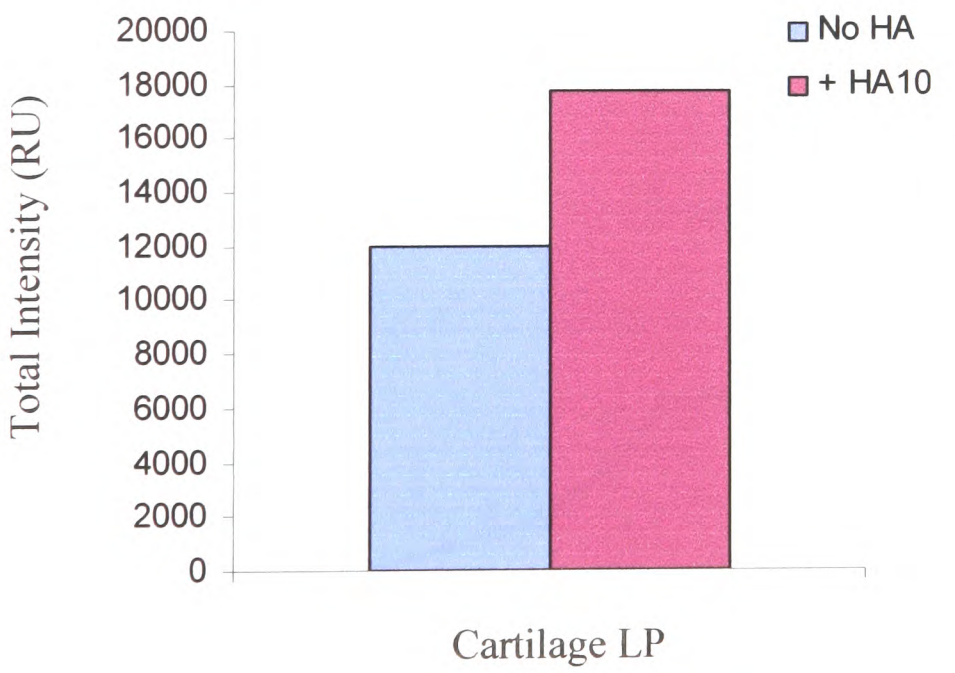

Figure 4.5 (**a**) SDS-PAGE analysis of cLP collected from gel filtration in the absence or presence of HA10 (Figure 4.1a and 4.1b) followed by densitometry using the Scion Image software (**b**). Total intensity was calculated using the equation; (band area) x (band intensity-background intensity) and is displayed in relative units (RU).

a

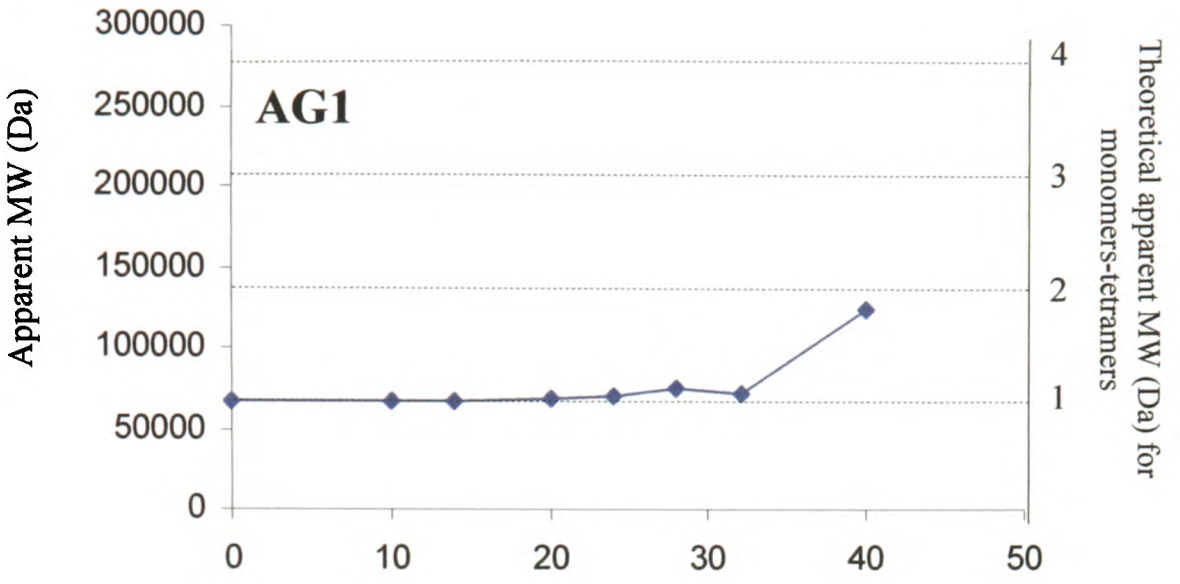

b

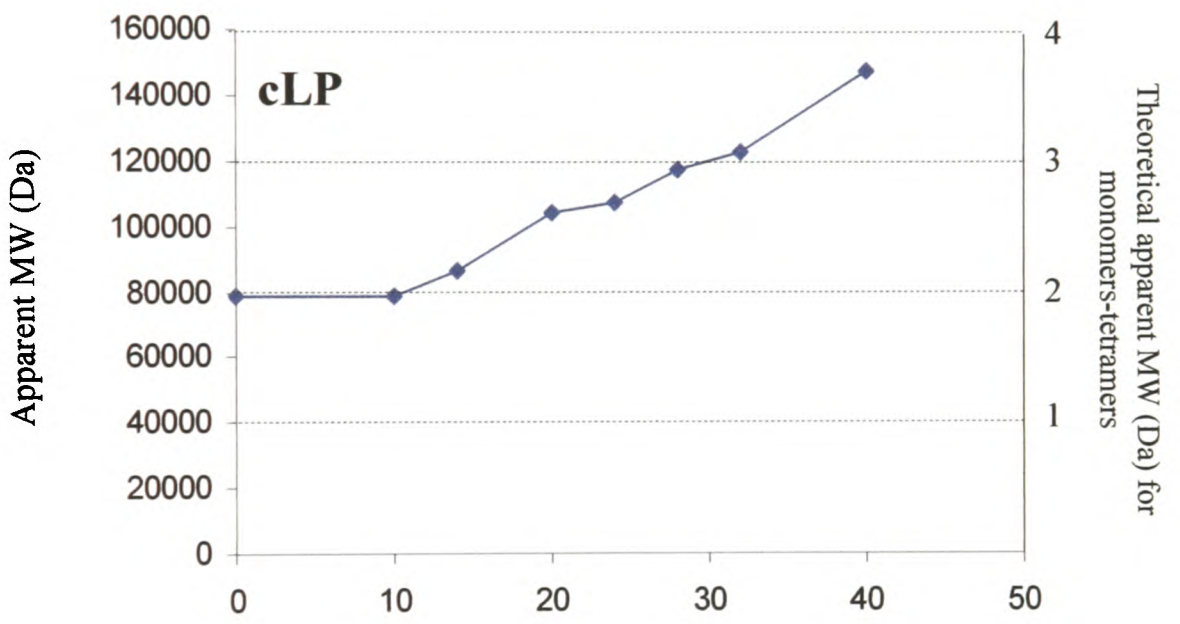

c

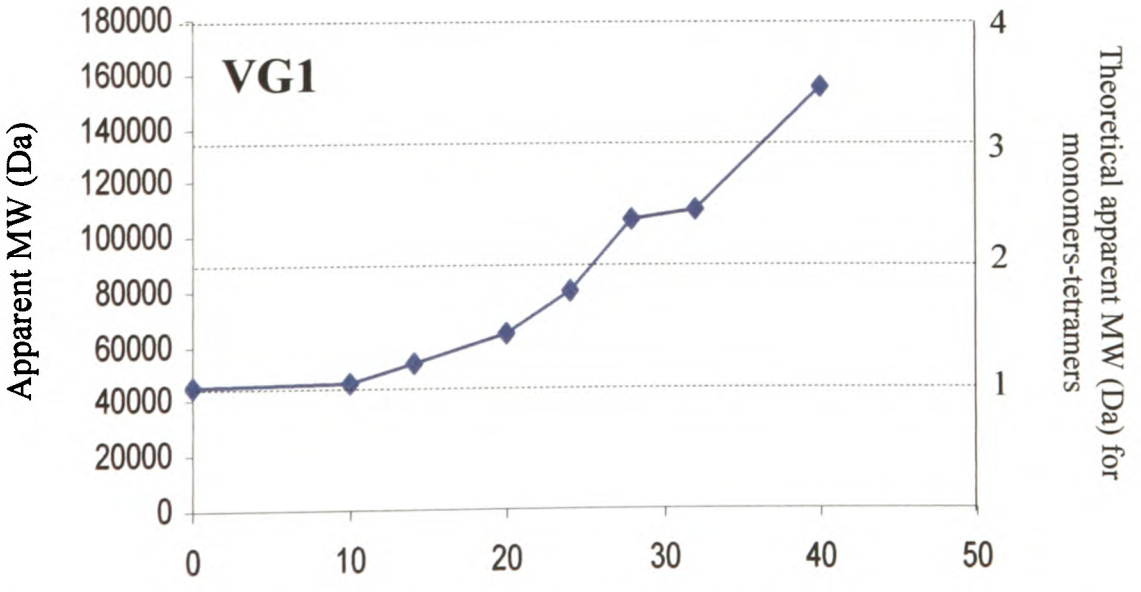

Figure 4.6 The apparent molecular weights derived from the calibration curve in Figure 4.2a (left axis) using the Biosep-SEC-S2000 gel filtration column are plotted against oligosaccharide length (10-, 14-, 20-, 24-, 28-, 32- and 40-mers) for AG1 (**a**) cLP (**b**) and VG1 (**c**). The theoretical molecular weights (dashed line) for 2, 3 and 4 molecules were extrapolated from the monomeric experimental values for AG1 (67 kDa), cLP (40 kDa) and VG1 (45 kDa).

and 32-mers (Figure 4.1 and 4.6). For example, HA32 (~6 kDa) only causes a small shift in the running position of AG1 compared to that in the absence of HA (corresponding to a change of 8 kDa). However, in the presence of HA40 (7.6 kDa) a bimodal peak distribution is observed where the first peak elutes at 13.4 min and the second at 14.5 min corresponding to apparent molecular masses of 122 and 67 kDa, respectively (Figure 4.7 and 4.6). The size of the higher molecular weight species is consistent with it containing two AG1 molecules bound to an oligomer of ~40 sugars in length (the HA40 preparation is likely to be a mixture of HA36-40-mers (Mahoney *et al.* 2001a)) indicating that potentially two AG1 molecules can interact with HA of ~ 40 sugars. From Figure 4.4a, it can be seen that no cross-linking product is formed for VG1 in the presence of HA24 (a size proposed to bind 2 VG1 molecules see above) consistent with a lack of protein-protein interaction between neighbouring versican G1-domains bound to a common HA chain. Similarly, cross-linking experiments on AG1 in the presence of HA40 (Figure 4.4a) also show no protein self-association.

To investigate protein-protein interactions cLP and AG1 were mixed in the absence of HA where a single peak was observed at 13.8 min corresponding to an apparent molecular weight of 98 kDa, which is significantly larger than either cLP or AG1 individually (Figure 4.8a) providing evidence for an interaction between these recombinant proteins in solution. Consistent with this, Figure 4.4b shows that a species of ~90 kDa was formed when cLP and AG1 were incubated together in the presence of a cross-linking reagent (band 2); MALDI-TOF mass spectrometry analysis of this species following in-gel trypsin digestion, identified peptides from both cLP and AG1 (see Figure 4.9 and Table 4.1) confirming that both proteins were

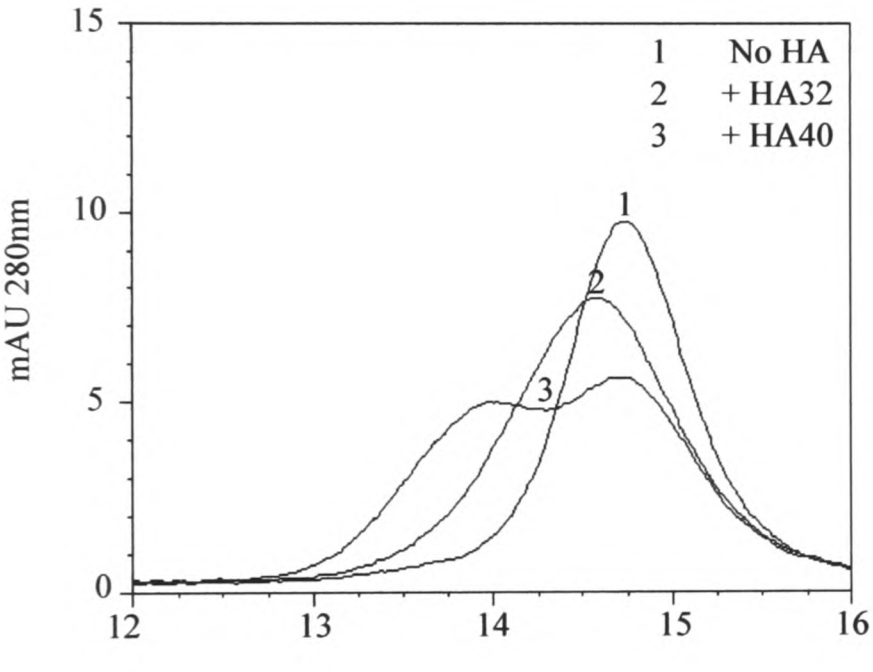

Figure 4.7 Interactions of AG1 with HA oligosaccharides of varying length. Gel filtrations chromatograms for AG1 alone (1) or in the presence of HA32 (2) or HA40 (3).

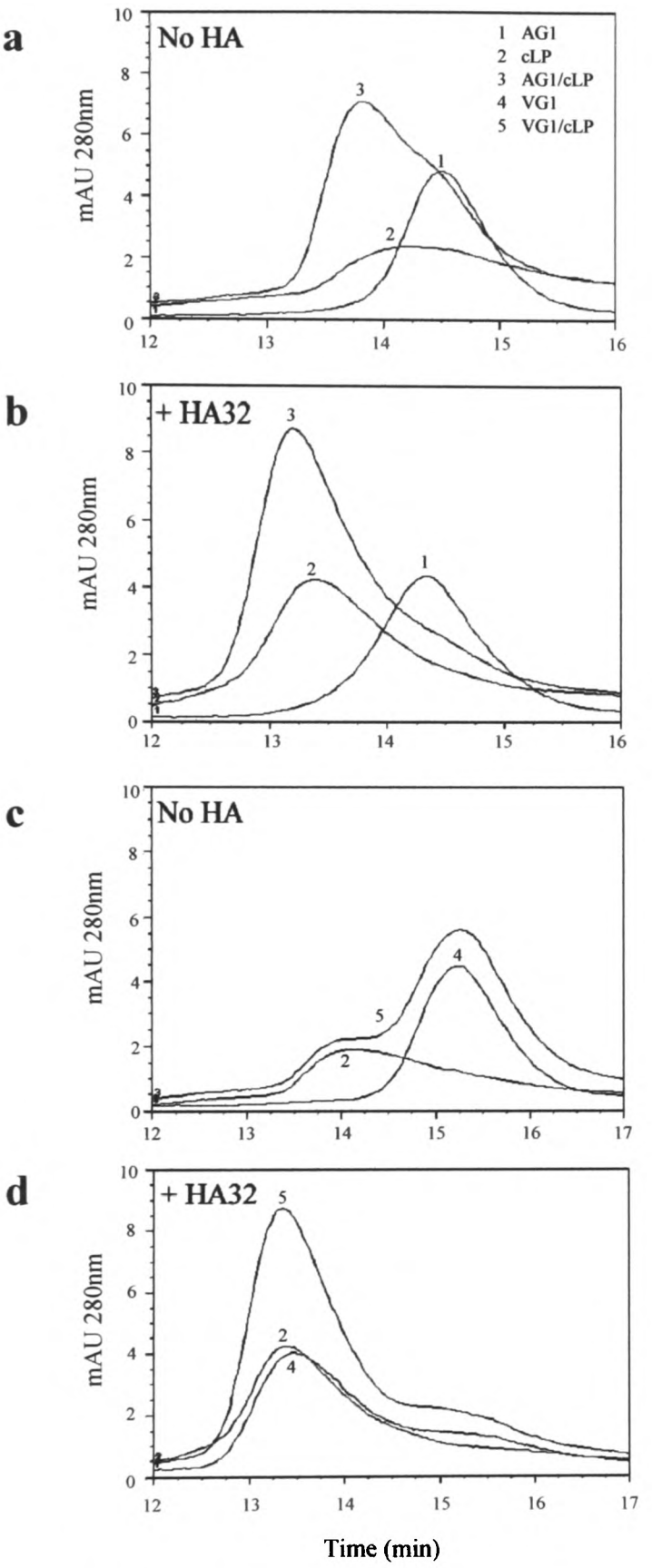

Figure 4.8 Protein-protein interactions and formation of cLP-stabilised complexes. Gel filtration chromatograms for AG1 and cLP run individually ((1) and (2), respectively), or together (3) in the absence of HA (**a**) or presence of HA32 (**b**). **c**) cLP (2) and VG1 (4) run individually or together (5) in the absence of HA. **d**) cLP (2) and VG1 (4) run individually or together (5) in the presence of HA32.

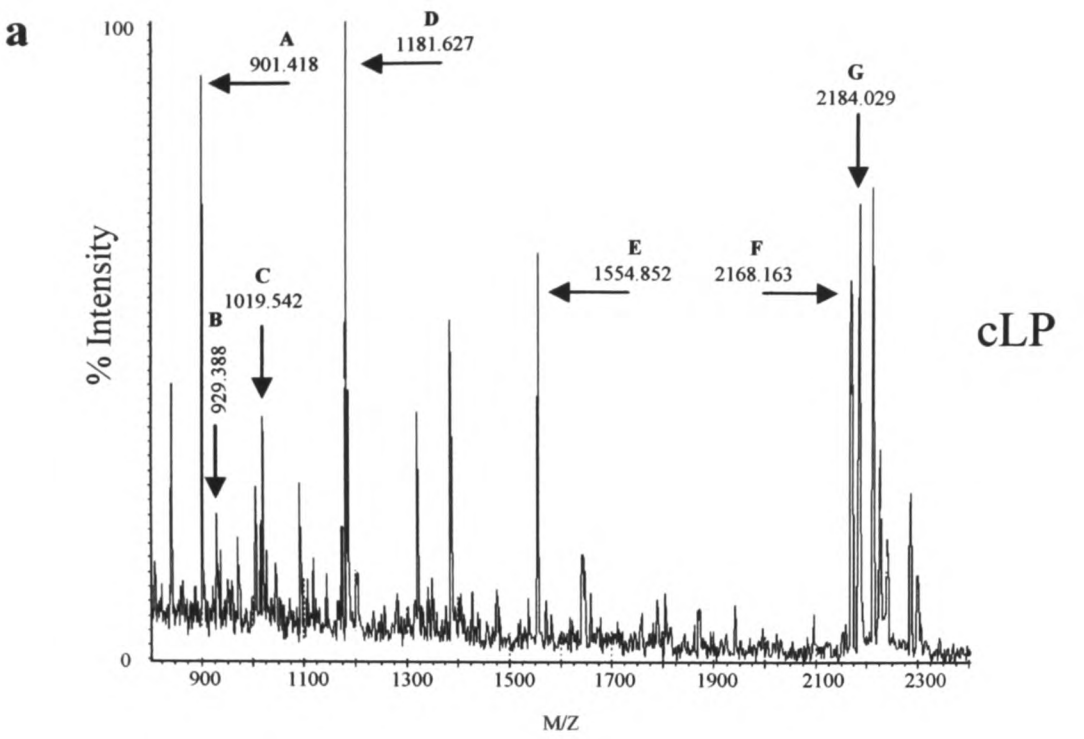

Figure 4.9 Mass fingerprint analysis for cartilage link protein and the G1-domains of aggrecan and versican. The three recombinant proteins were run on SDS-PAGE under reducing conditions (i.e., ß-mercaptoethanol) the bands excised and in-gel digested with tryspin. Mass fingerprints for cLP (**a**), VG1 (**b**) and AG1 (**c**) were obtained using MALDI-TOF mass spectrometry. Specific peptides for cLP (A-G), VG1 (H-O) and AG1 (P-W) were identified using the ProFound™ data analysis software (see Table 4.1). The majority of the unlabelled peaks correspond to either reactive cysteine derivatives (mainly with acrylamide) or keratin contaminants.

Table 4.1 Peptides identified as being cartilage link protein, G1-versican or G1-aggrecan specific are labelled alphabetically below. The residue coverage expectation values were determined using the ProFound™ search engine. The expectation values* for cLP, VG1 and AG1 were 0.008, 0.042 and 0.004, respectively.

Assignment	Expected Mass of Peptide (Da)	Experimental Mass [M+H]	Corresponding Peptide Sequence	Residue Coverage
cLP				
A	900.409	901.434	TYGGYQGR	104-111
B	928.379	929.424	NYGFWDDK	237-243
C	1018.534	1019.541	VGQIFAAWK	289-297
D	1180.619	1181.636	FYYLIHPTK	261-269
E	1553.819[a]	1554.827	EVDVFVSMGYHKK	91-103
F	2167.159	2168.128	AIHQAENGPHLLVEAEQAK	29-48
G	2183.025	2183.976	GGSDSDASLVITDLTLEDYGR	116-136
VG1				
H	941.449	942.456	FTFEEAAK	241-248
I	963.398	964.405	ECENQDAR	249-256
J	1077.612	1078.620	LLASDAGLYR	100-109
K	1183.581	1184.588	YTLNFEAAQK	141-150
L	1313.735	1314.743	LATVGELQAAWR	257-268
M	1385.711	1386.719	ETTVLVAQNGNIK	60-72
N	1490.689	1491.697	FENQTGFPPPDSR	308-320
O	1905.020	1906.027	VSVPTHPEAVGDSLTVVK	81-99
AG1				
P	882.475	883.484	YPIHTPR	192-198
Q	890.504	891.513	GIVFHYR	133-139
R	928.460	929.468	YTLDFDR	145-151
S	1178.639	1179.647	VRVNSAYQDK	75-84
T	1184.725	1185.733	EVVLLVATEGR	64-74
U	1441.850	1442.857	EKEVVLLVATEGR	62-74
V	1890.915	1891.629	TVYVHANQTGYPDPSSR	308-324
W	2269.210	2270.214	VSLPNYPAIPSDATLEVQSR	85-105

[a] peptide has oxidized Met-98

*An expectation value of 0 is a perfect match and a value of 1.0 means that at least 1 similar match would be expected when searching a database that does not include the protein sequence (i.e., less confidence).

present in the cross-linking product (Table 4.2). Furthermore, an interaction is seen between these proteins in microtitre plate assays where either AG1 or cLP are immobilised and incubated with biotinylated cLP or AG1, respectively (Figure 4.10a and 4.10c). This indicates that these human recombinant proteins are able to interact in the absence of HA in both solution and solid phase assays, which has been well established for the native proteins previously (Caterson and Baker 1978; Franzen *et al.* 1981; Thornton *et al.* 1987). However, when cLP and VG1 were mixed, the resulting elution profile is essentially the superposition of the proteins run individually (Figure 4.8c). In addition, only peptides from cLP, which runs as a dimer in the absence of HA, were identified in the cross-linking product (band 4) derived from the cLP/VG1 mixture (see Figures 4.4b, Figure 4.11a and Table 4.2) indicating no direct interaction between cLP and VG1 in solution. However, biotinylated-cLP and biotinylated-VG1 are capable of binding immobilized VG1 and cLP respectively, in a microtitre plate assay (see Figure 4.10b and 4.10c). This is consistent with results obtained by others using recombinant human cartilage link protein and G1-versican in solid phase experiments (i.e., by surface plasmon resonance (Matsumoto *et al.* 2003; Shi *et al.* 2004) and ELISA-like assays (Shi *et al.* 2004)). Plate assays in the presence of 0.5 M NaCl or at pH 5.8 also resulted in a positive interaction between biotinylated-cLP and AG1 or VG1 demonstrating that the high salt strength (0.5 M) used in gel-filtration or the lower pH (5.8) used in the dissociative and associative incubation conditions is not responsible for the lack of the cLP-VG1 interaction (Figure 4.10a and 4.10b). Additionally, removal of the *N*-linked glycans from VG1 did not promote its interaction with cLP in solution; VG1 treated with PNGase F gave essentially the same result as for the untreated material in cross-linking/MS experiments (Table 4.2) indicating that glycosylation was not responsible for the lack

Table 4.2 Protein/protein interactions determined by MALDI-TOF mass spectrometry. Peptides were identified using in-gel trypsin digestion of protein cross-linking products formed in the absence or presence of HA oligosaccharides of defined length.

Cross-linking Product	Link protein Peptides[a]	G1-domain Peptides[a]
cLP/G1-aggrecan[b]		
No HA		
Band 1	A,D,E,F,G	None detected
Band 2	A,D,F,G	P,W
+HA32		
Band 3	A,D,E,F,G	P,Q,W
cLP/G1-aggrecan[c]		
+HA32	A,D,E,F	P,Q,W
cLP/G1-versican		
No HA[b]	A,C,D,E,F	None detected
+HA10	A,B,D,E,F,G	None detected
+HA20	A,B,D,E,F,G	None detected
+HA24	A,B,F,G	L,N
+HA28	A,D,E,F,G	J,L,N,O
+HA32[b]	A,D,E,F,G	J,L,N,O
cLP/G1-versican[c]		
No HA	A,B,D,F,G	None
+HA32	A,C,D,F,G	L,N,O

[a] *Peptides are defined in Table 4.1.*
[b] *Bands excised from SDS-PAGE gels representing cross-linking products in Figure 4.4b.*
[c] *VG1 and AG1 were treated with the PNGase F enzyme.*

a

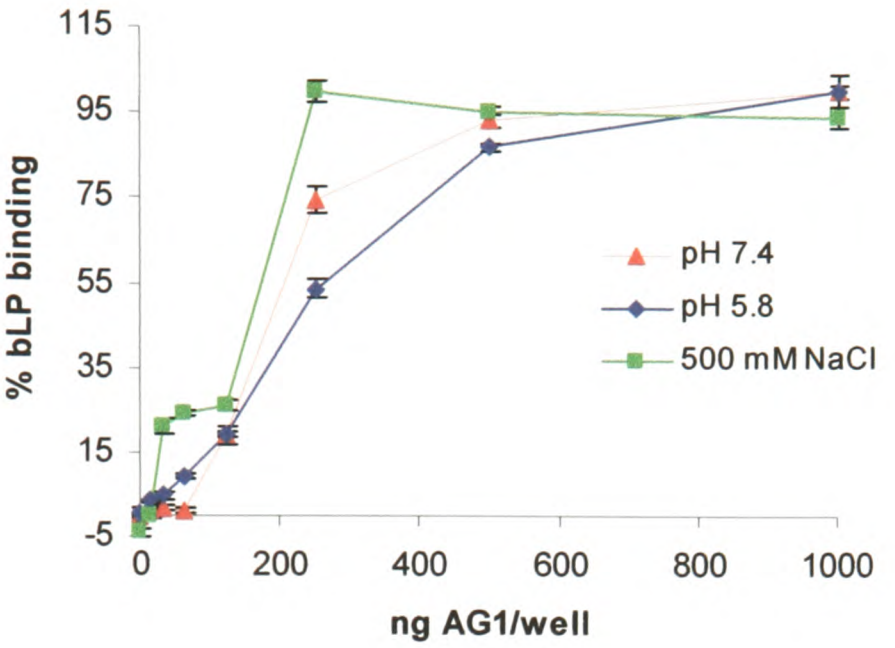

b

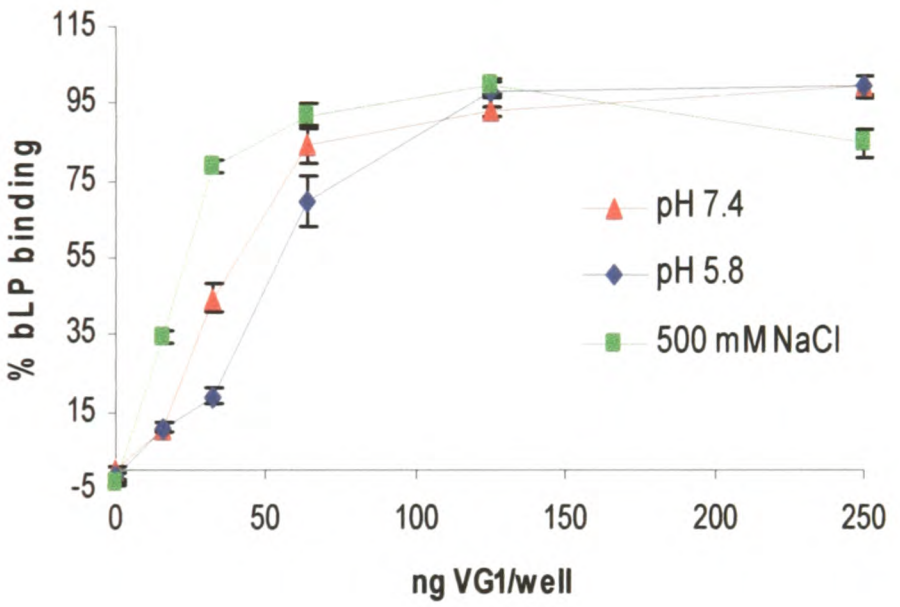

c

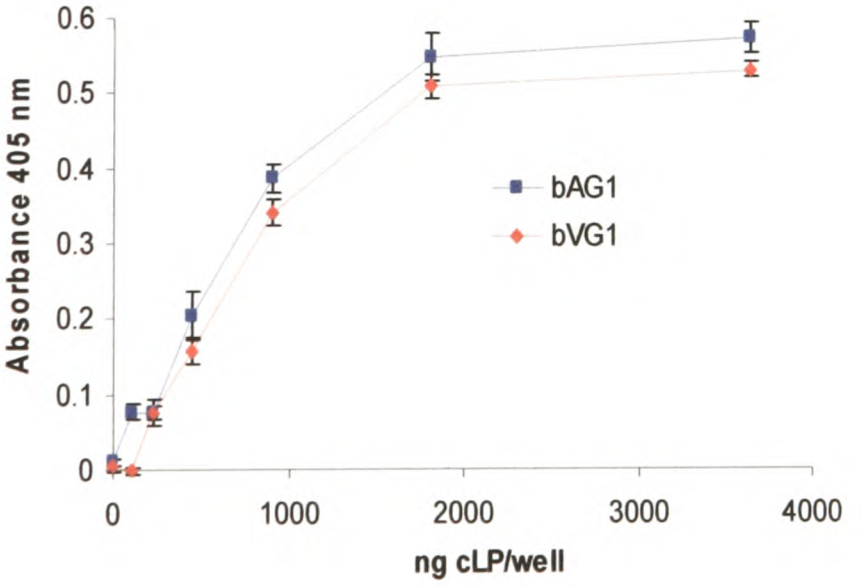

Figure 4.10. Interactions of G1-aggrecan and G1-versican to cartilage link protein. Binding of bLP (6.6 pmol/well) to increasing amounts of AG1 (**a**) or VG1 (**b**) coated on microtitre plates at pH 7.4 and 5.8 or at pH 7.4 with 500 mM salt (see section 2.11.3). Values are plotted as mean percentages of binding (n=4) ±S.E. (**c**) Binding of bAG1 (13.3 pmol/well) or bVG1 3.3 (pmol/well) to increasing amounts of cLP coated on microtitre plates using standard assays buffer conditions. Values are plotted as mean absorbance (n=4) ±S.E.

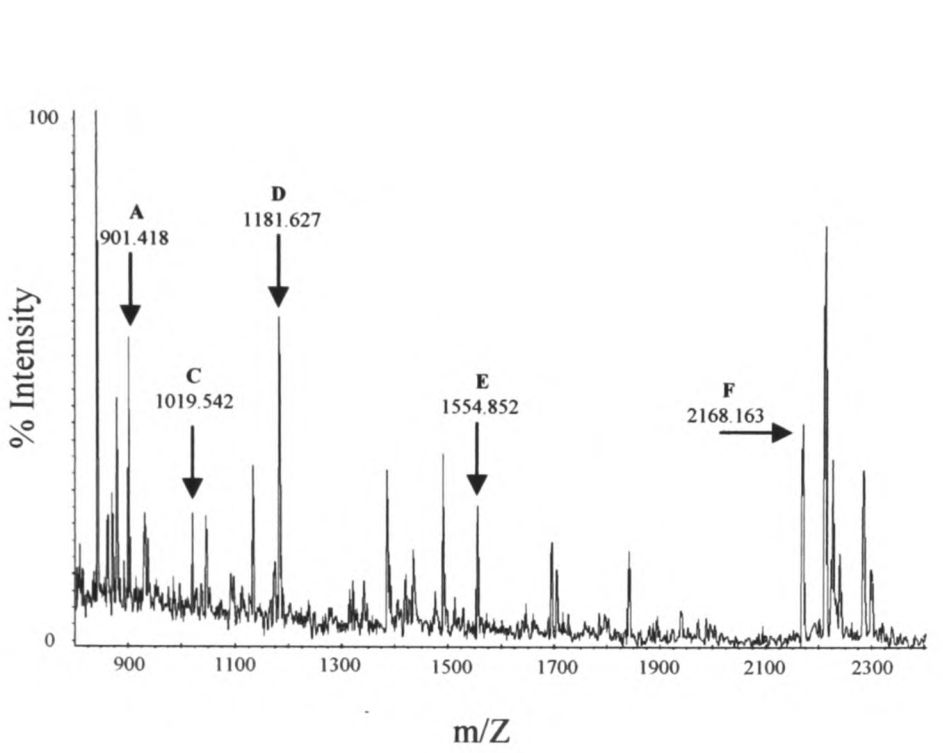

Figure 4.11 MALDI-TOF/MS tryptic peptide map for cross-linking products derived from cLP and VG1 mixtures in the absence (**a**) and presence (**b**) of HA32; these products correspond to bands 4 and 5, respectively, on Fig. 4b. Mass peaks (m/Z) labeled (A-G) represent cLP-specific peptides and mass peaks (H-O) represent VG1 specific peptides as defined in Table 4.1.

of interaction between VG1 and cLP. Therefore, VG1 behaves differently than AG1, where no demonstrable interaction is observed with cLP in solution.

4.3 Formation of link protein-stabilised complexes

The ability of our human recombinant proteins to form ternary complexes was initially assessed by gel filtration where cLP was added to either AG1 or VG1 in the presence of HA32 oligosaccharides. As can be seen from Figure 4.8, the addition of HA32 to the cLP/AG1 mixture produced a peak that shifted to a higher apparent molecular weight (136 kDa) than the peak observed for the cLP/AG1 complex in the absence of HA (98 kDa); panels b and a, respectively. MALDI-TOF MS confirmed that peptides from both cLP and AG1 were observed in the cross-linking product (band 3 on Figure 4.4b) when HA32 was present (see Table 4.2), which has an apparent molecular weight of ~90 kDa on SDS-PAGE (Figure 4.4b) consistent with a 1:1 stoichiometry of cLP:AG1. A similar result was obtained previously with native link protein and the G1-domain of aggrecan (Faltz *et al.* 1979). Interestingly, the cLP/AG1 cross-linking product (band 3) becomes more clearly demarcated and less diffuse in the presence of HA32 (Figure 4.4b). This may be caused by a stronger association of cLP and AG1 in the ternary complex (Hardingham 1979) or a change in orientation allowing more cross-linking by BS^3, which links primary amines separated by ~12 Å. Although no direct interaction is observed between VG1 and cLP on gel filtration (Figure 4.8c), a mixture of cLP, VG1 and HA32 produced a peak that shifted to a higher apparent molecular weight (~122 kDa; Figure 4.8d). Protein cross-linking was utilised to assess if this shift observed in gel filtration represented a cLP stabilised ternary complex. When HA32 was added to the cLP/VG1 mixture, both peptide species were observed in the cross-linking product (band 5 on Figure 4.4b, Figure

4.11b and Table 4.2) indicating that a protein/protein interaction between cLP and VG1 does indeed occur in the presence of HA; and the cross-linking product formed between cLP and VG1 in the presence of HA32 was ~80 kDa (Figure 4.4b), which is consistent with a 1:1 association of these proteins. Further analysis by MALLS determined a molecular weight for the complex of 85 ± 5 kDa (Figure 4.3d), which is in good agreement with the theoretical mass of 86 kDa for a 1:1:1 cLP/VG1/HA32 complex (assuming a value of 40 kDa for both cLP and VG1). Cross-linking experiments with other HA oligosaccharides (i.e., 10-, 20-, 24- or 28-mers) showed that HA24 was the minimum sized oligomer that gave rise to a detectable protein/protein interaction between cLP and VG1 (Table 4.2). This is consistent with the gel filtration data where a single symmetrical peak was seen for cLP and VG1 in the presence of HA24, whereas a bimodal 'superposition' of the individual proteins was observed with HA10 or HA20 (Figure 4.12). Therefore, a HA oligosaccharide of between 22-24 sugars in length is required to facilitate the protein/protein interaction between cLP and VG1. A similar observation was observed with the native aggrecan and link protein by Kimura *et al.* 1979, where HA ~24-mers were the minimum sized oligomers that could compete for complex assembly in rat chondrosarcoma cultures. Finally, treatment of AG1 or VG1 with PNGase F did not affect their ability to interact with cLP in the presence of HA, indicating that glycosylation of these G1 domains is not essential for ternary complex formation (Table 4.2 and Figure 4.13).

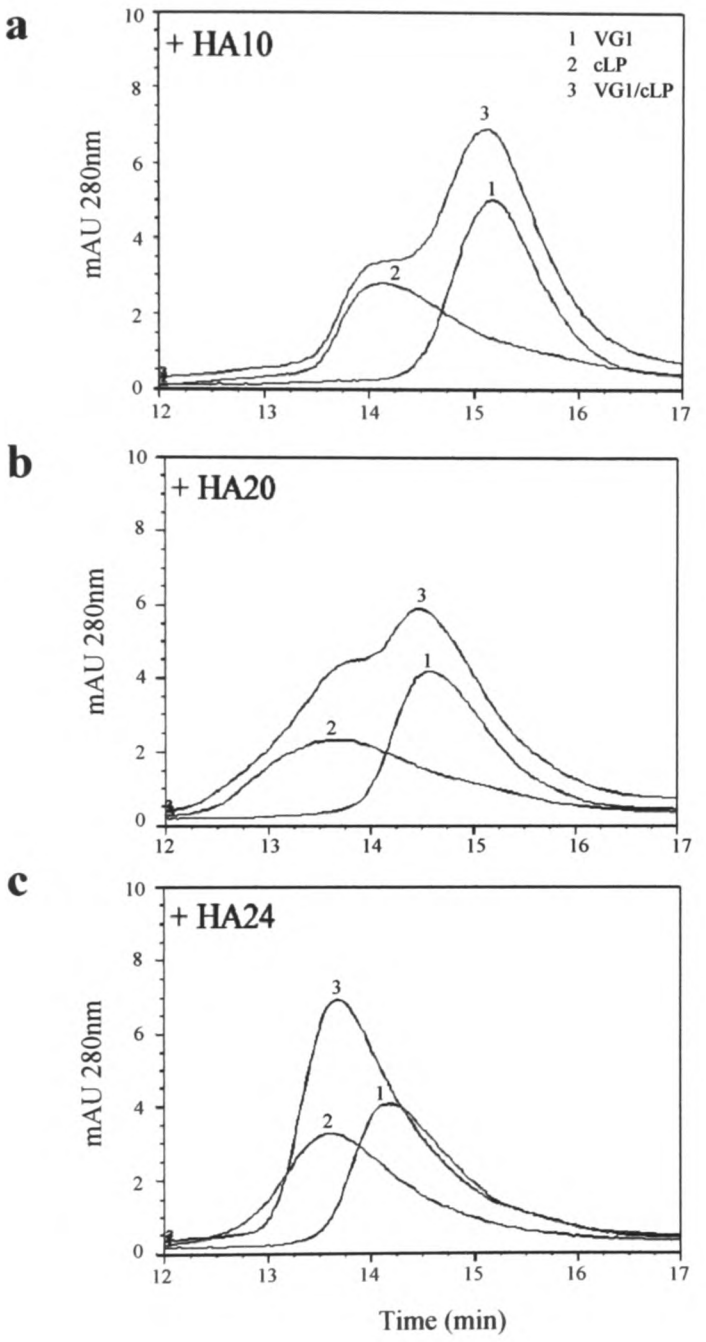

Figure 4.12 Interactions between cartilage link protein and G1-versican in the presence of different sizes of HA oligosaccharide. Gel filtration chromatograms of VG1 and cLP run individually ((1) and (2), respectively) or together (3) in the presence of HA10 **(a)** HA20 **(b)** or HA24 **(c)**.

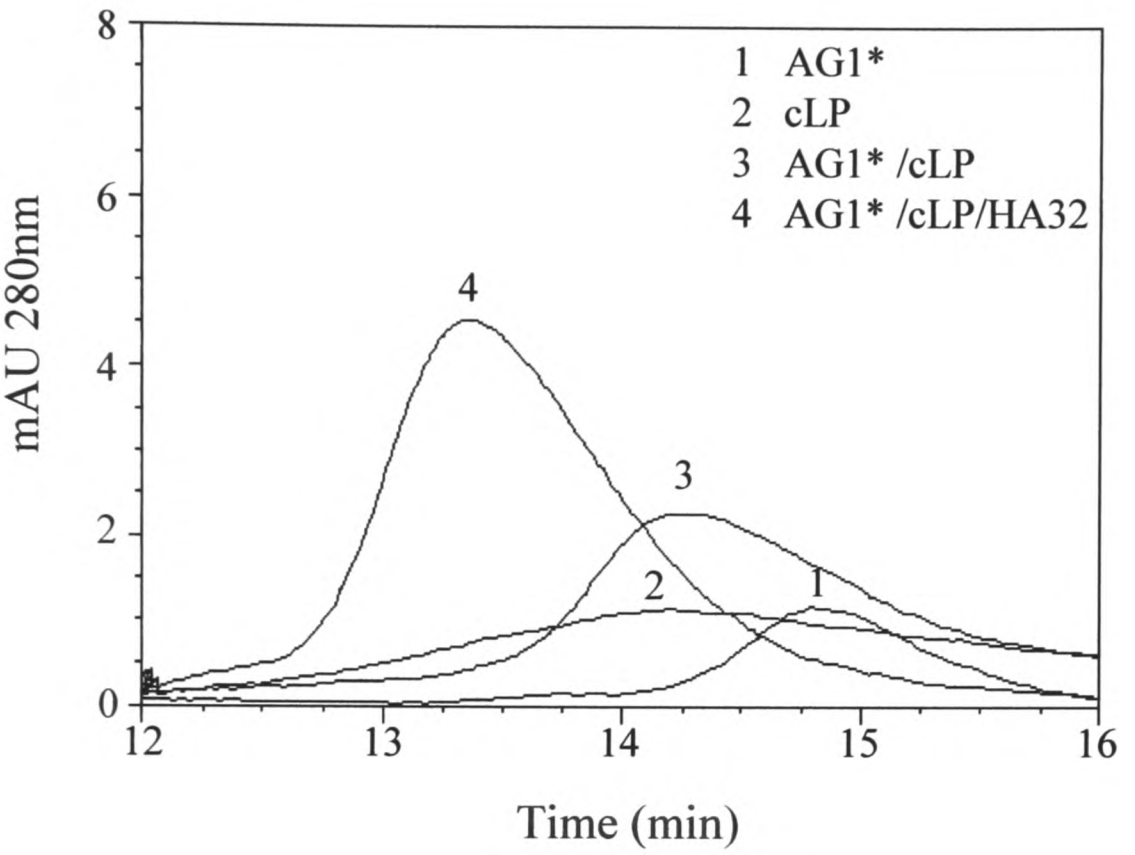

Figure 4.13 Gel filtration experiments were performed to assess the functional activity of PNGase F treated AG1 (AG1*). AG1* (1) and untreated cLP (2) were run individually, or together, in the absence (3) or presence of HA32 (4). AG1* maintained its ability to interact with cLP in the absence and presence of HA32.

4.4 Discussion

The recombinant proteins expressed in *Drosophila* S2 cells displayed properties identical to those reported for the native proteins. For example, cLP formed dimers as described previously for the native bovine and porcine proteins (Tang *et al.* 1979; Bonnet *et al.* 1985; Thornton *et al.* 1987). cLP was also capable of interacting with AG1 in solution and solid phase experiments. In addition, cLP formed stabilised ternary complex with AG1 and in the presence of HA as described previously for the native proteins (Hardingham and Muir 1972; Hascall and Heinegaard 1974a).

The ability of cLP to interact with AG1 in the absence of HA was observed in three different techniques (i.e., gel filtration, cross-linking/MALDI-TOF MS analysis and microtitre plate assays). Although gel filtration is a non-equilibrium technique (i.e., a system where the ligands are separated during the analysis), a shift in the elution position or hydrodynamic volume is nevertheless observed for the AG1/cLP mixture compared to the individual components alone indicating that the proteins can indeed interact prior to analysis. This is not surprising, given that their concentrations in the mixture prior to loading were 375 nM (AG1) and 750 nM (cLP) respectively, higher than the K_d (47-73 nM) for this interaction recently reported in Surface Plasmon Resonance (SPR) analysis (Matsumoto *et al.* 2003; Shi *et al.* 2004). Interestingly, in gel filtration studies, a larger apparent molecular weight is observed for the cLP/AG1/HA32 complex (136 kDa) compared to the mass of AG1/cLP (98 kDa). This may be due to a change in the aggregate dimensions (Buckwalter *et al.* 1984) or increased stability of the proteins upon the formation of a cooperative ternary complex (Hardingham 1979).

In contrast to AG1 and cLP, no interaction between VG1 and cLP is seen in gel filtration or protein cross-linking experiments (performed at equilibrium) where both proteins were at concentrations (635 nM and 750 nM for VG1 and cLP, respectively) above the K_d (16-131 nM) reported for the interaction by SPR (Matsumoto *et al.* 2003; Shi *et al.* 2004). It must also be noted that the lack of interaction between cLP and VG1 is not an artefact caused by HPLC purification of the proteins as when cLP and VG1 were prepared using the Mono-S purification scheme (see Chapter 3) and combined in the absence of guanidine they gave essentially identical profiles on gel filtration to the HPLC purified material (Figure 4.14). Therefore, there appears to be a genuine difference in the association of cLP with AG1 and VG1 in solution. This is supported in the experiments of Shi *et al.,* where co-incubation of cLP and VG1 prior to binding immobilised HA on a SPR sensor chip did not alter the association kinetics compared to those for the individual proteins, consistent with a lack of interaction of these molecules in solution. Conversely, pre-incubation of cLP with AG1, which form a complex in solution, promoted the association of these proteins with HA (Shi *et al.* 2004). However, in solid phase microtitre plate assays, cLP is able to interact with both AG1 and VG1, which is consistent with recent studies using human recombinant cartilage link protein and the G1-domains of aggrecan and versican (Shi *et al.* 2004). Interestingly, Matsumoto *et al.* 2003 report that cLP interacts with VG1 via the double Link modules and not the immunoglobulin (Ig) domain as is the case for AG1. This may underlie the differences seen in this study between cLP and VG1 where the dimerisation state of cLP could potentially mask its direct interaction with VG1 in solution via the double Link modules. Therefore, a reduced level of dimer formation at the lower concentration used in plate assays (Rosenberg *et al.* 1991), modification of lysine residues (Bonnet *et al.* 1985) with biotin or

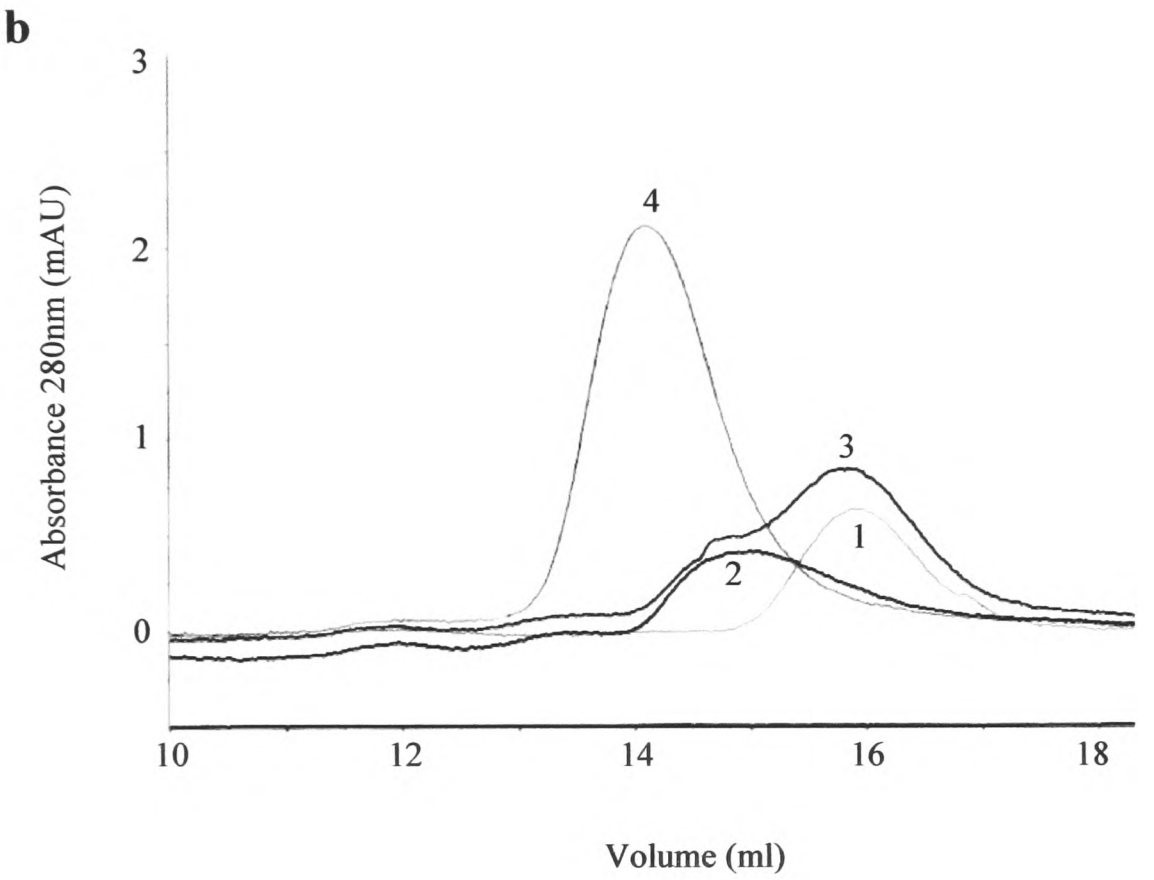

Figure 4.14 Biosep-SEC-S2000 gel filtration using Mono-S purified cLP (163 nM) and VG1 (500 nM). Chromatograms of VG1 and cLP run individually ((1) and (2), respectively) or together in the absence (3) or presence of ~2 M excess HA32 (4).

immobilisation of cLP on the microtitre plate could potentially disrupt dimerisation and unmask the potential binding site resulting in the positive cLP interaction with VG1. Native cartilage link protein has also been proposed to contain two sites of self-association, one of which is abolished when link protein binds HA10-16-mers (Bonnet *et al.* 1985). Given the similarities between the native and recombinant cLP, it was thought possible that the binding of HA to cLP and/or VG1 might effect a conformational change in their HA-binding domains (as occurs for TSG-6 (Blundell *et al.* 2003)) allowing a protein-protein interaction to occur. However, no change in the gel filtration profile or protein cross-linking was seen for cLP/VG1 in the presence of HA10 (i.e., a size of HA of insufficient length to accommodate both proteins on a single chain); see Figures 4.4a and 4.12a and Table 4.2. However, in the presence of longer HA oligosaccharides (>HA22-24) an association binding site in cLP may become unmasked allowing VG1 to interact, forming a link protein stabilised complex as observed and cross-linking experiments and supported by MALLS (Figure 4.3 and Table 4.2).

Large differences in elution position were also observed with the individual proteins in the presence of HA oligosaccharides above a certain length that could be interpreted as changes from monomeric to multimeric binding. It must be noted that the concentration of AG1 (375 nM) loaded on the column was higher than the K_d values previously reported for the monomeric binding of AG1 (17-42 nM) to HA oligosaccharides (10-18-mers) by equilibrium dialysis in solution (Cleland 1979; Nieduszynski *et al.* 1980). In addition, individual concentrations loaded on the column for cLP (750 nM) and VG1 (635 nM) were also higher than then K_d (10-40 nM) established for native link protein to HA in solution (Lyon and Nieduszynski

1983) and human recombinant versican (4-18 nM) binding to HA either by equilibrium dialysis (LeBaron *et al.* 1992) or SPR (Matsumoto *et al.* 2003; Shi *et al.* 2004), respectively. Although some non-equilibrium effects cannot be ruled out, it was expected that the HA-protein complexes formed would elute close to their stoichiometric positions. VG1 for example, has an apparent molecular weight of 45 kDa by gel filtration in the absence (~40 kDa from MALLS) or presence of HA10, but shifts to an apparent molecular weight of 79 kDa in the presence of HA24. Therefore, HA24 appears to be capable of accommodating two molecules of VG1. In fact, for VG1 the hydrodynamic volume increases proportionally to oligosaccharide length (Figure 4.6c), where the apparent molecular weights of VG1 in the presence of HA 24-, 32- and 40-mers are 79, 109, and 155 kDa (Figure 4.6c), respectively. Using the apparent molecular weight for VG1 derived from gel filtration (45 kDa), the ratio of VG1 molecules to HA 24, 32- and 40-mers are 1.8, 2.4, and 3.4 VG1, respectively indicating the possibility of multimeric binding of VG1 to oligosaccharides with increasing size. A similar conclusion was derived previously for native hyaluronectin and HA oligosaccharides (Courel *et al.* 2002). However, in this case the number of hyaluronectin molecules was proportional to the number of decasaccahride units (the minimum sized that can accommodate VG1 binding (see section 3.5.1)) within the HA oligosaccharide. For example, HA 10, 20 and 40-mers can accommodate 1, 2 and 4 hyaluronectin molecules, respectively (Courel *et al.* 2002). The lack of a VG1 cross-linking product in the presence of HA24 suggests that this potential multimeric interaction with the sugar may not be mediated by protein-protein interactions. This is in contrast to the cooperative complex formed with VG1, cLP and HA observed in MALLS (Figure 4.3c and d) or cross-linking (Figure 4.4b and Table 4.2). For cLP individually, a change from ~80 to ~100 kDa is observed in the presence of HA20

suggesting that the oligosaccharide can accommodate only two cLP molecules (Figure 4.6b). Interestingly, the change in apparent molecular weight might result from cLP rearrangement when bound to the oligosaccharide (i.e., forming an asymmetric complex). Further experiments using MALLS will be needed to support this hypothesis. Using 40 kDa as the monomeric value for cLP (half the apparent molecular mass of the dimer), the ratio of cLP molecules to HA 24, 32- and 40-mers are 2.5, 3.1, and 3.7, respectively (Figure 4.6b). Therefore, like VG1, there it seems likely that multimeric binding of cLP to HA oligosaccharides occurs with increasing size.

In contrast to the results for cLP and VG1, HA20, HA24 and HA32 were unable to accommodate the binding of two AG1-domains (Figure 4.6a and 4.7). However, HA of ~40 sugars in length appears to support the interaction of two aggrecan molecules, but even in this case there was a significant amount of free AG1 (i.e., an apparent molecular mass of 67 kDa), which may be a result of insufficient amounts of HA40 in the reaction mixture. It seems likely that the binding of aggrecan to HA 'footprints' a considerably larger region of HA than either cLP or VG1 where AG1 potentially stabilises a HA conformation that inhibits the binding of another adjacent AG1 molecule (i.e., negative cooperativity). However, it is clear that AG1 binding to HA does not affect the interaction of a neighbouring link protein molecule (i.e., cLP and AG1 can both bind to HA32 (Figure 4.8b and 4.4b)). This is interesting since it has been reported that the G1-domain of AG1 binds HA in a random manner leaving free HA between bound molecules (Morgelin *et al.* 1988; Morgelin *et al.* 1995). It was determined from these electron microscopy studies that HA undergoes an apparent shortening on interaction with AG1, where the closest centre-to-centre distance

between adjacent G1-domains is 12 nm or approximately 50 sugars (Morgelin *et al.* 1995). This supports the gel filtration experiments where it appears that ~20 sugars are free between each bound AG1 molecule.

In summary, the interactions with cLP with AG1 or VG1 were compared in solution and in solid phase experiments. Unlike, AG1, in the absence of HA, VG1 did not interact in solution phase (gel filtration and protein cross-linking) with cLP. However, VG1 could form protein-protein ternary complexes with cLP in the presence of HA oligosaccharides of ≥24 sugars in length. In addition, the length of HA required to accommodate two G1-domains was different for versican and aggrecan. These studies indicate that there are considerable complexities in the details of link protein/CSPG interactions and this may lead to aggregates with HA of diverse quaternary structure.

5 Preparation and application of fluorescent HA oligosaccharides

5.1 Introduction

Hyaluronan oligosaccharides have diverse and interesting biological functions both *in vitro* and *in vivo*, such as induction of angiogenesis (Slevin *et al.* 2002), regulation of macrophage inflammatory responses (Noble *et al.* 1996) and suppression of tumour growth (possibly by disrupting endogenous CD44 HA-receptor binding to its ligand (Toole 2004)). In addition to these cellular activities, HA oligosaccharides of defined length can be used to characterise HA-protein interactions as discussed in chapters 3 and 4.

Polymeric HA can be digested with testicular hyaluronidase to yield even-numbered saturated oligosaccharides (HA4 being the shortest produced). The resultant oligomers are then typically purified by size exclusion chromatography (Hardingham and Muir 1973; Hascall and Heinegaard 1974b; Lesley *et al.* 2000) or anion-exchange chromatography (Almond *et al.* 1998b; Mahoney *et al.* 2001a; Tawada *et al.* 2002; Blundell *et al.* 2004a). Proper characterisation of HA oligosaccharides after preparation is essential to ensure purity and homogeneity prior to experimental use. This is of particular importance since attention has been drawn to the possibility of contaminants in HA preparations which may effect the results of experiments (Mahoney *et al.* 2001a). One highly sensitive technique to assess oligosaccharide purity is fluorophore-assisted carbohydrate electrophoresis (FACE). This procedure introduces a fluorophore at the reducing end carbohydrate by reductive amination

(Starr *et al.* 1996) prior to electrophoresis (see Figure 5.1). The choice of fluorophore is of particular importance because it may affect some of the physical properties of the oligosaccharide, or in the case of short oligomers the biological activity (i.e., protein binding) and therefore have a direct consequence on its experimental performance. This chapter describes the advantages of using the fluorophore 2-aminobenzoic acid (2AA; see Table 5.1) in the preparation and application of fluorescent HA oligosaccharides for use in a range of analytical techniques (i.e., FACE, MALDI-TOF mass spectrometry, electrophorectic mobility shift assays (EMSA) and fluorimetry).

5.2 Preparation of hyaluronan oligosaccharides

HA oligosaccharides of between 4 and 10 saccharides were prepared as described in (Blundell *et al.* 2004a), where medical grade hyaluronan was digested with 100 U of enzyme per milligram of HA for 3 h at 37 °C and purified by anion-exchange using a linear gradient of 0 mM–100 mM NaCl. Here, in order to maximize the production of longer length oligosaccharides (~20-40-mers), hyaluronan was resuspended at 1 mg/ml and partially digested with varying amounts of ovine testicular hyaluronidase (1, 5 or 10 U of enzyme per milligram HA) for 1 hr at 37 °C as described in section 2.15. Digests were analysed with anion-exchange chromatography employing a logarithmic ionic elution gradient (Figure 5.2). Peaks representing various even length oligosaccharides were present after treatment with 5 and 10 but not 1 U enzyme per milligram HA (Figure 5.2). Oligosaccharide lengths were estimated by counting peak fractions, which was made difficult by the presence of an unexpected high UV absorbing contaminant (black arrow; Figure 5.2). Subsequent digests and purification were performed using a different Milli-Q water source which eliminated this contaminant. More importantly the logarithmic gradient was capable of maintaining

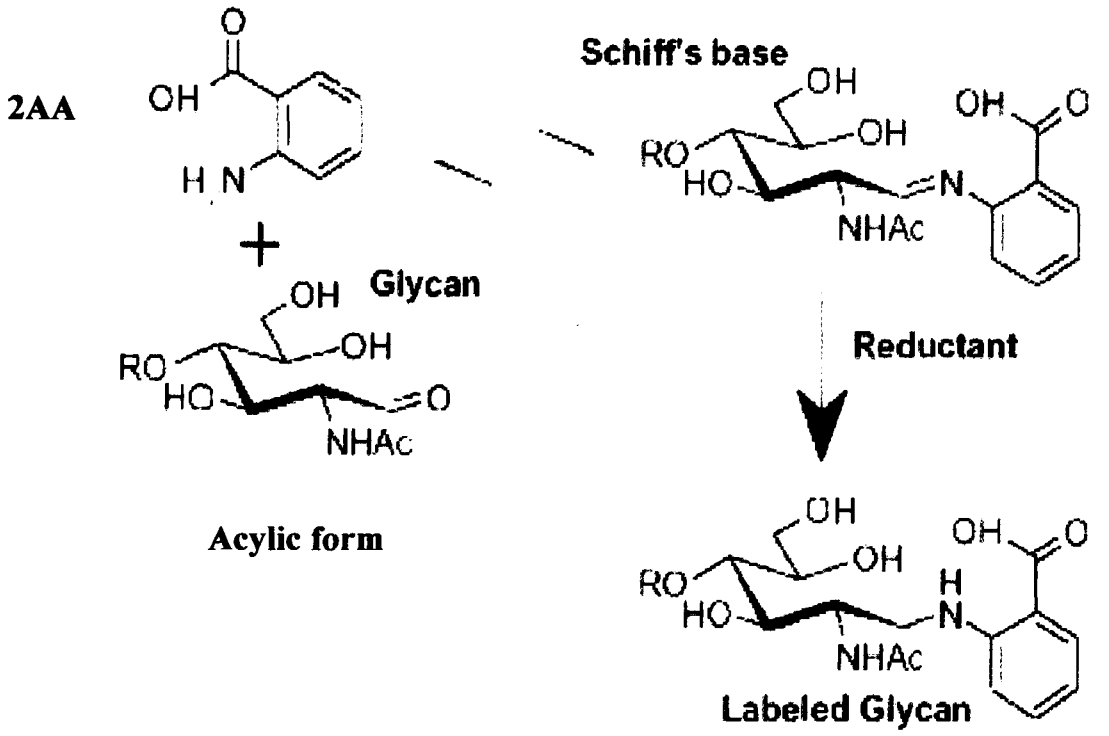

Figure 5.1 A schematic representation of the reductive amination reaction with the fluorophore 2-aminobenzoic acid (2AA). The labelling reaction involves a two step process. The first is the Schiff's base formation, which requires a glycan (R=linked saccharides) with a free reducing sugar that is in equilibrium between the ring closed (cyclic) and ring open (acyclic) forms. The low pH (~2) caused by the acetic acid in the reaction buffer opens the ring. This allows the primary amine group of the 2AA to perform a nucleophilic attack on the carbonyl carbon of the acyclic reducing sugar residue to form a partially stable Schiff's base. The second step is the reduction where the Schiff's base imine group is chemically reduced by cyanoborohydride to give a stable 2AA-labelled glycan. The information and picture was compiled from the ProZyme, Inc. product data sheet for 2-aminobenzoic acid.

Table 5.1 The properties of various fluorophores that have been reported to label glycans.

Fluorophore	Structure	Charge	M_r	λ Excitation	λ Emission
2- aminobenzoic acid (2AA) (Bigge *et al.*, 1995)	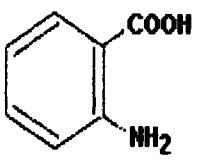	negative	137.1	330 nm[a]	425 nm[a]
2-aminoacridone (AMAC) (Calabro *et al.*, 2000a)	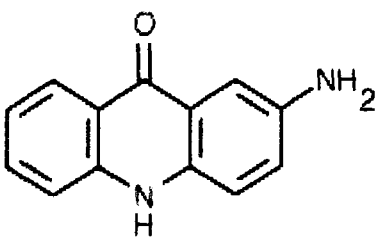	neutral	210.2	425 nm[b]	530 nm[b]
8-amino-1,3,6-naphtalene trisulphonic acid (ANTS) (Jackson *et al.*, 1994)	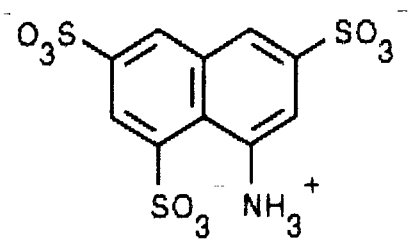	negative	381.33	353 nm[b]	520 nm[b]

[a] taken from Ito *et al.*, 1998
[b] taken from molecular probes website (http://www.probes.com)

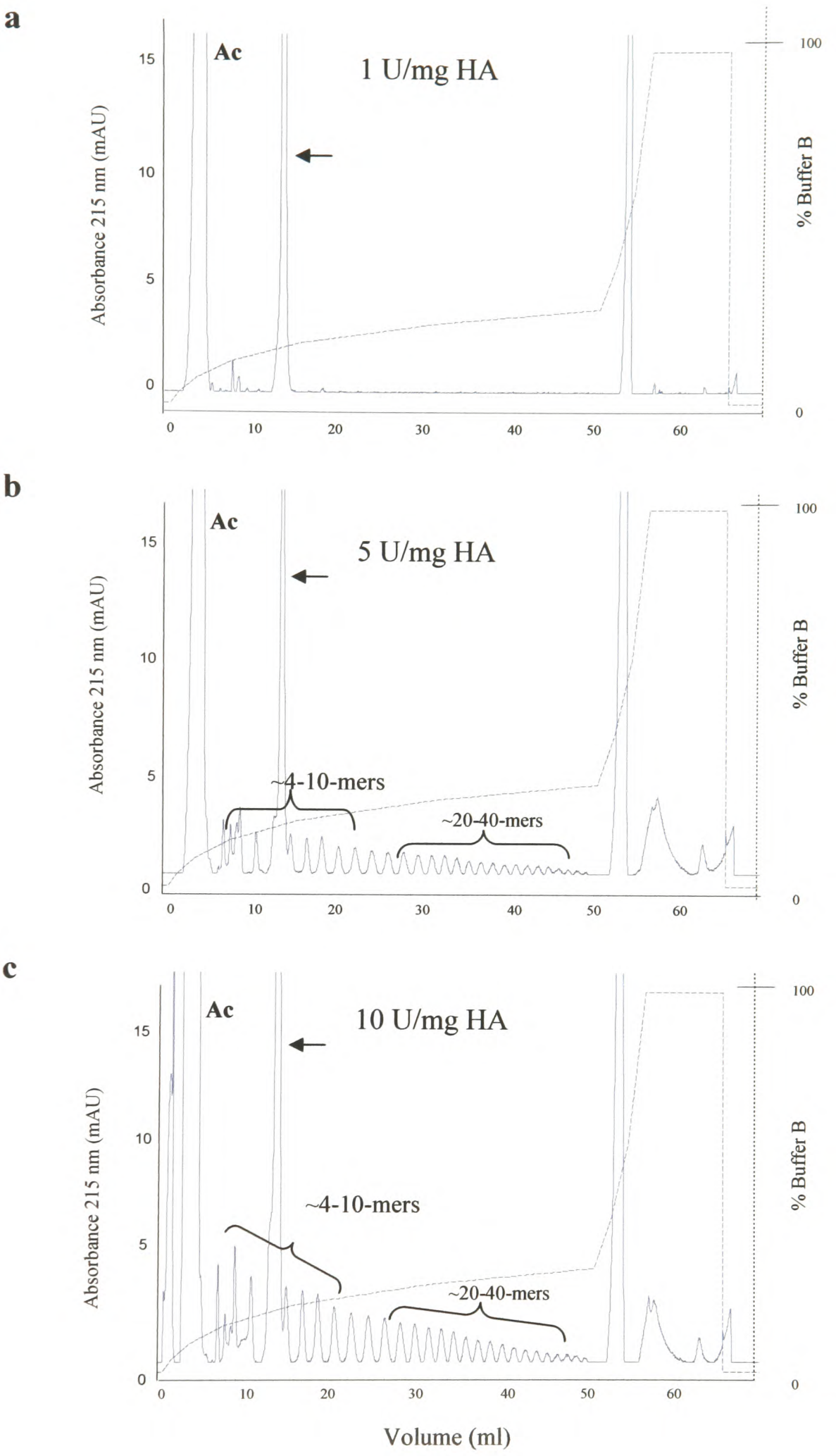

Figure 5.2 Equivalent amounts (200 µg) of polymeric hyaluronan (1 mg/ml) digested with 1 U (**a**), 5 U (**b**) or 10 U (**c**) ovine hyaluronidase for 1 hr at 37 °C were analysed by anion-exchange chromatography. Oligosaccharides were eluted with a logarithmic NaCl gradient (dashed line) and sizes estimated by counting the peaks. The acetate peak (Ac) and the high UV absorbing contaminant (arrow) are indicated. The logarithmic gradient was run at 1 ml/min and buffer B is 1 M NaCl.

equidistant separation of even numbered HA oligosaccharides up to at least to 40-mers, and perhaps longer. An increase in peak signal (~2-fold) at 215 nm for the longer length oligosaccharides was observed with 10 U compared to 5 U of enzyme (Figure 5.2) indicating that the former enzyme concentration was a more effective for the production of longer length oligosaccharides. Therefore, all subsequent hyaluronan digestions were performed with 10 U of enzyme per milligram HA, which were then fluorescently labelled with 2AA by reductive amination prior to purification using essentially identical conditions (Figure 5.3a and b). An equivalent separation of oligosaccharides was observed after 2AA derivatisation; a HA 10-mer made and characterised in Blundell *et al.* 2004a, labelled with 2AA was used to calibrate peak elution positions (Figure 5.3c). In addition a ~2-fold increase in absorbance at 215 nm was seen after fluorescent labelling with 2AA compared to the same amount of underivatised digest, which greatly facilitated peak detection. This is not surprising since 2AA has a significant optical absorbance between 200-220 nm (Ito *et al.* 1998). The absorbance could also be selectively monitored at 330 nm, a wavelength specific for the fluorophore (Ito *et al.* 1998), although this was less sensitive than at 215 nm (Figure 5.3b). Thus, the combination of 2AA labelling and a logarithmic gradient enhanced both the separation and identification of oligosaccharide peaks.

5.3 Fluorophore assisted carbohydrate electrophoresis (FACE)

Carbohydrate electrophoresis of peak fractions from ion exchange (Figure 5.3) was performed on large gels (12 cm x 14 cm) to allow all 2AA labelled oligosaccharides to be visualised on a single gel (Figure 5.4a). The negative charge on 2AA at pH 8.4 facilitated the separation of the HA oligosaccharides as a function of their length and

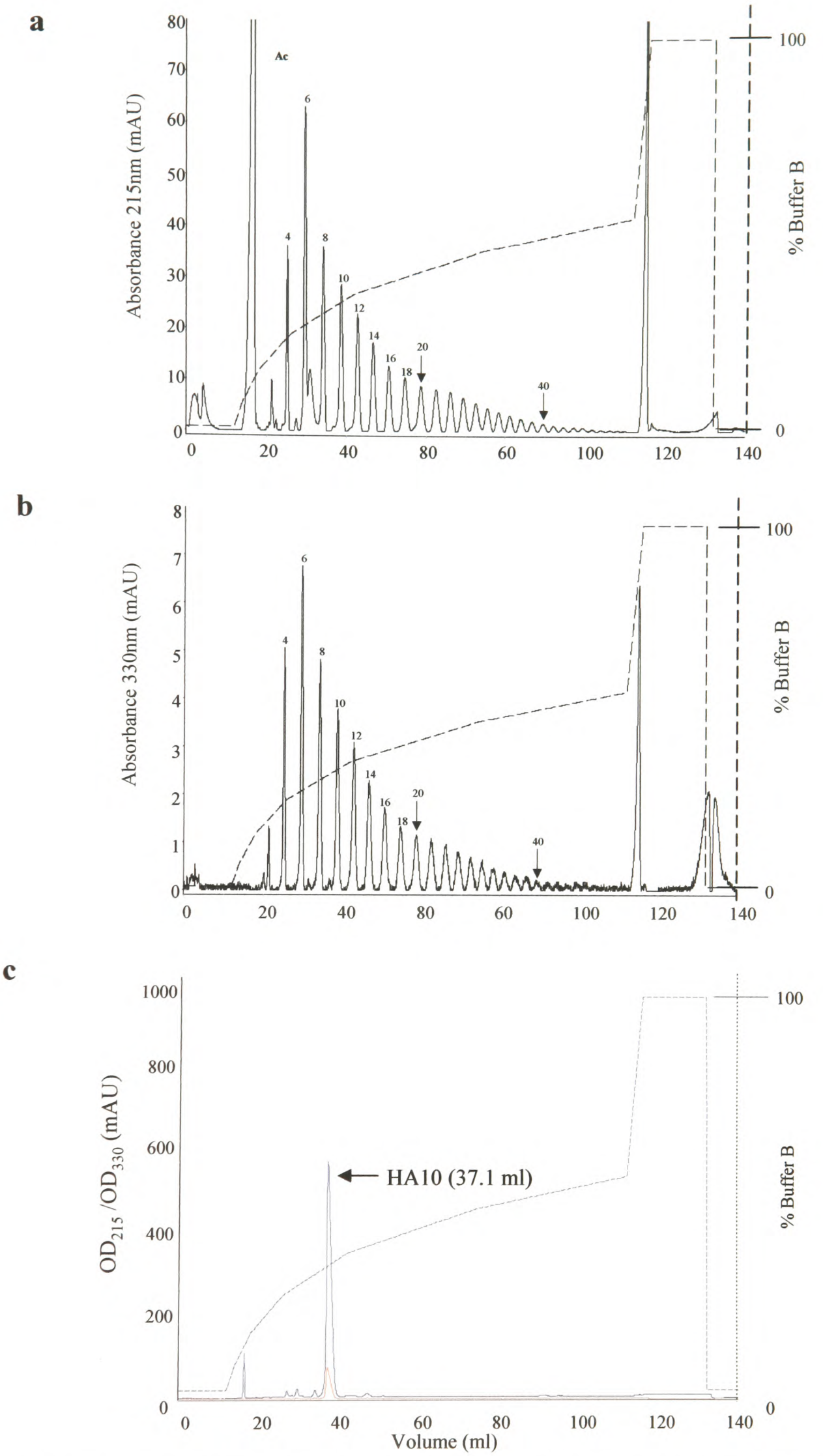

Figure 5.3. Fluorescently labelled (2AA) HA oligosaccharides observed at 215 nm (**a**) or 330 nm (**b**) were eluted using a logarithmic NaCl concentration gradient (dashed line). The oligosaccharide lengths were calibrated using a labelled 10-mer (**c**) monitored at both 215 nm (blue) and 330 nm (red). The acetate peak (Ac) is also indicated. The logarithmic gradient was run at 2 ml/min and buffer B is 0.5 M NaCl.

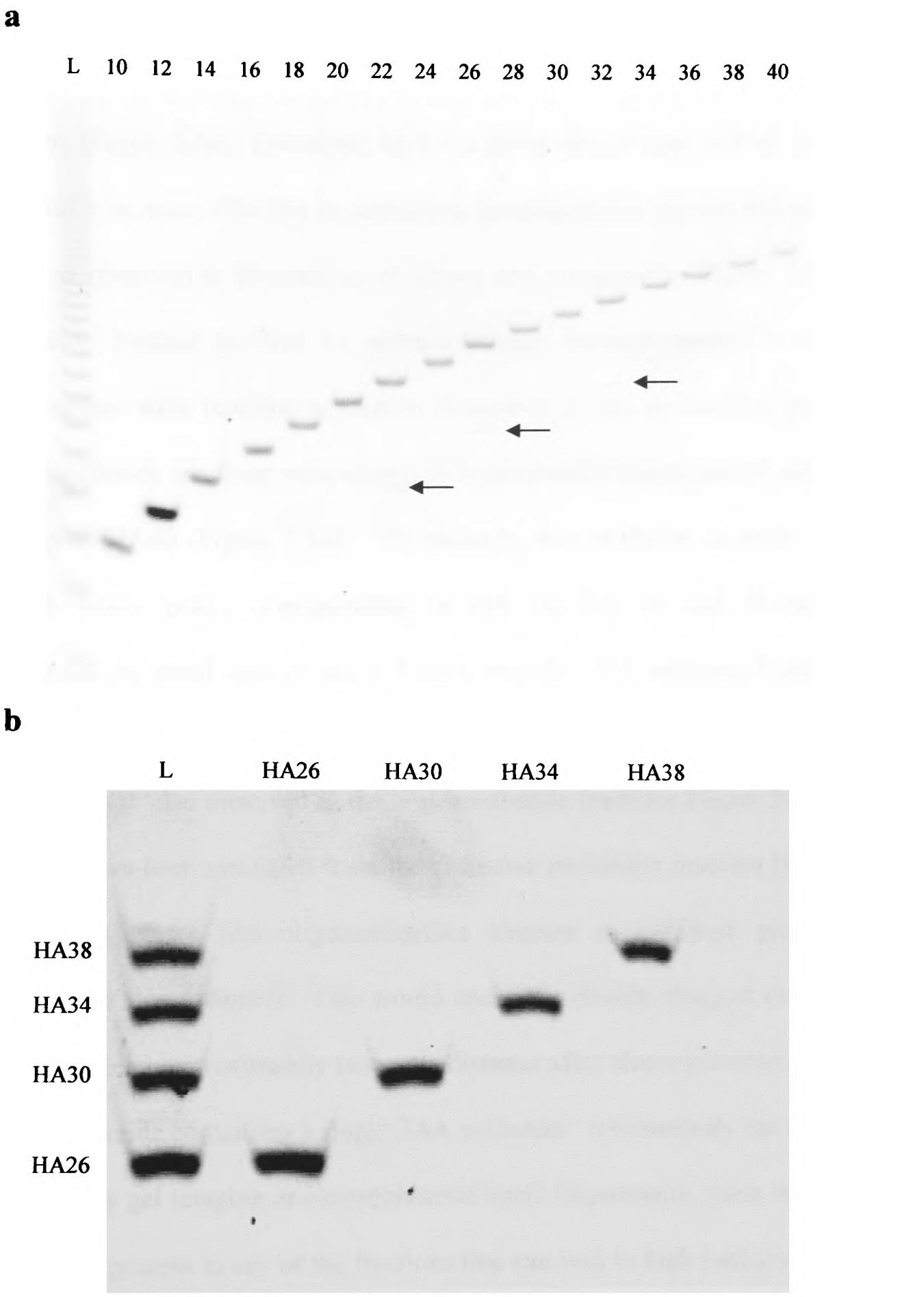

Figure 5.4 Gel electrophoresis of fluorescent HA oligosaccharides. (**a**) Purified 2AA-HA oligosaccharides of defined length (ranging from 10-40-mers) were run individually on native acrylamide gels and compared against a ladder from an unfractionated testicular hyaluronidase digest (L). The black arrows represents faint species (see section 5.3). 2AA-labelled HA 26-, 30-, 34-, and 38-mers are run individually (**b**) and compared with a mixture (L) of the same oligosaccharides, respectively.

charge during electrophoresis. In contrast, labelling with neutral fluorophore 2-aminoacridone (AMAC, see Table 5.1) gave rise to an inverted parabolic separation for 4-10-mers (Figure 5.5a). Therefore, 2AA is a better choice than AMAC for FACE analysis since it is more effective in separating heterogeneous shorter HA oligomers (<10-mers) as observed in Blundell *et al.* 2004a and presented in Figure 5.5b. Each oligosaccharide fraction purified by anion-exchange chromatography is separated from one another with baseline resolution (Figure 5.3). As determined by FACE, these oligosaccharide fractions were shown to be essentially homogenous with regard to length up to HA40 (Figure 5.4a). For example, this is shown in more detail in Figure 5.4b where peaks corresponding to HA 26, 30, 34 and 38-mers were electrophoresed on small gels (7 cm x 8 cm); no other HA oligosaccharides were visible in the respective fractions. However, faint lower molecular weight species (black arrows) were also observed in the oligosaccharide fractions Figure 5.4a. These species might have been produced from the reductive amination reaction (i.e., a side reaction product where two oligosaccharides become cross-linked producing a product with two fluorophores). This would cause the doubly charged cross-linked product to migrate at approximately twice the distance after electrophoresis compared to the oligosaccharide containing a single 2AA molecule. Alternatively the may be an artefact caused by gel imaging or electrophoresis itself. Importantly, there was also no excess free 2AA present in any of the fractions that can lead to high background when imaging the gel (Drummond *et al.* 2001). Therefore, the combination of 2AA labelling followed by anion-exchange described in section 5.2 results in homogenous oligosaccharide preparations and is an improvement on the linear gradient (Mahoney *et al.* 2001a) or molecular sieve approaches (Lesley *et al.* 2000) used previously which can result in heterogeneous mixtures of longer oligosaccharides. Taking

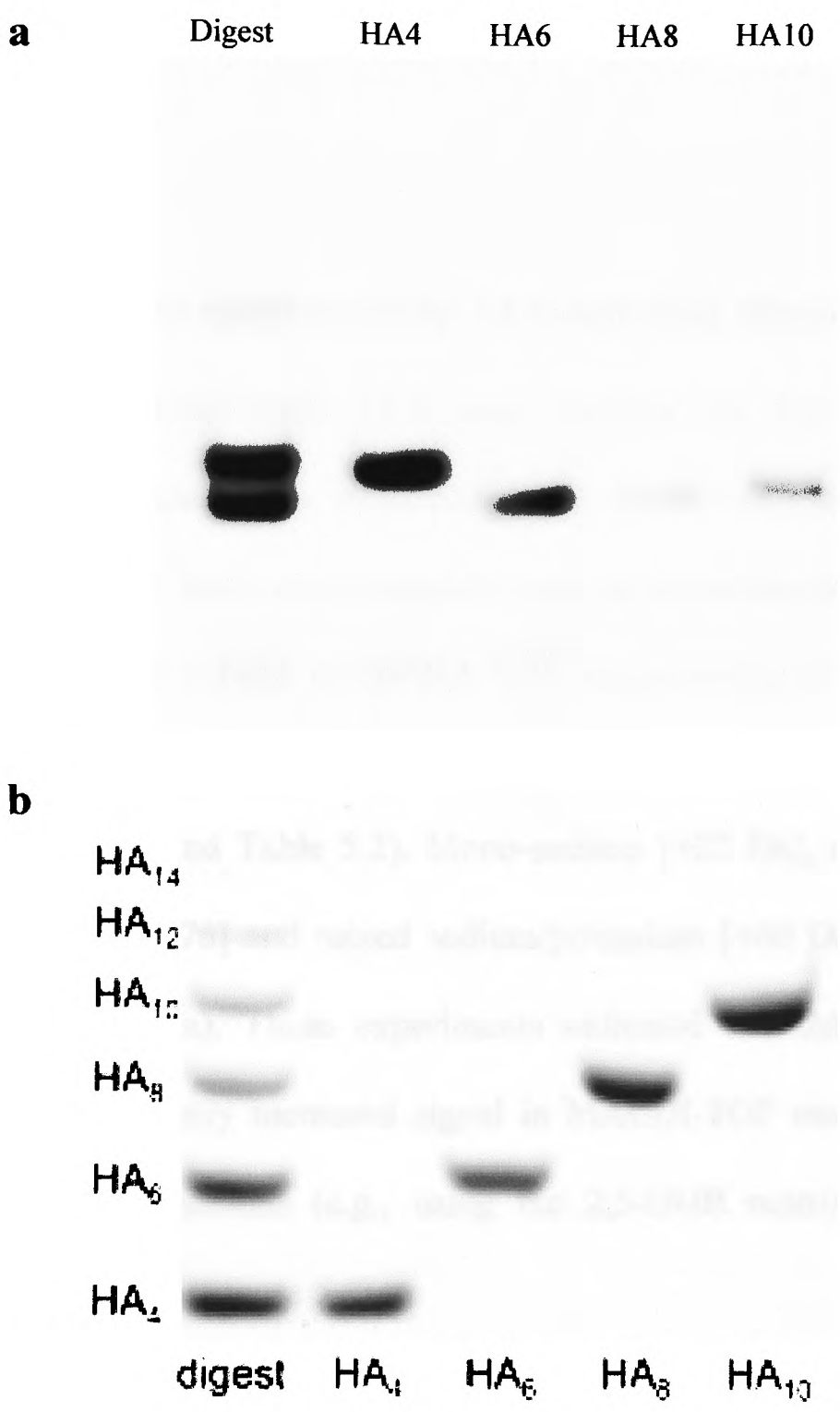

Figure 5.5 Gel electrophoresis of 2-aminoacridone (AMAC) labelled (**a**) and 2-aminobenzoic acid (2AA) labelled (**b**) HA 4-10-mers. The unfractionated (100 U/mg HA for 3 h 37 °C) digest is shown in the first lane in both **a** and **b**. Gel **b** was reproduced from Blundell *et al.*, 2004a.

advantage of this enhanced FACE separation caused by 2AA, defined HA ladders were prepared that facilitate the sizing of unknown mixtures of HA oligosaccharides, as commonly used for DNA restriction fragments. As an example, oligosaccharides with separation of four were mixed containing either 10, 14-.....38-mers and 12-,16-...40-mers (Figure 5.6).

5.4 MALDI-TOF mass spectrometry 2AA-labelled oligosaccharides

HA oligosaccharides labelled with 2AA were analysed by MALDI-TOF mass spectrometry in both negative-ion reflectron mode (4-10-mers) and negative-ion linear mode (12-40-mers). Each oligosaccharide had an experimental mass that was within error (ranging from 0.1-2.3 Da for HA 4-40, respectively) of their theoretical mass (M_r HA + M_r 2AA– 16) where the reductive amination results in the loss of an oxygen atom (Figure 5.7 and Table 5.2). Mono-sodium [+22 Da], mono-potassium [+38 Da], Di-potassium [+76] and mixed sodium/potassium [+60 Da] adducts were also identified (Figure 5.7a). These experiments indicated that 2AA-labelled HA oligosaccharides had a greatly increased signal in MALDI-TOF mass spectrometry under these particular conditions (e.g., using the 2,5-DHB matrix) compared to unlabelled oligosaccharides (Figure 5.8).

5.5 NMR spectroscopy

One dimensional NMR performed by Dr. Charles Blundell, University of Oxford was routinely performed on 2AA-labelled 4-, 6-, 8- and 10-mers to contain complete derivatisation and measure the stock solution concentrations prior to their use in biological assays. The 1D spectrum of 2AA-labelled HA4 (Figure 5.9), for example,

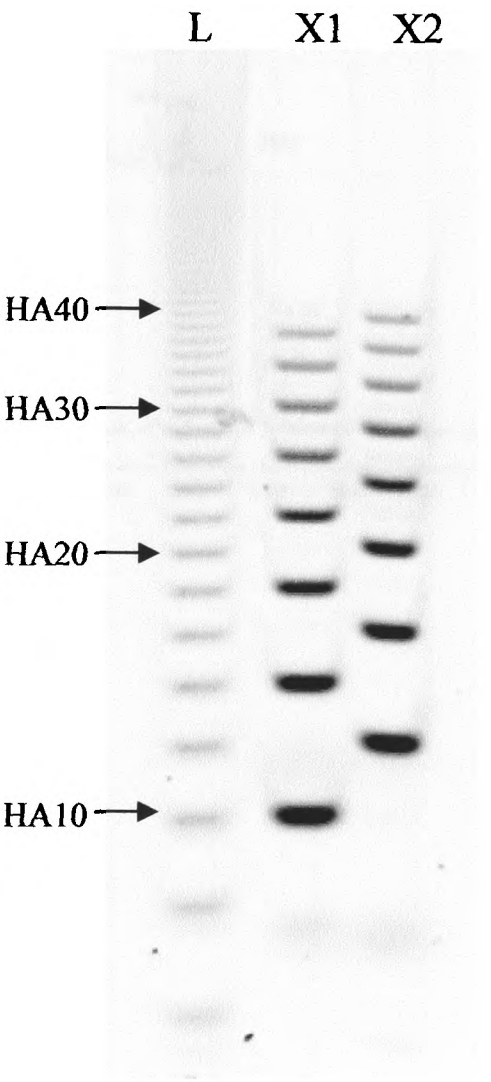

Figure 5.6 Gel electrophoresis of fluorescent HA oligosaccharides of defined ladders purified from a digest (X1= 10-, 14-, 18-, 22-, 26-, 30-, 34-, 38-mers and X2= 12-, 16-, 20-, 24-, 28-, 32-, 36-, 40-mers) are compared with that from a raw digest (L).

a

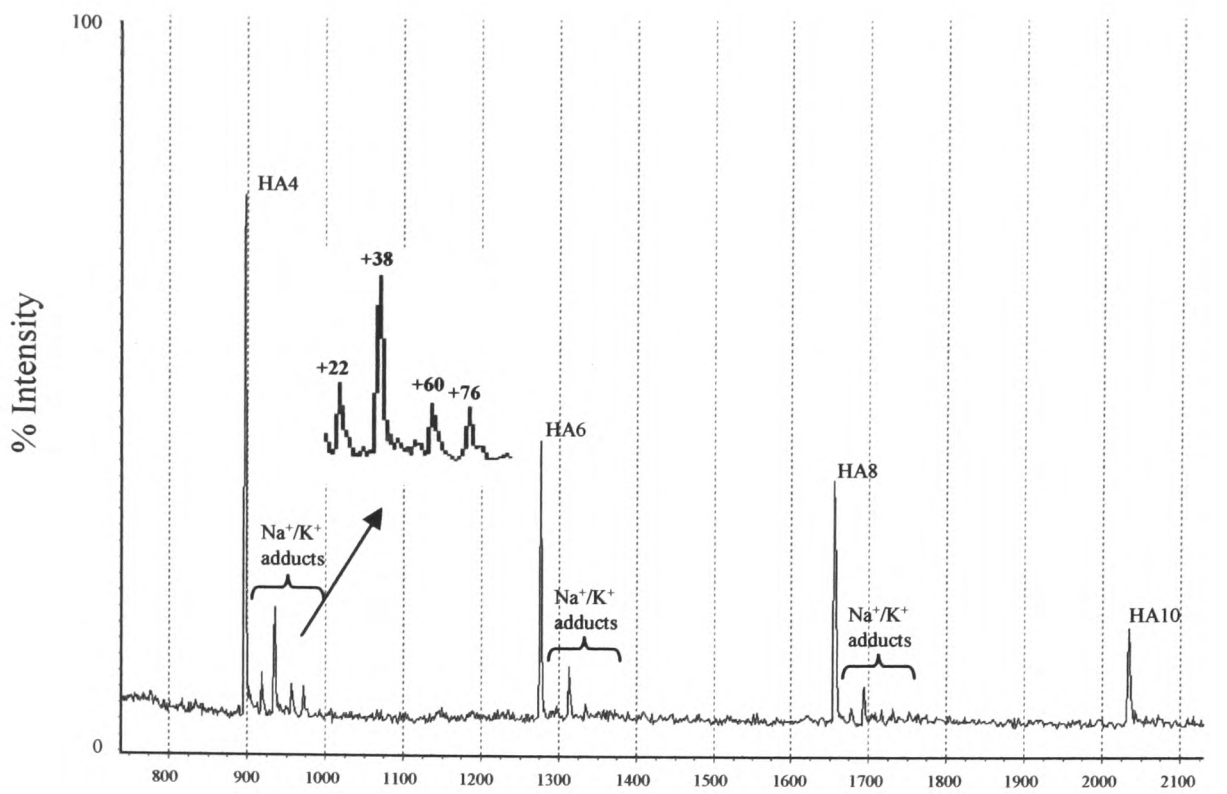

b

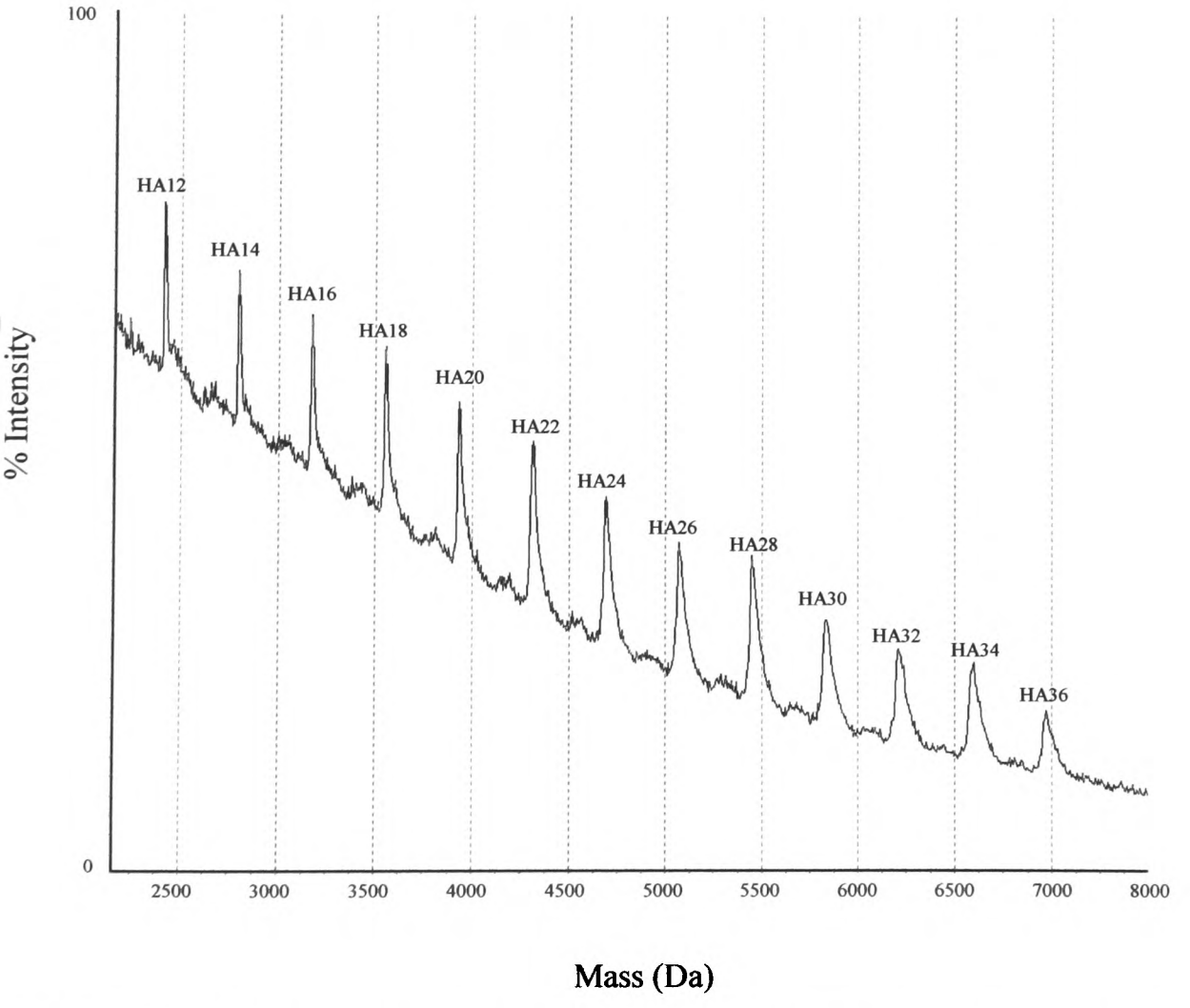

Figure 5.7 Mixtures of (**a**) short (4-10-mers) and (**b**) long (12-36-mers) 2AA-labelled oligosaccharides were analysed by MALDI-TOF mass spectrometry in the negative-ion reflectron and linear modes, respectively. Mono-sodium (+22 Da), di-sodium (+44 Da), mono-potassium (+38 Da), di-potassium (+76) and mixed (sodium and potassium, +60 Da) adducts were also observed in (**a**) in addition to the molecular ion.

Table 5.2 Comparison of theoretical and experimentally derived masses of 2AA-labelled oligosaccharides

HA	Theoretical M_r[a] $[M-H]^-$	Experimental M_r[b] $[M-H]^-$
4	896.3	896.2 ± 0.1
6	1275.5	1275.4 ± 0.1
8	1654.7	1654.6 ± 0.1
10	2033.7	2033.7 ± 0.1
12	2414.0	2414.0 ± 0.6
14	2793.4	2793.4 ± 0.3
16	3272.9	3172.4 ± 0.7
18	3552.0	3551.9 ± 0.9
20	3931.3	3931.1 ± 1.0
22	4310.6	4309.9 ± 1.2
24	4690.0	4689.2 ± 1.6
26	5069.3	5068.5 ± 2.7
28	5448.6	5447.8 ± 1.8
30	5827.9	5827.6 ± 2.0
32	6207.4	6207.9 ± 1.7
34	6586.6	6587.7 ± 4.5
36	6966.5	6965.4 ± 3.0
38	7345.2	7344.1 ± 3.4
40	7724.5	7726.8 ± 3.1

[a] Based on the mono- and average molecular masses for HA4-10 and HA12-40, respectively. [b] The mean and standard deviation of five measurements.

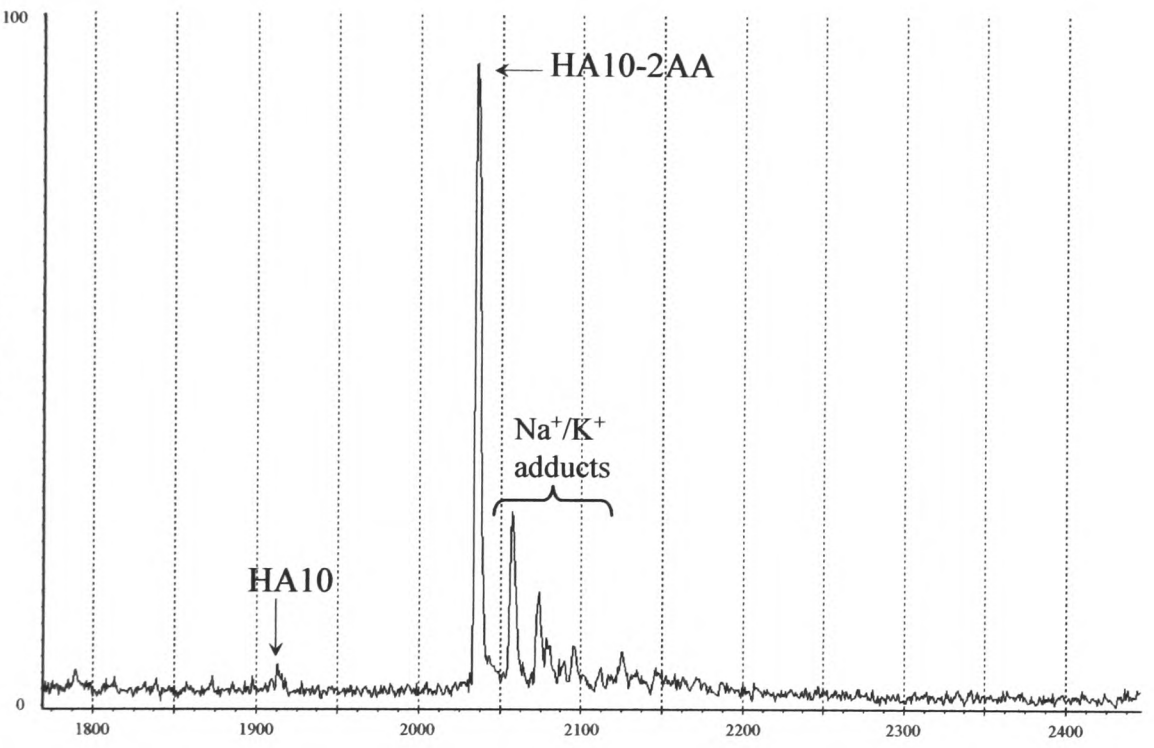

Figure 5.8 2AA derivatised HA oligosaccharides gave more intense signals in MALDI-TOF mass spectrometry than underivatised ones, when equal amounts (62.5 ng) were analysed simultaneously. Arrows denote HA10 (1912.6 Da) and HA10-2AA (2033.7 Da).

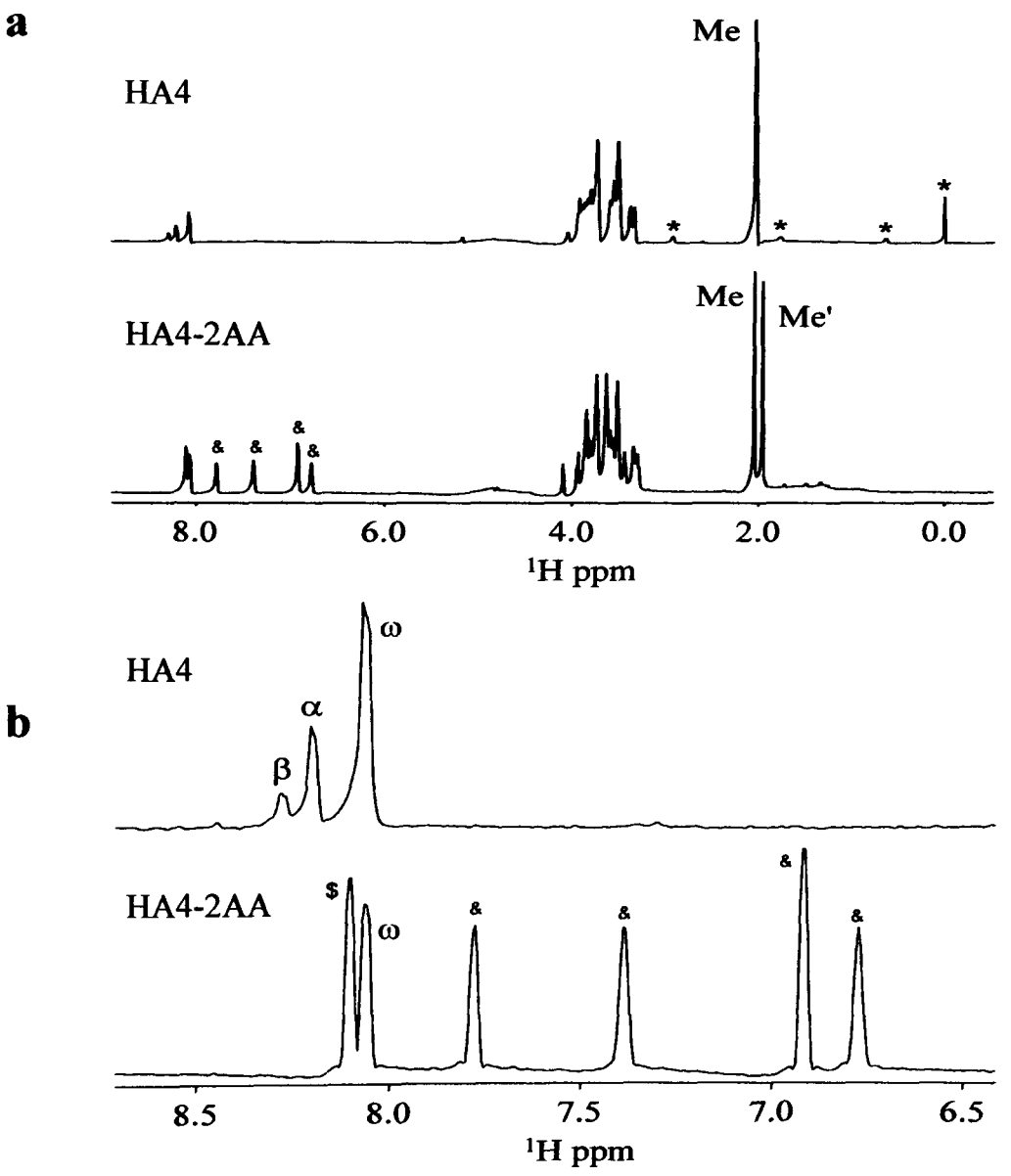

Figure 5.9 Comparison of underivatised HA4 and 2AA-labelled HA4 (HA4-2AA) by 1D NMR (750 MHz). (**a**) Complete spectra showing similarities (e.g. methyl, Me) and differences (e.g. Me') between unlabelled and labelled compounds. Resonances arising from the 2AA aromatic protons (&) and the reference compound DSS (*) are indicated. (**b**) Detail of the amide (α, ß, ω, $) and aromatic (&) proton regions. Resonances from free reducing termini (α, β) are clearly absent in the HA4-2AA sample.

has none of the resonances characteristic of the free reducing terminus (i.e., α, and β anomers), indicating it was fully derivatised; similar results were obtained for 2AA-labelled 6-, 8- and 10-mers (data not shown). Few resonances are clearly resolved in the 1D spectra, however those corresponding to the core of the labelled HA oligosaccharides that could be resolved were essentially unperturbed. For example, the methyl (Me) and amide (ω) protons from the internal GlcNAc ring (only two residues from the 2AA-labelled ring) are found at identical chemical shifts in both free and derivatised HA4 (Figure 5.9a). As expected, differences are observed in the 2AA-labelled ring; the methyl (Me') and amide ($) protons, for instance, are slightly perturbed (Figure 5.9a). These observations suggest that incorporation of the 2AA label into HA oligosaccharides produces only minor and local conformational changes.

5.6 The biological activity of 2AA-labelled HA oligosaccharides

Binding assays with the human recombinant proteins were performed to determine whether the 2AA label affected the biological activity of the oligosaccharides. Both excess HA10 and 2AA-labelled HA10 competed similarly for cLP, VG1 and AG1 binding to biotinylated polymeric HA (Figure 5.10) performed as described in section 2.11.1. It was shown previously that HA10 was the shortest length oligosaccharide capable of efficiently competing for the binding of polymeric HA to cLP, AG1, and VG1, as reported in section 3.5.1. Therefore, it can be concluded that the addition of the 2AA moiety to the reducing end termini of HA10 does not significantly interfere with its protein-binding activity.

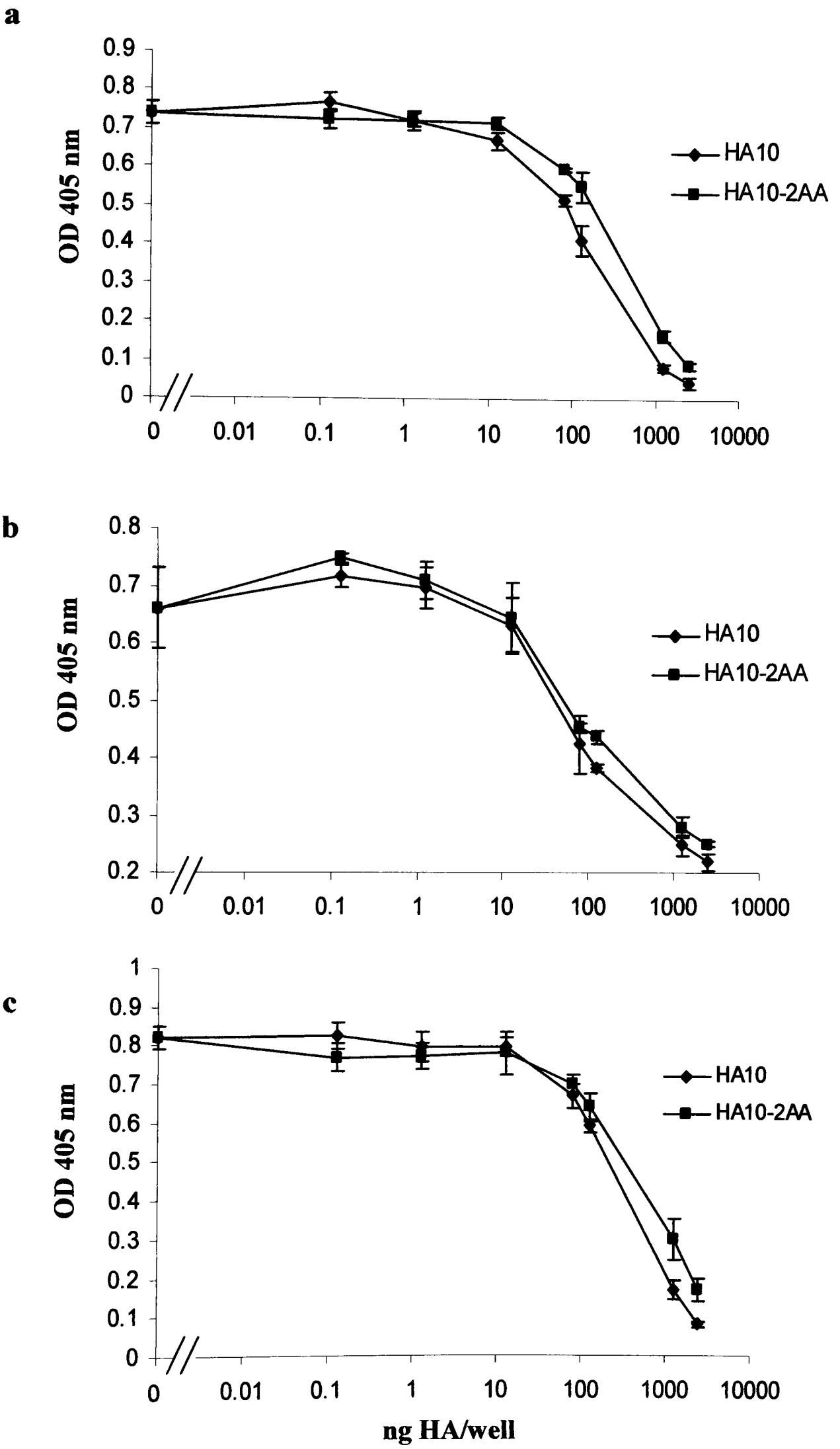

Figure 5.10 The biological activity of 2AA-labelled HA oligosaccharides was assessed by the binding of biotinylated polymeric HA (12.5 ng/well) to AG1 (**a**), cLP (**b**) and VG1 (**c**) coated plates in the presence or absence of HA10 and 2AA derivatised HA10 (HA10-2AA) oligosaccharides as described in section 2.11.1. The errors correspond to the standard deviation of four measurements.

5.7 Electrophorectic mobility shift assay (EMSA)

5.7.1 Preliminary EMSA with cLP, AG1 and VG1

An electrophoretic mobility shift assay (EMSA) was utilised to further investigate the binding of cLP, AG1 and VG1 with 2AA labelled HA oligosaccharides of defined lengths. In EMSA studies, it is common to utilise radiolabelled ligands (e.g. ^{35}S, ^{32}P) to probe interactions (Lane *et al.* 1992), as seen recently in investigations of the interaction between heparin and antithrombin III (Wu *et al.* 2002). However, in this case, given the of lack of sulphate or phosphate groups on HA, a fluorescent EMSA technique was favoured, which has also been recently used to study heparin-protein interactions (Lyon *et al.* 2004). In EMSA experiments, the protein retards the fluorescent oligosaccharide when bound to it, resulting in a band shift from the free sugar position; the charge on the 2AA ensures that a good separation was achieved. Initial EMSA experiments were performed at a resolving and stacking acrylamide gel concentration of 10 % and 4 % (w/v), respectively as described in section 2.21.1. As can be seen from Figure 5.11, all three proteins were capable of binding 2AA-labelled 10-, 24-, and 40-mers where both free and bound oligosaccharide bands are present. However, the bands corresponding to the bound oligosaccharide are diffuse, which probably results from non-equilibrium effects caused during electrophoresis. Therefore, careful considerations (low percentage acrylamide gels (4.5 % (w/v)), low voltage (40 V), low temperature (4 °C) and short run time 40 min see section 2.21.2) were taken to ensure that electrophoresis conditions did not promote dissociation of the oligosaccharide from the protein in further shift assays performed as described below (section 5.7.2).

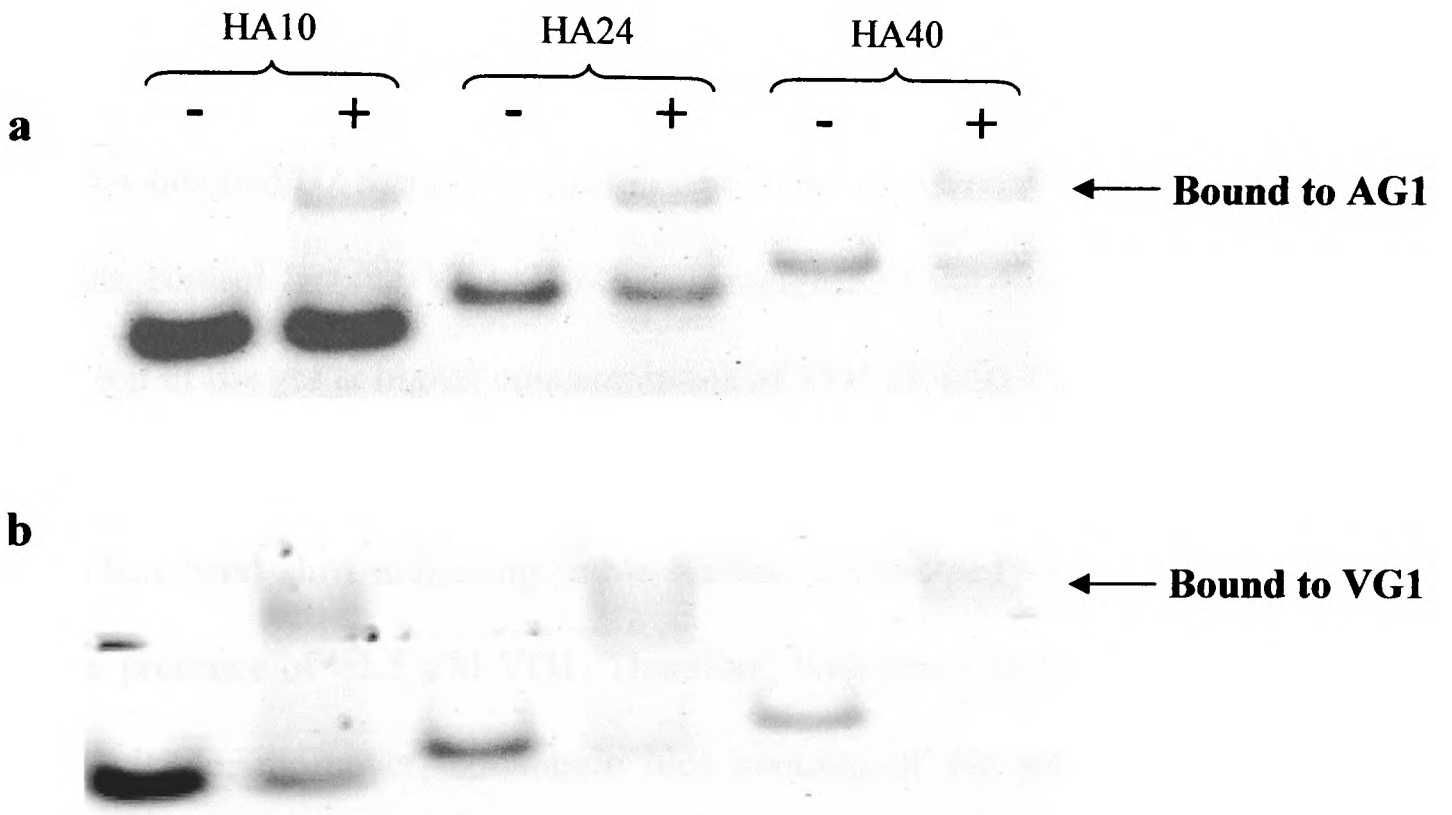

Figure 5.11 The interaction of 2AA-labelled HA oligosaccharides (10-, 24-, and 40-mers) with the recombinant proteins (5 μg) using an EMSA performed as described in section 2.21.1. Fluorescent oligosaccharides were analysed in the absence (-) or presence (+) of AG1 (**a**), VG1 (**b**) and cLP (**c**).

5.7.2 EMSA with VG1

Oligosaccharide samples of unknown concentrations (20-, 30- and 40-mers) were normalised to a known concentration of 2AA-labelled HA10 by densitometry as described in section 2.22. As shown in Figure 5.12a, an increasing amount of VG1 (0-10.7 μM) was added to 2AA-labelled HA 8-, 10-, 20-, 30-, and 40-mers (all at 2.2 μM). For 2AA-labelled HA8, no band shift is seen in the presence of 0.2-3.6 μM VG1 relative to the control lacking VG1. However, smearing of the free oligosaccharide towards the top of the gel at higher concentrations of VG1 (5.4-10.7 μM) suggests the sugar is binding very weakly to the protein under the conditions analysed here. In contrast, a clear band shift indicating stable binding is observed with 2AA-labelled HA10 in the presence of >1.8 μM VG1. Therefore, both free and bound fluorescent bands were visible; moreover, coomassie blue staining of the gel (Figure 5.12b) indicated that the VG1 protein and the shifted fluorescent HA10 bands run at identical positions. As seen in Figure 5.12a, at concentrations of VG1 (>7.1 μM), where 2AA-labelled HA10 is fully bound, the retarded fluorescent bands were less intense than free labelled HA10 bands. Since there was no fluorescence observed in the wells after electrophoresis, indicating that all bound protein is migrating into the gel, the difference in intensity suggests that fluorescence quenching is likely to be occurring in the binding site of VG1. Fluorescence emission scans further supported this hypothesis, where a significant decrease in emission at 400-450 nm (maximum for 2AA) was observed when equimolar amounts of labelled HA10 and VG1 were mixed compared to controls lacking protein (Figure 5.13). As a consequence of VG1 quenching the fluorescence of 2AA-labelled HA, only the free oligosaccharide could be reliably measured by densitometry analysis. Using this type of analysis it was found that between 0.9 and 1.8 μM of total VG1, the concentration of unbound

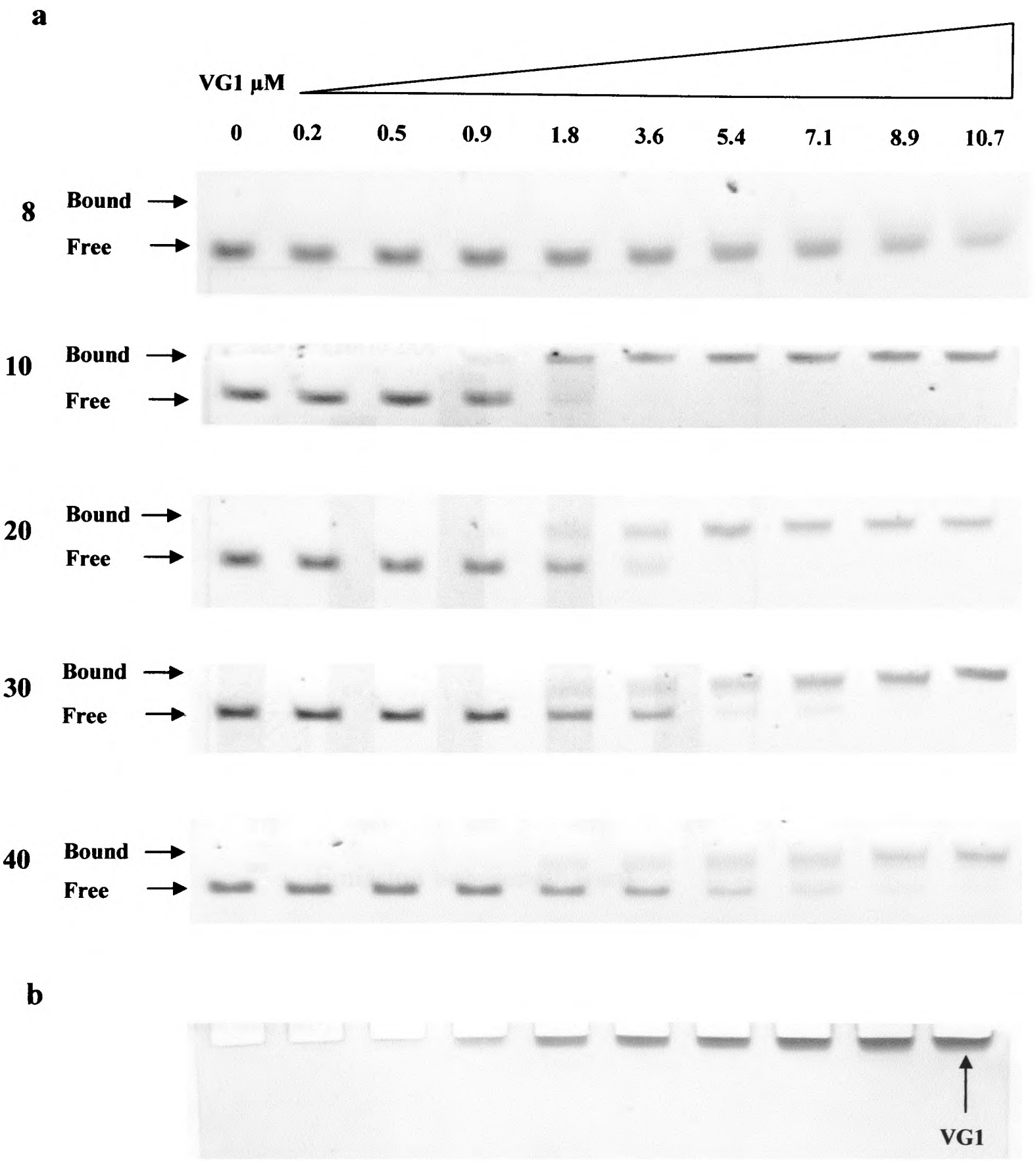

Figure 5.12 (**a**) Increasing concentrations of VG1 were mixed with a constant concentration (2.2 μM) of 2AA-labelled HA 8-, 10-, 20-, 30- and 40-mers and analysed by EMSA. (**b**) In the presence of 2AA-labelled HA10, VG1 protein bands (detected with coomassie-blue staining) co-localised with the bound fluorescent HA10 bands observed in (**a**).

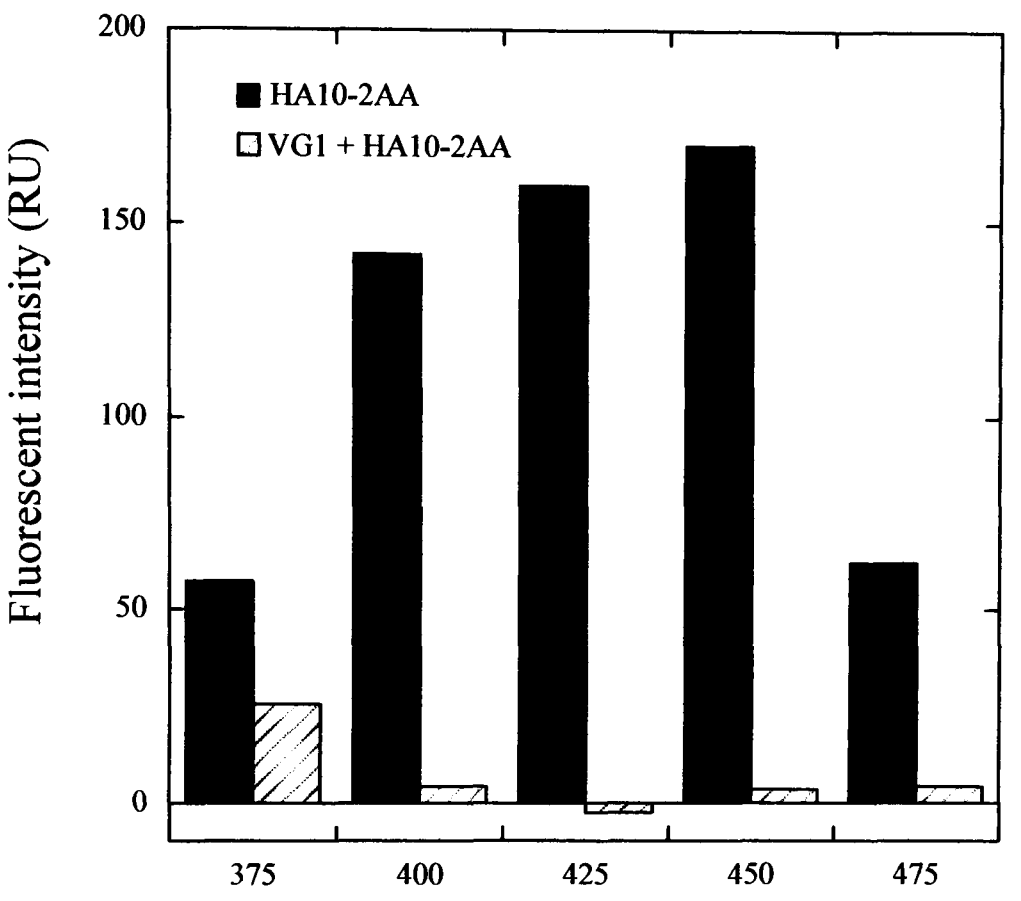

Figure 5.13. The fluorescence emitted from HA10-2AA is quenched in the presence of equimolar amounts of VG1 (VG1 + HA10-2AA). Fluorescent intensity is displayed in relative units (RU).

HA10 had reduced to around 50 % of its maximum value. Therefore, the derivation for the K_d of VG1 to 2AA-labelled HA10 using a single site model was attempted by densitometry analysis of the free oligosaccharide.

5.7.3 Derivation of the equilibrium binding constant for VG1 to HA10-2AA

Since only the free HA can be determined from densitometry for a given amount of total protein (P_t), the K_d has to be calculated based on free HA, P_t and total HA (H_t) rather than the free protein [P], which is the conventional method, but unknown in this case. Therefore, assuming a 1:1 stiochiometry between VG1 and HA10 and equilibrium kinetics (i.e. $H + P \rightleftharpoons HP$, where H represents the HA oligosaccharide and P the protein), equation (1) can be derived from the standard equations for the equilibrium dissociation constant K_d (Price and Dwek 1979). If θ is the fraction of free HA, as obtained from the EMSA experiment by densitometry (Figures 5.12a and 5.14), then r can be defined as the fraction of bound HA, as shown in equation (2), where H_t is the total concentration of HA.

$$r = \frac{[P]}{K_d + [P]} \qquad (1)$$

$$r \equiv (1-\theta) \equiv \frac{[HP]}{H_t} \qquad (2)$$

Use of equation (2) allows the amount of free protein to be calculated from the total protein concentration P_t, equation (3). Substitution of equation (3) into equation (1) results in equation (4) which can now be used to relate the amount of free HA, total protein and the K_d to each other. Thus, the equation can be used to model the EMSA experiment as performed here, and is quadratic in the variable r (equations (5-8)).

$$[P] = P_t - rH_t \qquad (3)$$

a

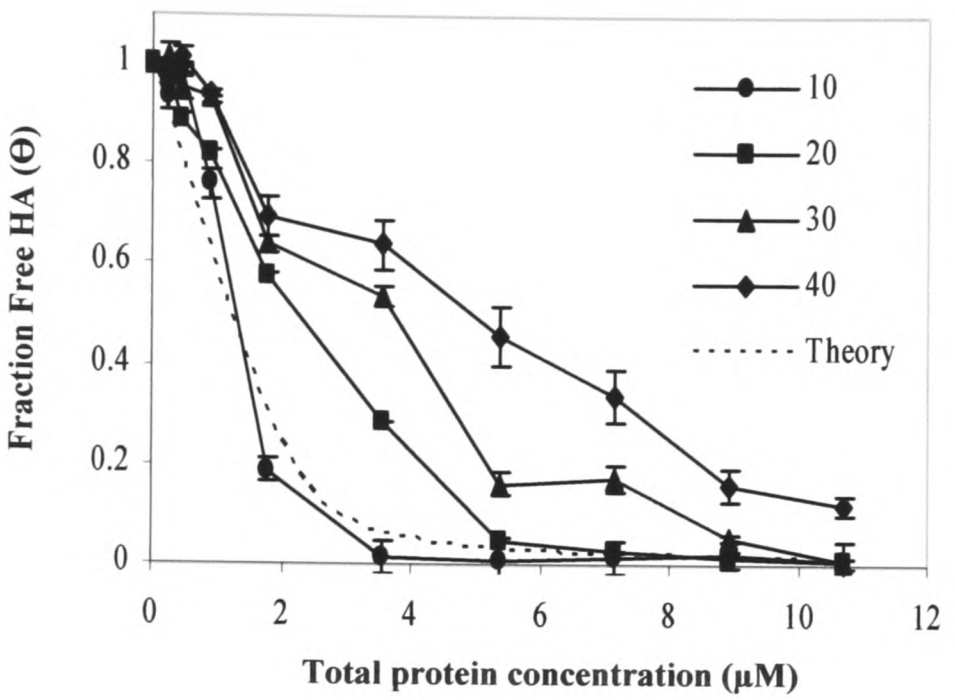

b

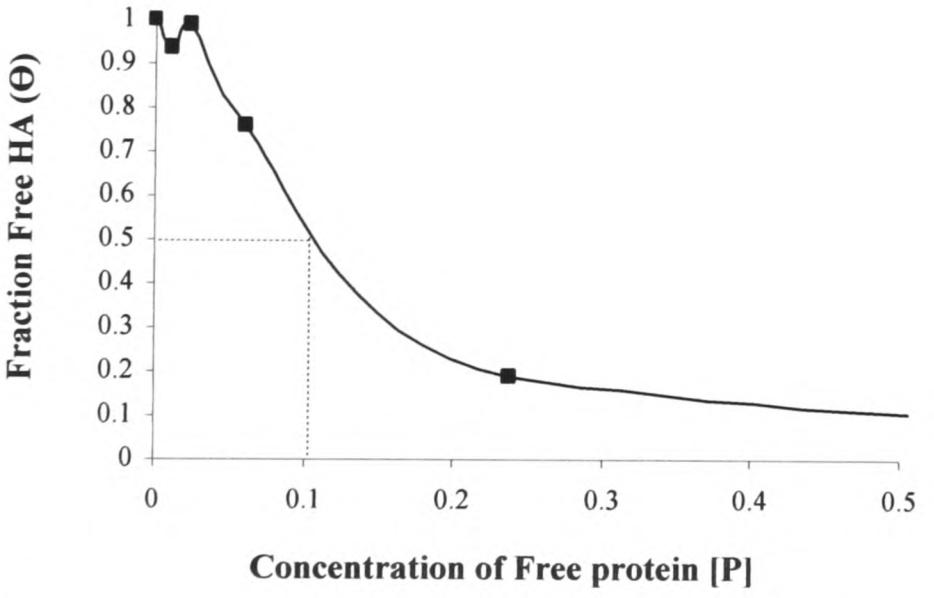

Figure 5.14 The fraction of the free oligosaccharide (θ) for labelled 10-, 20-, 30-, and 40-mers was calculated by densitometry analysis after EMSA and plotted against the total VG1 concentration (**a**). Each fluorescent band was measured three independent times to estimate the standard error. A theoretical curve (Theory) representing a K_d of 100 nM for binding of VG1 to HA10 is also shown. (**b**) Using a K_d of 100 nM allowed the θ value to be plotted against the predicted concentration of free protein [P] to produce the familiar plot, which yields the K_d at θ=0.5. For the longer length sugars (**a**) linear interpolation allowed the values of total protein corresponding to a θ value of 0.5 to be calculated. The values of 1.2, 2.3, 3.8 and 4.9 μM were recorded for HA 10-, 20-, 30- and 40-mers, respectively.

$$r = \frac{P_t - rH_t}{K_d + P_t - rH_t} \tag{4}$$

$$H_t r^2 - (K_d + H_t + P_t)r + P_t = 0 \tag{5}$$

$$ax^2 + bx + c = 0 \tag{6}$$

$$x = \frac{-b \pm \sqrt{b^2 - 4ac}}{2a} \tag{7}$$

$$r(P_t) = \frac{K_d + H_t + P_t - \sqrt{(K_d + H_t + P_t)^2 - 4H_t P_t}}{2H_t} \tag{8}$$

Equation (4) was fitted to the experimentally derived EMSA data for HA10 to determine the K_d, since P_t, H_t and r are known at each point. It can be seen that the experimental and theoretical curve are in good agreement with one another (Figure 5.14a), and yield a K_d value of 100 nM for the interaction of HA10 with VG1 under the conditions used here. Therefore, because of the above circumstance (i.e., the free protein [P] is unknown) the concentration of total protein where $\theta = 0.5$ does not correspond to the K_d (see Figure 5.14a). However, solving the quadratic equation (7 and 8) for variable r as a function of P_t using a K_d of 100 nM allows the substitution of r values into equation (3). It must be noted that negative square root in the quadratic was determined to be the real value since the positive square root yielded r values >1 (unphysical). Therefore, the concentration of free protein [P] can be calculated and plotted against θ values for HA10 as seen in Figure 5.14b.

Experiments with longer HA oligosaccharides (i.e., HA 20-, 30-, and 40-mers), which are likely to bind multiple VG1 molecules (Courel *et al.* 2002), also gave rise to clear shifts in HA mobility, as shown in Figures 5.12a and 5.14. However,

interpretation of this data and hence calculation of K_d values becomes much more difficult since the equation becomes binomial.

5.8 Discussion

The fluorophore 2-aminobenzoic acid (2AA; also referred to as anthranilic acid) has been used previously to enhance HPLC, capillary and gel electrophoreses of glycans isolated from cells, proteins and lipids (Anumula 1994; Bigge *et al.* 1995; Sato *et al.* 1997; Anumula and Dhume 1998; Anumula and Du 1999; Huang *et al.* 2000; Neville *et al.* 2004). Labelling with 2AA has also been used for separation and sequencing of heterogeneous heparan sulphate derived saccharides (Turnbull *et al.* 1999; Shriver *et al.* 2000) and for structural profiling of keratan sulphates (Whitham *et al.* 1999). In addition, 2AA-labelling does not disrupt biological activity in enzyme-substrate fluorescent assays (Gershkovich and Kholodovych 1996). This chapter describes the advantages of labelling HA oligosaccharides with 2AA for use in a range of analytical techniques.

In combination with a logarithmic gradient, as used previously for the purification of oligonucleotides (Tashlitskil and Oretskaya 1997), 2AA labelling enhanced the UV absorbance between 200 and 220 nm facilitating the purification and detection of homogeneous even-numbered HA oligosaccharides at least up to 40-mers; it seems likely that longer oligomers (e.g., up to 50-mers) could be purified using this system. Additionally, 2AA-labelled HA oligosaccharides gave more intense signals in MALDI-TOF mass spectrometry, as has been reported previously for 2AA-labelled chicken ovalbumin oligosaccharides (Anumula and Dhume 1998). This enhancement is not surprising since the MALDI apparatus used here employs a UV laser to cause

ionization, and matrix compounds are selected on the basis of being good UV absorbers. Therefore, 2AA which has been used as a MALDI co-matrix for DNA (Zhang and Gross 2000) in its own right, is a UV absorber, and may be directly ionized. Various other fluorophores, including 2-aminoacridone (AMAC), have also been reported to increase glycan ionisation in MALDI-TOF experiments following derivatisation (Harvey 2003) however, AMAC-labelled HA oligosaccharides were not analysed.

Another advantage of 2AA derivatisation was the ability to enhance oligosaccharide migration in fluorophore-assisted carbohydrate electrophoresis (FACE) analysis. The negative charge on 2AA facilitated separation of the HA oligosaccharides as a function of their length and charge during electrophoresis (Figure 5.6 and 5.7b), without the necessity for borate in the running buffer or a stacking gel, as has been previously required for HA oligosaccharides derivatised with the neutral fluorophore AMAC (Calabro *et al.* 2000a; Calabro *et al.* 2000b; Mahoney *et al.* 2001a; Karousou *et al.* 2004). Therefore, AMAC which contains bulky aromatic groups (MW = 210.24, Table 5.1) and, significantly, has no charge does not enhance the migration of sugars during electrophoresis and is probably responsible for the problematic migration (parabolic inversion) of short HA oligosaccharides observed in Figure 5.7a, as reported previously (Calabro *et al.* 2000a; Mahoney *et al.* 2001a; Tawada *et al.* 2002). Another fluorophore, 8-amino-1,3,6-naphthalene trisulfonic acid (ANTS; see table 5.1), which is commonly used to analyse various glycans by electrophoresis (Jackson 1994), has also been used to label HA and chondroitin oligosaccharides (Tawada *et al.* 2002; Volpi 2003). While ANTS derivatised HA oligosaccharides (4-mers to 16-mers) display linear separation as a function of length (due to the three negatively

charged sulphate moieties on the fluorophore (Tawada *et al.* 2002)), it is rather bulky (MW = 381.33) and this may interfere with ligand-binding. Moreover, the sulphate moieties may modify the biological activity of the oligosaccharides, since several HA-binding proteins have been reported to also bind sulphated GAGs (Parkar and Day 1997; Weigel and Weigel 2003; Mahoney *et al.* 2004).

Crucially, the 2AA label was not observed to disrupt the biological activity of HA oligosaccharides in the assays performed here. For example, HA10-2AA was as effective a competitor as unlabelled HA10 for polymeric HA binding to cLP, VG1 and AG1, which is interesting considering that reductive amination breaks the integrity of the reducing terminal GlcNAc ring. This is somewhat surprising since a 10-mer is the minimum size that competes effectively for protein binding. The retention of activity may be due to the fact that 2-aminobenzoic acid has a three-dimensional structure very similar to D-glucuronic acid, and has a carboxylic acid in the same relative position as in HA, which could compensate for the breakage of the terminal sugar ring. What is clear however is that 2AA-labelled HA oligosaccharide can be used in fluorescence-based assays for investigation of HA-protein interactions, as we have demonstrated with EMSA.

A drawback of the EMSA approach used in this study is the inability to measure the free protein concentration, or the amount of bound oligosaccharide because of fluorescence quenching. This is in contrast to radiolabelled experiments (Wu *et al.* 2002). Recent structural work has shown that the binding groove of the Link module from human TSG-6 contains three tyrosine residues, and sequence alignments indicate that these are highly conserved (e.g., versican has tyrosines at these three

positions in the first Link module (Blundell *et al.* 2003)). It is proposed that these amino acids, with delocalised electrons, may be responsible for quenching the fluorescence of 2AA. Therefore, it is apparent that fluorescence quenching could have a wide application for studying the kinetics of HA-protein interactions.

A K_d of 100 nM was derived for the interaction of VG1 to HA10 by theoretical analysis of EMSA results. This is approximately nine times weaker than the K_d (4-18 nM) reported for recombinant versican binding to polymeric hyaluronan using equilibrium dialysis (LeBaron *et al.* 1992) or surface plasmon resonance (Matsumoto *et al.* 2003; Shi *et al.* 2004). This may result from the different conditions (salt strength, pH and temperature) in which the EMSA was performed (see section 2.21.2). Interestingly, for HA 20-, 30- and 40-mers, approximately two-, three- and four-times the respective amount of total VG1 was needed to retard 50 % of the oligosaccharide compared to HA10, (the minimum size even oligosaccharide that can accommodate the protein). In this regard the analytical gel filtration experiments described in chapter 4 indicate that these lengths of HA might support the binding of 2, 3, and potentially 4 proteins, respectively. It should be noted, that only a single bound protein is required per HA molecule to retard it in the EMSA assay. Therefore, if HA20 has more independent protein binding sites than HA10 (Courel *et al.* 2002), and the oligosaccharides are at the same molar concentration, then HA20 would require less protein to cause an equilibrium dissociation. Thus, the data appears inconsistent with site-independent protein binding to a multivalent HA oligosaccharide. One explanation for this is that the interaction of VG1 with >HA20 displays positive cooperativity in that the binding of VG1 to one site makes the binding to adjacent sites much more favourable. This would essentially create an all-

or-none paradigm where HA oligosaccharides partition into those saturated with protein and those with no protein bound. Clearly further work is required to establish the exact nature of this phenomenon. Comparison with EMSA experiments using other members of the Link module superfamily, where the binding is better characterised (such as TSG-6 or aggrecan) may be very revealing in this regard.

In conclusion, the advantages of labelling HA oligosaccharides with 2AA for their use in biological assays appears to result from it having a similar size (M_r= 137.1) and charge to that of D-glucuronic acid. Additionally, 2AA has no sulphate moieties that might interfere with oligosaccharide activity and is also highly fluorescent (Anumula 1994), which facilitates oligosaccharide detection. Therefore, a simple protocol for fluorescent labelling and separation of HA oligosaccharides is described, which does not perturb their biological function. This methodology will allow a range of fluorescence-based assays to be developed for the analysis of HA-protein interactions.

6 Discussion and future work

The work presented in this thesis describes the expression, purification and characterisation of human recombinant cartilage link protein (cLP) and the G1-domains of aggrecan (AG1) and versican (VG1). All three proteins investigated have an identical domain organisation containing an N-terminal immunoglobulin (Ig) fold followed by two contiguous Link modules. The recombinant proteins expressed in *Drosophila* S2 cells all had significant levels of *N*-linked glycosylation (~2 kDa) but this did not interfere with HA binding or ternary complex formation, despite the fact that the glycosylation machinery of insect cells is distinct from that of mammalian cells (Altmann *et al.* 1999). However, when AG1 was treated with PNGase F, no detectable binding of biotinylated HA was observed when the deglycosylated protein was immobilised on a microtitre plate (Figure 3.8). A similar finding has been reported previously for HA binding to recombinant AG1 in solid phase transbot assays (Watanabe *et al.* 1997a). Importantly, the removal of the *N*-linked glycans from AG1 did not alter its ability to bind cLP in solution or in forming a ternary complex with cLP and HA32 (see Figure 4.13 and Table 4.2). This indicates that *N*-glycosylation of the G1-domain of aggrecan is unlikely to play a significant role in its functional activity but rather that the deglycosylated AG1 has different properties when immobilised in microtitre plate assays to those seen in free solution (i.e., gel filtration and cross-linking MS). Therefore, it seems likely that the lack of AG1 activity in solid phase assays is an artefact caused by its immobilisation. In contrast the removal of *N*-linked glycans from VG1 did not have any affect on its functional activity regardless of the assay performed; PNGase F treatment of cLP did not affect its HA-binding properties. Therefore, it can be concluded that *N*-glycosylation is unlikely to be necessary for the functional activity or folding of cLP, aggrecan and

versican. Thus, the previous finding that the double Link module of AG1 and VG1 expressed in *E.coli* do not fold (McVey 2002) can now be interpreted as being due to a lack of the Ig domain rather than due to the absence of glycosylation.

As discussed in section 1.4 a link protein gene family consisting of four members denoted 'HAPLN' (HA and Proteoglycan LiNk protein Family) has recently been identified (Spicer *et al.* 2003) where cLP is renamed HAPLN-1. Each link protein gene was found to be located immediately adjacent to one of the four CSPG genes forming HAPLN-1/versican, HAPLN-2/brevican, HAPLN-3/aggrecan and HAPLN-4/neurocan gene pairs (Nomoto *et al.* 2002; Czipri *et al.* 2003; Spicer *et al.* 2003). The four encoded HAPLN proteins share 45-52 % overall amino acid identity where the least amount of similarity is seen in the immunoglobulin domain (Spicer *et al.* 2003). This is interesting given that the interaction between cartilage link protein and aggrecan in the absence of HA is mediated via the immunoglobulin domain (Perin *et al.* 1987; Grover and Roughley 1994; Watanabe *et al.* 1997a; Matsumoto *et al.* 2003), but at present, the specificity of HAPLN-CSPG interactions is not well established. As described in chapter 4, no evidence for the interaction of VG1 with cLP in the absence of HA in solution was observed either by gel filtration or cross-linking/MS analysis. However, in the study by Matsumoto *et al.* 2003 the binding of cLP to VG1 in solid phase assays was mediated via the Link modules of versican rather than the Ig domain. While this interaction may be an artefact caused by protein immobilisation it is possible that the association of cLP and VG1 is the context of a ternary complex is indeed mediated via VG1's Link module domains. If this is the case than aggrecan and versican may form distinct types of ternary complexes. The lack of solution phase association of cLP with VG1 may suggest that of these two proteins the preferred

partner for cLP is AG1 given their ability to bind directly in solution. For example, both cLP and aggrecan are expressed at high levels in cartilage while cLP and versican genes are not co-expressed to any significant degree in adult tissues (Spicer *et al.* 2003); versican is present a low levels in cartilage (Sztrolovics *et al.* 2002). Furthermore, the level of aggrecan was significantly reduced in the cartilage of mice lacking HAPLN-1 (Watanabe and Yamada 1999, 2002). It would also seem reasonable, given their common expression in brain, that both HAPLN-2 and 4 could form stabilised ternary complexes with the CSPGs neurocan and brevican (Spicer *et al.* 2003). However, is was reported that HAPLN-2 co-localises with the versican V2 splice variant in the brain (Oohashi *et al.* 2002) and recently HAPLN-1, which is also expressed in brain (Ripellino *et al.* 1989; Rauch *et al.* 1991), has been reported to interact with neurocan (Rauch *et al.* 2004). Therefore, it was suggested that HAPLN-1 and neurocan are likely to form ternary aggregates in the developing brain. The interaction between cLP and neurocan was shown to be mediated via the immunoglobulin domain (Rauch *et al.* 2004), similar to that observed for cLP and aggrecan (Perin *et al.* 1987; Watanabe *et al.* 1997a; Matsumoto *et al.* 2003). As discussed above, this is distinct from the mode of interaction for VG1 and cLP in the absence of HA, which is proposed to occur via the double Link modules (Matsumoto *et al.* 2003). It would be interesting to know if cLP and the G1-domain of neurocan could indeed interact directly in gel filtration or protein cross-linking experiments (i.e., in solution).

While cLP and VG1 did not interact with each other in the absence of HA in solution, in its presence they were able to form a ternary complex as analysed by cross-linking/MALDI-TOF MS. These experiments revealed that the binding of cLP and

VG1 to HA oligosaccharides of 24 sugars (or longer) promoted their association. It is clear that this study provides experimental evidence that ternary complexes consisting of hyaluronan, versican and cLP (HAPLN-1) can be reassembled *in vitro* and are likely to be present in tissue where the two proteins are co-expressed (Yamauchi *et al.* 1997; Czipri *et al.* 2003; Spicer *et al.* 2003). Therefore, cLP can form ternary complexes with aggrecan, versican and potentially neurocan (see above). Thus, it appears that HAPLN-1 has a wide specificity rather than partnering with just one CSPG. It is also important to note that in genetic rescue experiments only 15-20 % expression of HAPLN-1 was necessary for the survival in HAPLN-$1^{-/-}$ mice (Czipri *et al.* 2003). Therefore, it was suggested that additional members of the link protein family are probably contributing to the stability of the ECM via ternary complex formation with CSPGs (Czipri *et al.* 2003). For example, it was also noted that HAPLN-3 mRNA levels were as high as the HAPLN-1 in cartilage (Czipri *et al.* 2003) and recently HAPLN-3 and versican were found co-localised in smooth muscle cells (Ogawa *et al.* 2004). It appears that a wide range of aggregates containing one of four HAPLNs and CSPGs can be formed and contribute to the structural integrity of tissue. Clearly, a better understanding the temporal expression and mode of binding between members of the link protein family, CSPGs and HA will be important in understanding differences in tissue specific extracellular matrix assembly. In this regard, current work to express HAPLN-3 and other members of the link protein family to investigate their interactions with CSPGs will be insightful.

Another interesting observation from this work is the potential positive cooperative interaction between VG1 and hyaluronan (see chapter 5). The first indication of this was the finding from microtitre plate assays that HA 10-mers and 12-mers appeared

to be less efficient competitors than polymeric HA for immobilised VG1 binding (Figure 3.7). Additional evidence from gel filtration experiments (Figure 4.6) showed that that longer oligosaccharides (HA 24-, 32- and 40-mers) could potentially accommodate 2, 3, and 4 VG1 molecules respectively (a VG1 molecule for every 10 sugars), indicating that oligomers of 10-12 sugars should be effective competitors. Together, these initial results suggested that VG1 may have increased affinity for HA with increasing size. However, these microtitre plate and gel filtration experiments were unable to give any quantitative measure of how bound VG1 affected the affinity for the binding of additional VG1 molecules to adjacent sites. Data from EMSA experiments was capable of giving some insight, where it appears that HA oligosaccharides can partition into those saturated with VG1 and those with no VG1 bound. This would indicate that a positive cooperative interaction between VG1 and HA oligosaccharides with increasing length is occurring (discussed in chapter 5). The observation of positive cooperativity is surprising given the homology between VG1 and the G1-domain of aggrecan, which has an identical domain organisation, yet does not display cooperative behaviour, where it is reported to bind to polymeric HA in a random fashion such that free HA was observed between bound molecules (Morgelin *et al.* 1988; Morgelin *et al.* 1995). In this regard, the results obtained here for AG1 on gel filtration experiments (chapter 4) reveal that the binding of AG1 'footprints' a large region of HA since HA32 is not able to accommodate two proteins and HA of somewhere between 34 and 40 sugars can. If it is assumed that the AG1 binding site is a HA decasaccharide then on binding of two AG1 proteins to HA40 approximately half of the HA chain will not be in direct contact with the protein. One possible explanation for the spacing of aggrecan on HA is that its binding stabilises a conformation of HA that inhibits the binding of another aggrecan close by (i.e.,

negative cooperativity). However, in the presence of link protein, uninterrupted regions of bound protein form (Morgelin *et al.* 1988; Morgelin *et al.* 1995), consistent with the presence of protein-protein interactions where cLP stabilises aggrecan to form an undissociable cooperative ternary complex with HA (Hardingham 1979). As discussed above, distinct, cooperative complexes also form between VG1 and HA in the presence of cLP (Chapter 4), where the protein-protein interaction most likely occurs between both Link module domains (see above), rather than via the Ig domain (Matsumoto *et al.* 2003). Thus, factors such as these might underlie the observed differences in cooperativity exhibited by aggrecan and versican both alone and in the presence of link protein. The biological ramifications of these physical differences, and whether the positive cooperativity displayed by VG1 alone has any *in vivo* function, remains unclear at present. It is tempting to speculate whether this positive cooperativity is contributing to the disruption of cell adhesion and promotion of proliferation observed when VG1 is over expressed in NIH3T3 fibroblasts (Yang *et al.* 1999). However, further studies are required to establish if the cooperativity implied by the EMSA experiments could indeed occur *in vivo*, and whether its nature is similar to the interaction between versican and link protein (i.e., involving Link module-Link module interactions). Although longer HA oligosaccharides (i.e., 24-, 32- and 40-mers) also showed potential for multimeric binding to sites to cLP by gel filtration (Figure 4.6), no difference in competition was observed between HA 10-mers and polymeric HA (Figure 3.7). Additionally, given the lack of material, EMSA experiments using cLP such as those performed for with VG1 (Figure 5.12) were not performed. Future EMSA experiments with both cLP and AG1 will help shed light on these interactions.

With regard to the production of fluorescently labelled HA oligosaccharides, it was essential that highly characterised proteins (cLP, VG1 and AG1) were used for the assessment of their binding activities. One of the more intriguing results obtained from the studies using fluorescent HA oligosaccharides was the ability of VG1 to quench the fluorescence upon binding indicating that Fluorescent Resonance Energy Transfer (FRET) type experiments can be pursued. This technique involves the distance-dependent interaction between the electronic excited states of two fluorophores where the excitation is transferred from a donor fluorophore to an acceptor fluorophore without emission of a photon (Stryer and Haugland 1967). In most applications, the donor and acceptor fluorophores are different, in which case FRET can be detected by the appearance of sensitised fluorescence of the acceptor or by quenching of donor fluorescence. In our experiments the donor fluorophore was the 2AA-labelled HA oligosaccharides and the acceptor or quenching fluorophores are most likely the tyrosines in the HA-binding site of the protein (see Figure 2.1). Given that all functional members of the Link module superfamily have tyrosines in their binding grove (Mahoney *et al.* 2001b; Blundell *et al.* 2003), FRET type experiments can be used to assess the binding kinetics between members of the Link module superfamily and HA oligosaccharides labelled with 2AA. Fluorescent labelling of hyaluronan oligosaccharides could also be useful in cell culture experiments for monitoring oligosaccharide protein interactions as observed previously for fluorescein-labelled hyaluronan (Evanko and Wight 1999). Since the 2AA is quenched by the binding of Link modules, labelling oligosaccharides with 2-aminoacridone (AMAC) may be a more suitable given its emission wavelength is higher than 2AA (see Table 5.1) making the sugars less likely to be quenched. Although AMAC labelled heparin oligosaccharides have been reported to be

biologically active (Lyon *et al.* 2004) it remains uncertain how AMAC labelling will effect HA oligosaccharides. Clearly, fluorescent labelling of HA oligosaccharides could prove to be a highly effective method for the investigation of HA-protein interactions *in vitro*.

In summary the major results of this work are as follows:

- Cartilage link protein (cLP) and the G1-domains of aggrecan (AG1) and versican (VG1) expressed in *Drosophila* S2 cells were purified to homogeneity either by reverse-phase HPLC or high resolution ion-exchange chromatography.
- All three proteins contained *N*-linked glycosylation as assessed by both SDS-PAGE and MALDI-TOF mass spectrometry before and after PNGase F treatment.
- All three proteins were demonstrated to be functionally active with regard to HA binding as reported previously for the native proteins.
- All three proteins maintained their functional activity after biotinylation and bVG1 and bAG1 were used to stain hyaluronan in tissue.
- cLP and VG1 but not AG1 maintained their ability to bind HA after PNGase F treatment on solid phase microtitre plate assays.
- Longer HA oligosaccharides (HA24, 32 and 40) could accommodate more than one cLP or VG1 molecules.
- HA40 but not HA32 was capable of accommodating two AG1 molecules.
- AG1 interacted with cLP in both solution phase (gel filtration and cross-linking/MALDI-TOF MS) and solid phase microtitre plate assays.

- VG1 did not interact with cLP in solution phase experiments but did on microtitre plate assays.
- VG1 and cLP formed ternary complexes in the presence of HA oligosaccharides of 24 but not 20 sugars in length.
- PNGase F treated AG1 and VG1 maintained their ability to form ternary complexes with cLP.
- HA oligosaccharides labelled with 2-aminobenzoic acid from four to 40 sugars in length were purified to homogeneity by ion exchange chromatography using a logarithmic gradient.
- Molecular weight and purity characterisation of HA oligosaccharides is facilitated by 2AA derivatisation since it enhances signals in MALDI-TOF mass spectrometry and improves FACE (fluorophore-assisted carbohydrate electrophoresis) analysis by avoiding the inverted parabolic migration characteristic of 2-aminoacridone (AMAC) labelled sugars.
- The small size and shape of the fluorophore maintains the biological activity of the derivatised oligosaccharides, as demonstrated by their ability to compete for polymeric hyaluronan binding VG1, AG1 and cLP.
- An electrophoretic mobility shift assay was used to study VG1 binding to labelled HA 8-, 10-, 20-, 30- and 40-mers and, although no stable VG1 binding was observed to labelled 8-mers, the equilibrium dissociation constant (100 nM) for VG1 with HA10 was estimated from densitometry analysis of the free oligosaccharide.

7 References

Acharya, S., Foletta, V.C., Lee, J.W., Rayborn, M.E., Rodriguez, I.R., Young, W.S., 3rd and Hollyfield, J.G. (2000) SPACRCAN, a novel human interphotoreceptor matrix hyaluronan-binding proteoglycan synthesized by photoreceptors and pinealocytes. *J Biol Chem*, **275**, 6945-6955.

Almond, A., Brass, A. and Sheehan, J.K. (1998a) Dynamic exchange between stabilized conformations predicted for hyaluronan tetrasaccharides: comparison of molecular dynamics simulations with available NMR data. *Glycobiology*, **8**, 973-980.

Almond, A., Brass, A. and Sheehan, J.K. (1998b) Deducing polymeric structure from aqueous molecular dynamics simulations of oligosaccharides: predictions from simulations of hyaluronan tetrasaccharides compared with hydrodynamic and X-ray fibre diffraction data. *J Mol Biol*, **284**, 1425-1437.

Altmann, F., Staudacher, E., Wilson, I.B. and Marz, L. (1999) Insect cells as hosts for the expression of recombinant glycoproteins. *Glycoconj J*, **16**, 109-123.

Anumula, K.R. (1994) Quantitative determination of monosaccharides in glycoproteins by high-performance liquid chromatography with highly sensitive fluorescence detection. *Anal Biochem*, **220**, 275-283.

Anumula, K.R. and Dhume, S.T. (1998) High resolution and high sensitivity methods for oligosaccharide mapping and characterization by normal phase high performance liquid chromatography following derivatization with highly fluorescent anthranilic acid. *Glycobiology*, **8**, 685-694.

Anumula, K.R. and Du, P. (1999) Characterization of carbohydrates using highly fluorescent 2-aminobenzoic acid tag following gel electrophoresis of glycoproteins. *Anal Biochem*, **275**, 236-242.

Aspberg, A., Adam, S., Kostka, G., Timpl, R. and Heinegard, D. (1999) Fibulin-1 is a ligand for the C-type lectin domains of aggrecan and versican. *J Biol Chem*, **274**, 20444-20449.

Aspberg, A., Miura, R., Bourdoulous, S., Shimonaka, M., Heinegard, D., Schachner, M., Ruoslahti, E. and Yamaguchi, Y. (1997) The C-type lectin domains of lecticans, a family of aggregating chondroitin sulfate proteoglycans, bind tenascin-R by protein-protein interactions independent of carbohydrate moiety. *Proc Natl Acad Sci U S A*, **94**, 10116-10121.

Baldwin, C.T., Reginato, A.M., Smith, C., Jimenez, S.A. and Prockop, D.J. (1989) Structure of cDNA clones coding for human type II procollagen. The alpha 1(II) chain is more similar to the alpha 1(I) chain than two other alpha chains of fibrillar collagens. *Biochem J*, **262**, 521-528.

Banerji, S., Ni, J., Wang, S.X., Clasper, S., Su, J., Tammi, R., Jones, M. and Jackson, D.G. (1999) LYVE-1, a new homologue of the CD44 glycoprotein, is a lymph-specific receptor for hyaluronan. *J Cell Biol*, **144**, 789-801.

Bayliss, M.T. (1990) Proteoglycan structure and metabolism during maturation and ageing of human articular cartilage. *Biochem Soc Trans*, **18**, 799-802.

Bekku, Y., Su, W.-D., et al. (2003) Molecular cloning of Bral2, a novel brain-specific link protein, and immunohistochemical colocalization with brevican in perineuronal nets. *Molecular and Cellular Neuroscience*, **24**, 148-159.

Bertrand, P. and Delpech, B. (1985) Interaction of hyaluronectin with hyaluronic acid oligosaccharides. *J Neurochem*, **45**, 434-439.

Bigge, J.C., Patel, T.P., Bruce, J.A., Goulding, P.N., Charles, S.M. and Parekh, R.B. (1995) Nonselective and efficient fluorescent labeling of glycans using 2-amino benzamide and anthranilic acid. *Anal Biochem*, **230**, 229-238.

Blumenkrantz, N. and Asboe-Hansen, G. (1973) New method for quantitative determination of uronic acids. *Anal Biochem*, **54**, 484-489.

Blundell, C.D., DeAngelis, P.L., Day, A.J. and Almond, A. (2004a) Use of 15N-NMR to resolve molecular details in isotopically-enriched carbohydrates: sequence-specific observations in hyaluronan oligomers up to decasaccharides. *Glycobiology*, **14**, 999-1009.

Blundell, C.D., Mahoney, D.J., Almond, A., DeAngelis, P.L., Kahmann, J.D., Teriete, P., Pickford, A.R., Campbell, I.D. and Day, A.J. (2003) The link module from ovulation- and inflammation-associated protein TSG-6 changes conformation on hyaluronan binding. *J Biol Chem*, **278**, 49261-49270.

Blundell, C.D., Seyfried, N.T. and Day, A.J. (2004b) Structural and functional diversity of hyaluronan-binding proteins. *Chemistry and Biology of Hyaluronan*, (H. G. Garg and C.A Hales Ed), Elsevier Press, Amsterdam, The Netherlands, 184-204.

Bonnet, F., Dunham, D.G. and Hardingham, T.E. (1985) Structure and interactions of cartilage proteoglycan binding region and link protein. *Biochem J*, **228**, 77-85.

Bost, F., Diarra-Mehrpour, M. and Martin, J.P. (1998) Inter-alpha-trypsin inhibitor proteoglycan family--a group of proteins binding and stabilizing the extracellular matrix. *Eur J Biochem*, **252**, 339-346.

Brakebusch, C., Seidenbecher, C.I., et al. (2002) Brevican-deficient mice display impaired hippocampal CA1 long-term potentiation but show no obvious deficits in learning and memory. *Mol Cell Biol*, **22**, 7417-7427.

Buckwalter, J.A. and Rosenberg, L.C. (1982) Electron microscopic studies of cartilage proteoglycans. Direct evidence for the variable length of the chondroitin sulfate-rich region of proteoglycan subunit core protein. *J Biol Chem*, **257**, 9830-9839.

Buckwalter, J.A., Rosenberg, L.C. and Tang, L.H. (1984) The effect of link protein on proteoglycan aggregate structure. An electron microscopic study of the molecular architecture and dimensions of proteoglycan aggregates reassembled from the proteoglycan monomers and link proteins of bovine fetal epiphyseal cartilage. *J Biol Chem*, **259**, 5361-5363.

Calabro, A., Benavides, M., Tammi, M., Hascall, V.C. and Midura, R.J. (2000a) Microanalysis of enzyme digests of hyaluronan and chondroitin/dermatan sulfate by fluorophore-assisted carbohydrate electrophoresis (FACE). *Glycobiology*, **10**, 273-281.

Calabro, A., Hascall, V.C. and Midura, R.J. (2000b) Adaptation of FACE methodology for microanalysis of total hyaluronan and chondroitin sulfate composition from cartilage. *Glycobiology*, **10**, 283-293.

Calabro, A., Midura, R., Wang, A., West, L., Plaas, A. and Hascall, V.C. (2001) Fluorophore-assisted carbohydrate electrophoresis (FACE) of glycosaminoglycans. *Osteoarthritis Cartilage*, **9 Suppl A**, S16-22.

Camenisch, T.D. and McDonald, J.A. (2000) Hyaluronan . Is Bigger Better? *Am. J. Respir. Cell Mol. Biol.*, **23**, 431-433.

Carrette, O., Nemade, R.V., Day, A.J., Brickner, A. and Larsen, W.J. (2001) TSG-6 is concentrated in the extracellular matrix of mouse cumulus oocyte complexes through hyaluronan and inter-alpha-inhibitor binding. *Biol Reprod*, **65**, 301-308.

Caterson, B. and Baker, J. (1978) The interaction of link proteins with proteoglycan monomers in the absence of hyaluronic acid. *Biochem Biophys Res Commun*, **80**, 496-503.

Chen, Q., Cai, S., Shadrach, K.G., Prestwich, G.D. and Hollyfield, J.G. (2004) Spacrcan binding to hyaluronan: molecular and biochemical studies. *Matrix Biology Institute*, Proceedings from Hyaluronan (2003), http://www.matrixbiologyinstitute.org/ha2003/ch2009/index.htm.

Cheung, W.F., Cruz, T.F. and Turley, E.A. (1999) Receptor for hyaluronan-mediated motility (RHAMM), a hyaladherin that regulates cell responses to growth factors. *Biochem Soc Trans*, **27**, 135-142.

Chu, B. (1991) *Laser light scattering: basic principle and practice*, 2nd Ed., Academic Press, Boston.

Cleland, R.L. (1979) Binding of hyaluronic acid oligosaccharides by cartilage proteoglycan. *Biochem Biophys Res Commun*, **87**, 1140-1145.

Courel, M.-N., Maingonnat, C., Tranchepain, F., Deschrevel, B., Vincent, J.-C., Bertrand, P. and Delpech, B. (2002) Importance of Hyaluronan Length in a Hyaladherin-Based Assay for Hyaluronan. *Analytical Biochemistry*, **302**, 285-290.

Csoka, A.B., Frost, G.I. and Stern, R. (2001) The six hyaluronidase-like genes in the human and mouse genomes. *Matrix Biology*, **20**, 499-508.

Czipri, M., Otto, J.M., et al. (2003) Genetic rescue of chondrodysplasia and the perinatal lethal effect of cartilage link protein deficiency. *J Biol Chem*, **278**, 39214-39223.

Day, A.J. (1999) The structure and regulation of hyaluronan-binding proteins. *Biochem Soc Trans*, **27**, 115-121.

Day, A.J. (2001) http:www.glycoforum.gr.jp/science/hyaluronan/HA16/HA16E.html.

Day AJ, A.J., Rugg, M.S., Mahoney, D.J. and Milner, C.M. (2004) Role of hyaluronan-binding proteins in ovulation. *Matrix Biology Institute*, Proceedings from Hyaluronan (2003) http://www.matrixbiologyinstitute.org/ha2003/ch2008/index.htm.

Day, A.J. and Prestwich, G.D. (2002) Hyaluronan-binding proteins: tying up the giant. *J Biol Chem*, **277**, 4585-4588.

Day, A.J. and Sheehan, J.K. (2001) Hyaluronan: polysaccharide chaos to protein organisation. *Curr Opin Struct Biol*, **11**, 617-622.

Day JM, Olin, A.I., Murdoch, A.D., Canfield, A., Sasaki, T., Timpl, R., Hardingham, T.E. and Aspberg, A. (2004) Alternative Splicing in the Aggrecan G3 Domain Influences Binding Interactions with Tenascin-C and Other Extracellular Matrix Proteins. *J. Biol. Chem.*, **279**, 12511-12518.

de la Motte, C.A., Hascall, V.C., Drazba, J., Bandyopadhyay, S.K. and Strong, S.A. (2003) Mononuclear Leukocytes Bind to Specific Hyaluronan Structures on Colon Mucosal Smooth Muscle Cells Treated with Polyinosinic Acid:Polycytidylic Acid: Inter-{alpha}-Trypsin Inhibitor Is Crucial to Structure and Function. *Am J Pathol*, **163**, 121-133.

DeAngelis, P.L. (1999) Hyaluronan synthases: fascinating glycosyltransferases from vertebrates, bacterial pathogens, and algal viruses. *Cell Mol Life Sci*, **56**, 670-682.

DeAngelis, P.L. (2002) Evolution of glycosaminoglycans and their glycosyltransferases: Implications for the extracellular matrices of animals and the capsules of pathogenic bacteria. *Anat Rec*, **268**, 317-326.

Deb, T.B. and Datta, K. (1996) Molecular cloning of human fibroblast hyaluronic acid-binding protein confirms its identity with P-32, a protein co-purified with splicing factor SF2. Hyaluronic acid-binding protein as P-32 protein, co-purified with splicing factor SF2. *J Biol Chem*, **271**, 2206-2212.

Doege, K.J., Sasaki, M., Kimura, T. and Yamada, Y. (1991) Complete coding sequence and deduced primary structure of the human cartilage large aggregating proteoglycan, aggrecan. Human-specific repeats, and additional alternatively spliced forms. *J Biol Chem*, **266**, 894-902.

Dours-Zimmermann, M. and Zimmermann, D. (1994) A novel glycosaminoglycan attachment domain identified in two alternative splice variants of human versican. *J. Biol. Chem.*, **269**, 32992-32998.

Drickamer, K. (1999) C-type lectin-like domains. *Curr Opin Struct Biol*, **9**, 585-590.

Drummond, K.J., Yates, E.A. and Turnbull, J.E. (2001) Electrophoretic sequencing of heparin/heparan sulfate oligosaccharides using a highly sensitive fluorescent end label. *Proteomics*, **1**, 304-310.

Dudhia, J. and Hardingham, T.E. (1990) The primary structure of human cartilage link protein. *Nucleic Acids Res*, **18**, 2214.

Engstrom-Laurent, A. (1989) Changes in hyaluronan concentration in tissues and body fluids in disease states. *Ciba Found Symp*, **143**, 233-240; discussion 240-237, 281-235.

Esko, J.D. and Lindahl, U. (2001) Molecular diversity of heparan sulfate. *J. Clin. Invest.*, **108**, 169-173.

Evanko, S.P. and Wight, T.N. (1999) Intracellular localization of hyaluronan in proliferating cells. *J Histochem Cytochem*, **47**, 1331-1342.

Faltz, L.L., Caputo, C.B., Kimura, J.H., Schrode, J. and Hascall, V.C. (1979) Structure of the complex between hyaluronic acid, the hyaluronic acid-binding region, and the link protein of proteoglycan aggregates from the swarm rat chondrosarcoma. *J Biol Chem*, **254**, 1381-1387.

Faltz, L.L., Reddi, A.H., Hascall, G.K., Martin, D., Pita, J.C. and Hascall, V.C. (1979) Characteristics of proteoglycans extracted from the Swarm rat chondrosarcoma with associative solvents. *J Biol Chem*, **254**, 1375-1380.

Fosang, A.J. and Hardingham, T.E. (1989) Isolation of the N-terminal globular protein domains from cartilage proteoglycans. Identification of G2 domain and its lack of interaction with hyaluronate and link protein. *Biochem J*, **261**, 801-809.

Franzen, A., Bjornsson, S. and Heinegard, D. (1981) Cartilage proteoglycan aggregate formation. Role of link protein. *Biochem J*, **197**, 669-674.

Fraser, J.R., Laurent, T.C. and Laurent, U.B. (1997) Hyaluronan: its nature, distribution, functions and turnover. *J Intern Med*, **242**, 27-33.

Friedlander, D.R., Milev, P., Karthikeyan, L., Margolis, R.K., Margolis, R.U. and Grumet, M. (1994) The neuronal chondroitin sulfate proteoglycan neurocan binds to the neural cell adhesion molecules Ng-CAM/L1/NILE and N-CAM, and inhibits neuronal adhesion and neurite outgrowth. *J Cell Biol*, **125**, 669-680.

Funderburgh, J.L. (2000) Keratan sulfate: structure, biosynthesis, and function. *Glycobiology*, **10**, 951-958.

Gardell, S., Baker, J., Caterson, B., Heinegard, D. and Roden, L. (1980) Link protein and a hyaluronic acid-binding region as components of aorta proteoglycan. *Biochem Biophys Res Commun*, **95**, 1823-1831.

Gary, S.C. and Hockfield, S. (2000) BEHAB/brevican: an extracellular matrix component associated with invasive glioma. *Clin Neurosurg*, **47**, 72-82.

Gary, S.C., Kelly, G.M. and Hockfield, S. (1998) BEHAB/brevican: a brain-specific lectican implicated in gliomas and glial cell motility. *Curr Opin Neurobiol*, **8**, 576-581.

Gershkovich, A.A. and Kholodovych, V.V. (1996) Fluorogenic substrates for proteases based on intramolecular fluorescence energy transfer (IFETS). *J Biochem Biophys Methods*, **33**, 135-162.

Goetinck, P.F., Stirpe, N.S., Tsonis, P.A. and Carlone, D. (1987) The tandemly repeated sequences of cartilage link protein contain the sites for interaction with hyaluronic acid. *J Cell Biol*, **105**, 2403-2408.

Grover, J. and Roughley, P.J. (1993) Versican gene expression in human articular cartilage and comparison of mRNA splicing variation with aggrecan. *Biochem J*, **291 (Pt 2)**, 361-367.

Grover, J. and Roughley, P.J. (1994) The expression of functional link protein in a baculovirus system: analysis of mutants lacking the A, B and B' domains. *Biochem J*, **300 (Pt 2)**, 317-324.

Grumet, M., Flaccus, A. and Margolis, R.U. (1993) Functional characterization of chondroitin sulfate proteoglycans of brain: interactions with neurons and neural cell adhesion molecules. *J Cell Biol*, **120**, 815-824.

Grumet, M., Milev, P., Sakurai, T., Karthikeyan, L., Bourdon, M., Margolis, R.K. and Margolis, R.U. (1994) Interactions with tenascin and differential effects on cell adhesion of neurocan and phosphacan, two major chondroitin sulfate proteoglycans of nervous tissue. *J Biol Chem*, **269**, 12142-12146.

Hardingham, T.E. (1979) The role of link-protein in the structure of cartilage proteoglycan aggregates. *Biochem J*, **177**, 237-247.

Hardingham,T.E.(1998) http://www.glycoforum.gr.jp/hyaluronan/HA05/HA05E.html.

Hardingham, T.E. (2004) Solution Properties of Hyaluronan. *Chemistry and Biology of Hyaluronan*, Elsevier Ltd. (H.G. Garg and C.A. Hales), 1-19.

Hardingham, T.E. and Fosang, A.J. (1992) Proteoglycans: many forms and many functions. *Faseb J*, **6**, 861-870.

Hardingham, T.E., Fosang, A.J. and Dudhia, J. (1994) The structure, function and turnover of aggrecan, the large aggregating proteoglycan from cartilage. *Eur J Clin Chem Clin Biochem*, **32**, 249-257.

Hardingham, T.E. and Muir, H. (1972) The specific interaction of hyaluronic acid with cartillage proteoglycans. *Biochim Biophys Acta*, **279**, 401-405.

Hardingham, T.E. and Muir, H. (1973) Binding of oligosaccharides of hyaluronic acid to proteoglycans. *Biochem J*, **135**, 905-908.

Harvey, D.J. (2003) Matrix-assisted laser desorption/ionization mass spectrometry of carbohydrates and glycoconjugates. *International Journal of Mass Spectrometry*, **226**, 1-35.

Hascall, V.C. and Heinegaard, D. (1974a) Aggregation of cartilage proteoglycans. I. The role of hyaluronic acid. *J Biol Chem*, **249**, 4232-4241.

Hascall, V.C. and Heinegaard, D. (1974b) Aggregation of cartilage proteoglycans. II. Oligosaccharide competitors of the proteoglycan-hyaluronic acid interaction. *J Biol Chem*, **249**, 4242-4249.

Hascall, V.C., Majors, A.K., De La Motte, C.A., Evanko, S.P., Wang, A., Drazba, J.A., Strong, S.A. and Wight, T.N. (2004) Intracellular hyaluronan: a new frontier for inflammation? *Biochim Biophys Acta*, **1673**, 3-12.

Heinrikson, R.L. and Meredith, S.C. (1984) Amino acid analysis by reverse-phase high-performance liquid chromatography: precolumn derivatization with phenylisothiocyanate. *Anal Biochem*, **136**, 65-74.

Hirakawa, S., Oohashi, T., Su, W.D., Yoshioka, H., Murakami, T., Arata, J. and Ninomiya, Y. (2000) The brain link protein-1 (BRAL1): cDNA cloning, genomic structure, and characterization as a novel link protein expressed in adult brain. *Biochem Biophys Res Commun*, **276**, 982-989.

Horton, M.R., Shapiro, S., Bao, C., Lowenstein, C.J. and Noble, P.W. (1999) Induction and regulation of macrophage metalloelastase by hyaluronan fragments in mouse macrophages. *J Immunol*, **162**, 4171-4176.

Huang, Z., Prickett, T., Potts, M. and Helm, R.F. (2000) The use of the 2-aminobenzoic acid tag for oligosaccharide gel electrophoresis. *Carbohydr Res*, **328**, 77-83.

Iozzo, R.V. (1998) Matrix proteoglycans: from molecular design to cellular function. *Annu Rev Biochem*, **67**, 609-652.

Isogai, Z., Aspberg, A., Keene, D.R., Ono, R.N., Reinhardt, D.P. and Sakai, L.Y. (2002) Versican Interacts with Fibrillin-1 and Links Extracellular Microfibrils to Other Connective Tissue Networks. *J. Biol. Chem.*, **277**, 4565-4572.

Itano, N., Sawai, T., et al. (1999) Three isoforms of mammalian hyaluronan synthases have distinct enzymatic properties. *J Biol Chem*, **274**, 25085-25092.

Ito, A.S., Turchiello, R.D., Hirata, I.Y., Cezari, M.H., Meldal, M. and Juliano, L. (1998) Fluorescent properties of amino acids labeled with ortho-aminobenzoic acid. *Biospectroscopy*, **4**, 395-402.

Jackson, D.G. (2003) The lymphatics revisited: new perspectives from the hyaluronan receptor LYVE-1. *Trends Cardiovasc Med*, **13**, 1-7.

Jackson, D.G., Prevo, R., Clasper, S. and Banerji, S. (2001) LYVE-1, the lymphatic system and tumor lymphangiogenesis. *Trends Immunol*, **22**, 317-321.

Jackson, P. (1994) High-resolution polyacrylamide gel electrophoresis of fluorophore-labeled reducing saccharides. *Methods Enzymol*, **230**, 250-265.

Jackson, R.L., Busch, S.J. and Cardin, A.D. (1991) Glycosaminoglycans: molecular properties, protein interactions, and role in physiological processes. *Physiol Rev*, **71**, 481-539.

Kahmann, J.D., O'Brien, R., Werner, J.M., Heinegard, D., Ladbury, J.E., Campbell, I.D. and Day, A.J. (2000) Localization and characterization of the hyaluronan-binding site on the link module from human TSG-6. *Structure Fold Des*, **8**, 763-774.

Karousou, E.G., Porta, G., De Luca, G. and Passi, A. (2004) Analysis of fluorophore-labelled hyaluronan and chondroitin sulfate disaccharides in biological samples. *J Pharm Biomed Anal*, **34**, 791-795.

Kimata, K., Oike, Y., Tani, K., Shinomura, T., Yamagata, M., Uritani, M. and Suzuki, S. (1986) A large chondroitin sulfate proteoglycan (PG-M) synthesized before chondrogenesis in the limb bud of chick embryo. *J. Biol. Chem.*, **261**, 13517-13525.

Kimura, J.H., Hardingham, T.E., Hascall, V.C. and Solursh, M. (1979) Biosynthesis of proteoglycans and their assembly into aggregates in cultures of chondrocytes from the Swarm rat chondrosarcoma. *J Biol Chem*, **254**, 2600-2609.

Knudson, C.B. and Knudson, W. (2001) Cartilage proteoglycans. *Semin Cell Dev Biol*, **12**, 69-78.

Kohda, D., Morton, C.J., Parkar, A.A., Hatanaka, H., Inagaki, F.M., Campbell, I.D. and Day, A.J. (1996) Solution structure of the link module: a hyaluronan-binding domain involved in extracellular matrix stability and cell migration. *Cell*, **86**, 767-775.

Krusius, T., Gehlsen, K. and Ruoslahti, E. (1987) A fibroblast chondroitin sulfate proteoglycan core protein contains lectin-like and growth factor-like sequences. *J. Biol. Chem.*, **262**, 13120-13125.

Kusche-Gullberg, M. and Kjellen, L. (2003) Sulfotransferases in glycosaminoglycan biosynthesis. *Curr Opin Struct Biol*, **13**, 605-611.

Lane, D., Prentki, P. and Chandler, M. (1992) Use of gel retardation to analyze protein-nucleic acid interactions. *Microbiol Rev*, **56**, 509-528.

Laurent, T.C. and Fraser, J.R. (1992) Hyaluronan. *Faseb J*, **6**, 2397-2404.

Laurent, T.C., Ryan, M. and Pietruszkiewicz, A. (1960) Fractionation of hyaluronic acid. The polydispersity of hyaluronic acid from the bovine vitreous body. *Biochim Biophys Acta*, **42**, 476-485.

LeBaron, R.G., Zimmermann, D.R. and Ruoslahti, E. (1992) Hyaluronate binding properties of versican. *J Biol Chem*, **267**, 10003-10010.

Lesley, J., Hascall, V.C., Tammi, M. and Hyman, R. (2000) Hyaluronan binding by cell surface CD44. *J Biol Chem*, **275**, 26967-26975.

Lundell, A., Olin, A.I., Morgelin, M., al-Karadaghi, S., Aspberg, A. and Logan, D.T. (2004) Structural Basis for Interactions between Tenascins and Lectican C-Type Lectin Domains: Evidence for a Crosslinking Role for Tenascins. *Structure*, **12**, 1495-1506.

Lyon, M., Deakin, J.A., Lietha, D., Gherardi, E. and Gallagher, J.T. (2004) The interactions of hepatocyte growth factor / scatter factor and its NK1 and NK2 variants with glycosaminoglycans using a modified gel mobility shift assay: Elucidation of the minimal size of binding and activatory oligosaccharides. *J Biol Chem,* **279**, 43560-43567.

Lyon, M. and Nieduszynski, I.A. (1983) A study of equilibrium binding of link protein to hyaluronate. *Biochem J*, **213**, 445-450.

Mahoney, D.J., Aplin, R.T., Calabro, A., Hascall, V.C. and Day, A.J. (2001a) Novel methods for the preparation and characterization of hyaluronan oligosaccharides of defined length. *Glycobiology*, **11**, 1025-1033.

Mahoney, D.J., Blundell, C.D. and Day, A.J. (2001b) Mapping the hyaluronan-binding site on the link module from human tumor necrosis factor-stimulated gene-6 by site-directed mutagenesis. *J Biol Chem*, **276**, 22764-22771.

Mahoney, D.J., Whittle, J.D., Milner, C.M., Clark, S.J., Mulloy, B., Buttle, D.J., Jones, G.C., Day, A.J. and Short, R.D. (2004) A method for the non-covalent immobilization of heparin to surfaces. *Anal Biochem*, **330**, 123-129.

Margolis, R.U. and Margolis, R.K. (1994) Aggrecan-versican-neurocan family proteoglycans. *Methods Enzymol*, **245**, 105-126.

Matsumoto, K., Shionyu, M., Go, M., Shimizu, K., Shinomura, T., Kimata, K. and Watanabe, H. (2003) Distinct interaction of versican/PG-M with hyaluronan and link protein. *J Biol Chem*, **278**, 41205-41212.

McVey, G.F. (2002) The Expression, Purification and Characterisation of Hyaluronan-binding Domains from Extracelluar Matrix Proteins. D.Phil Thesis, University of Oxford, 1-176.

Meyer, K. and Palmer, J.W. (1934) The Polysaccharide of the Vitreous Humor. *J. Biol. Chem.*, **107**, 629-634.

Milner, C.M. and Day, A.J. (2003) TSG-6: a multifunctional protein associated with inflammation. *J Cell Sci*, **116**, 1863-1873.

Mjaatvedt, C.H., Yamamura, H., Capehart, A.A., Turner, D. and Markwald, R.R. (1998) TheCspg2Gene, Disrupted in thehdfMutant, Is Required for Right Cardiac Chamber and Endocardial Cushion Formation. *Developmental Biology*, **202**, 56-66.

Morgelin, M., Paulsson, M., Hardingham, T.E., Heinegard, D. and Engel, J. (1988) Cartilage proteoglycans. Assembly with hyaluronate and link protein as studied by electron microscopy. *Biochem J*, **253**, 175-185.

Morgelin, M., Paulsson, M., Heinegard, D., Aebi, U. and Engel, J. (1995) Evidence of a defined spatial arrangement of hyaluronate in the central filament of cartilage proteoglycan aggregates. *Biochem J*, **307 (Pt 2)**, 595-601.

Mort, J.S., Poole, A.R. and Roughley, P.J. (1983) Age-related changes in the structure of proteoglycan link proteins present in normal human articular cartilage. *Biochem J*, **214**, 269-272.

Muir, H. (1995) The chondrocyte, architect of cartilage. Biomechanics, structure, function and molecular biology of cartilage matrix macromolecules. *Bioessays*, **17**, 1039-1048.

Nagase, T., Ishikawa, K., Suyama, M., Kikuno, R., Miyajima, N., Tanaka, A., Kotani, H., Nomura, N. and Ohara, O. (1998) Prediction of the coding sequences of unidentified human genes. XI. The complete sequences of 100 new cDNA clones from brain which code for large proteins in vitro. *DNA Res*, **5**, 277-286.

Neame, P.J. and Barry, F.P. (1993) The link proteins. *Experientia (Basel)*, **49**, 393-402.

Neame, P.J., Christner, J.E. and Baker, J.R. (1986) The primary structure of link protein from rat chondrosarcoma proteoglycan aggregate. *J Biol Chem*, **261**, 3519-3535.

Nedvetzki, S., Gonen, E., et al. (2004) RHAMM, a receptor for hyaluronan-mediated motility, compensates for CD44 in inflamed CD44-knockout mice: A different interpretation of redundancy. *PNAS*, **101**, 18081-18086.

Nentwich, H.A., Mustafa, Z., et al. (2002) A novel allelic variant of the human TSG-6 gene encoding an amino acid difference in the CUB module. Chromosomal localization, frequency analysis, modeling, and expression. *J Biol Chem*, **277**, 15354-15362.

Neville, D.C., Coquard, V., Priestman, D.A., Te Vruchte, D.J., Sillence, D.J., Dwek, R.A., Platt, F.M. and Butters, T.D. (2004) Analysis of fluorescently labeled glycosphingolipid-derived oligosaccharides following ceramide glycanase digestion and anthranilic acid labeling. *Anal Biochem*, **331**, 275-282.

Nieduszynski, I.A., Sheehan, J.K., Phelps, C.F., Hardingham, T.E. and Muir, H. (1980) Equilibrium-binding studies of pig laryngeal cartilage proteoglycans with hyaluronate oligosaccharide fractions. *Biochem J*, **185**, 107-114.

Noble, P.W., McKee, C.M., Cowman, M. and Shin, H.S. (1996) Hyaluronan fragments activate an NF-kappa B/I-kappa B alpha autoregulatory loop in murine macrophages. *J Exp Med*, **183**, 2373-2378.

Nomoto, H., Oohashi, T., Hirakawa, S., Ueki, Y., Ohtsuki, H. and Ninomiya, Y. (2002) Human BRAL1 and BCAN genes that belong to the link-module superfamily are tandemly arranged on chromosome 1q21-23. *Acta Med Okayama*, **56**, 25-29.

Oegema, T.R., Jr., Hascall, V.C. and Dziewiatkowski, D.D. (1975) Isolation and characterization of proteoglycans from the swarm rat chondrosarcoma. *J Biol Chem*, **250**, 6151-6159.

Ogawa, H., Oohashi, T., et al. (2004) Lp3/Hapln3, a novel link protein that co-localizes with versican and is coordinately up-regulated by platelet-derived growth factor in arterial smooth muscle cells. *Matrix Biol*, **23**, 287-298.

Olin, A.I., Morgelin, M., Sasaki, T., Timpl, R., Heinegard, D. and Aspberg, A. (2001) The proteoglycans aggrecan and Versican form networks with fibulin-2 through their lectin domain binding. *J Biol Chem*, **276**, 1253-1261.

Oohashi, T., Hirakawa, S., Bekku, Y., Rauch, U., Zimmermann, D.R., Su, W.D., Ohtsuka, A., Murakami, T. and Ninomiya, Y. (2002) Bral1, a brain-specific link protein, colocalizing with the versican V2 isoform at the nodes of Ranvier in developing and adult mouse central nervous systems. *Mol Cell Neurosci*, **19**, 43-57.

Parkar, A.A. and Day, A.J. (1997) Overlapping sites on the Link module of human TSG-6 mediate binding to hyaluronan and chrondroitin-4-sulphate. *FEBS Lett*, **410**, 413-417.

Parkar, A.A., Kahmann, J.D., Howat, S.L., Bayliss, M.T. and Day, A.J. (1998) TSG-6 interacts with hyaluronan and aggrecan in a pH-dependent manner via a common functional element: implications for its regulation in inflamed cartilage. *FEBS Lett*, **428**, 171-176.

Perin, J.P., Bonnet, F., Thurieau, C. and Jolles, P. (1987) Link protein interactions with hyaluronate and proteoglycans. Characterization of two distinct domains in bovine cartilage link proteins. *J Biol Chem*, **262**, 13269-13272.

Perrimon, N. and Bernfield, M. (2000) Specificities of heparan sulphate proteoglycans in developmental processes. *Nature*, **404**, 725-728.

Philipson, L.H. and Schwartz, N.B. (1984) Subcellular localization of hyaluronate synthetase in oligodendroglioma cells. *J Biol Chem*, **259**, 5017-5023.

Plaas, A.H., West, L., Midura, R.J. and Hascall, V.C. (2001) Disaccharide composition of hyaluronan and chondroitin/dermatan sulfate. Analysis with fluorophore-assisted carbohydrate electrophoresis. *Methods Mol Biol*, **171**, 117-128.

Politz, O., Gratchev, A., et al. (2002) Stabilin-1 and -2 constitute a novel family of fasciclin-like hyaluronan receptor homologues. *Biochem J*, **362**, 155-164.

Prehm, P. (1984) Hyaluronate is synthesized at plasma membranes. *Biochem J*, **220**, 597-600.

Prevo, R., Banerji, S., Ferguson, D.J., Clasper, S. and Jackson, D.G. (2001) Mouse LYVE-1 is an endocytic receptor for hyaluronan in lymphatic endothelium. *J Biol Chem*, **276**, 19420-19430.

Prevo, R., Banerji, S., Ni, J. and Jackson, D.G. (2004) Rapid plasma membrane-endosomal trafficking of the lymph node sinus and high endothelial venule scavenger receptor/homing receptor stabilin-1 (feel-1/clever-1). *J Biol Chem*, **279**, 52580-52592.

Price, N.C. and Dwek, R.A. (1979) *Principles and problems in physical chemistry for biochemists (Second Edition)*. Oxford University Press, Oxford.

Rauch, U. (2004) Extracellular matrix components associated with remodeling processes in brain. *Cell Mol Life Sci*, **61**, 2031-2045.

Rauch, U., Gao, P., Janetzko, A., Flaccus, A., Hilgenberg, L., Tekotte, H., Margolis, R.K. and Margolis, R.U. (1991) Isolation and characterization of developmentally regulated chondroitin sulfate and chondroitin/keratan sulfate proteoglycans of brain identified with monoclonal antibodies. *J Biol Chem*, **266**, 14785-14801.

Rauch, U., Hirakawa, S., Oohashi, T., Kappler, J. and Roos, G. (2004) Cartilage link protein interacts with neurocan, which shows hyaluronan binding characteristics different from CD44 and TSG-6. *Matrix Biol*, **22**, 629-639.

Rauch, U., Karthikeyan, L., Maurel, P., Margolis, R.U. and Margolis, R.K. (1992) Cloning and primary structure of neurocan, a developmentally regulated, aggregating chondroitin sulfate proteoglycan of brain. *J Biol Chem*, **267**, 19536-19547.

Reardon, A., Heinegard, D., McLeod, D., Sheehan, J.K. and Bishop, P.N. (1998) The large chondroitin sulphate proteoglycan versican in mammalian vitreous. *Matrix Biol*, **17**, 325-333.

Ripellino, J.A., Margolis, R.U. and Margolis, R.K. (1989) Immunoelectron microscopic localization of hyaluronic acid-binding region and link protein epitopes in brain. *J Cell Biol*, **108**, 1899-1907.

Rosenberg, L., Choi, H.U., Tang, L.H., Pal, S., Johnson, T., Lyons, D.A. and Laue, T.M. (1991) Proteoglycans of bovine articular cartilage. The effects of divalent cations on the biochemical properties of link protein. *J Biol Chem*, **266**, 7016-7024.

Rosenberg, L., Tang, L.H., Pal, S., Johnson, T.L. and Choi, H.U. (1988) Proteoglycans of bovine articular cartilage. Studies of the direct interaction of link protein with hyaluronate in the absence of proteoglycan monomer. *J Biol Chem*, **263**, 18071-18077.

Salustri, A., Camaioni, A., Di Giacomo, M., Fulop, C. and Hascall, V. (1999) Hyaluronan and proteoglycans in ovarian follicles. *Hum Reprod Update*, **5**, 293-301.

Sandson, J., Hamerman, D. and Schwick, G. (1965) Altered properties of pathological hyaluronate due to a bound inter-alpha trypsin inhibitor. *Trans Assoc Am Physicians*, **78**, 304-313.

Sato, K., Okubo, A. and Yamazaki, S. (1997) Determination of monosaccharides derivatized with 2-aminobenzoic acid by capillary electrophoresis. *Anal Biochem*, **251**, 119-121.

Schagger, H. and von Jagow, G. (1987) Tricine-sodium dodecyl sulfate-polyacrylamide gel electrophoresis for the separation of proteins in the range from 1 to 100 kDa. *Anal Biochem*, **166**, 368-379.

Scher, D.M., Stolerman, E.S. and Di Cesare, P.E. (1996) Biologic markers of arthritis. *Am J Orthop*, **25**, 263-272.

Schneider, I. (1972) Cell lines derived from late embryonic stages of Drosophila melanogaster. *J Embryol Exp Morphol*, **27**, 353-365.

Schwartz, N.B., Domowicz, M., Krueger, R.C., Jr., Li, H. and Mangoura, D. (1996) Brain aggrecan. *Perspect Dev Neurobiol*, **3**, 291-306.

Seidenbecher, C.I., Richter, K., Rauch, U., Fässler, R., Garner, C.C. and Gundelfinger, E.D. (1995) Brevican, a Chondroitin Sulfate Proteoglycan of Rat Brain, Occurs as Secreted and Cell Surface Glycosylphosphatidylinositol-anchored Isoforms. *J. Biol. Chem.*, **270**, 27206-27212.

Shi, S., Grothe, S., Zhang, Y., O'Connor-McCourt, M.D., Poole, A.R., Roughley, P.J. and Mort, J.S. (2004) Link protein has greater affinity for versican than aggrecan. *J Biol Chem.* **279,** 12060-12066

Shriver, Z., Raman, R., Venkataraman, G., Drummond, K., Turnbull, J., Toida, T., Linhardt, R., Biemann, K. and Sasisekharan, R. (2000) Sequencing of 3-O sulfate containing heparin decasaccharides with a partial antithrombin III binding site. *Proc Natl Acad Sci U S A*, **97**, 10359-10364.

Simpson, M.A., Wilson, C.M. and McCarthy, J.B. (2002) Inhibition of Prostate Tumor Cell Hyaluronan Synthesis Impairs Subcutaneous Growth and Vascularization in Immunocompromised Mice. *Am J Pathol*, **161**, 849-857.

Slevin, M., Krupinski, J., Kumar, S. and Gaffney, J. (1998) Angiogenic oligosaccharides of hyaluronan induce protein tyrosine kinase activity in endothelial cells and activate a cytoplasmic signal transduction pathway resulting in proliferation. *Lab Invest*, **78**, 987-1003.

Slevin, M., Kumar, S. and Gaffney, J. (2002) Angiogenic oligosaccharides of hyaluronan induce multiple signaling pathways affecting vascular endothelial cell mitogenic and wound healing responses. *J Biol Chem*, **277**, 41046-41059.

Spicer, A.P., Augustine, M.L. and McDonald, J.A. (1996) Molecular cloning and characterization of a putative mouse hyaluronan synthase. *J Biol Chem*, **271**, 23400-23406.

Spicer, A.P., Joo, A. and Bowling, R.A., Jr. (2003) A hyaluronan binding link protein gene family whose members are physically linked adjacent to chondroitin sulfate proteoglycan core protein genes: the missing links. *J Biol Chem*, **278**, 21083-21091.

Spicer, A.P. and McDonald, J.A. (1998) Characterization and molecular evolution of a vertebrate hyaluronan synthase gene family. *J Biol Chem*, **273**, 1923-1932.

Starr, C.M., Masada, R.I., Hague, C., Skop, E. and Klock, J.C. (1996) Fluorophore-assisted carbohydrate electrophoresis in the separation, analysis, and sequencing of carbohydrates. *J Chromatogr A*, **720**, 295-321.

Stern, R. (2003) Devising a pathway for hyaluronan catabolism: are we there yet? *Glycobiology*, **13**, 105R-115.

Stern, R. (2004) Devising a pathway for hyaluronan catabolism: How the goo gets cut. *Matrix Biology Institute*, Proceedings from Hyaluronan (2003), http://www.matrixbiologyinstitute.org/ha2003/ch2003/index.htm.

Stryer, L. and Haugland, R.P. (1967) Energy transfer: a spectroscopic ruler. *Proc Natl Acad Sci U S A*, **58**, 719-726.

Sztrolovics, R., Grover, J., Cs-Szabo, G., Shi, S.L., Zhang, Y., Mort, J.S. and Roughley, P.J. (2002) The characterization of versican and its message in human articular cartilage and intervertebral disc. *J Orthop Res*, **20**, 257-266.

Tammi, M.I., Day, A.J. and Turley, E.A. (2002) Hyaluronan and homeostasis: a balancing act. *J Biol Chem*, **277**, 4581-4584.

Tanford, C. (1961) *Physical Chemistry of Macromolecules*. John Wiley & Son's (New York).

Tang, L.H., Rosenberg, L., Reiner, A. and Poole, A.R. (1979) Proteoglycans from bovine nasal cartilage. Properties of a soluble form of link protein. *J Biol Chem*, **254**, 10523-10531.

Tashlitskil, V.N. and Oretskaya, T.S. (1997) Optimization of conditions for ion-pair HPLC of oligonucleotides. *Bioorg Khim*, **23**, 732-741.

Tawada, A., Masa, T., Oonuki, Y., Watanabe, A., Matsuzaki, Y. and Asari, A. (2002) Large-scale preparation, purification, and characterization of hyaluronan oligosaccharides from 4-mers to 52-mers. *Glycobiology*, **12**, 421-426.

Teriete, P., Banerji, S., et al. (2004) Structure of the regulatory hyaluronan binding domain in the inflammatory leukocyte homing receptor CD44. *Mol Cell*, **13**, 483-496.

Termeer, C., Benedix, F., et al. (2002) Oligosaccharides of Hyaluronan activate dendritic cells via toll-like receptor 4. *J Exp Med*, **195**, 99-111.

Termeer, C., Sleeman, J.P. and Simon, J.C. (2003) Hyaluronan--magic glue for the regulation of the immune response? *Trends Immunol*, **24**, 112-114.

Thornton, D.J., Sheehan, J.K. and Nieduszynski, I.A. (1987) A study of the interaction between cartilage proteoglycan and link protein. *Biochem J*, **248**, 943-951.

Timpl, R., Sasaki, T., Kostka, G. and Chu, M.L. (2003) Fibulins: a versatile family of extracellular matrix proteins. *Nat Rev Mol Cell Biol*, **4**, 479-489.

Toole, B.P. (1990) Hyaluronan and its binding proteins, the hyaladherins. *Curr Opin Cell Biol*, **2**, 839-844.

Toole, B.P. (2002) Hyaluronan promotes the malignant phenotype. *Glycobiology*, **12**, 37R-42R.

Toole, B.P. (2004) Hyaluronan: From extracellular glue to pericellular cue. *Nat Rev Cancer*, **4**, 528-539.

Toole, B.P. and Hascall, V.C. (2002) Hyaluronan and Tumor Growth. *Am J Pathol*, **161**, 745-747.

Trowbridge, J.M. and Gallo, R.L. (2002) Dermatan sulfate: new functions from an old glycosaminoglycan. *Glycobiology*, **12**, 117R-125.

Turnbull, J.E., Hopwood, J.J. and Gallagher, J.T. (1999) A strategy for rapid sequencing of heparan sulfate and heparin saccharides. *Proc Natl Acad Sci U S A*, **96**, 2698-2703.

Volpi, N. (2003) Milligram-scale preparation and purification of oligosaccharides of defined length possessing the structure of chondroitin from defructosylated capsular polysaccharide K4. *Glycobiology*, **13**, 635-640.

Watanabe, H., Cheung, S.C., Itano, N., Kimata, K. and Yamada, Y. (1997a) Identification of hyaluronan-binding domains of aggrecan. *J Biol Chem*, **272**, 28057-28065.

Watanabe, H., Nakata, K., Kimata, K., Nakanishi, I. and Yamada, Y. (1997b) Dwarfism and age-associated spinal degeneration of heterozygote cmd mice defective in aggrecan. *Proc Natl Acad Sci U S A*, **94**, 6943-6947.

Watanabe, H. and Yamada, Y. (1999) Mice lacking link protein develop dwarfism and craniofacial abnormalities. *Nat Genet*, **21**, 225-229.

Watanabe, H. and Yamada, Y. (2002) Chondrodysplasia of gene knockout mice for aggrecan and link protein. *Glycoconj J*, **19**, 269-273.

Wedemeyer, J., Tsai, M. and Galli, S.J. (2000) Roles of mast cells and basophils in innate and acquired immunity. *Curr Opin Immunol*, **12**, 624-631.

Weigel, J.A. and Weigel, P.H. (2003) Characterization of the Recombinant Rat 175-kDa Hyaluronan Receptor for Endocytosis (HARE). *J. Biol. Chem.*, **278**, 42802-42811.

Weigel, P.H. (2004) Current progress and limitations in understanding the molecular and cellular functions of hyaluronan synthases. *Matrix Biology Institute*, Proceedings from Hyaluronan (2003), http://www.matrixbiologyinstitute.org/ha2003/ch2002/index.htm.

Weigel, P.H., Hascall, V.C. and Tammi, M. (1997) Hyaluronan synthases. *J Biol Chem*, **272**, 13997-14000.

Weissmann, B. and Meyer, K. (1954) The Structure of Hyalobiuronic Acid and of Hyaluronic Acid from Umbilical Cord. *J.Am. Chem.Soc.*, **76**, 17531757.

Whitham, K.M., Hadley, J.L., Morris, H.G., Andrew, S.M., Nieduszynski, I.A. and Brown, G.M. (1999) An improved method for the structural profiling of keratan sulfates: analysis of keratan sulfates from brain and ovarian tumors. *Glycobiology*, **9**, 285-291.

Wight, T.N. (2002) Versican: a versatile extracellular matrix proteoglycan in cell biology. *Curr Opin Cell Biol*, **14**, 617-623.

Wight, T.N. and Merrilees, M.J. (2004) Proteoglycans in Atherosclerosis and Restenosis: Key Roles for Versican. *Circ Res*, **94**, 1158-1167.

Wisniewski, H.G. and Vilcek, J. (2004) Cytokine-induced gene expression at the crossroads of innate immunity, inflammation and fertility: TSG-6 and PTX3/TSG-14. *Cytokine Growth Factor Rev*, **15**, 129-146.

Wisniewski, H.-G. and Vilcek, J. (1997) TSG-6: An IL-1 /TNF-inducible protein with anti-inflammatory activity. *Cytokine & Growth Factor Reviews*, **8**, 143-156.

Wu, Z.L., Zhang, L., Beeler, D.L., Kuberan, B. and Rosenberg, R.D. (2002) A new strategy for defining critical functional groups on heparan sulfate. *Faseb J*, **16**, 539-545.

Yamada, H., Watanabe, K., Shimonaka, M. and Yamaguchi, Y. (1994) Molecular cloning of brevican, a novel brain proteoglycan of the aggrecan/versican family. *J. Biol. Chem.*, **269**, 10119-10126.

Yamaguchi, Y. (2000) Lecticans: organizers of the brain extracellular matrix. *Cell Mol Life Sci*, **57**, 276-289.

Yamauchi, S., Cheng, H., Neame, P., Caterson, B. and Yamauchi, M. (1997) Identification, partial characterization, and distribution of versican and link protein in bovine dental pulp. *J Dent Res*, **76**, 1730-1736.

Yang, B., Yang, B.L., Savani, R.C. and Turley, E.A. (1994) Identification of a common hyaluronan binding motif in the hyaluronan binding proteins RHAMM, CD44 and link protein. *Embo J*, **13**, 286-296.

Yang, B.L., Zhang, Y., Cao, L. and Yang, B.B. (1999) Cell adhesion and proliferation mediated through the G1 domain of versican. *J Cell Biochem*, **72**, 210-220.

Zanin, M.K., Bundy, J., Ernst, H., Wessels, A., Conway, S.J. and Hoffman, S. (1999) Distinct spatial and temporal distributions of aggrecan and versican in the embryonic chick heart. *Anat Rec*, **256**, 366-380.

Zeng, C., Toole, B.P., Kinney, S.D., Kuo, J.W. and Stamenkovic, I. (1998) Inhibition of tumor growth in vivo by hyaluronan oligomers. *Int J Cancer*, **77**, 396-401.

Zhang, L.K. and Gross, M.L. (2000) Matrix-assisted laser desorption/ionization mass spectrometry methods for oligodeoxynucleotides: improvements in matrix, detection limits, quantification, and sequencing. *J Am Soc Mass Spectrom*, **11**, 854-865.

Zhao, M., Yoneda, M., Ohashi, Y., Kurono, S., Iwata, H., Ohnuki, Y. and Kimata, K. (1995) Evidence for the Covalent Binding of SHAP, Heavy Chains of Inter-alpha-Trypsin Inhibitor, to Hyaluronan. *J. Biol. Chem.*, **270**, 26657-26663.

Zhou, B., McGary, C.T., Weigel, J.A., Saxena, A. and Weigel, P.H. (2003) Purification and molecular identification of the human hyaluronan receptor for endocytosis. *Glycobiology*, **13**, 339-349.

Zhou, B., Weigel, J.A., Fauss, L. and Weigel, P.H. (2000) Identification of the hyaluronan receptor for endocytosis (HARE). *J Biol Chem*, **275**, 37733-37741.

Zhou, X.H., Brakebusch, C., et al. (2001) Neurocan is dispensable for brain development. *Mol Cell Biol*, **21**, 5970-5978.

Zimmermann, D.R., Dours-Zimmermann, M.T., Schubert, M. and Bruckner-Tuderman, L. (1994) Versican is expressed in the proliferating zone in the epidermis and in association with the elastic network of the dermis. *J Cell Biol*, **124**, 817-825.

Zimmermann, D.R. and Ruoslahti, E. (1989) Multiple domains of the large fibroblast proteoglycan, versican. *EMBO J*, **8**, 2975-2981.